iScience

CellPress

Article

Catalytic Asymmetric Formal [3+2] Cycloaddition of Azoalkenes with 3-Vinylindoles: Synthesis of 2,3-Dihydropyrroles

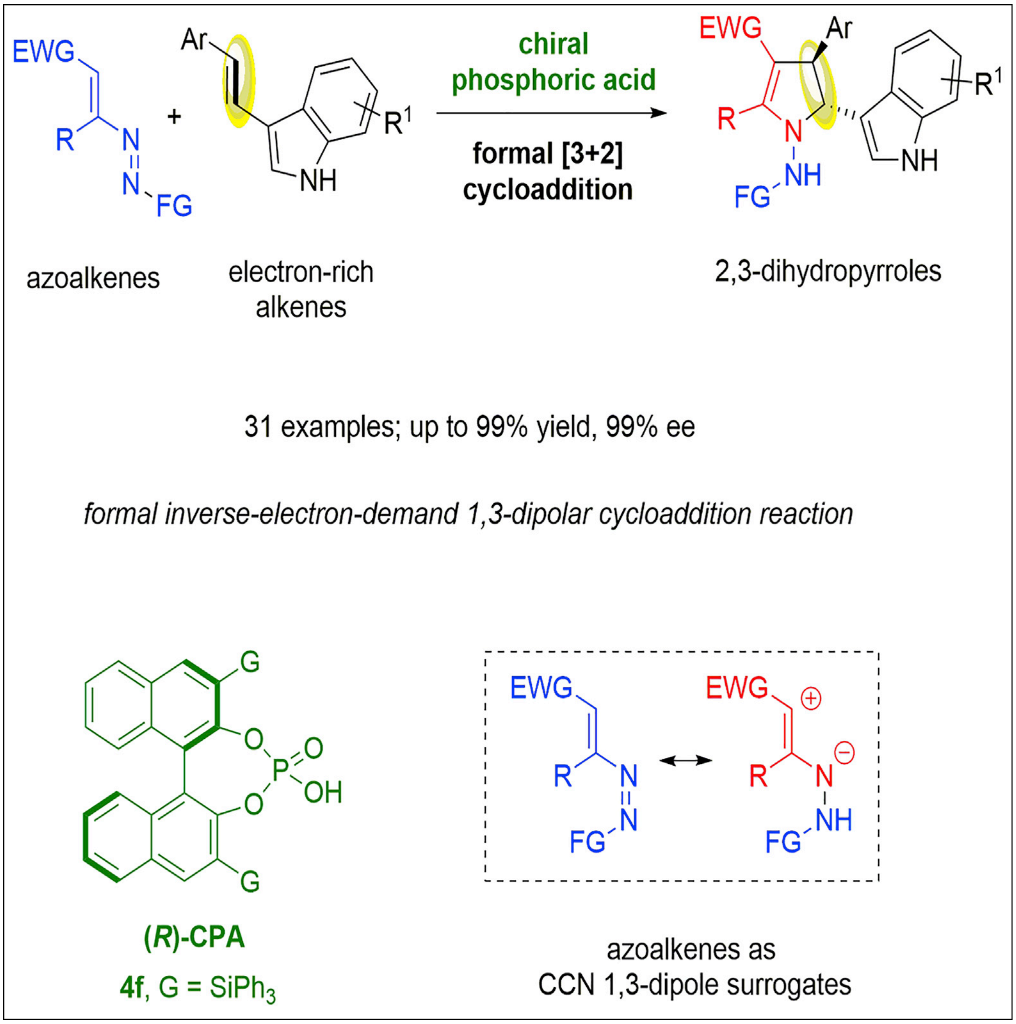

Guang-Jian Mei, Wenrui Zheng, Théo P. Gonçalves, Xiwen Tang, Kuo-Wei Huang, Yixin Lu

chmlyx@nus.edu.sg

HIGHLIGHTS

Chiral phosphoric acid catalyzed formal [3 + 2] cycloaddition reaction

2,3-Dihydropyrroles were enantioselectively synthesized

Azoalkenes served as 3-atom synthons

Mei et al., iScience *23*, 100873
February 21, 2020
https://doi.org/10.1016/j.isci.2020.100873

iScience

CellPress

Article

Catalytic Asymmetric Formal [3+2] Cycloaddition of Azoalkenes with 3-Vinylindoles: Synthesis of 2,3-Dihydropyrroles

Guang-Jian Mei,[1] Wenrui Zheng,[1] Théo P. Gonçalves,[2] Xiwen Tang,[1] Kuo-Wei Huang,[2] and Yixin Lu[1,3,4,5,*]

SUMMARY

Chiral phosphoric acid-catalyzed highly enantioselective formal [3 + 2] cycloaddition reaction of azoalkenes with 3-vinylindoles has been established. Under mild conditions, the projected cycloaddition proceeded smoothly, affording a variety of 2,3-dihydropyrroles in high yields and excellent enantioselectivities, and also in a diastereospecific manner. As opposed to the common 4-atom synthons in the previous literature reports, azoalkenes served as 3-atom synthons. Besides, the observed selectivity was supported by primary theoretical calculation. The unique chemistry of azoalkenes disclosed herein will empower asymmetric synthesis of nitrogen-containing ring structural motifs in a broader context.

INTRODUCTION

1,3-Dipolar cycloadditions are well-established synthetic strategies in organic chemistry for the preparation of five-membered heterocyclic ring systems (Coldham and Hufton, 2005; Fang and Wang, 2018; Gothelf and Jørgensen, 1998; Hashimoto and Maruoka, 2015; Kissane and Maguire, 2010; Stanley and Sibi, 2008). In a typical normal-electron-demand 1,3-dipolar cycloaddition, nucleophilic 1,3-dipoles and electron-deficient dipolarophiles are utilized. Asymmetric versions of such cycloadditions often rely on synthetic strategy that lowers the lowest unoccupied molecular orbital (LUMO) of dipolarophiles (Cheng et al., 2019; Hashimoto et al., 2007; Kano et al., 2005; Liu et al., 2008; Pascual-Escudero et al., 2016; Sibi et al., 2004; Tong et al., 2013; Wang et al., 2015; Xu et al., 2018; Yang et al., 2017). In stark contrast, inverse-electron-demand 1,3-dipolar cycloadditions utilizing electrophilic 1,3-dipoles and nucleophilic dipolarophiles are much less common. Among the reported catalytic asymmetric inverse-electron-demand 1,3-dipolar cycloadditions, nitrones and vinyl ethers are commonly employed reaction partners (Figure 1) (Ashizawa et al., 2006; Bayón et al., 2000a, 2000b; Hashimoto et al., 2011; Hori et al., 1998; Jensen et al., 1999, 2000; Jiao et al., 2008; Mikami et al., 2001; Seerden et al., 1994, 1995, 1997, Simonsen et al., 1999a, 1999b, Suga et al., 2007, 2010; Yanagisawa et al., 2011) To date, there are only a handful of exceptions (Bartlett et al., 2017; Liu et al., 2016; Sohtome et al., 2017; Xu et al., 2015; Zhu et al., 2014). Sodeoka et al.' employment of nitrile oxides as electrophilic 1,3-dipoles and Feng's utilization of enecarbamates as nucleophilic dipolarophiles are interesting examples, among others. To design inverse-electron-demand 1,3-dipolar cycloaddition processes, we recognized the importance of introducing alternative electrophilic 1,3-dipole surrogates, which ideally could be easily combined with various dipolarophiles, thus allowing for ready creation of useful molecular architectures.

Azoalkenes, also known as 1,2-diaza-1,3-dienes, have proven to be versatile synthetic building blocks in organic chemistry (Attanasi et al., 2002a, 2002b, 2009; Attanasi and Filippone, 1997; Lopes et al., 2018; Wei et al., 2019). Their characteristic 1,3-conjugate systems have been utilized synthetically; azoalkenes were shown to be a valuable acceptor in 1,4-conjugate additions, displaying excellent reactivity toward a wide variety of nucleophiles (Attanasi et al., 2011a, 2011b, 2012, 2013a, 2013b; Ciccolini et al., 2019; Mantenuto et al., 2015; Miles et al., 2015; Preti et al., 2010). Another attractive synthetic application of azoalkenes is the cycloaddition reaction, which serves as a powerful strategy for the construction of nitrogen-containing heterocycles. In the currently available mode of cycloaddition, Wang and others employed azoalkenes as 4-atom (A_4) synthons (**Int-I**), making use of C4 electrophilicity and N1 nucleophilicity of azoalkenes for various asymmetric formal [4 + n] cycloaddition processes (Chen et al., 2012; Gao et al., 2013; Huang et al., 2016; Tong et al., 2014; Wei et al., 2017, 2018; Wei and Wang, 2015; Zhang et al., 2018; Zhang and Song, 2018). Very recently, our group discovered an azoalkene-enabled enantioselective

[1]Department of Chemistry, National University of Singapore, 3 Science Drive 3, Singapore 117543, Singapore

[2]KAUST Catalysis Center and Division of Physical Sciences and Engineering, King Abdullah University of Science and Technology, Thuwal 23955-6900, Saudi Arabia

[3]Joint School of National University of Singapore and Tianjin University, International Campus of Tianjin University, Binhai New City, Fuzhou, Fujian 359297, PR China

[4]National University of Singapore (Suzhou) Research Institute, 377 Lin Quan Street, Suzhou Industrial Park, Suzhou, 215123, China

[5]Lead Contact

*Correspondence: chmlyx@nus.edu.sg

https://doi.org/10.1016/j.isci.2020.100873

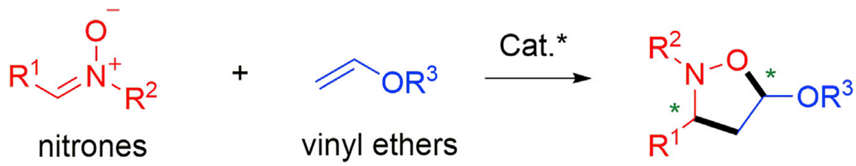

Figure 1. Inverse-Electron-Demand 1,3-Dipolar Cycloadditions Utilizing Nitrones and Vinyl Ethers

dearomatization of indoles (Mei et al., 2020). Given the ubiquitous existence of nitrogen-containing cyclic structural motifs, we questioned whether it might be possible to utilize azoalkenes as a carbon-carbon-nitrogen (CCN) 1,3-diplole surrogate, a 3-atom (A_3) synthon (**Int-II**) in asymmetric formal [3 + 2] cycloaddition reactions, and thereby to access a broad range of nitrogen-containing ring systems (Attanasi et al., 2002a, 2002b, 2005, 2013a, 2013b; Clarke et al., 1983; Karapetyan et al., 2008; Mari et al., 2017; Ran et al., 2017; Sommer, 1979). We reasoned the hydrazine-enamine tautomerization could play a key role, and fine-tuning of the system and judicious selection of potential reaction partners are of crucial importance to the successful implementation of synthetic plans (Figure 2). In particular, we believe that the current under-developed status of inverse-electron-demand 1,3-dipolar cycloadditions, in combination of rich chemistry of azoalkenes and anticipated broad applicability of the methodology, make the proposed strategy highly attractive and worthwhile investigating.

2,3-Dihydropyrroles are common structural motifs that are widely present in biologically significant molecules, and they are also valuable intermediates in organic synthesis (Augeri et al., 2005; Cantín et al., 1999; Hertel and Xu, 2002; Herzon and Myers, 2005; Kawase et al., 1999; Marti and Carreira, 2005; Petersen and Nielsen, 2013). Although approaches to access racemic 2,3-dihydropyrroles are well documented (El-Sepelgy et al., 2018; Jiang et al., 2017; Liang et al., 2017, 2018; Ma et al., 2018; Zhu et al., 2009, 2011), reports on catalytic asymmetric synthesis of 2,3-dihydropyrroles are scarce. In an early example, Gong et al. documented a catalytic asymmetric formal [3 + 2] cycloaddition reaction between isocyanoesters and nitroolefins for the synthesis of optically enriched 2,3-dihydropyrroles (Guo et al., 2008). More recently, Miura and Murakami, as well as the Fokin group, reported enantioselective preparation of 2,3-dihydropyrroles via RhII-catalyzed asymmetric annulations of triazoles with alkenes (Kwok et al., 2014; Miura et al., 2013). As part of our continuous interests in developing enantioselective cycloaddition reactions for the preparation various heterocyclic ring systems (Chan et al., 2019; Han et al., 2014, 2016; Li et al., 2019; Ni et al., 2017; Yao et al., 2016; Wu et al., 2019), we questioned the feasibility of establishing an effective asymmetric synthesis of 2,3-dihydropyrroles via a formal [3 + 2] cycloaddition reaction, by utilizing azoalkenes as an electrophilic CCN 1,3-dipole surrogate and employing simple 3-vinylindoles (Gioia et al., 2008; Li et al., 2018; Sun et al., 2016; Tan et al., 2011; Yang et al., 2019; Zhang et al., 2018; Zheng et al., 2015) as a C2 reaction partner (Figure 3). In this report, we document a formal

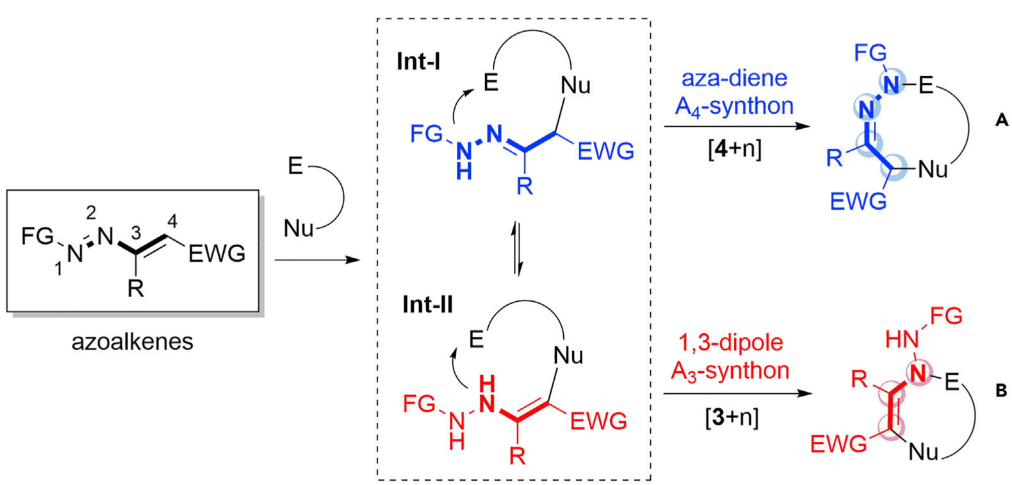

Figure 2. Employment of Azoalkenes As a Reaction Partner in Enantioselective Formal Cycloaddition Reactions

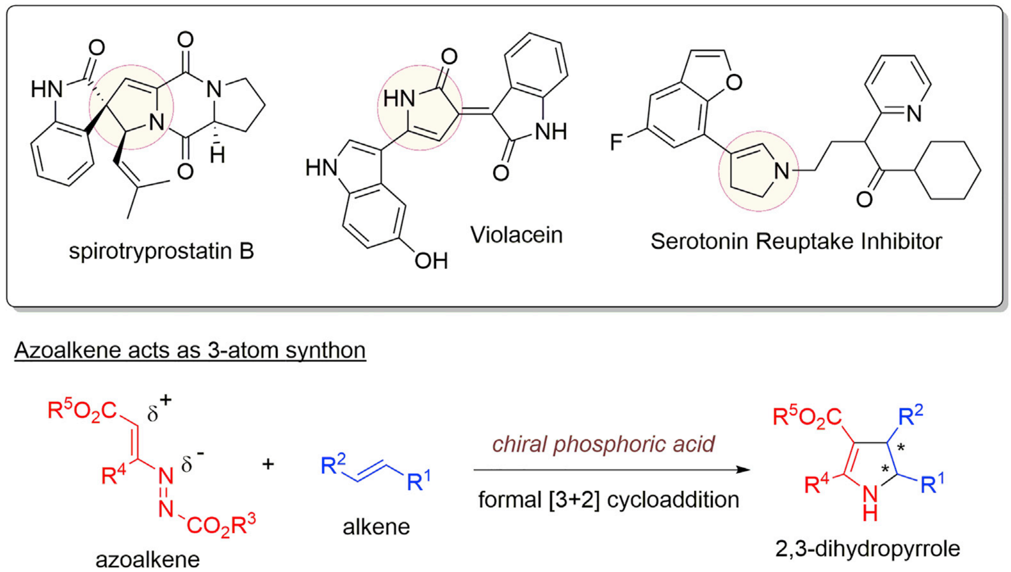

Figure 3. Our Hypothesis: Construction of 2,3-Dihydropyrroles from Azoalkenes and Simple Alkenes

[3 + 2] cycloaddition reaction for enantioselective creation of 2,3-dihydropyrroles under the catalysis of chiral phosphoric acid (CPA) (Akiyama, 2007; Terada, 2008, 2010; Wu et al., 2015; Yu et al., 2011). The projected progress could be identified as a formal inverse-electron-demand 1,3-dipolar cycloaddition reaction, wherein azoalkene served as a CCN 1,3-dipole surrogate, a 3-atom synthon.

RESULTS AND DISCUSSION

Reaction Development

Our investigation was initiated by identifying optimal conditions for the model reaction between azoalkene **1a** and vinylindole **2a** (Table 1). TRIP-CPA **4a** effectively catalyzed the reaction, furnishing 2,3-dihydropyrrole **3a** in excellent yield and moderate stereoselectivities (entry 1). The solvent screening was subsequently carried out, and chloroform was found to be the best solvent (entries 1–5). Next, the catalytic effects of different CPA catalysts (**4b**–**f**) were examined. Catalysts **4b** and **4e** had excellent controls on diastereoselectivities, but enantiomeric controls were less ideal (entries 6 and 9). Although **4c** was less effective (entry 7), **4d** was completely ineffective (entry 8). To our delight, the $SiPh_3$-derived CPA **4f** was found to be an excellent catalyst, leading to the formation of 2,3-dihydropyrrole **3a** in excellent yield and excellent enantioselectivity and diastereoselectivity (entry 10). Lowering the reaction temperature or adding molecular sieves did not result in enhancement (entries 11 and 12). Under the optimized reaction conditions, the desired 2,3-dihydropyrrole **3a** was obtained in 96% yield, and with 94% *ee* and >20:1 dr.

Scope

With the optimal reaction conditions in hand, the substrate scope with regard to azoalkenes was evaluated (Table 2). Azoalkenes bearing different R^1 groups such as methyl (**1a**), ethyl (**1b**), and *n*-propyl (**1c**) were well tolerated. When azoalkenes containing different C=C double bond appended ester groups, e.g., CO_2Et (**1a**), CO_2Me (**1d**), $CO_2{}^tBu$ (**1e**), CO_2Bn (**1f**), and $CO_2{}^iPr$ (**1g**) were utilized, consistently high chemical yields and enantio- and diastereoselectivities were attainable.

The reaction scope with regard to vinylindoles was subsequently investigated (Figure 4). Different substituted aryl groups could be installed at the terminal position of vinylindoles, regardless of electronic nature and substitution pattern (**3h**–**3o**). Moreover, vinylindoles bearing a dichloro-substituted phenyl ring (**3p**), a 2-naphthalenyl (**3q**), or a 2-thiophenyl substituent (**3r**) were found suitable for the reaction. In all the examples examined, the desired 2,3-dihydropyrrole products were obtained in high yields and with excellent ee values and all the reactions proceeded in a diastereospecific manner.

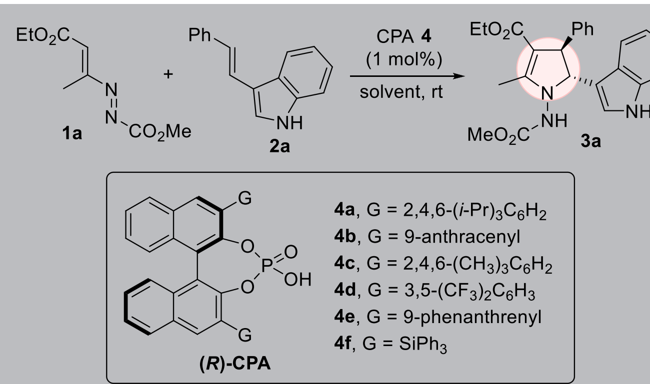

Entry	4	Solvent	Yield (%)[a]	*ee* (%)[b]	Dr[c]
1	4a	CH_2Cl_2	95	70	6:1
2	4a	Toluene	90	53	8:1
3	4a	THF	<5	–	–
4	4a	DCE	85	70	7:1
5	4a	$CHCl_3$	86	72	11:1
6	4b	$CHCl_3$	80	28	>20:1
7	4c	$CHCl_3$	92	62	7:1
8	4d	$CHCl_3$	95	0	2:1
9	4e	$CHCl_3$	88	54	>20:1
10	4f	$CHCl_3$	96	94	>20:1
11[d]	4f	$CHCl_3$	94	92	>20:1
12[e]	4f	$CHCl_3$	92	91	>20:1

Table 1. Optimization of the Reaction Conditions

Reaction conditions: **1a** (0.1 mmol), **2a** (0.12 mmol), and the catalyst (0.001 mmol) in the solvent specified (1 mL) at room temperature for 0.5 h.

[a]Yields refer to isolated yields.

[b]The *ee* values were determined by HPLC analysis on a chiral stationary phase.

[c]The dr values were determined by ^{1}H NMR analysis of the crude mixture.

[d]The reaction was carried out at 0°C.

[e]Molecular sieves (4 Å) were added.

The indole moieties in the vinylindole structures could also be varied, and the results are summarized in Figure 5. A wide range of vinylindoles bearing various substituted indoles were employed, and the corresponding 2,3-dihydropyrrole products **3** (**3s**−**3z**, **3a′**−**3e′**) were obtained in good to very good yields, and with consistently excellent enantioselectivities, as well as perfect diastereoselectivities. Notably, the electronic nature and position of the indole substituents did not appear to have much influence on the reaction, and this trend held true for 5,6-dichloro-substituted substrate (**3e′**). The absolute configurations of 2,3-dihydropyrrole products were assigned based on X-ray crystallographic analysis of **3y**.

Mechanistic Investigations

We carried out a few further experiments to gain a better understanding of this reaction process. When methyl-substituted vinylindole **2b** was employed, only a moderate ee value of 64% was obtained (Scheme 1 Equation 1), which suggested the importance of aryl moiety in vinylindole substrates for asymmetric induction. When 2-methyl-substituted vinylindole **2c** was utilized, a dearomatization of indole occurred,

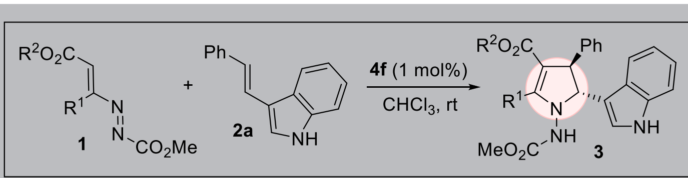

Entry	R^1/R^2(1)	3	Yield (%)[a]	*ee* (%)[b]	Dr[c]
1	Me/Et(**1a**)	3a	96	94	>20:1
2	Et/Et(**1b**)	3b	90	95	>20:1
3	*n*Pr/Et(**1c**)	3c	94	83	>20:1
4	Me/Me(**1d**)	3d	85	94	>20:1
5	Me/*t*Bu(**1e**)	3e	86	92	>20:1
6	Me/Bn(**1f**)	3f	95	91	>20:1
7	Me/*i*Pr(**1g**)	3g	92	91	>20:1

Table 2. Employing Different Azoalkenes

Reaction conditions: **1** (0.1 mmol), **2a** (0.12 mmol), and **4f** (0.001 mmol) in $CHCl_3$ (1 mL) at room temperature for 0.5 h.

[a]Yields refer to isolated yields.

[b]The *ee* values were determined by HPLC analysis on a chiral stationary phase.

[c]The dr values were determined by ^1H NMR analysis of the crude mixture.

furnishing the pyrroloindoline product **5** in good yield and excellent enantioselectivity (Scheme 1 Equation 2). It is intriguing to note that such subtle difference in substrate structure could result in totally different chemoselectivity. The presence of a 2-methyl group may render indole higher nucleophilicity at the C3-position, thus favoring the dearomative process (Mei et al., 2020). Furthermore, no reaction was observed when *N*-methyl vinylindole **2d** was employed (Scheme 1 Equation 3), indicating the indispensability of hydrogen bonding interactions between CPA and the substrates, not only in asymmetric induction but also in reaction activation.

On the basis of our experimental results, we have also constructed the models with the aid of computation using **1a** and **2a** as substrates to obtain some insights into the reaction selectivity. A plausible reaction pathway was proposed (Figure 6) where the asymmetric 1,4-addition of vinylindole **2a** to azoalkene **1a** is initiated via a hydrogen-bonding activation mode and both substrates can be activated simultaneously by the CPA catalyst within its chiral pockets. Vinylindole **2a** adopts the *s-cis* geometry in order to reach the electrophilic site in **1a**. The resulting intermediate **A** has its conformation locked for the *5-exo* attack [3 + 2] of the iminic N to the spatially adjacent C=C bond (N1-C 3.98 Å, path a) to afford the experimentally observed product after proton transfer and tautomerization steps. Alternatively, hydrazone-enamine tautomerization may occur, furnishing intermediate **B**, which undergoes cyclization to afford the observed [3 + 2] product **3a** via path c. In comparison, the *6-exo* [4 + 2] attack was deemed difficult to occur. In intermediate **A**, path b is unfavorable, likely due to the ring strain under such a rigid structure (N2-C 5.32 Å), whereas in intermediate **B**, pathway d is unlikely because of the reduced nucleophilicity of the amide nitrogen. Indeed, the [4 + 2] products formed via path b or d were never observed in this reaction.

Conclusions

In conclusion, we have established a formal [3 + 2] cycloaddition reaction, utilizing azoalkenes as an electrophilic reaction component and simple alkenes as a nucleophilic partner. In the presence of chiral phosphoric acid, the reaction proceeded smoothly, furnishing a wide range of functionalized 2,3-dihydropyrroles in good yields and in a highly enantioselective and diastereospecific manner. It is noteworthy that the projected progress could be identified as a formal inverse-electron-demand 1,3-dipolar cycloaddition reaction, wherein azoalkenes served as CCN 1,3-dipole surrogates, 3-atom synthons, as opposed to the common 4-atom synthons in the previous literature reports. With the current successful demonstration of chiral 2,3-dihydropyrrole synthesis and theoretical understanding of the observed chemoselectivity,

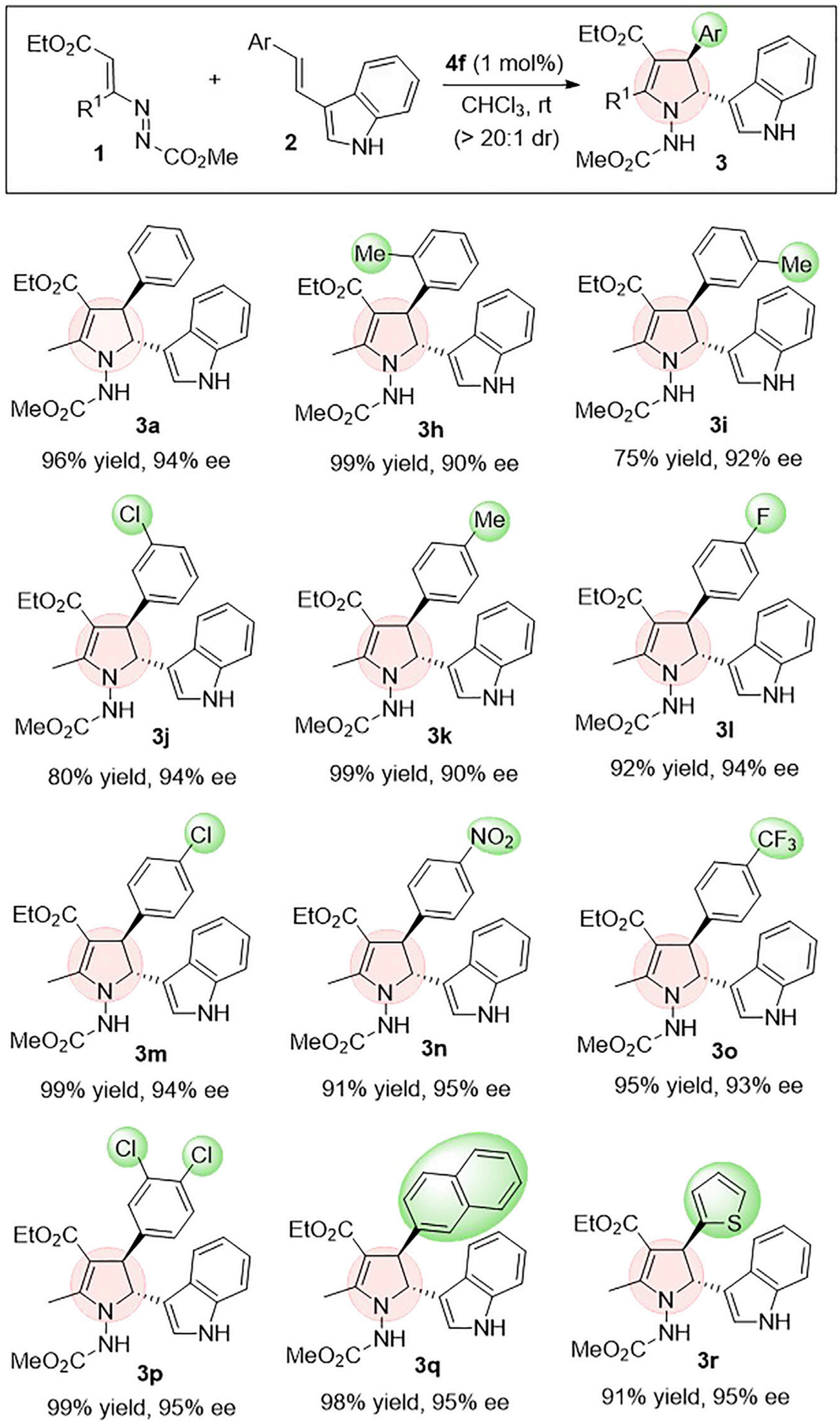

Figure 4. Reaction Scope of Vinylindoles

Reaction conditions: **1** (0.1 mmol), **2** (0.12 mmol), and **4f** (0.001mmol) in $CHCl_3$ (1 mL) at room temperature for 0.5 h. Yields refer to isolated yields; the *ee* values were determined by HPLC analysis on a chiral stationary phase.

we anticipate the unique chemistry of azoalkenes disclosed herein will empower asymmetric synthesis of nitrogen-containing ring structural motifs in a broader context. Our findings in this direction will be reported in due course.

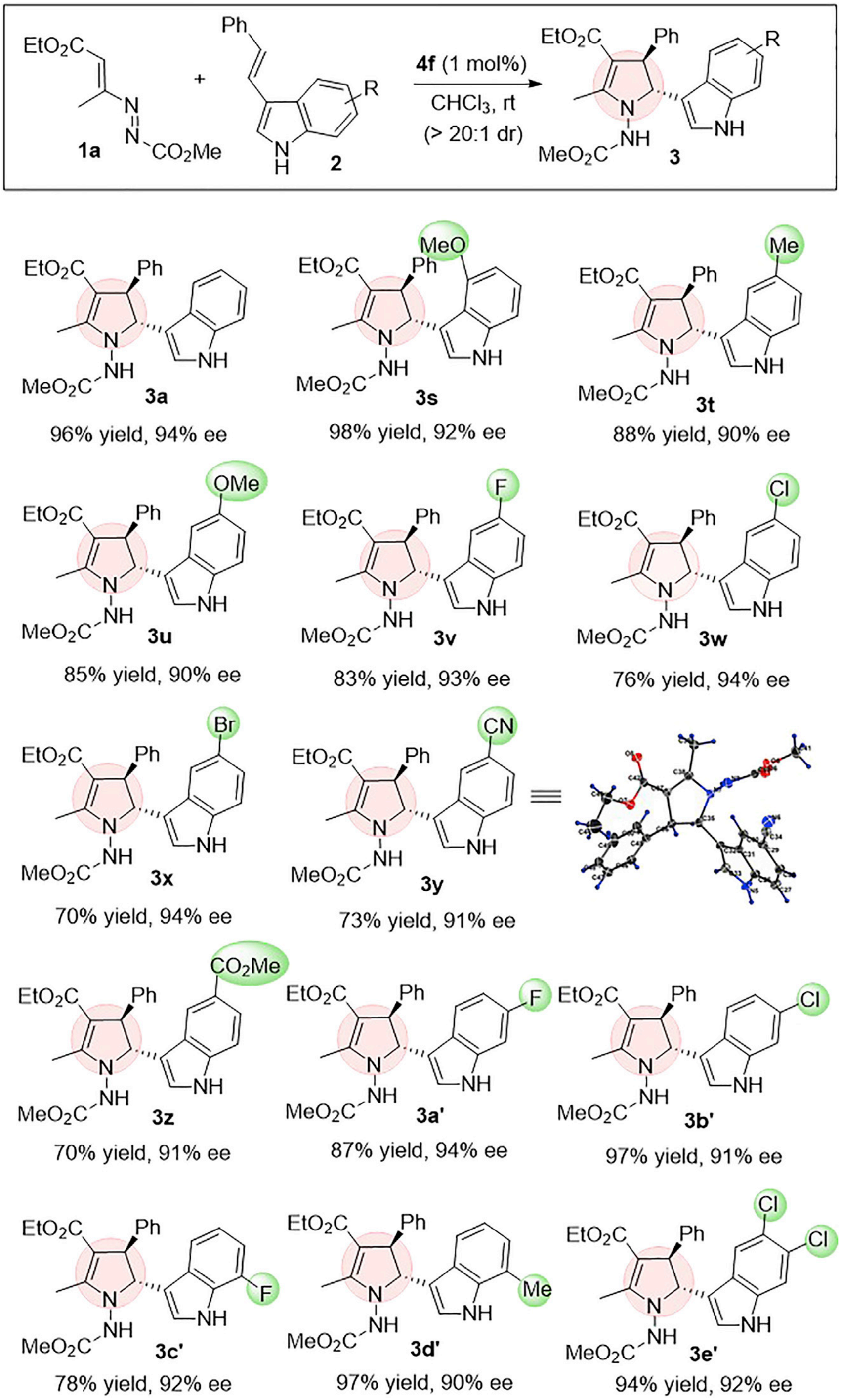

Figure 5. Further Reaction Scope of vinylindoles

Reaction conditions: **1a** (0.1 mmol), **2** (0.12 mmol), and **4f** (0.001 mmol) in $CHCl_3$ (1 mL) at room temperature for 0.5 h. Yields refer to isolated yields; the ee values were determined by HPLC analysis on a chiral stationary phase. The absolute configurations of the annulation products were assigned based on X-ray crystallographic analysis of **3y** (CCDC 1957145).

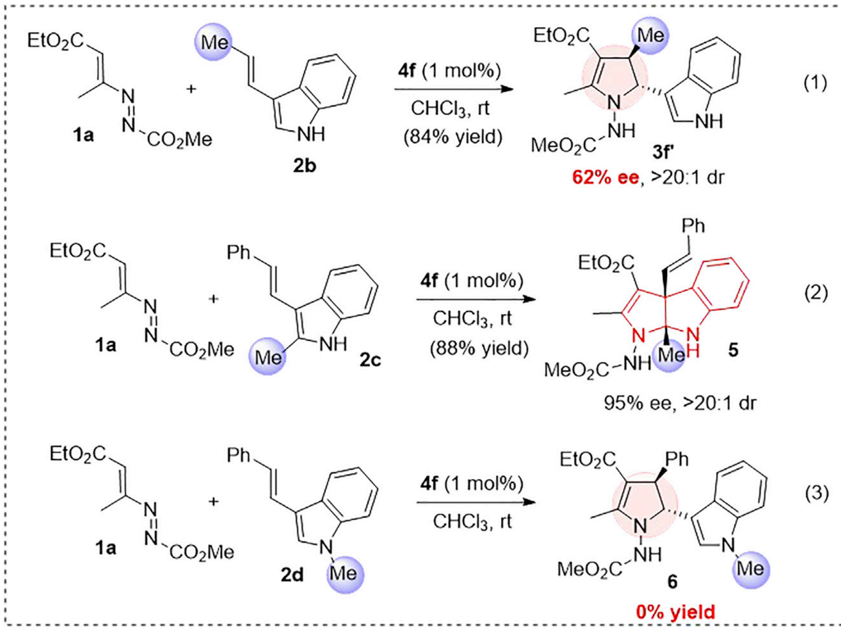

Scheme 1. Control Experiments

Limitations of the Study

A brief examination showed that the present method is not compatible with N-methyl-substituted vinylindole and 2-methyl-substituted vinylindole for the construction of corresponding 2,3-dihydropyrroles.

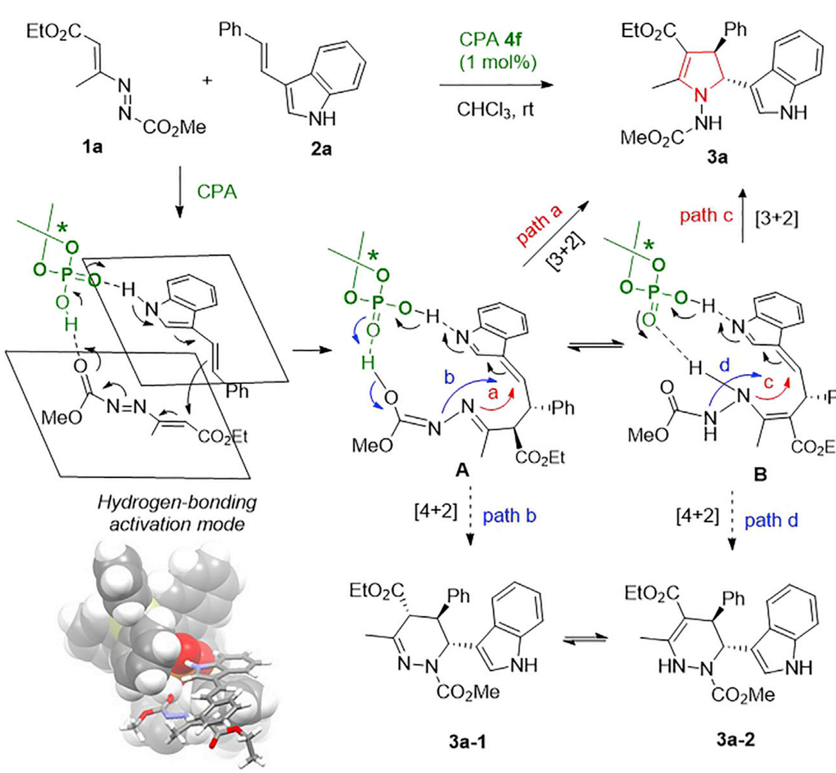

Figure 6. A Plausible Reaction Mechanism Accounting for the Selectivity

METHODS

All methods can be found in the accompanying Transparent Methods supplemental file.

SUPPLEMENTAL INFORMATION

Supplemental Information can be found online at https://doi.org/10.1016/j.isci.2020.100873.

ACKNOWLEDGMENTS

Y.L. thanks the Singapore National Research Foundation, Prime Minister's Office for the NRF Investigatorship Award (R-143-000-A15-281). Financial supports from the National University of Singapore (R-143-000-695-114 & C-141-000-092-001) and the National Natural Science Foundation of China (21672158 & 21702077) are also gratefully acknowledged.

AUTHOR CONTRIBUTIONS

Methodology, G.-J.M., W.Z., and X.T.; Investigation, G.-J.M.; Calculation, T.P.G. and K.-W.H.; Writing – Original Draft & Review & Editing, G.-J.M. and Y.L.; Conceptualization & Project Administration, G.-J.M. and Y.L.; Supervision, Y.L.

DECLARATION OF INTERESTS

The authors declare no competing interests.

Received: December 30, 2019
Revised: January 13, 2020
Accepted: January 27, 2020
Published: February 21, 2020

REFERENCES

Akiyama, T. (2007). Stronger Bronsted acids. Chem. Rev. *107*, 5744–5758.

Ashizawa, T., Ohtsuki, N., Miura, T., Ohya, M., Shinozaki, T., Ikeno, T., and Yamada, T. (2006). endo-Selective asymmetric inverse electron-demand 1,3-dipolar cycloaddition reaction of nitrones. Heterocycles *68*, 1801–1810.

Attanasi, O.A., and Filippone, P. (1997). Working twenty years on conjugated azo alkenes (and environs) to find new entries in organic synthesis. Synlett *12*, 1128–1140.

Attanasi, O.A., De Crescen-tini, L., Favi, G., Filippone, P., Mantellini, F., and Santeusanio, S. (2002a). Straightforward entry into 5-Hydroxy-1-aminopyrrolines and the corresponding pyrroles from 1,2-Diaza-1,3-butadienes. J. Org. Chem. *67*, 8178–8181.

Attanasi, O.A., De Crescentini, L., Filippone, P., Mantellini, F., and Santeusanio, S. (2002). 1,2-Diaza-1,3-butadienes: just a nice class of compounds, or powerful tools in organic chemistry? Reviewing an experience. ARKIVOC *2002*, 274–292.

Attanasi, O.A., Favi, G., Filip-pone, P., Golobič, A., Stanovnik, B., and Svete, J. (2005). Unexpected behavior of the reaction between 1,2-diaza-1,3-butadienes and 3-dimethylaminopropenoates: a useful entry to new pyrrolines, pyrroles, and oxazolines. J. Org. Chem. *70*, 4307–4431.

Attanasi, O.A., De Crescentini, L., Favi, G., Filippone, P., Mantellini, F., Perrulli, F.R., and Santeusanio, S. (2009). Cultivating the passion to build heterocycles from 1,2-Diaza-1,3-dienes: the force of imagination. Eur. J. Org. Chem. *2009*, 3109–3127.

Attanasi, O.A., De Crescentini, L., Favi, G., Mantellini, F., and Nicolini, S. (2011a). Divergent regioselective synthesis of 2,5,6,7-tetrahydro-1H-1,4-diazepin-2-ones and 5H-1,4-benzodiazepines. J. Org. Chem. *76*, 8320–8328.

Attanasi, O.A., De Crescentini, L., Favi, G., Nicolini, S., Perrulli, F.R., and Santeusanio, S. (2011b). 1,3,5-Trisubstituted and 5-acyl-1,3-disubstituted hydantoin derivatives via novel sequential three-component reaction. Org. Lett. *13*, 353–355.

Attanasi, O.A., Bartoccini, S., Favi, G., Giorgi, G., Perrulli, F.R., and Santeusanio, S. (2012). Powerful approach to heterocyclic skeletal diversity by sequential three-component reaction of amines, isothiocyanates, and 1,2-diaza-1,3-dienes. J. Org. Chem. *77*, 1161–1167.

Attanasi, O.A., Bianchi, L., Campisi, L.A., De Crescentini, L., Favi, G., and Mantellini, F. (2013a). A novel solvent-free approach to imidazole containing nitrogen-bridgehead heterocycles. Org. Lett. *15*, 3646–3649.

Attanasi, O.A., Favi, G., Geronikaki, A., Mantellini, F., Mosca-telli, G., and Paparisva, A. (2013b). Synthesis of densely functionalized 3a,4-dihydro-1H-pyrrolo[1,2-b]pyrazoles via base mediated domino reaction of vinyl malononitriles with 1,2-diaza-1,3-dienes. Org. Lett. *15*, 2624–2627.

Augeri, D.J., Robl, J.A., Betebenner, D.A., Magnin, D.R., Khanna, A., Robertson, J.G., Wang, A., Simpkins, L.M., Taunk, P., Huang, Q., et al. (2005). Discovery and preclinical profile of saxagliptin (BMS-477118): A highly potent, long-acting, orally active dipeptidyl peptidase IV inhibitor for the treatment of type 2 diabetes. J. Med. Chem. *48*, 5025–5037.

Bartlett, S.L., Sohtome, Y., Hashizume, D., White, P.S., Sawamura, M., Johnson, J.S., and Sodeoka, M. (2017). Catalytic enantioselective [3 + 2] cycloaddition of alpha-keto ester enolates and nitrile oxides. J. Am. Chem. Soc. *139*, 8661–8666.

Bayón, P., de March, P., Espinosa, M., Figueredo, M., and Font, J. (2000a). Use of chiral Ti(IV) complexes in the cycloaddition of C,N-diphenylnitrone to tert-butyl vinyl ether. Tetrahedron Asymmetry *11*, 1757–1765.

Bayón, P., de March, P., Figueredo, M., Font, J., and Medrano, J. (2000b). Use of chiral B(III) complexes in the cycloaddition of C,N-diphenylnitrone to tert-butyl vinyl ether. Tetrahedron Asymmetry *11*, 4269–4278.

Cantín, Á., Moya, P., Castillo, M.-A., Primo, J., Miranda, M.A., and Primo-Yúfera, E. (1999). Isolation and synthesis of N-(2-Methyl-3-oxodec-8-enoyl)-2-pyrroline and 2-(Hept-5-enyl)-3-methyl-4-oxo-6,7,8,8a-tetrahydro-4H-pyrrolo[2,1-b]1,3-oxazine – two new fungal metabolites with in vivo anti-Juvenile-hormone and insecticidal activity. Eur. J. Org. Chem. *1999*, 221–226.

Chan, W.L., Tang, X., Zhang, F., Quek, G., Mei, G.J., and Lu, Y. (2019). Phosphine-catalyzed (3+2) annulation of isoindigos with allenes: enantioselective formation of two vicinal quaternary stereogenic centers. Angew. Chem. Int. Ed. *58*, 6260–6264.

Chen, J.R., Dong, W.R., Candy, M., Pan, F.F., Jorres, M., and Bolm, C. (2012). Enantioselective synthesis of dihydropyrazoles by formal [4+1] cycloaddition of in situ-derived azoalkenes and sulfur ylides. J. Am. Chem. Soc. *134*, 6924–6927.

Cheng, F., Kalita, S.J., Zhao, Z.-N., Yang, X., Zhao, Y., Schneider, U., Shibata, N., and Huang, Y.-Y. (2019). Diastereodivergent asymmetric 1,3-dipolar cycloaddition of azomethine ylides and β-fluoroalkyl vinylsulfones: low copper(II) catalyst loading and theoretical studies. Angew. Chem. Int. Ed. https://doi.org/10.1002/anie.201908227.

Ciccolini, C., De Crescentini, L., Mantellini, F., Santeusanio, S., and Favi, G. (2019). Zn(II)-Catalyzed addition of aromatic/heteroaromatic C(sp(2))-H to azoalkenes: a polarity-reversed arylation of carbonyl compounds. Org. Lett. *21*, 4388–4391.

Clarke, S.J., Davies, D.E., and Gilchrist, T.L. (1983). Competing [4 + 2] and [3 + 2] cycloaddition in the reactions of nucleophilic olefins with ethyl 3-(toluene-p-sulphonylazo)but-2-enoate. J. Chem. Soc. Perkin Trans. *1*, 1803–1807.

Coldham, I., and Hufton, R. (2005). Intramolecular dipolar cycloaddition reactions of azomethine ylides. Chem. Rev. *105*, 2765–2810.

El-Sepelgy, O., Brzozowska, A., Sklyaruk, J., Jang, Y.K., Zubar, V., and Rueping, M. (2018). Cooperative metal-ligand catalyzed intramolecular hydroamination and hydroalkoxylation of allenes using a stable iron catalyst. Org. Lett. *20*, 696–699.

Fang, X., and Wang, C.J. (2018). Catalytic asymmetric construction of spiropyrrolidines via 1,3-dipolar cycloaddition of azomethine ylides. Org. Biomol. Chem. *16*, 2591–2601.

Gao, S., Chen, J.R., Hu, X.Q., Cheng, H.G., Lu, L.Q., and Xiao, W.J. (2013). Copper-catalyzed enantioselective inverse electron-demand hetero-diels–alder reactions of diazadienes with enol ethers: efficient synthesis of chiral pyridazines. Adv. Synth. Catal. *355*, 3539–3544.

Gioia, C., Hauville, A., Bernardi, L., Fini, F., and Ricci, A. (2008). Organocatalytic asymmetric diels-alder reactions of 3-vinylindoles. Angew. Chem. Int. Ed. *47*, 9236–9239.

Gothelf, K.V., and Jørgensen, K.A. (1998). Asymmetric 1,3-dipolar cycloaddition reactions. Chem. Rev. *98*, 863–910.

Guo, C., Xue, M.X., Zhu, M.K., and Gong, L.Z. (2008). Organocatalytic asymmetric formal [3+2] cycloaddition reaction of isocyanoesters to nitroolefins leading to highly optically active dihydro-pyrroles. Angew. Chem. Int. Ed. *47*, 3414–3417.

Han, X., Yao, W., Wang, T., Tan, Y.R., Yan, Z., Kwiatkowski, J., and Lu, Y. (2014). Asymmetric synthesis of spiropyrazolones through phosphine-catalyzed [4+1] annulation. Angew. Chem. Int. Ed. *53*, 5643–5647.

Han, X., Chan, W.-L., Yao, W., Wang, Y., and Lu, Y. (2016). Phosphine-mediated highly enantioselective spirocyclization with ketimines as substrates. Angew. Chem. Int. Ed. *55*, 6492–6496.

Hashimoto, T., and Maruoka, K. (2015). Recent advances of catalytic asymmetric 1,3-dipolar cycloadditions. Chem. Rev. *115*, 5366–5412.

Hashimoto, T., Omote, M., Kano, T., and Maruoka, K. (2007). Asymmetric 1,3-dipolar cycloadditions of nitrones and methacrolein catalyzed by chiral bis-titanium lewis acid: a dramatic effect of N-substituent on nitrone. Org. Lett. *9*, 4805–4808.

Hashimoto, T., Omote, M., and Maruoka, K. (2011). Asymmetric inverse-electron-demand 1,3-dipolar cycloaddition of C,N-cyclic azomethine imines: an umpolung strategy. Angew. Chem. Int. Ed. *50*, 3489–3492.

Hertel, L.W.. and Xu, Y.-C. (2002). PrepAration of pyrrolidine and pyrroline derivatives having effects on serotonin related systems. WO2000000196A1.

Herzon, S.B., and Myers, A.G. (2005). Enantioselective synthesis of stephacidin B. J. Am. Chem. Soc. *127*, 5342–5344.

Hori, K., Ito, J., Ohta, T., and Furukawa, I. (1998). Palladium(II)-catalyzed 1,3-dipolar cycloaddition of nitrones with enol ethers. Tetrahedron *54*, 12737–12744.

Huang, R., Chang, X., Li, J., and Wang, C.J. (2016). Cu(I)-Catalyzed asymmetric multicomponent cascade inverse electron-demand aza-diels-alder/nucleophilic addition/ring-opening reaction involving 2-methoxyfurans as efficient dienophiles. J. Am. Chem. Soc. *138*, 3998–4001.

Jensen, K.B., Hazell, R.G., and Jørgensen, K.A. (1999). Copper(II)-Bisoxazoline catalyzed asymmetric 1,3-dipolar cycloaddition reactions of nitrones with electron-rich alkenes. J. Org. Chem. *64*, 2353–2360.

Jensen, K.B., Roberson, M., and Jørgensen, K.A. (2000). Catalytic enantioselective 1,3-dipolar cycloaddition reactions of cyclic nitrones: a simple approach for the formation of optically active isoquinoline derivatives. J. Org. Chem. *65*, 9080–9084.

Jiang, B., Meng, F.F., Liang, Q.J., Xu, Y.H., and Loh, T.P. (2017). Palladium-catalyzed direct intramolecular C-N bond formation: access to multisubstituted dihydropyrroles. Org. Lett. *19*, 914–917.

Jiao, P., Nakashima, D., and Yamamoto, H. (2008). Enantioselective 1,3-dipolar cycloaddition of nitrones with ethyl vinyl ether: the difference between Bronsted and Lewis acid catalysis. Angew. Chem. Int. Ed. *47*, 2411–2413.

Kano, T., Hashimoto, T., and Maruoka, K. (2005). Asymmetric 1,3-dipolar cycloaddition reaction of nitrones and acrolein with a bis-titanium catalyst as chiral lewis acid. J. Am. Chem. Soc. *127*, 11926–11927.

Karapetyan, V., Mkrtchyan, S., Schmidt, A., Attanasi, O.A., Favi, G., Mantellini, F., Villinger, A., Fischer, C., and Langer, P. (2008). .Diversity-oriented synthesis of functionalized 1-aminopyrroles by regioselective zinc chloride-catalyzed, one-pot 'conjugate addition/cyclization' reactions of 1,3-Bis(silyl enol ethers) with 1,2-Diaza-1,3-butadienes. Adv. Synth. Catal. *350*, 1331–1336.

Kawase, M., Sakagami, H., Kusama, K., Motohashi, N., and Saito, S. (1999). α-Trifluoromethylated acyloins induce apoptosis in human oral tumor cell lines. Bioorg. Med. Chem. Lett. *9*, 3113–3118.

Kissane, M., and Maguire, A.R. (2010). Asymmetric 1,3-dipolar cycloadditions of acrylamides. Chem. Soc. Rev. *39*, 845–883.

Kwok, S.W., Zhang, L., Grimster, N.P., and Fokin, V.V. (2014). Catalytic asymmetric transannulation of NH-1,2,3-triazoles with olefins. Angew. Chem. Int. Ed. *53*, 3452–3456.

Li, C., Xu, D.-N., Ma, C., Mei, G.-J., and Shi, F. (2018). Diastereo- and enantioselective construction of dihydrobenzo[e]indole scaffolds via catalytic asymmetric [3 + 2] cycloannulations. J. Org. Chem. *83*, 9190–9200.

Li, K., Goncalves, T.P., Huang, K.W., and Lu, Y. (2019). Dearomatization of 3-nitroindoles by a phosphine-catalyzed enantioselective [3+2] annulation reaction. Angew. Chem. Int. Ed. *58*, 5427–5431.

Liang, H., Yan, F., Dong, X., Liu, Q., Wei, X., Liu, S., Dong, Y., and Liu, H. (2017). Palladium-catalyzed cascade metallo-ene/Suzuki coupling reaction of allenamides. Chem. Commun. *53*, 3138–3141.

Liang, H., Meng, L., Chi, X., Yao, S., Chen, H., Jiao, L., Liu, Q., Zhang, D., Liu, H., and Dong, Y. (2018). Palladium/copper Co-catalyzed cascade metallo-ene/sonogashira coupling reaction of allenamides. Asian J. Org. Chem. *7*, 1793–1796.

Liu, W.-J., Chen, X.-H., and Gong, L.-Z. (2008). Direct assembly of aldehydes, amino esters, and anilines into chiral imidazolidines via Bronsted acid catalyzed asymmetric 1,3-dipolar cycloadditions. Org. Lett. *10*, 5357–5360.

Liu, X., Wang, Y., Yang, D., Zhang, J., Liu, D., and Su, W. (2016). Catalytic asymmetric inverse-electron-demand 1,3-dipolar cycloaddition of C,N-cyclic azomethine imines with azlactones: access to chiral tricyclic tetrahydroisoquinolines. Angew. Chem. Int. Ed. *55*, 8100–8103.

Lopes, S.M.M., Cardoso, A.L., Lemos, A., and Pinho e Melo, T.M.V.D. (2018). Recent advances in the chemistry of conjugated nitrosoalkenes and azoalkenes. Chem. Rev. *118*, 11324–11352.

Ma, X., Liu, L., Wang, J., Xi, X., Xie, X., and Wang, H. (2018). Rhodium-catalyzed annulation of alpha-imino carbenes with alpha,beta-unsaturated ketones: construction of multisubstituted 2,3-dihydropyrrole/pyrrole rings. J. Org. Chem. *83*, 14518–14526.

Mantenuto, S., Mantellini, F., Favi, G., and Attanasi, O.A. (2015). Divergent construction of pyrazoles via Michael addition of N-arylhydrazones to 1,2-diaza-1,3-dienes. Org. Lett. *17*, 2014–2017.

Mari, G., Crescentini, L.D., Favi, G., Lombardi, P., Fiorillo, G., Giorgi, G., and Mantellini, F. (2017). Heteroring-annulated pyrrolino-tetrahydroberberine analogues. Asian J. Org. Chem. *6*, 720–727.

Marti, C., and Carreira, E.M. (2005). Total synthesis of (−)-Spirotryprostatin B: synthesis and related studies. J. Am. Chem. Soc. *127*, 11505–11515.

Mei, G.J., Tang, X., Tasdan, Y., and Lu, Y. (2020). Enantioselective dearomatization of indoles by an azoalkene-enabled (3+2) reaction: access to pyrroloindolines. Angew. Chem. Int. Ed. *59*, 648–652.

Mikami, K., Ueki, M., Matsumoto, Y., and Terada, M. (2001). Tetranuclear titanium 7,7′-modified binaphtholate cluster as a novel chiral Lewis acid catalyst. Chirality *13*, 541–544.

Miles, D.H., Guasch, J., and Toste, F.D. (2015). A nucleophilic strategy for enantioselective intermolecular alpha-amination: access to enantioenriched alpha-arylamino ketones. J. Am. Chem. Soc. *137*, 7632–7635.

Miura, T., Tanaka, T., Hiraga, K., Stewart, S.G., and Murakami, M. (2013). Stereoselective synthesis of 2,3-dihydropyrroles from terminal alkynes, azides, and alpha,beta-unsaturated aldehydes via N-sulfonyl-1,2,3-triazoles. J. Am. Chem. Soc. *135*, 13652–13655.

Ni, H., Tang, X., Zheng, W., Yao, W., Ullah, N., and Lu, Y. (2017). Enantioselective phosphine-catalyzed formal [4+4] annulation of α,β-unsaturated imines and allene ketones: construction of eight-membered rings. Angew. Chem. Int. Ed. *56*, 14222–14226.

Pascual-Escudero, A., de Cozar, A., Cossio, F.P., Adrio, J., and Carretero, J.C. (2016). Alkenyl arenes as dipolarophiles in catalytic asymmetric 1,3-dipolar cycloaddition reactions of azomethine ylides. Angew. Chem. Int. Ed. *55*, 15334–15338.

Petersen, M.T., and Nielsen, T.E. (2013). Tandem ring-closing metathesis/isomerization reactions for the total synthesis of violacein. Org. Lett. *15*, 1986–1989.

Preti, L., Attanasi, O.A., Caselli, E., Favi, G., Ori, C., Davoli, P., Felluga, F., and Prati, F. (2010). One-Pot synthesis of imidazole-4-carboxylates by microwave-assisted 1,5-electrocyclization of azavinyl azomethine ylides. Eur. J. Org. Chem. *2010*, 4312–4320.

Ran, G.Y., Gong, M., Yue, J.F., Yang, X.X., Zhou, S.L., Du, W., and Chen, Y.C. (2017). Asymmetric cascade assembly of 1,2-Diaza-1,3-dienes and alpha,beta-unsaturated aldehydes via dienamine activation. Org. Lett. *19*, 1874–1877.

Seerden, J.-P.G., Schotte op Reimer, A.W.A., and Scheeren, H.W. (1994). Asymmetric 13-dipolar cycloaddition of nitrones with ketene acetals catalyzed by chiral oxazaborolidines. Tetrahedron Lett. *35*, 4419–4422.

Seerden, J.-P.G., Kuypers, M.M.M., and Scheeren, H.W. (1995). Dramatic solvents effects on the enantioselectivity of chiral oxazaborolidine catalyzed asymmetric 1,3-dipolar cycloadditions of nitrones with ketene acetals. Tetrahedron Asymmetry *6*, 1441–1450.

Seerden, J.-P.G., Boeren, M.M.M., and Scheeren, H.W. (1997). 1,3-Dipolar cycloaddition reactions of nitrones with alkyl vinyl ethers catalyzed by chiral oxazaborolidines. Tetrahedron *53*, 11843–11852.

Sibi, M.P., Ma, Z., and Jasperse, C.P. (2004). Exo selective enantioselective nitrone cycloadditions. J. Am. Chem. Soc. *126*, 718–719.

Simonsen, K.B., Anker Jørgensen, K., Hu, Q.-S., and Pu, L. (1999a). The first highly diastereo- and enantioselective polymeric catalyst for the 1,3-cycloaddition reaction of nitrones with alkenes. Chem. Commun. 811–812.

Simonsen, K.B., Bayón, P., Hazell, R.G., Gothelf, K.V., and Jørgensen, K.A. (1999b). Catalytic enantioselective inverse-electron demand 1,3-dipolar cycloaddition reactions of nitrones with alkenes. J. Am. Chem. Soc. *121*, 3845–3853.

Sohtome, Y., Nakamura, G., Muranaka, A., Hashizume, D., Lectard, S., Tsuchimoto, T., Uchiyama, M., and Sodeoka, M. (2017). Naked d-orbital in a centrochiral Ni(II) complex as a catalyst for asymmetric [3+2] cycloaddition. Nat. Commun. *8*, 14875.

Sommer, S. (1979). Reactions with azo compounds. 6. [3 + 2]-Cycloadditions of azoalkenes to enamines - "criss-cross" cycloadditions to azoalkenes. Angew. Chem. *91*, 756–757.

Stanley, L.M., and Sibi, M.P. (2008). Enantioselective copper-catalyzed 1,3-dipolar cycloadditions. Chem. Rev. *108*, 2887–2902.

Suga, H., Ishimoto, D., Higuchi, S., Ohtsuka, M., Arikawa, T., Tsuchida, T., Kakehi, A., and Baba, T. (2007). Dipole-LUMO/Dipolarophile-HOMO controlled asymmetric cycloadditions of carbonyl ylides catalyzed by chiral lewis acids. Org. Lett. *9*, 4359–4362.

Suga, H., Higuchi, S., Ohtsuka, M., Ishimoto, D., Arikawa, T., Hashimoto, Y., Misawa, S., Tsuchida, T., Kakehi, A., and Baba, T. (2010). Inverse electron demand asymmetric cycloadditions of cyclic carbonyl ylides catalyzed by chiral Lewis acids—scope and limitations of diazo and olefinic substrates. Tetrahedron *66*, 3070–3089.

Sun, X.-X., Zhang, H.-H., Li, G.-H., Meng, L., and Shi, F. (2016). Diastereo- and enantioselective construction of an indole-based 2,3-dihydrobenzofuran scaffold via catalytic asymmetric [3+2] cyclizations of quinone monoimides with 3-vinylindoles. Chem. Commun. *52*, 2968–2971.

Tan, B., Hernandez-Torres, G., and Barbas, C.F. (2011). Highly efficient hydrogen-bonding catalysis of the Diels-Alder reaction of 3-vinylindoles and methyleneindolinones provides carbazolespirooxindole skeletons. J. Am. Chem. Soc. *133*, 12354–12357.

Terada, M. (2008). Binaphthol-derived phosphoric acid as a versatile catalyst for enantioselective carbon-carbon bond forming reactions. Chem. Commun. 4097–4112.

Terada, M. (2010). Chiral phosphoric acids as versatile catalysts for enantioselective transformations. Synthesis *2010*, 1929–1982.

Tong, M.-C., Chen, X., Tao, H.-Y., and Wang, C.-J. (2013). Catalytic asymmetric 1,3-dipolar cycloaddition of two different ylides: facile access to chiral 1,2,4-triazinane frameworks. Angew. Chem. Int. Ed. *52*, 12377–12380.

Tong, M.C., Chen, X., Li, J., Huang, R., Tao, H., and Wang, C.J. (2014). Catalytic asymmetric synthesis of [2,3]-fused indoline heterocycles through inverse-electron-demand aza-Diels-Alder reaction of indoles with azoalkenes. Angew. Chem. Int. Ed. *53*, 4680–4684.

Wang, C.-S., Zhu, R.-Y., Zheng, J., Shi, F., and Tu, S.-J. (2015). Enantioselective construction of spiro [indoline-3,2′-pyrrole] framework via catalytic asymmetric 1,3-dipolar cycloadditions using allenes as equivalents of alkynes. J. Org. Chem. *80*, 512–520.

Wei, L., and Wang, C.J. (2015). The catalytic asymmetric synthesis of tetrahydropyridazines via inverse electron-demand aza-Diels-Alder reaction of enol ethers with azoalkenes. Chem. Commun. *51*, 15374–15377.

Wei, L., Zhou, Y., Song, Z.M., Tao, H.Y., Lin, Z., and Wang, C.J. (2017). Copper(I)-Catalyzed asymmetric desymmetrization through inverse-electron-demand aza-diels-alder reaction: efficient access to tetrahydropyridazines bearing a unique alpha-chiral silane moiety. Chem. Eur. J. *23*, 4995–4999.

Wei, L., Zhu, Q., Song, Z.M., Liu, K., and Wang, C.J. (2018). Catalytic asymmetric inverse electron demand Diels-Alder reaction of fulvenes with azoalkenes. Chem. Commun. *54*, 2506–2509.

Wei, L., Shen, C., Hu, Y.Z., Tao, H.Y., and Wang, C.J. (2019). Enantioselective synthesis of multi-nitrogen-containing heterocycles using azoalkenes as key intermediates. Chem. Commun. *55*, 6672–6684.

Wu, H., He, Y.P., and Shi, F. (2015). Recent advances in chiral phosphoric acid catalyzed asymmetric reactions for the synthesis of enantiopure indole derivatives. Synthesis *47*, 1990–2016.

Wu, M., Han, Z., Li, K., Wu, J., Ding, K., and Lu, Y. (2019). Cyclohexyl-fused, spirobiindane-derived, phosphine-catalyzed synthesis of tricyclic gamma-lactams and kinetic resolution of gamma-substituted allenoates. J. Am. Chem. Soc. *141*, 16362–16373.

Xu, Y., Liao, Y., Lin, L., Zhou, Y., Li, J., Liu, X., and Feng, X. (2015). Catalytic asymmetric inverse-electron demand 1,3-dipolar cycloaddition of isoquinolinium methylides with enecarbamates by a chiral N,N′-Dioxide/Ag(I) complex. ACS Catal. *6*, 589–592.

Xu, S., Zhang, Z.-M., Xu, B., Liu, B., Liu, Y., and Zhang, J. (2018). Enantioselective regiodivergent synthesis of chiral pyrrolidines with two quaternary stereocenters via ligand-controlled copper(I)-catalyzed asymmetric 1,3-dipolar cycloadditions. J. Am. Chem. Soc. *140*, 2272–2283.

Yanagisawa, A., Izumiseki, A., Sugita, T., Kushihara, N., and Yoshida, K. (2011). Catalytic asymmetric cycloaddition reaction of alkenyl trichloroacetates with nitrones. Synlett *2012*, 107–112.

Yang, X., Cheng, F., Kou, Y.-D., Pang, S., Shen, Y.-C., Huang, Y.-Y., and Shibata, N. (2017). Catalytic asymmetric 1,3-dipolar cycloaddition of β-fluoroalkylated α,β-unsaturated 2-pyridylsulfones with nitrones for chiral fluoroalkylated isoxazolidines and γ-amino alcohols. Angew. Chem. Int. Ed. *56*, 1510–1514.

Yang, X., Zhou, Y.-H., Yang, H., Wang, S.-S., Ouyang, Q., Luo, Q.-L., and Guo, Q.-X. (2019). Asymmetric Diels-Alder reaction of 3-vinylindoles and nitroolefins promoted by multiple hydrogen bonds. Org. Lett. *21*, 1161–1164.

Yao, W., Dou, X., Wen, S., Wu, J., Vittal, J.J., and Lu, Y. (2016). Enantioselective desymmetrization of cyclohexadienones via an intramolecular Rauhut-Currier reaction of allenoates. Nat. Commun. *7*, 13024.

Yu, J., Shi, F., and Gong, L.Z. (2011). Bronsted-acid-catalyzed asymmetric multicomponent reactions for the facile synthesis of highly enantioenriched structurally diverse nitrogenous heterocycles. Acc. Chem. Res. *44*, 1156–1171.

Zhang, Z.-J., and Song, J. (2018). An isothiourea-catalyzed asymmetric formal [4 + 2] cycloaddition of in situ generated azoalkenes with C1 ammonium enolates. Org. Chem. Front. *5*, 2578–2582.

Zhang, L.-L., Zhang, J.-W., Xiang, S.-H., Guo, Z., and Tan, B. (2018). Remote control of axial chirality: synthesis of spirooxindole-urazoles via desymmetrization of ATAD. Org. Lett. *20*, 6022–6026.

Zheng, H., Liu, X., Xu, C., Xia, Y., Lin, L., and Feng, X. (2015). Regio- and enantioselective aza-Diels-Alder reactions of 3-vinylindoles: a concise synthesis of the antimalarial spiroindolone NITD609. Angew. Chem. Int. Ed. *54*, 10958–10962.

Zhu, Y., Zhai, C., Yue, Y., Yang, L., and Hu, W. (2009). One-pot three-component tandem reaction of diazo compounds with anilines and unsaturated ketoesters: a novel synthesis of 2,3-dihydropyrrole derivatives. Chem. Commun. 1362–1364.

Zhu, Y., Zhai, C., Yang, L., and Hu, W. (2011). Highly regioselective, three-component reactions of diazoacetates with anilines and β,γ-unsaturated α-keto esters: 1,2-addition versus 1,4-addition. Eur. J. Org. Chem. *2011*, 1113–1124.

Zhu, R.Y., Wang, C.S., Zheng, J., Shi, F., and Tu, S.J. (2014). Organocatalytic asymmetric inverse-electron-demand 1,3-dipolar cycloaddition of N,N′-cyclic azomethine imines. J. Org. Chem. *79*, 9305–9312.

iScience, Volume *23*

Supplemental Information

Catalytic Asymmetric Formal

[3+2] Cycloaddition of Azoalkenes

with 3-Vinylindoles: Synthesis of 2,3-Dihydropyrroles

Guang-Jian Mei, Wenrui Zheng, Théo P. Gonçalves, Xiwen Tang, Kuo-Wei Huang, and Yixin Lu

Data S1. Spectra of Products: Related to Table 2, Figures 4,5 and Scheme 1

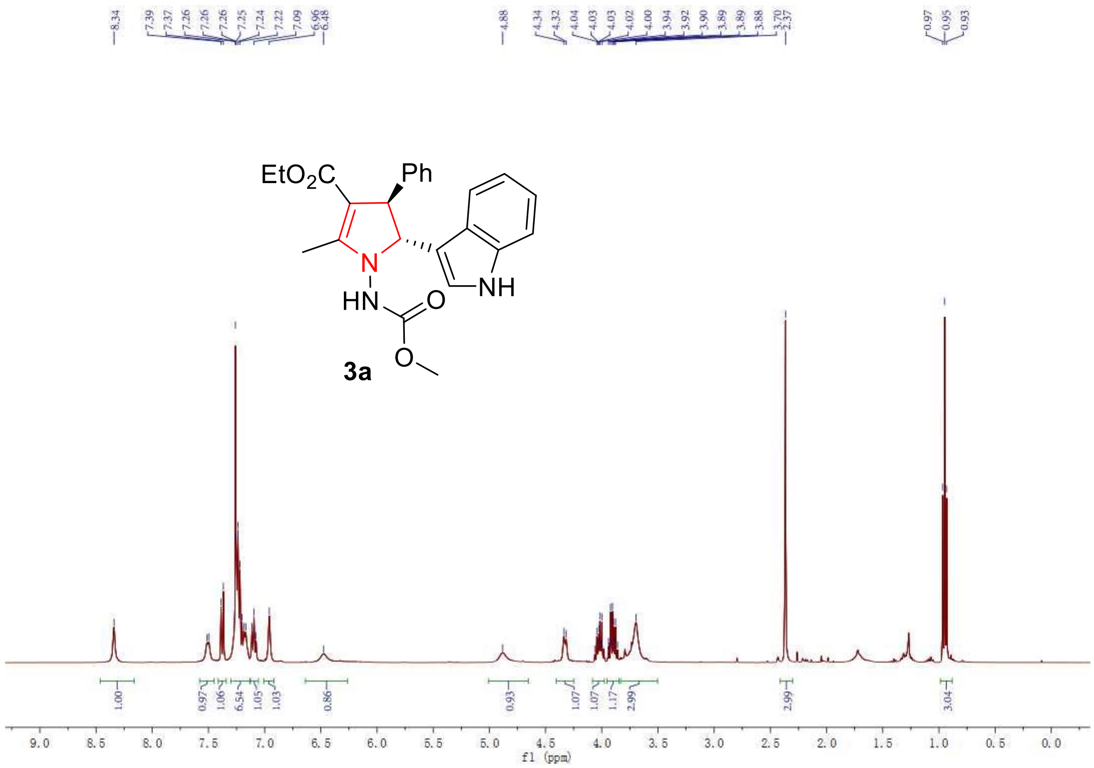

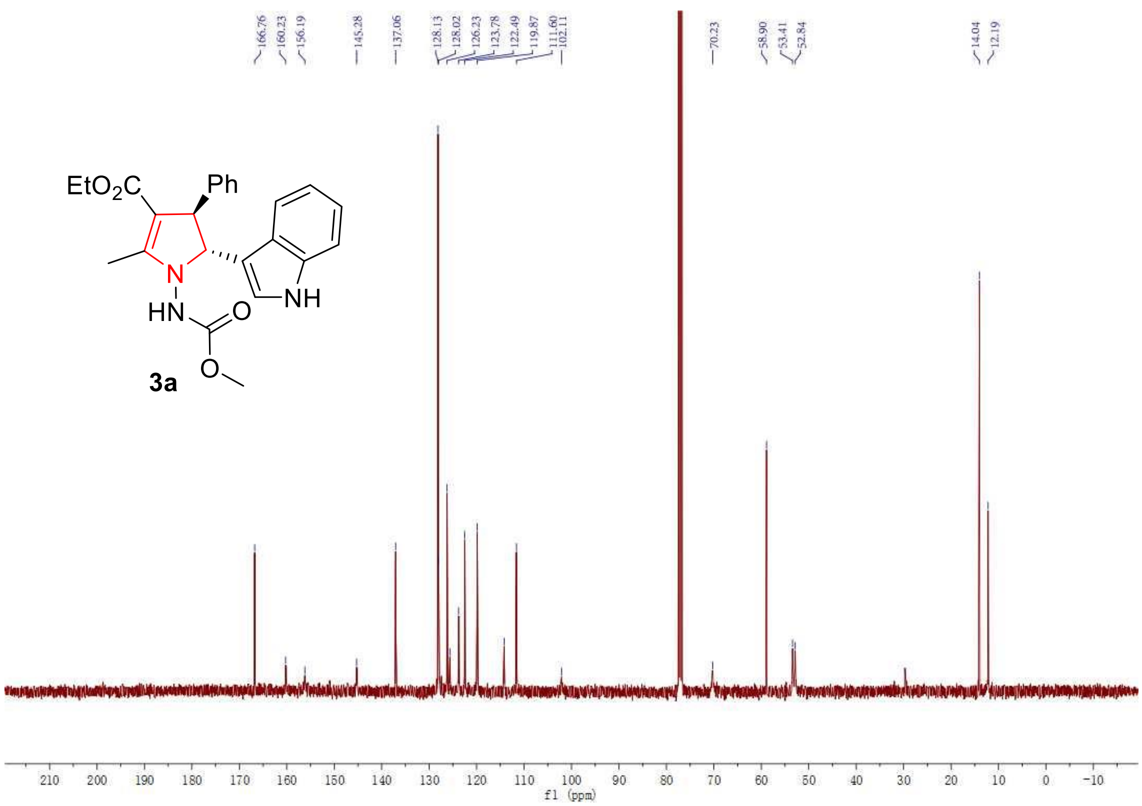

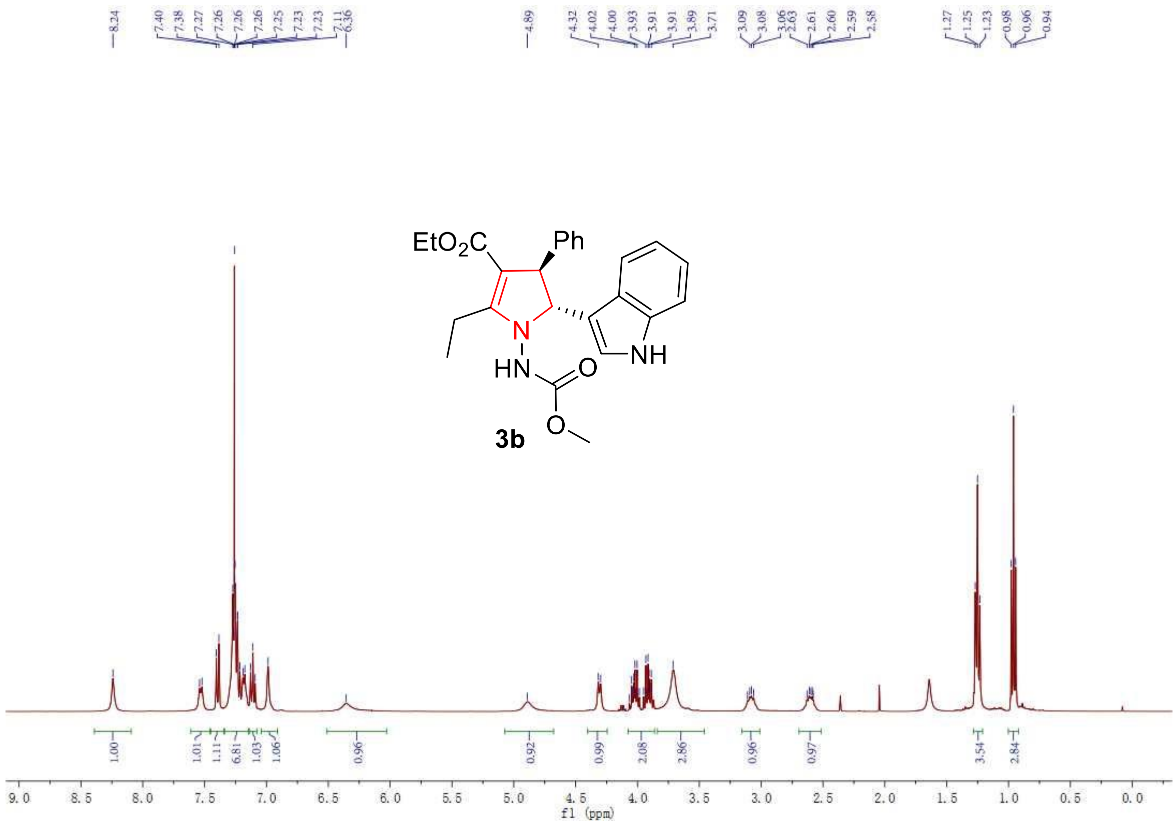
8.24
7.40
7.38
7.27
7.26
7.26
7.26
7.25
7.23
7.23
7.11
6.36
4.89
4.32
4.02
4.00
3.93
3.91
3.91
3.89
3.71
3.09
3.08
3.06
2.63
2.61
2.60
2.59
2.58
1.27
1.25
1.23
0.98
0.96
0.94
EtO2C
Ph
N
HN
O
O
NH
3b
1.00
1.01
1.11
6.81
1.03
1.06
0.96
0.92
0.99
2.08
2.86
0.96
0.97
3.54
2.84
9.0 8.5 8.0 7.5 7.0 6.5 6.0 5.5 5.0 4.5 4.0 3.5 3.0 2.5 2.0 1.5 1.0 0.5 0.0
f1 (ppm)

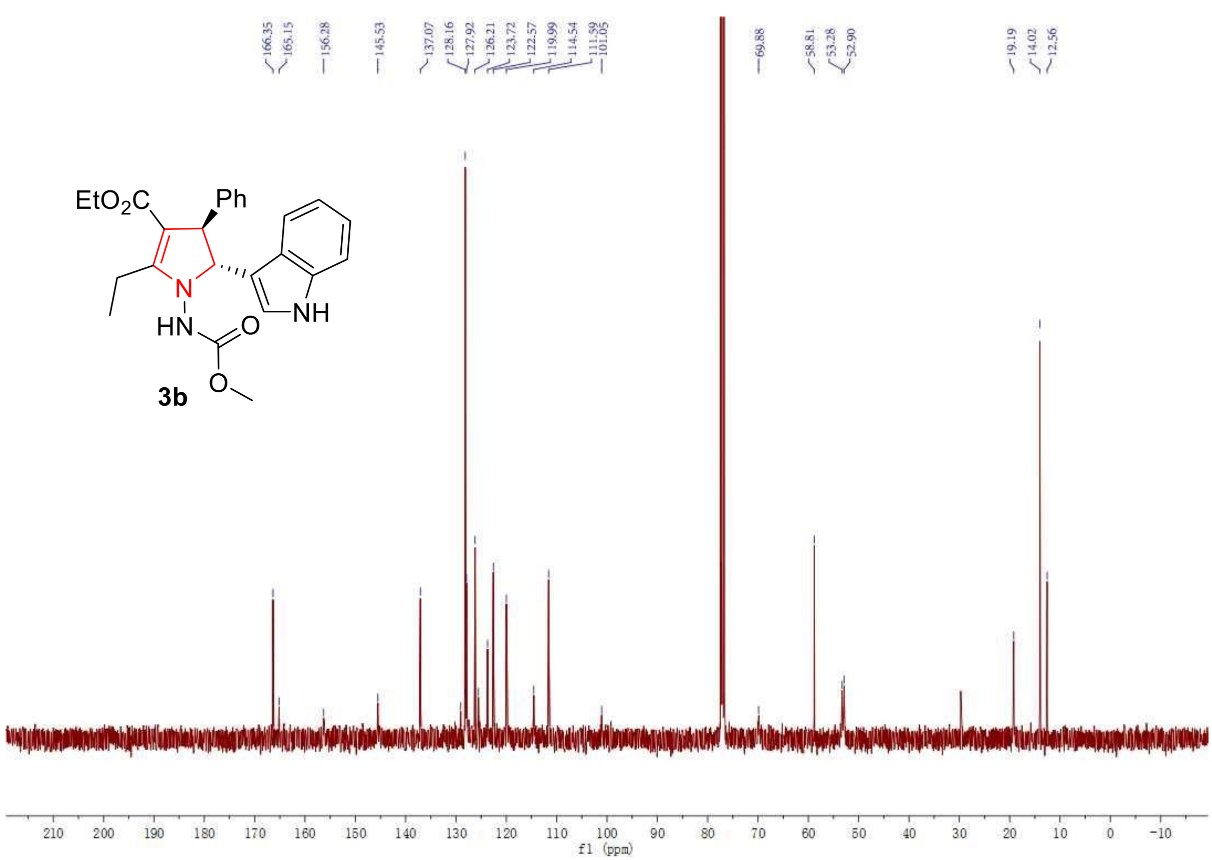
166.35
165.15
156.28
145.53
137.07
128.16
127.92
126.21
123.72
122.57
119.99
114.54
111.59
101.05
69.88
58.81
53.28
52.90
19.19
14.02
12.56
EtO2C
Ph
N
HN
O
O
NH
3b
210 200 190 180 170 160 150 140 130 120 110 100 90 80 70 60 50 40 30 20 10 0 -10
f1 (ppm)

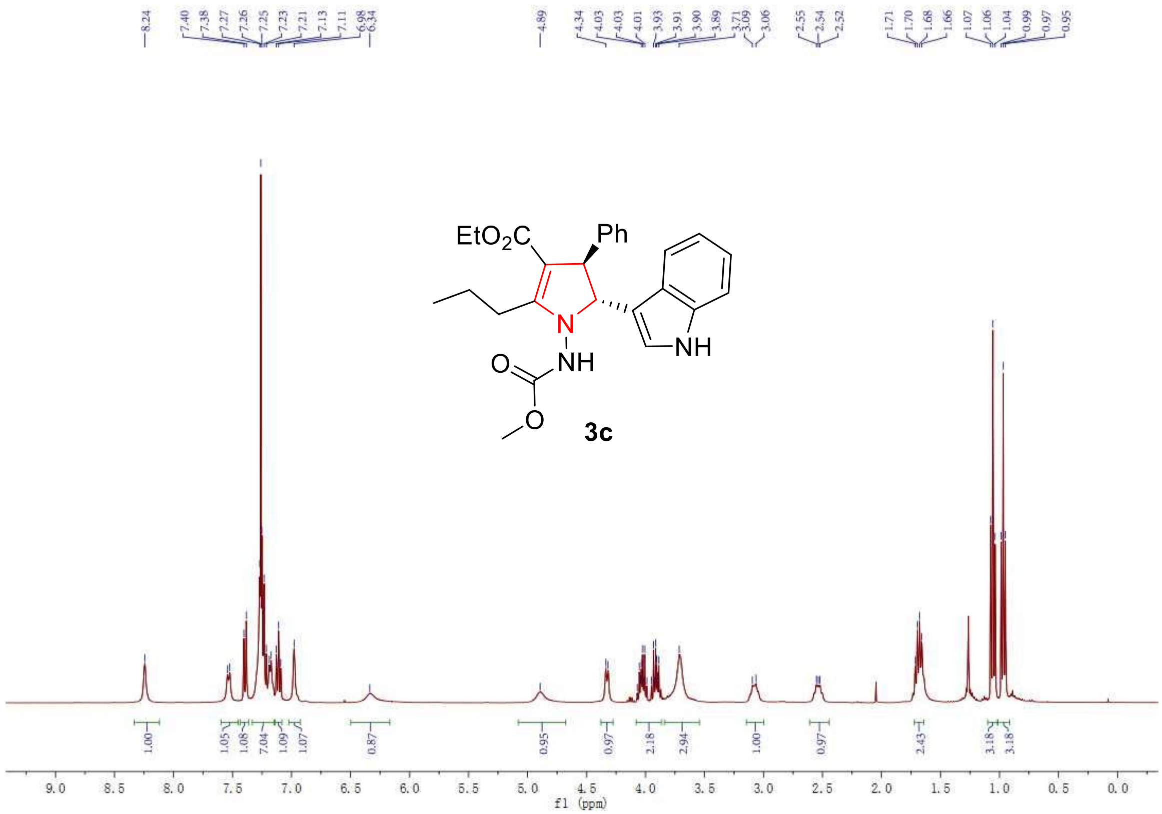
8.24
7.40 7.38 7.27 7.26 7.25 7.23 7.21 7.13 7.11 6.98 6.34
4.89
4.34 4.03 4.03 4.01 3.93 3.91 3.90 3.89 3.71 3.09 3.06
2.55 2.54 2.52
1.71 1.70 1.68 1.66 1.07 1.06 1.04 0.99 0.97 0.95
EtO2C
Ph
N
NH
NH
O
O
3c
1.00 1.05 1.08 7.04 1.09 1.07 0.87 0.95 0.97 2.18 2.94 1.00 0.97 2.43 3.18 3.18
9.0 8.5 8.0 7.5 7.0 6.5 6.0 5.5 5.0 4.5 4.0 3.5 3.0 2.5 2.0 1.5 1.0 0.5 0.0
f1 (ppm)

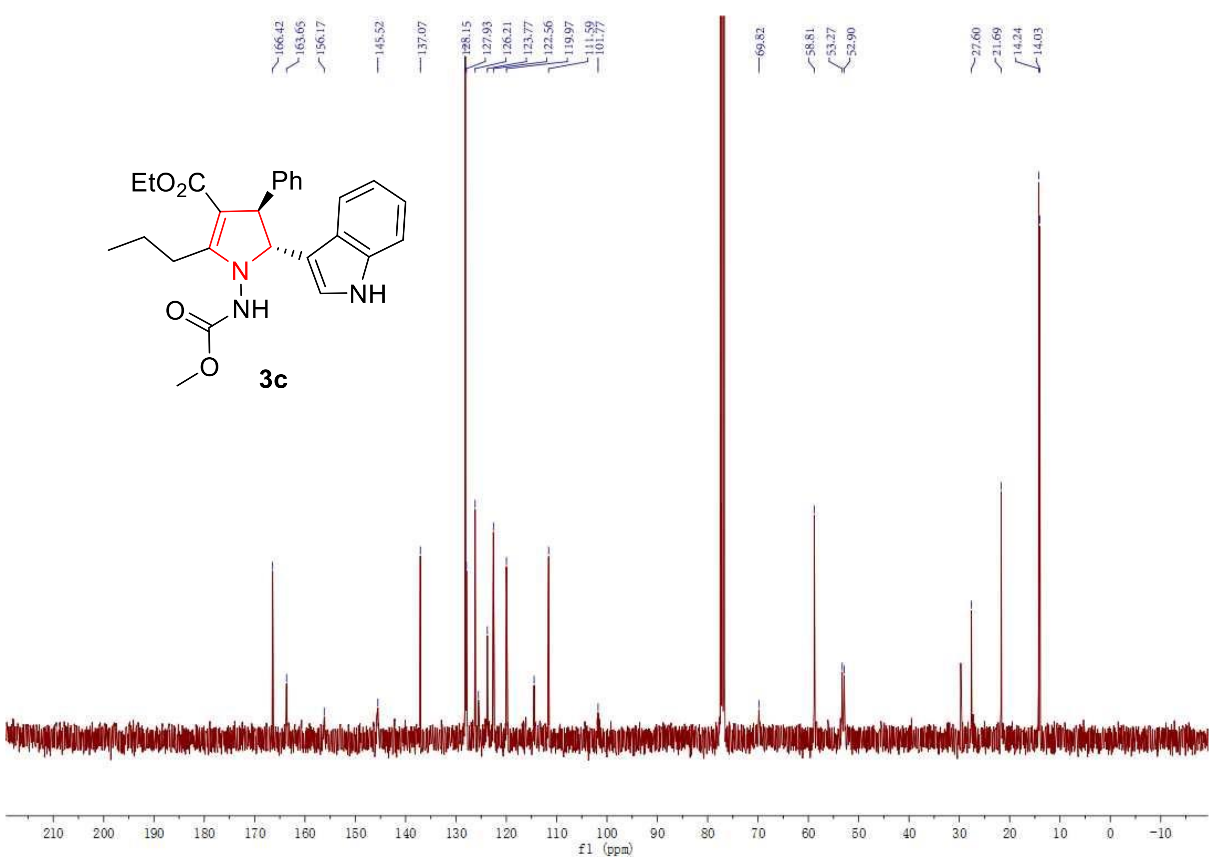
166.42 163.65 156.17 145.52 137.07 128.15 127.93 126.21 123.77 122.56 119.97 111.59 101.77
69.82 58.81 53.27 52.90 27.60 21.69 14.24 14.03
EtO2C
Ph
N
NH
NH
O
O
3c
210 200 190 180 170 160 150 140 130 120 110 100 90 80 70 60 50 40 30 20 10 0 -10
f1 (ppm)

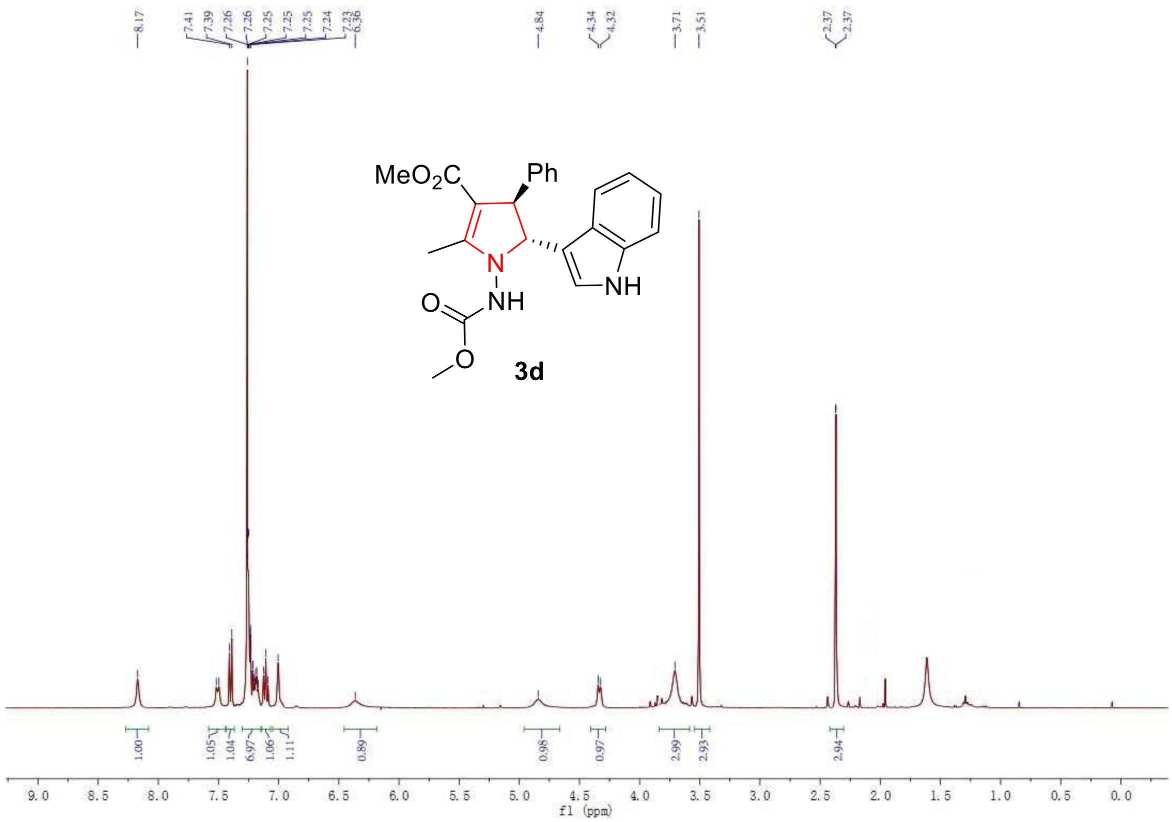
8.17
7.41
7.39
7.26
7.26
7.25
7.25
7.25
7.24
7.23
6.36
4.84
4.34
4.32
3.71
3.51
2.37
2.37
MeO2C
Ph
N
NH
NH
O
O
3d
1.00
1.05
1.04
6.97
1.06
1.11
0.89
0.98
0.97
2.99
2.93
2.94
9.0 8.5 8.0 7.5 7.0 6.5 6.0 5.5 5.0 4.5 4.0 3.5 3.0 2.5 2.0 1.5 1.0 0.5 0.0
f1 (ppm)

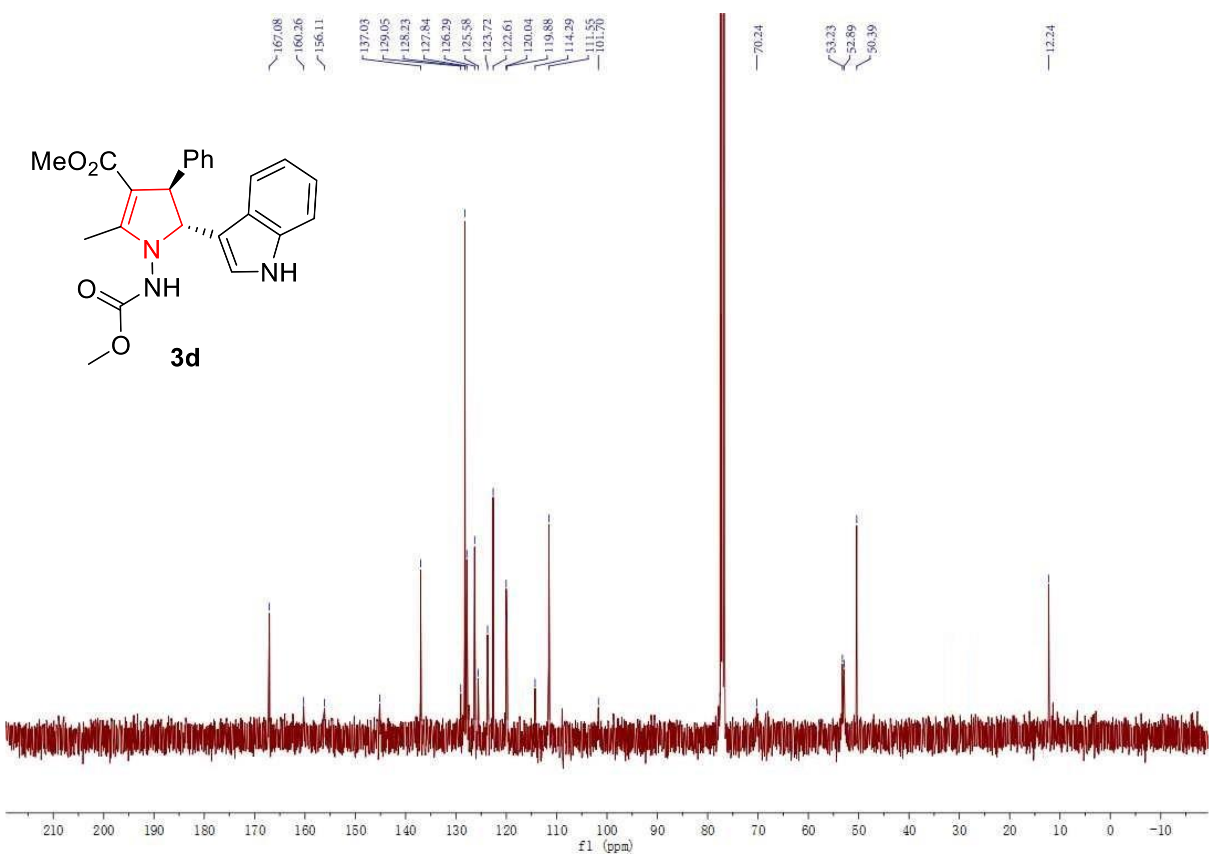
167.08
160.26
156.11
137.03
129.05
128.23
127.84
126.29
125.58
123.72
122.61
120.04
119.88
114.29
111.55
101.70
70.24
53.23
52.89
50.39
12.24
MeO2C
Ph
N
NH
NH
O
O
3d
210 200 190 180 170 160 150 140 130 120 110 100 90 80 70 60 50 40 30 20 10 0 -10
f1 (ppm)

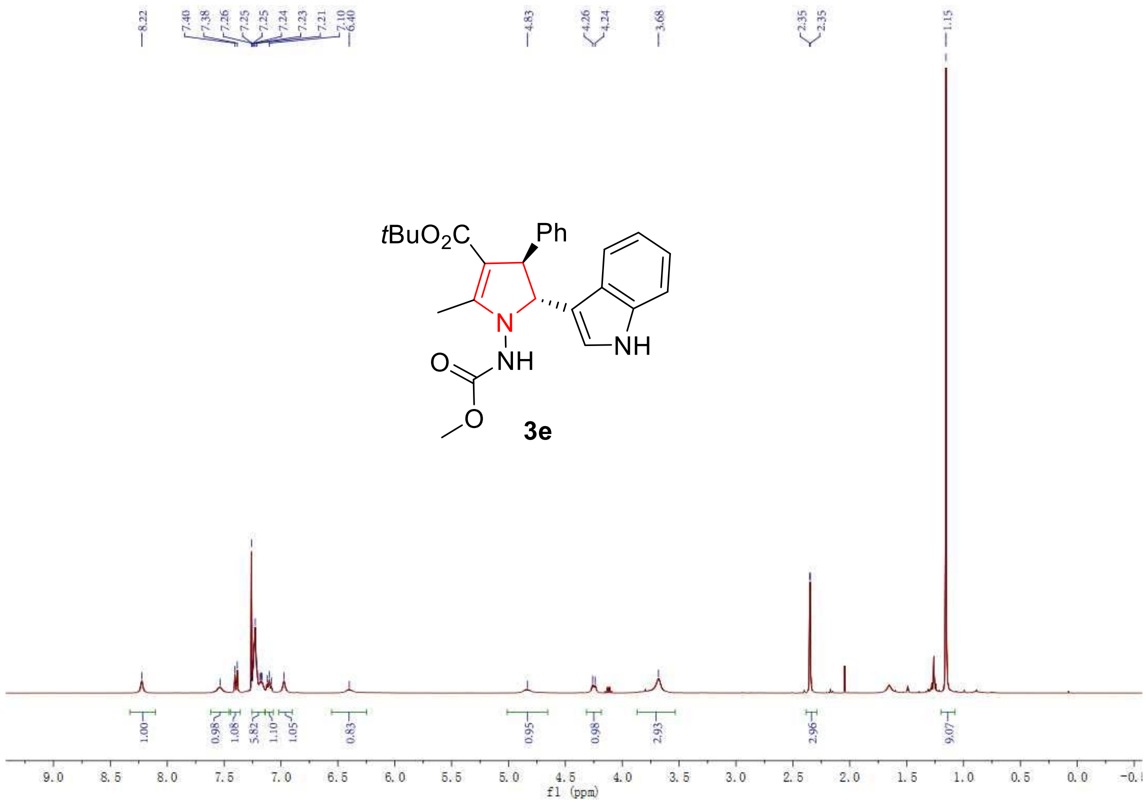
8.22
7.40
7.38
7.26
7.25
7.25
7.24
7.23
7.21
7.10
6.40
4.83
4.26
4.24
3.68
2.35
2.35
1.15
tBuO2C
Ph
N
NH
O
NH
O
3e
1.00
0.98
1.08
5.82
1.10
1.05
0.83
0.95
0.98
2.93
2.96
9.07
f1 (ppm)

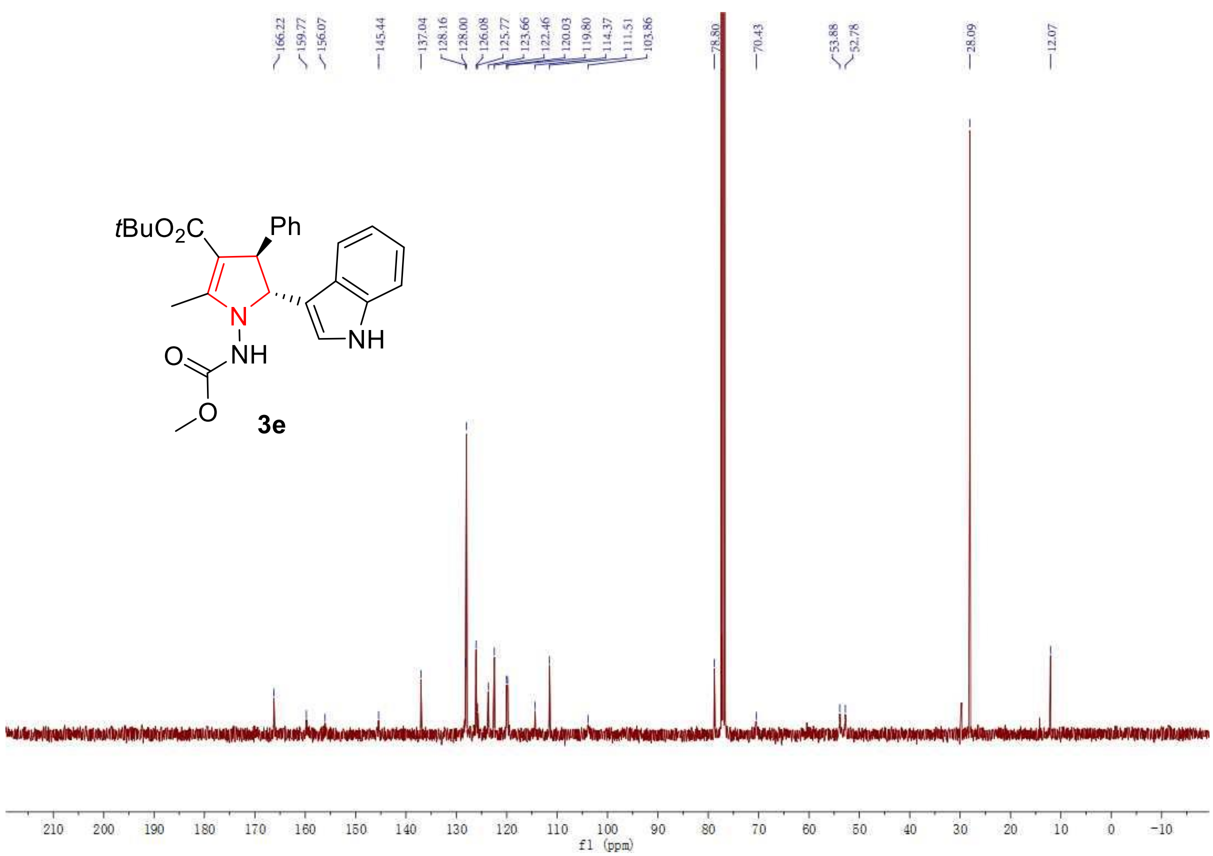
166.22
159.77
156.07
145.44
137.04
128.16
128.00
126.08
125.77
123.66
122.46
120.03
119.80
114.37
111.51
103.86
78.80
70.43
53.88
52.78
28.09
12.07
tBuO2C
Ph
N
NH
O
NH
O
3e
f1 (ppm)

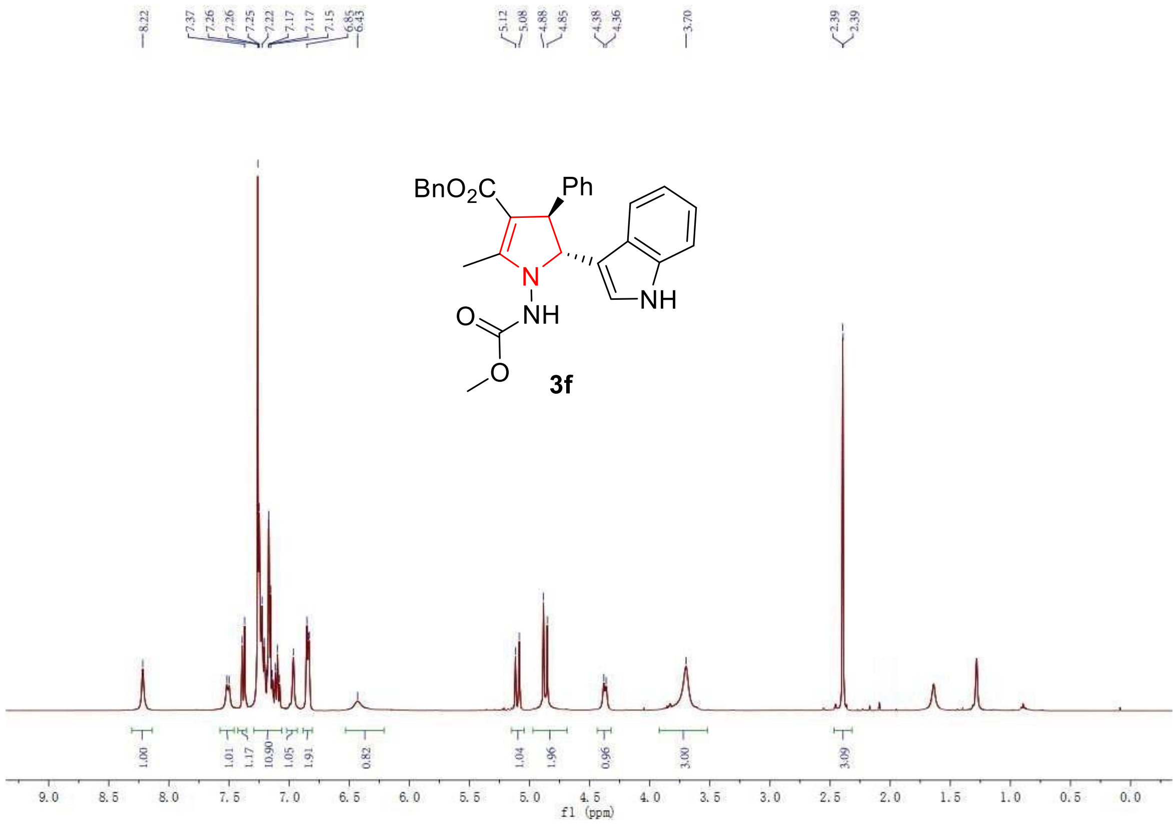
8.22
7.37
7.26
7.26
7.25
7.22
7.17
7.17
7.15
6.85
6.43
5.12
5.08
4.88
4.85
4.38
4.36
3.70
2.39
2.39
BnO2C
Ph
N
NH
NH
O
O
3f
1.00
1.01
1.17
10.90
1.05
1.91
0.82
1.04
1.96
0.96
3.00
3.09
f1 (ppm)

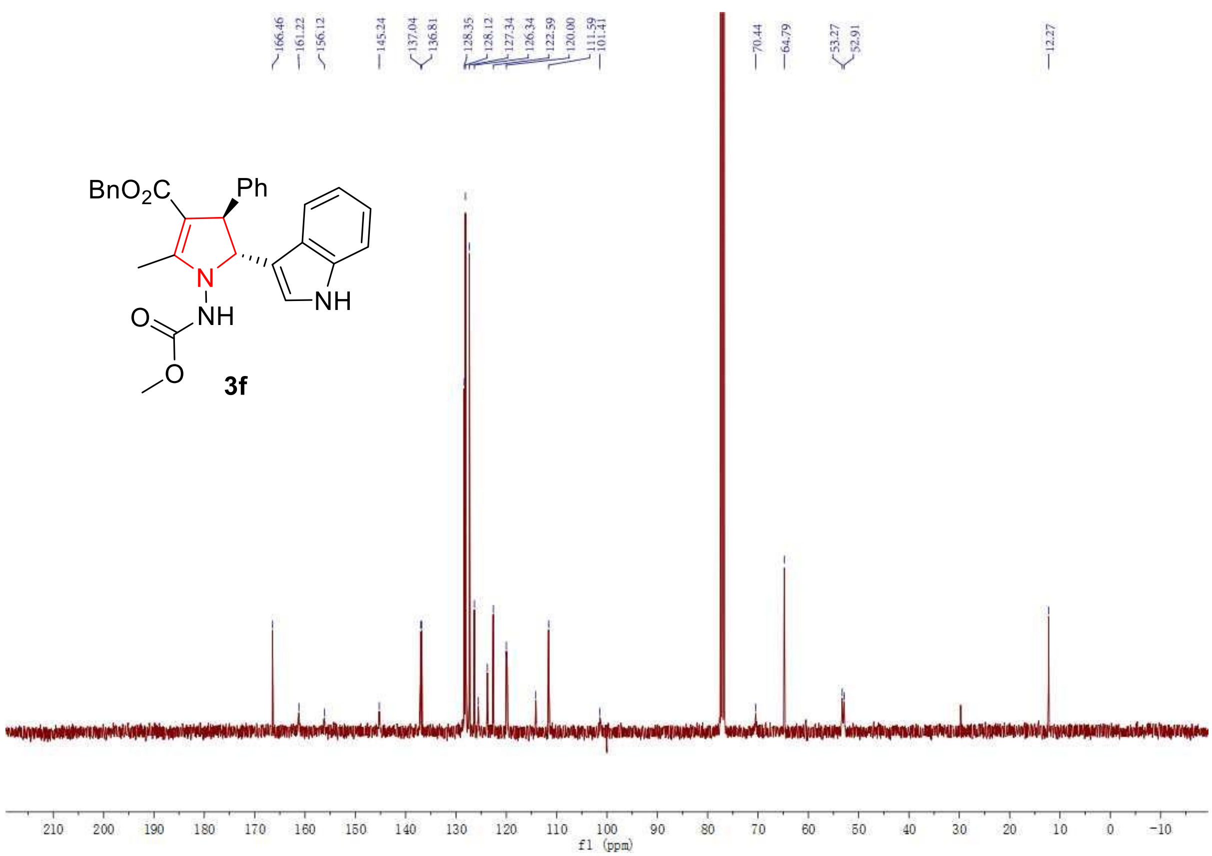
166.46
161.22
156.12
145.24
137.04
136.81
128.35
128.12
127.34
126.34
122.59
120.00
111.59
101.41
70.44
64.79
53.27
52.91
12.27
BnO2C
Ph
N
NH
NH
O
O
3f
f1 (ppm)

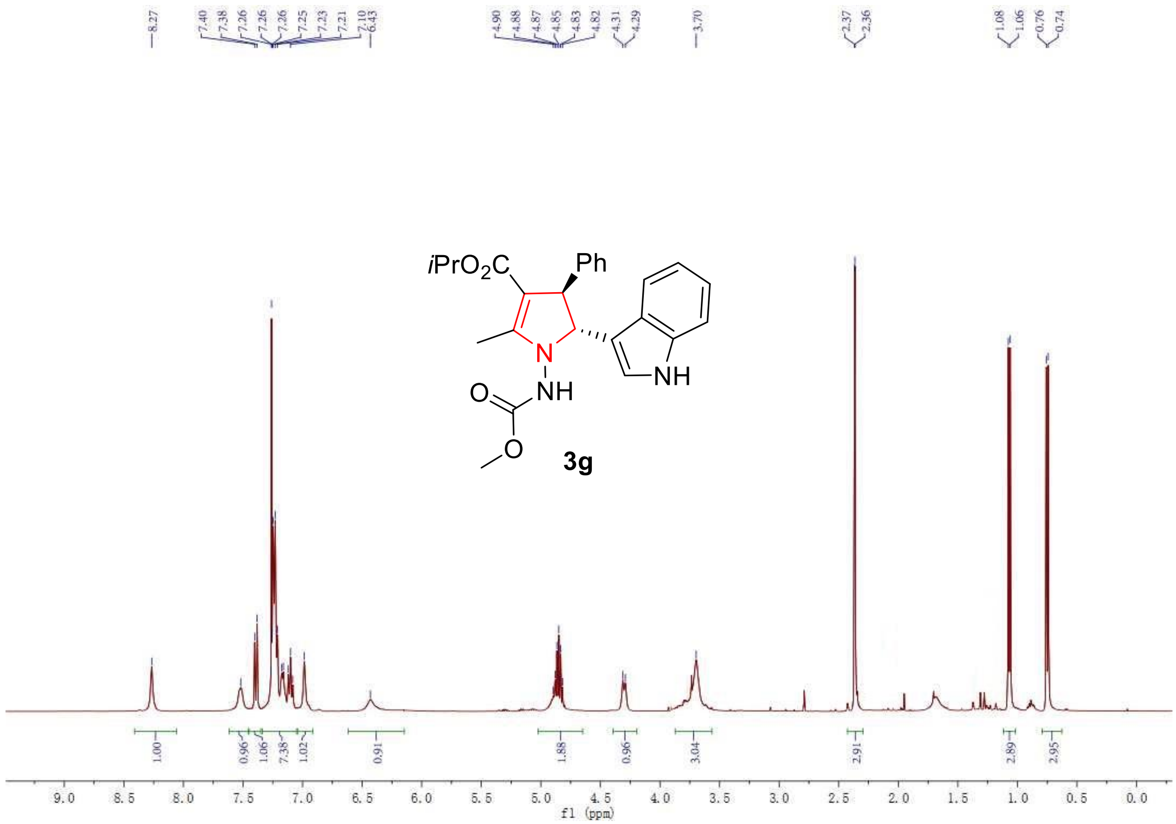
8.27
7.40 7.38 7.26 7.26 7.26 7.25 7.23 7.21 7.10 6.43
4.90 4.88 4.87 4.85 4.83 4.82 4.31 4.29
3.70
2.37 2.36
1.08 1.06 0.76 0.74
*i*PrO2C
Ph
N
NH
O
O
NH
3g
1.00 0.96 1.06 7.38 1.02 0.91 1.88 0.96 3.04 2.91 2.89 2.95
9.0 8.5 8.0 7.5 7.0 6.5 6.0 5.5 5.0 4.5 4.0 3.5 3.0 2.5 2.0 1.5 1.0 0.5 0.0
f1 (ppm)

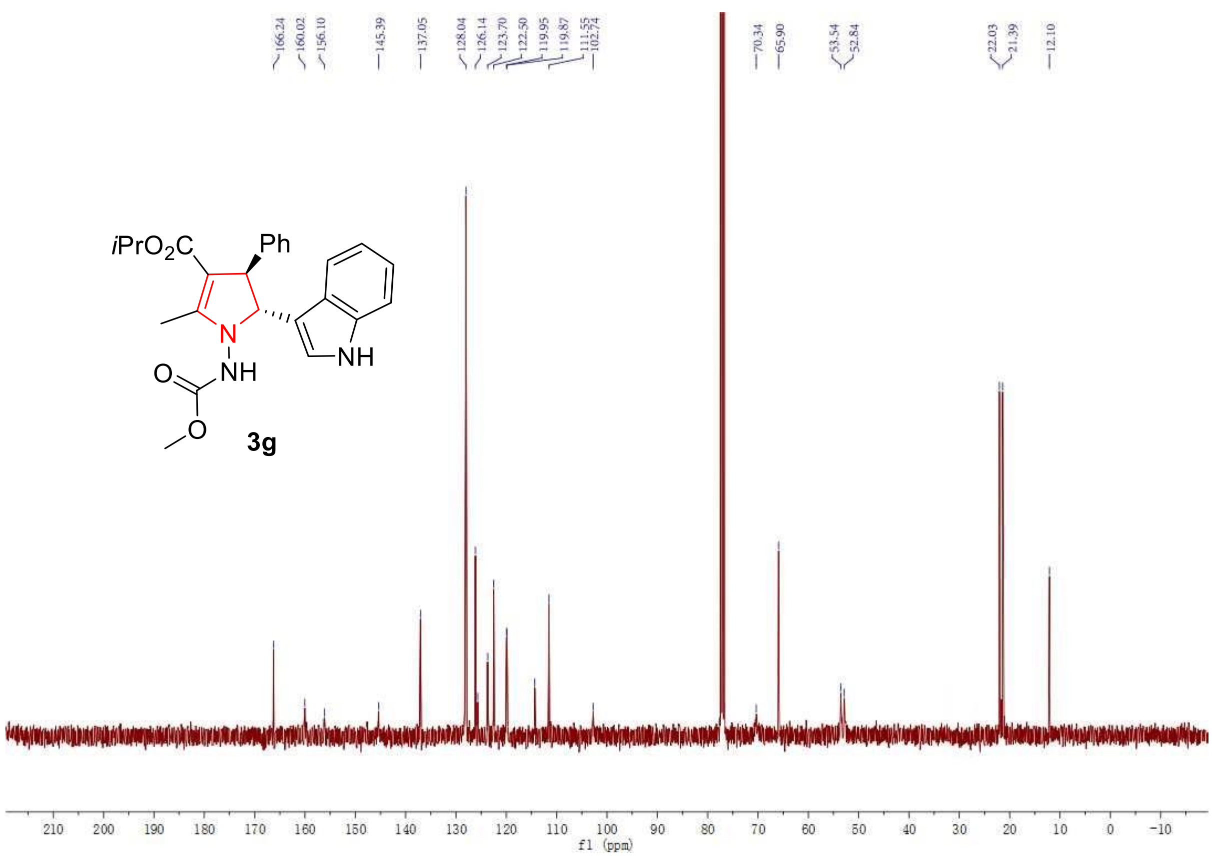
166.24 160.02 156.10
145.39
137.05
128.04 126.14 123.70 122.50 119.95 119.87 111.55 102.74
70.34
65.90
53.54 52.84
22.03 21.39
12.10
*i*PrO2C
Ph
N
NH
O
O
NH
3g
210 200 190 180 170 160 150 140 130 120 110 100 90 80 70 60 50 40 30 20 10 0 -10
f1 (ppm)

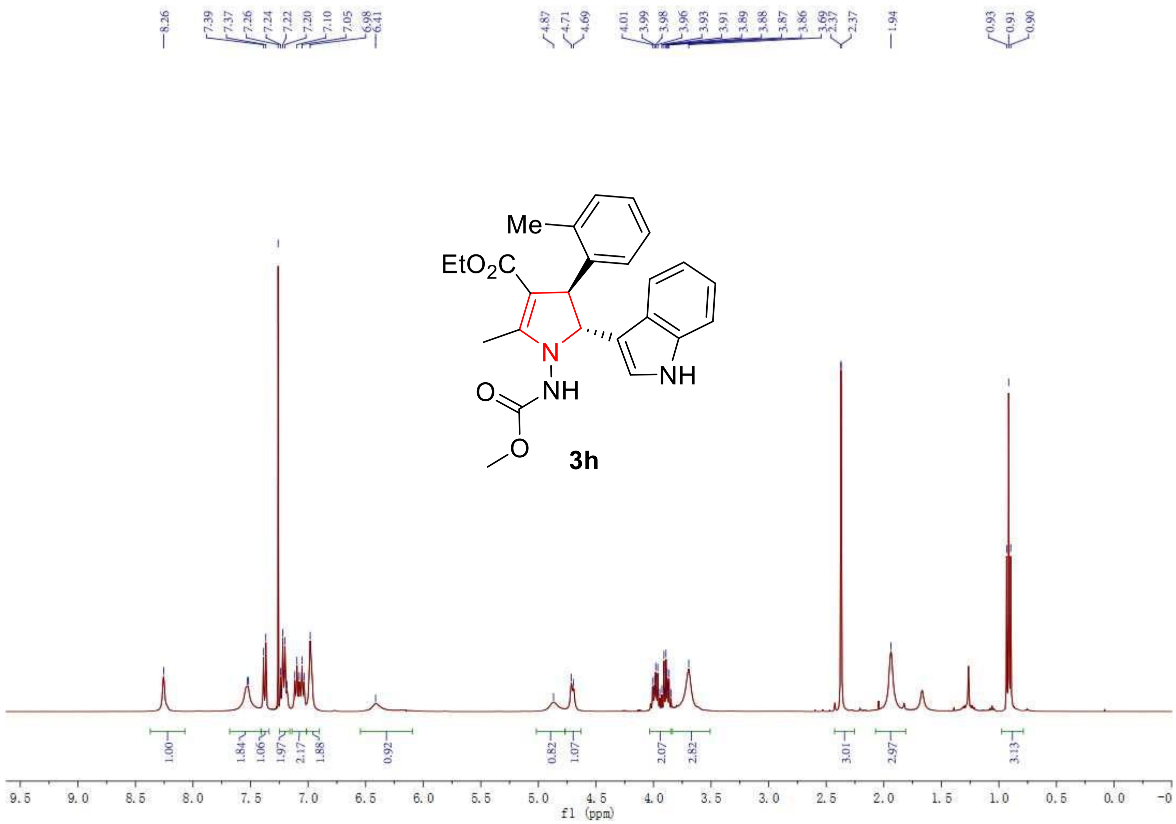
8.26
7.39
7.37
7.26
7.24
7.22
7.20
7.10
7.05
6.98
6.41
4.87
4.71
4.69
4.01
3.99
3.98
3.96
3.93
3.91
3.89
3.88
3.87
3.86
3.69
2.37
2.37
1.94
0.93
0.91
0.90
Me
EtO2C
N
NH
NH
O
O
3h
1.00
1.84
1.06
1.97
2.17
1.88
0.92
0.82
1.07
2.07
2.82
3.01
2.97
3.13
f1 (ppm)

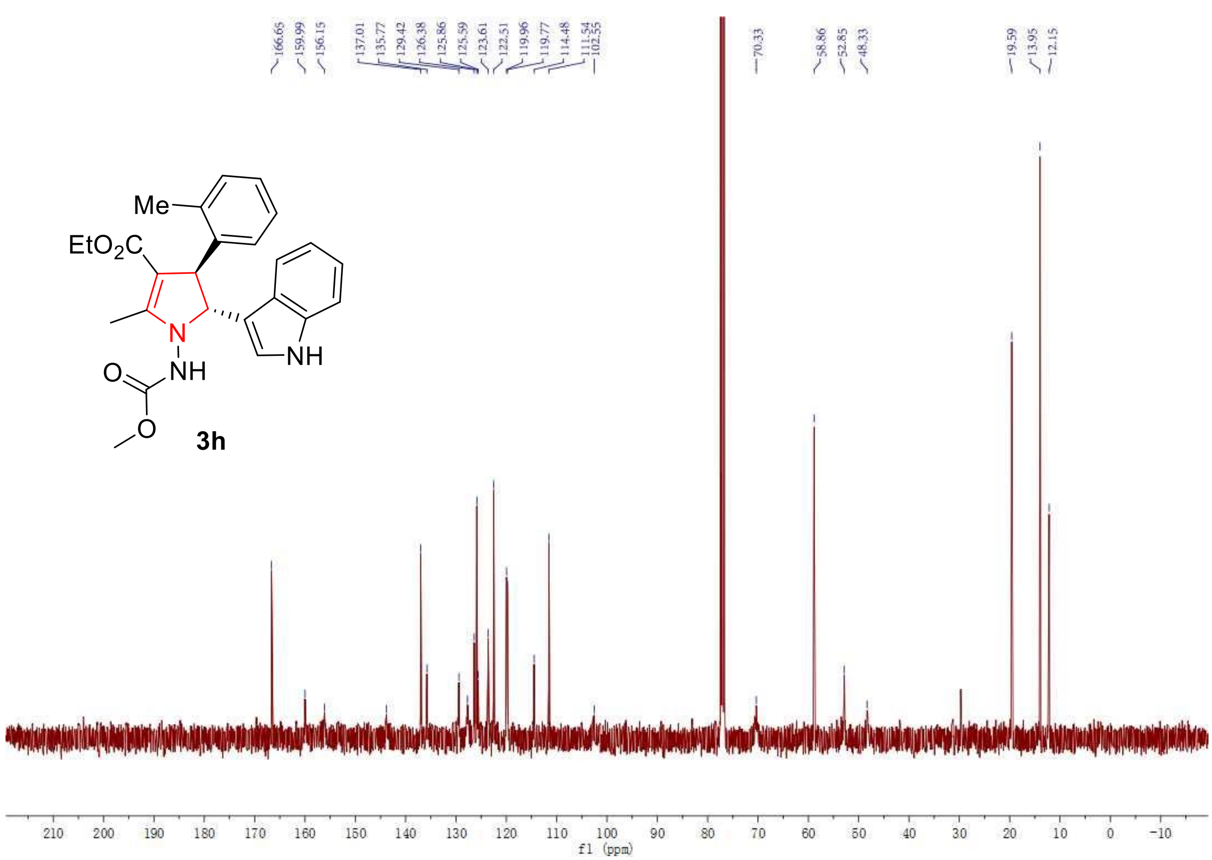
166.65
159.99
156.15
137.01
135.77
129.42
126.38
125.86
125.59
123.61
122.51
119.96
119.77
114.48
111.54
102.55
70.33
58.86
52.85
48.33
19.59
13.95
12.15
Me
EtO2C
N
NH
NH
O
O
3h
f1 (ppm)

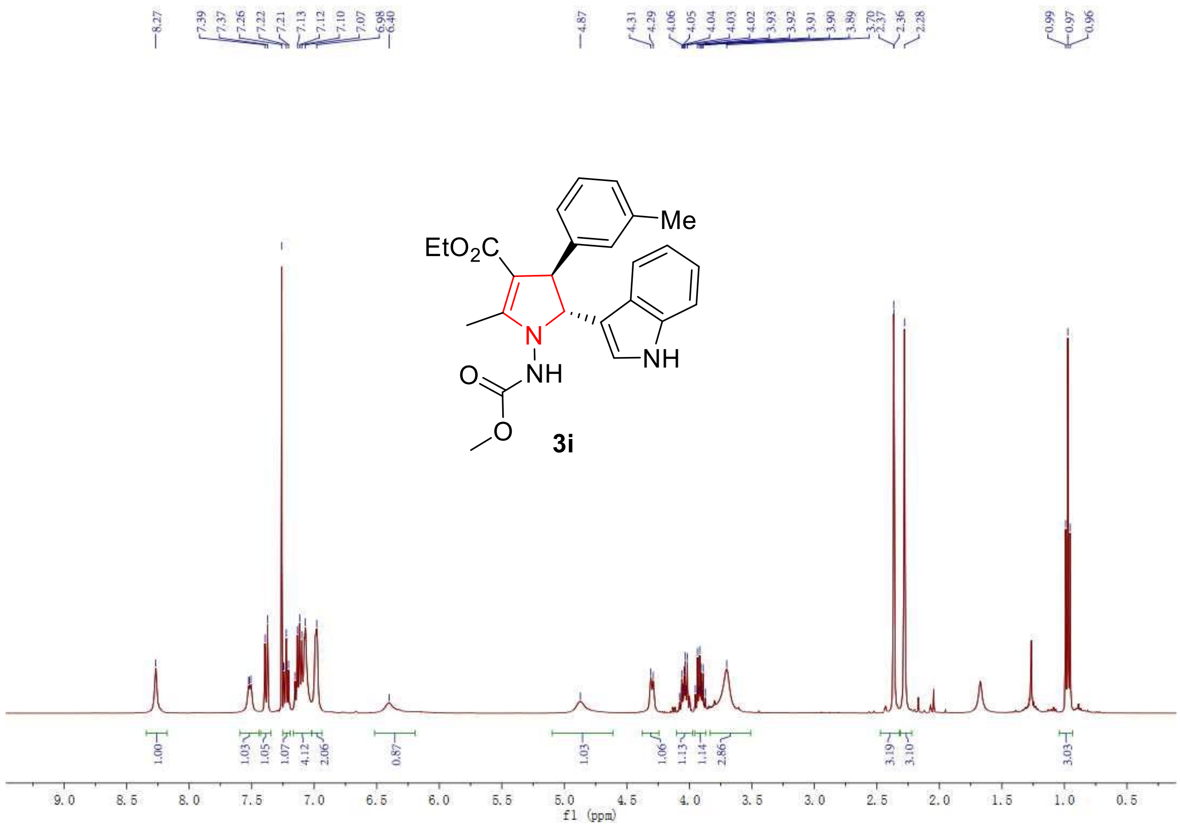

8.27
7.39
7.37
7.26
7.22
7.21
7.13
7.12
7.10
7.07
6.98
6.40
4.87
4.31
4.29
4.06
4.05
4.04
4.03
4.02
3.93
3.92
3.91
3.90
3.89
3.70
2.37
2.36
2.28
0.99
0.97
0.96
EtO_2C
Me
N
NH
NH
O
O
3i
1.00
1.03
1.05
1.07
4.12
2.06
0.87
1.03
1.06
1.13
1.14
2.86
3.19
3.10
3.03
9.0 8.5 8.0 7.5 7.0 6.5 6.0 5.5 5.0 4.5 4.0 3.5 3.0 2.5 2.0 1.5 1.0 0.5
f1 (ppm)

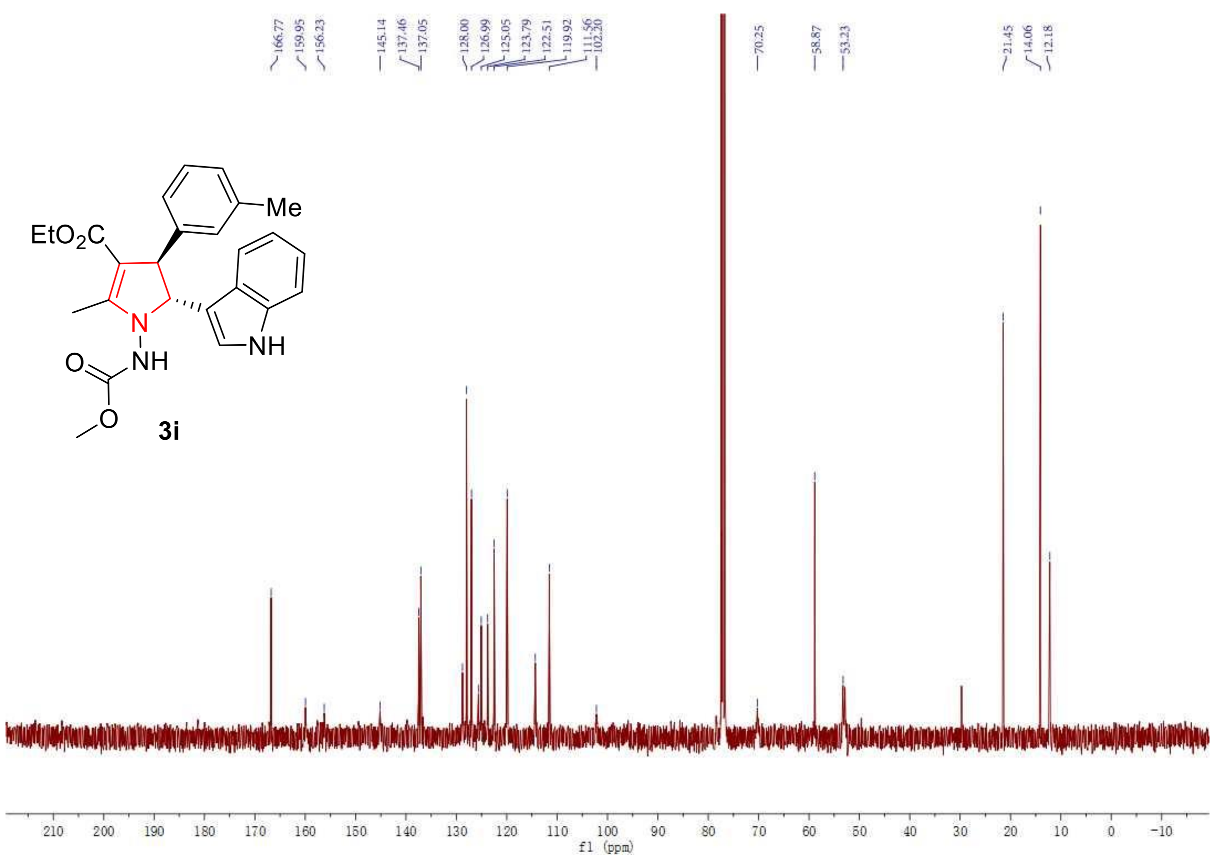

166.77
159.95
156.23
145.14
137.46
137.05
128.00
126.99
125.05
123.79
122.51
119.92
111.56
102.20
70.25
58.87
53.23
21.45
14.06
12.18
EtO_2C
Me
N
NH
NH
O
O
3i
210 200 190 180 170 160 150 140 130 120 110 100 90 80 70 60 50 40 30 20 10 0 -10
f1 (ppm)

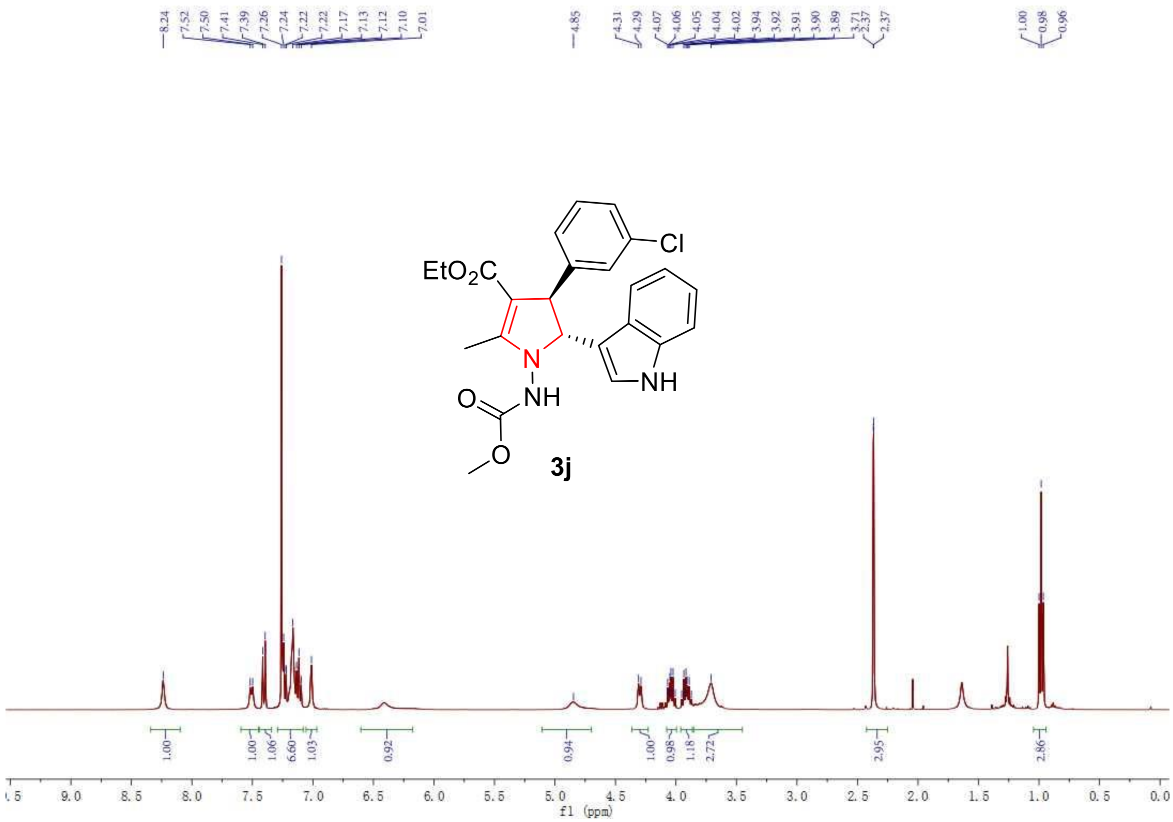

EtO2C
Cl
N
NH
O
NH
O
3j
f1 (ppm)

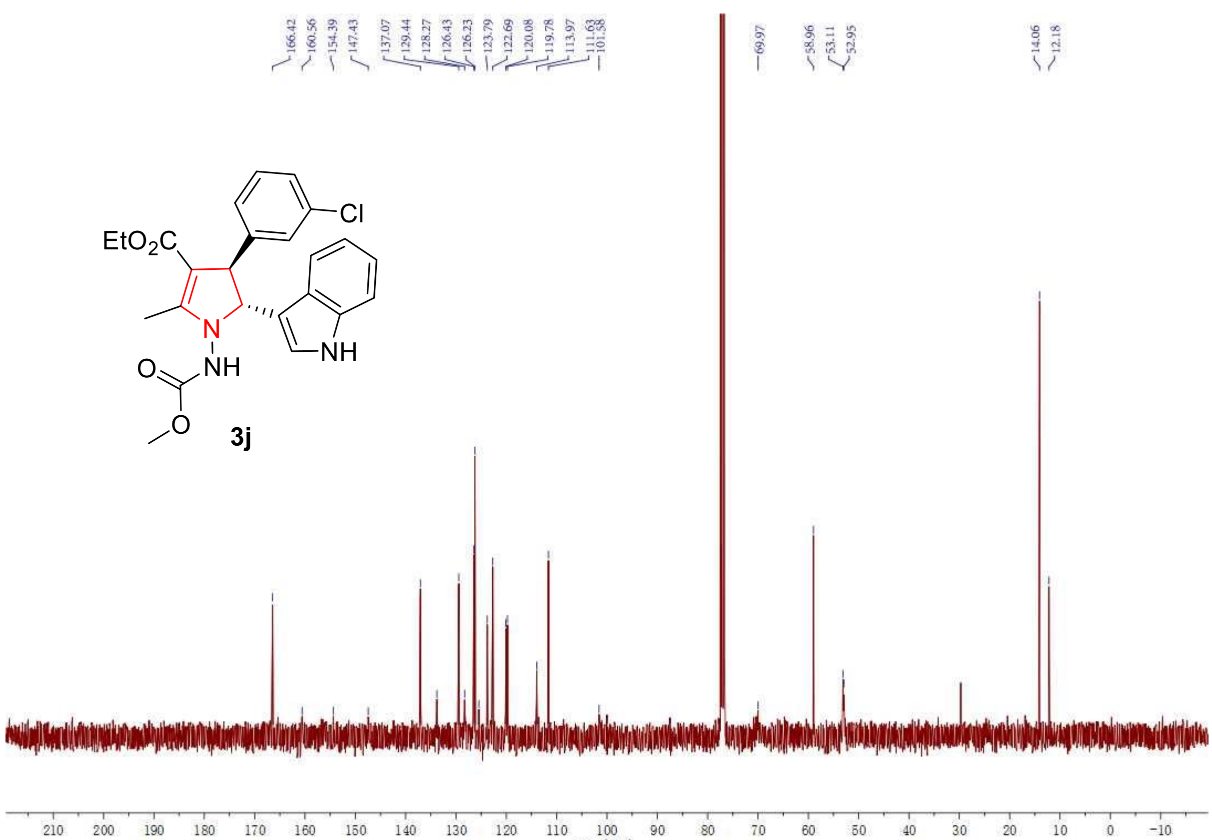

EtO2C
Cl
N
NH
O
NH
O
3j
f1 (ppm)

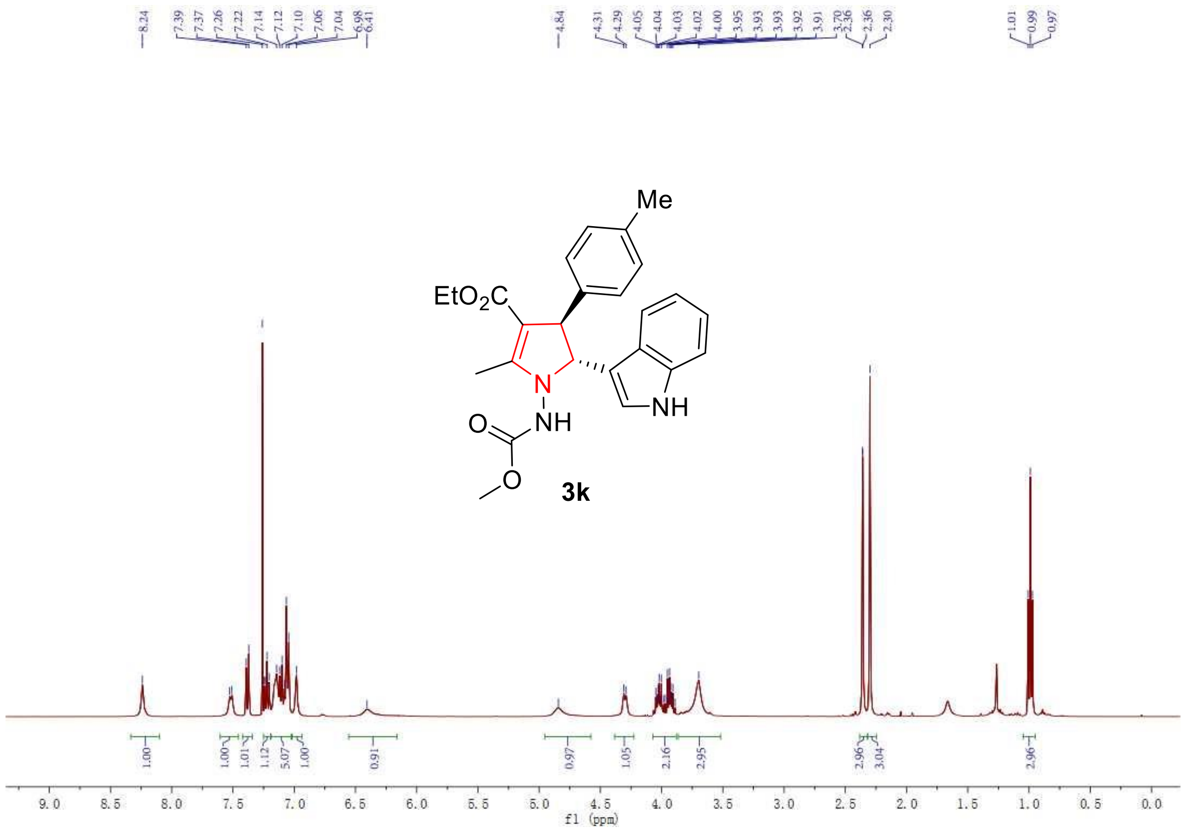

8.24
7.39
7.37
7.26
7.22
7.14
7.12
7.10
7.06
7.04
6.98
6.41
4.84
4.31
4.29
4.05
4.04
4.03
4.02
4.00
3.95
3.93
3.93
3.92
3.91
3.70
2.36
2.30
1.01
0.99
0.97
Me
EtO2C
N
NH
NH
O
O
3k
1.00
1.00
1.01
1.12
5.07
1.00
0.91
0.97
1.05
2.16
2.95
2.96
3.04
2.96
9.0
8.5
8.0
7.5
7.0
6.5
6.0
5.5
5.0
4.5
4.0
3.5
3.0
2.5
2.0
1.5
1.0
0.5
0.0
f1 (ppm)

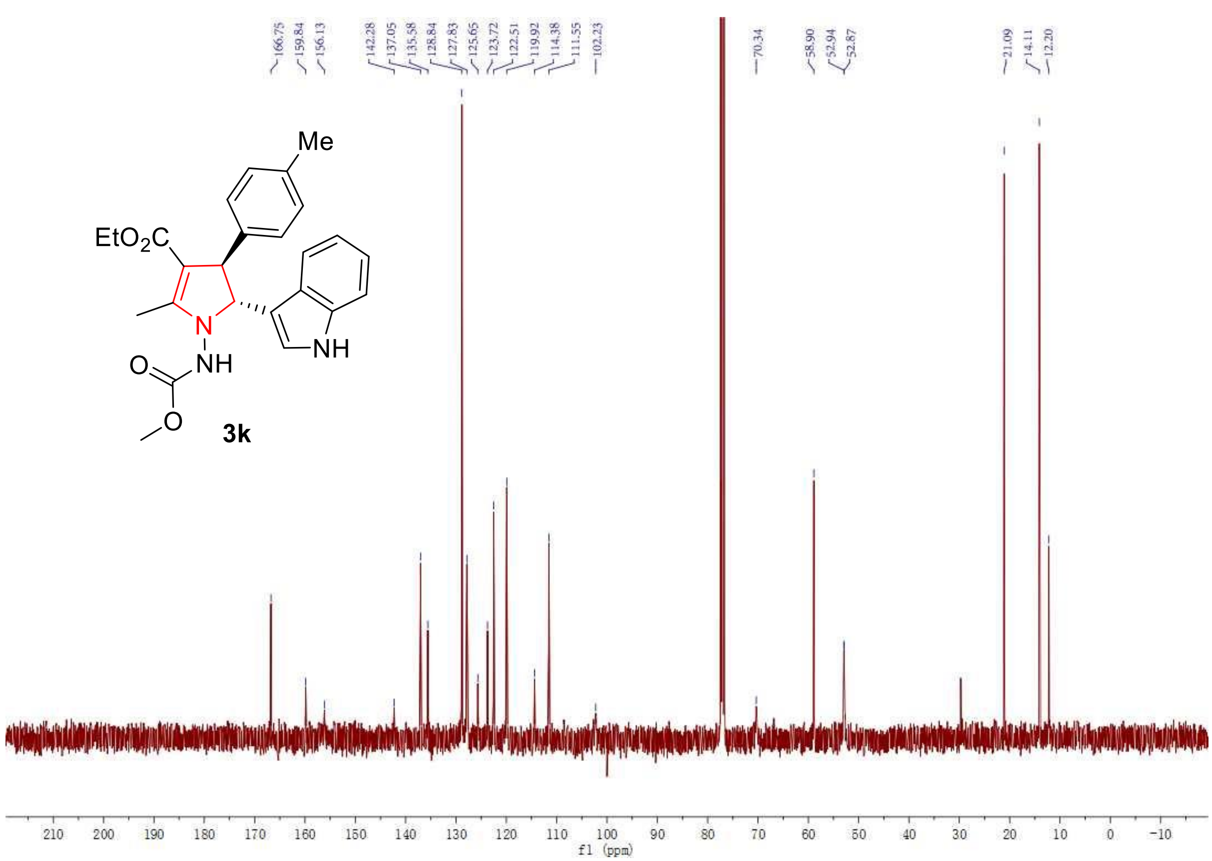

166.75
159.84
156.13
142.28
137.05
135.58
128.84
127.83
125.65
123.72
122.51
119.92
114.38
111.55
102.23
70.34
58.90
52.94
52.87
21.09
14.11
12.20
Me
EtO2C
N
NH
NH
O
O
3k
210
200
190
180
170
160
150
140
130
120
110
100
90
80
70
60
50
40
30
20
10
0
-10
f1 (ppm)

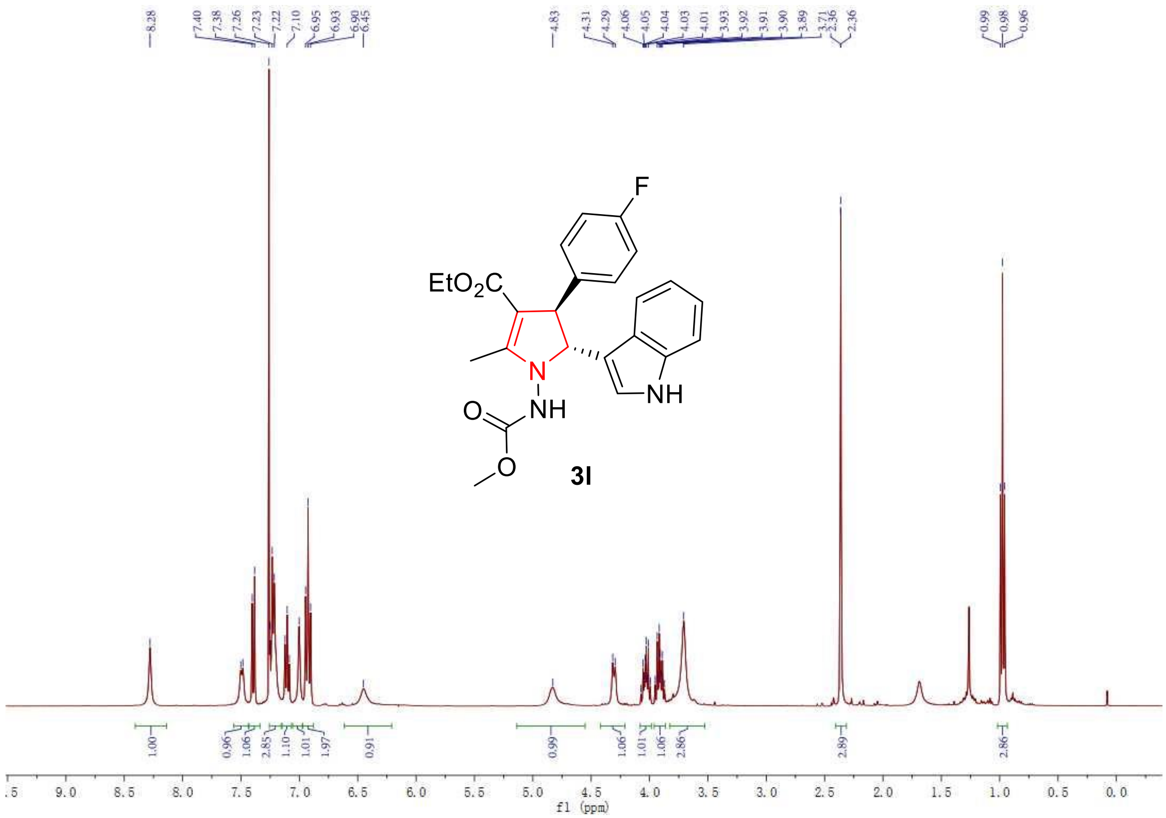
8.28
7.40 7.38 7.26 7.23 7.22 7.10 6.95 6.93 6.90 6.45
4.83
4.31 4.29 4.06 4.05 4.04 4.03 4.01 3.93 3.92 3.91 3.90 3.89 3.71 2.36 2.36
0.99 0.98 0.96
F
EtO2C
N
NH
NH
O
O
3l
1.00 0.96 1.06 2.85 1.10 1.01 1.97 0.91 0.99 1.06 1.01 1.06 2.86 2.89 2.86
f1 (ppm)

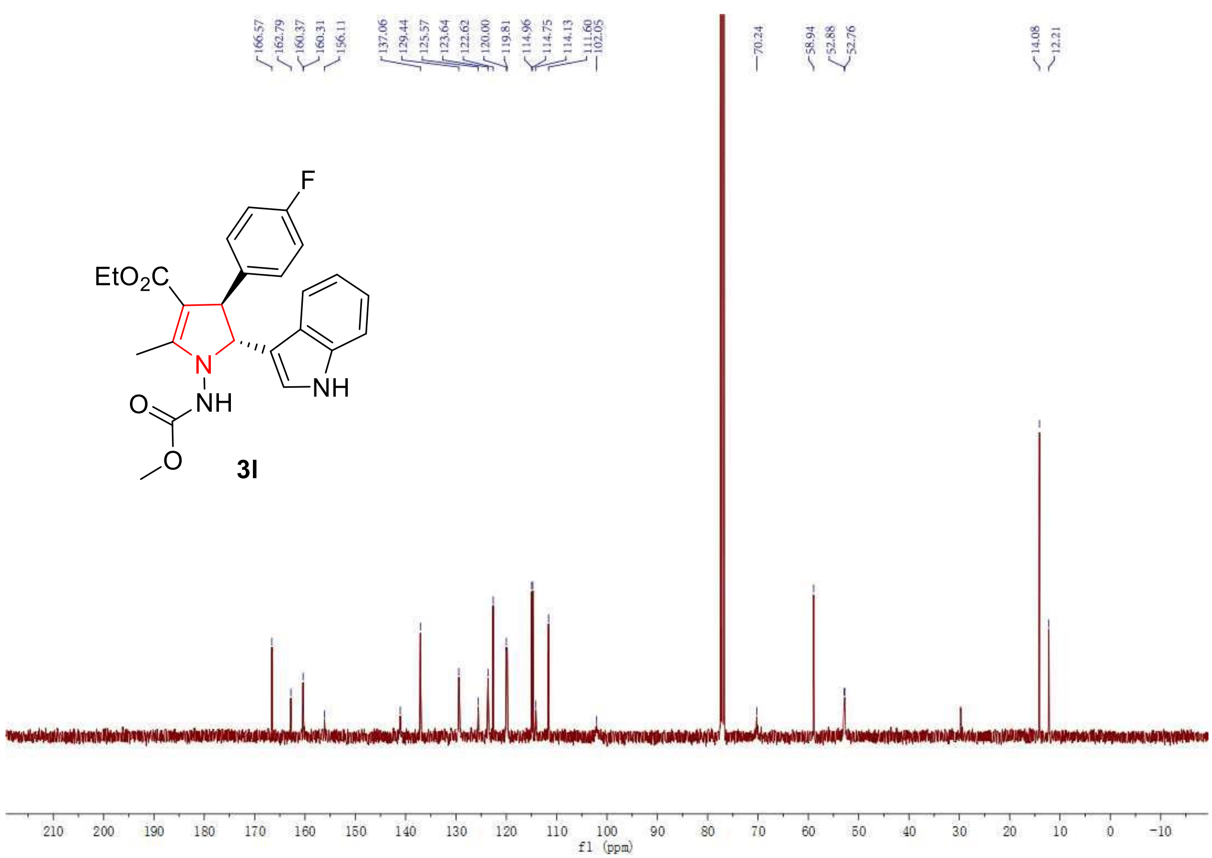
166.57 162.79 160.37 160.31 156.11
137.06 129.44 125.57 123.64 122.62 120.00 119.81 114.96 114.75 114.13 111.60 102.05
70.24
58.94 52.88 52.76
14.08 12.21
F
EtO2C
N
NH
NH
O
O
3l
f1 (ppm)

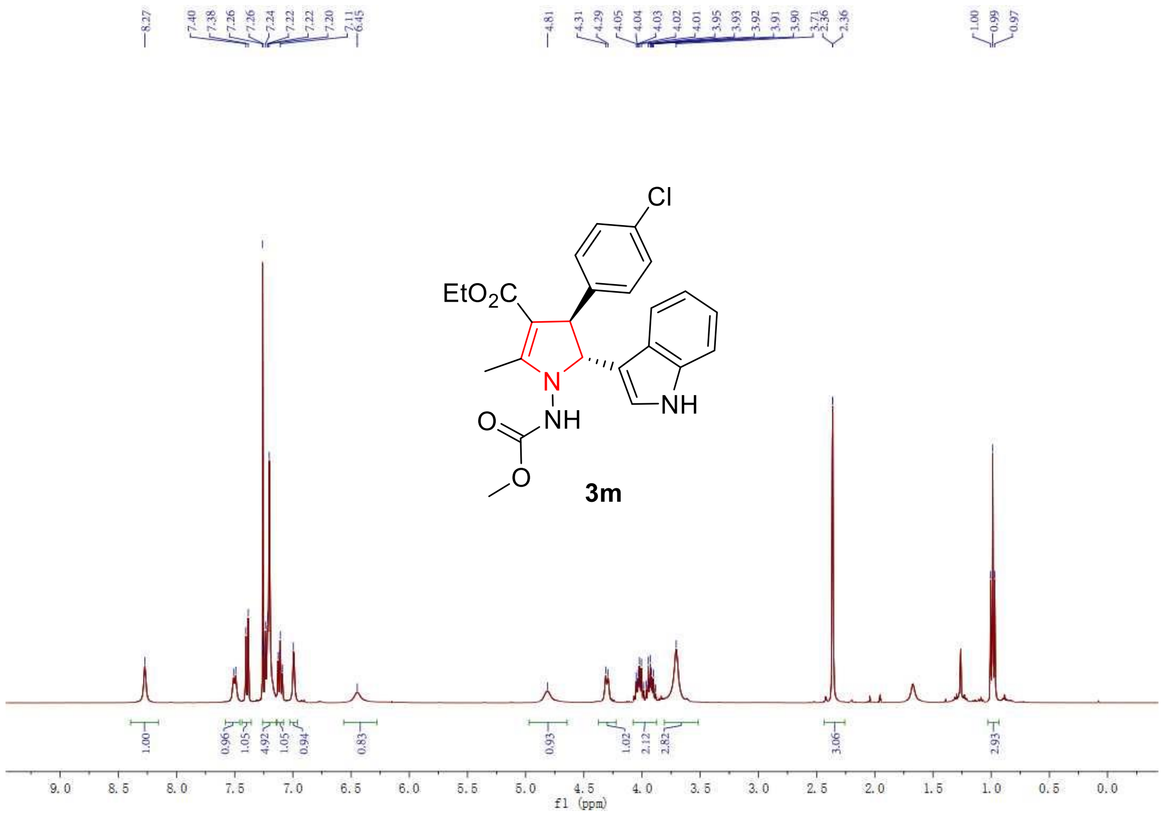
8.27
7.40 7.38 7.26 7.26 7.24 7.22 7.22 7.20 7.11 6.45
4.81
4.31 4.29 4.05 4.04 4.03 4.02 4.01 3.95 3.93 3.92 3.91 3.90 3.71 2.36 2.36
1.00 0.99 0.97
EtO2C
Cl
N
NH
O
NH
O
3m
1.00 0.96 1.05 4.92 1.05 0.94 0.83 0.93 1.02 2.12 2.82 3.06 2.93
f1 (ppm)

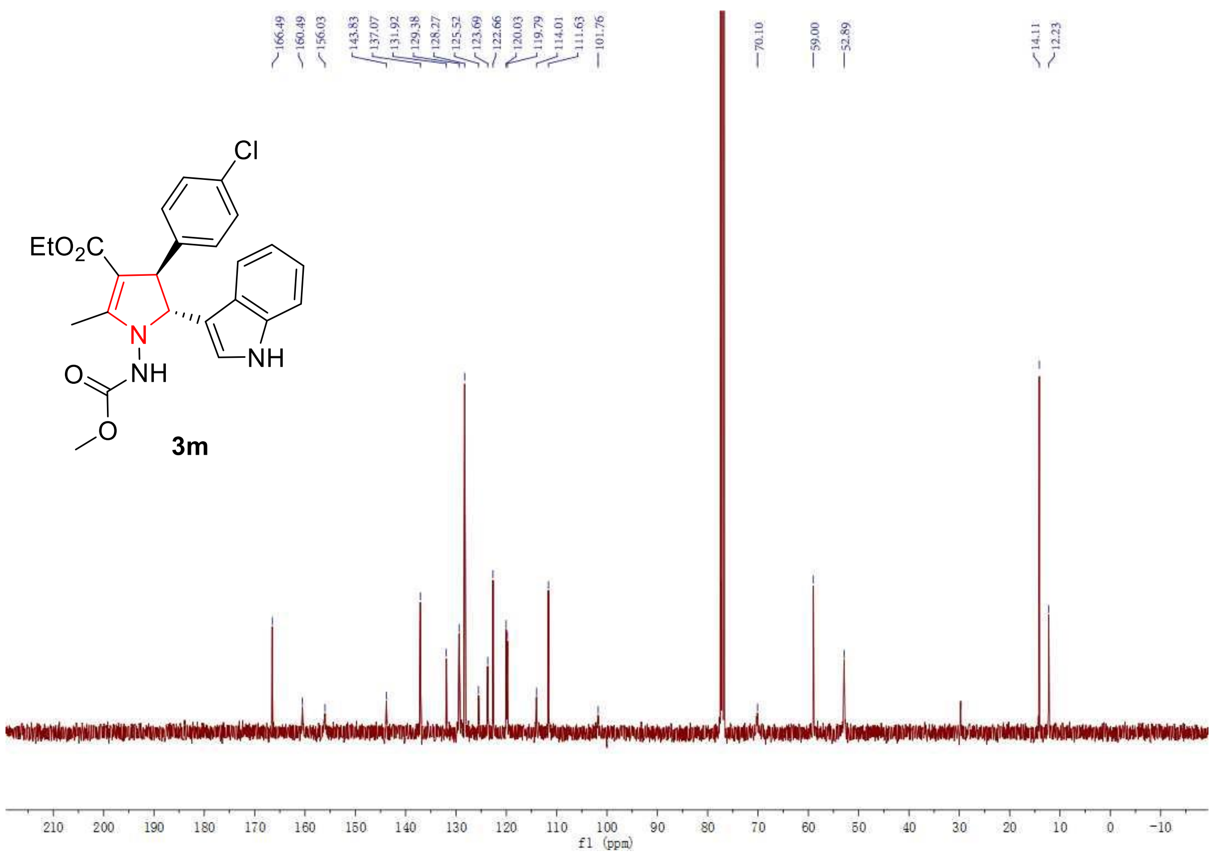
166.49 160.49 156.03
143.83 137.07 131.92 129.38 128.27 125.52 123.69 122.66 120.03 119.79 114.01 111.63 101.76
70.10
59.00
52.89
14.11 12.23
EtO2C
Cl
N
NH
O
NH
O
3m
f1 (ppm)

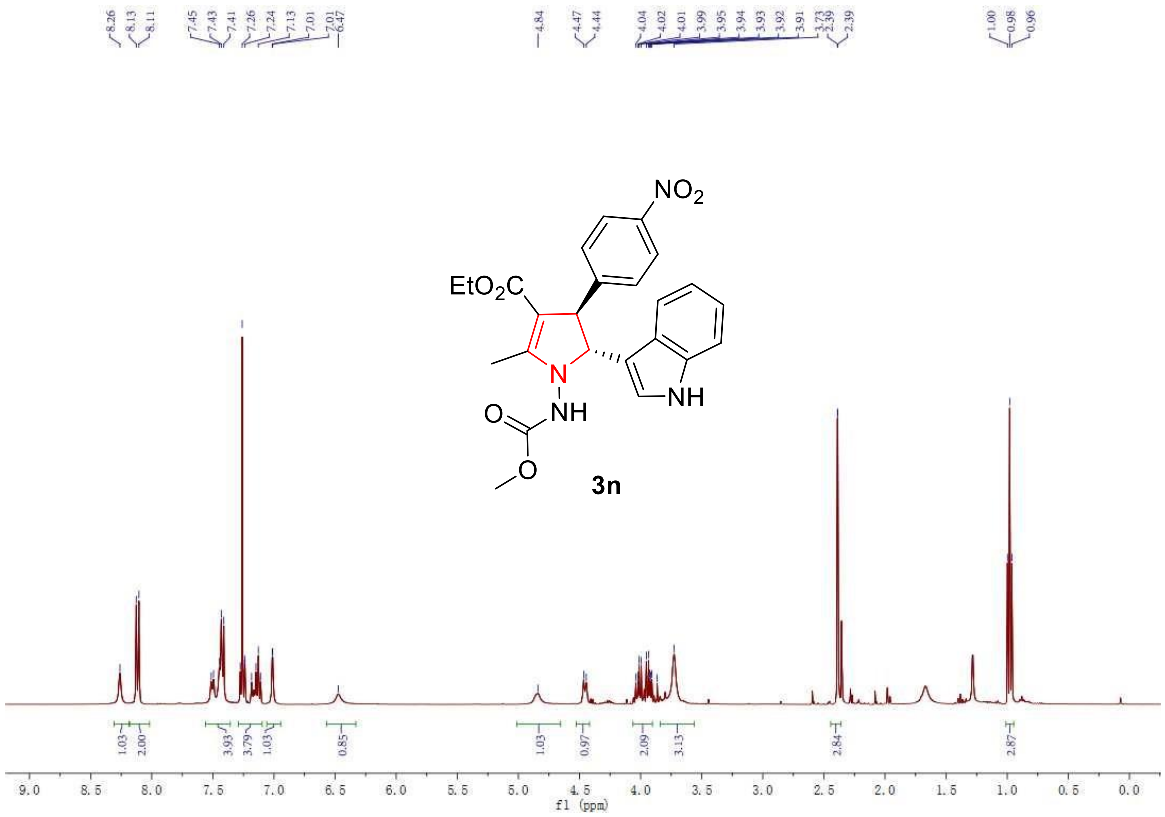
8.26 8.13 8.11 7.45 7.43 7.41 7.26 7.24 7.13 7.01 7.01 6.47 4.84 4.47 4.44 4.04 4.02 4.01 3.99 3.95 3.94 3.93 3.92 3.91 3.73 2.39 2.39 1.00 0.98 0.96
NO2
EtO2C
N
NH
O
O
NH
3n
1.03 2.00 3.93 3.79 1.03 0.85 1.03 0.97 2.09 3.13 2.84 2.87
9.0 8.5 8.0 7.5 7.0 6.5 6.0 5.5 5.0 4.5 4.0 3.5 3.0 2.5 2.0 1.5 1.0 0.5 0.0
f1 (ppm)

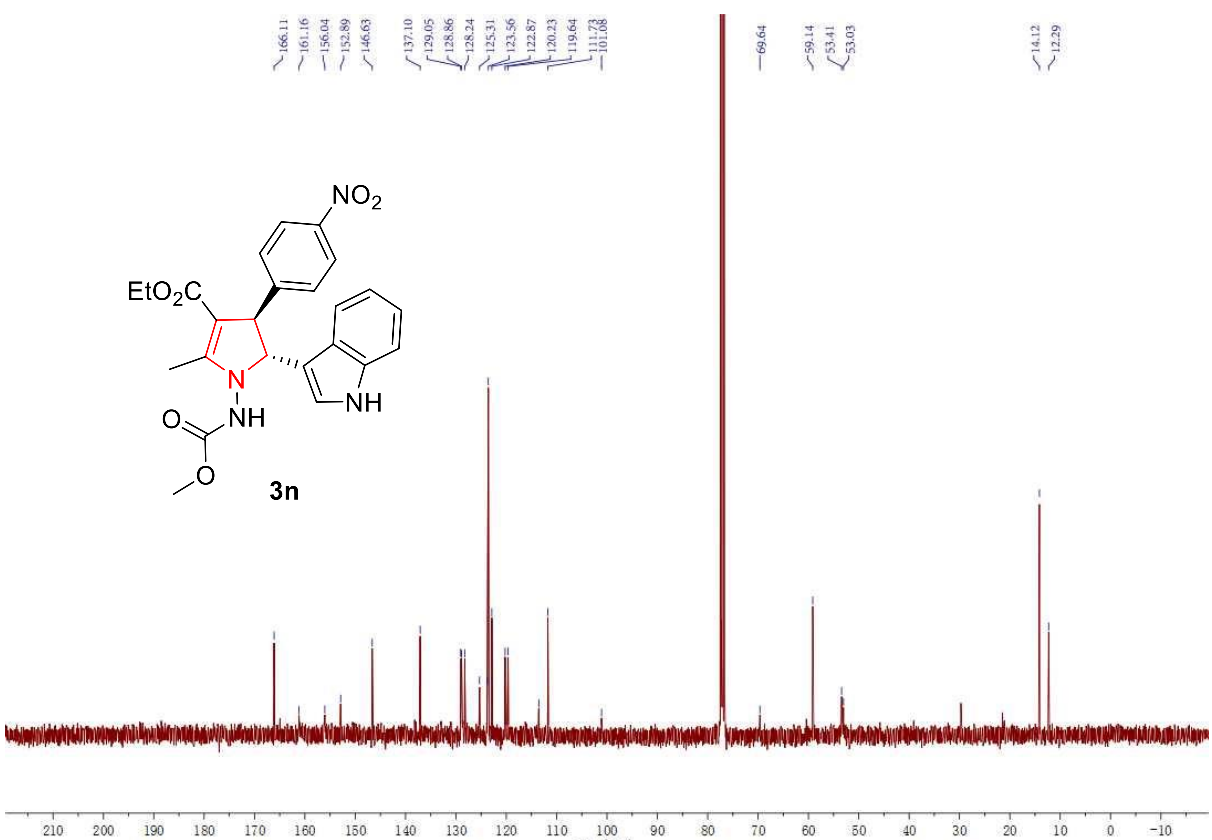
166.11 161.16 156.04 152.89 146.63 137.10 129.05 128.86 128.24 125.31 123.56 122.87 120.23 119.64 111.73 101.08 69.64 59.14 53.41 53.03 14.12 12.29
NO2
EtO2C
N
NH
O
O
NH
3n
210 200 190 180 170 160 150 140 130 120 110 100 90 80 70 60 50 40 30 20 10 0 -10
f1 (ppm)

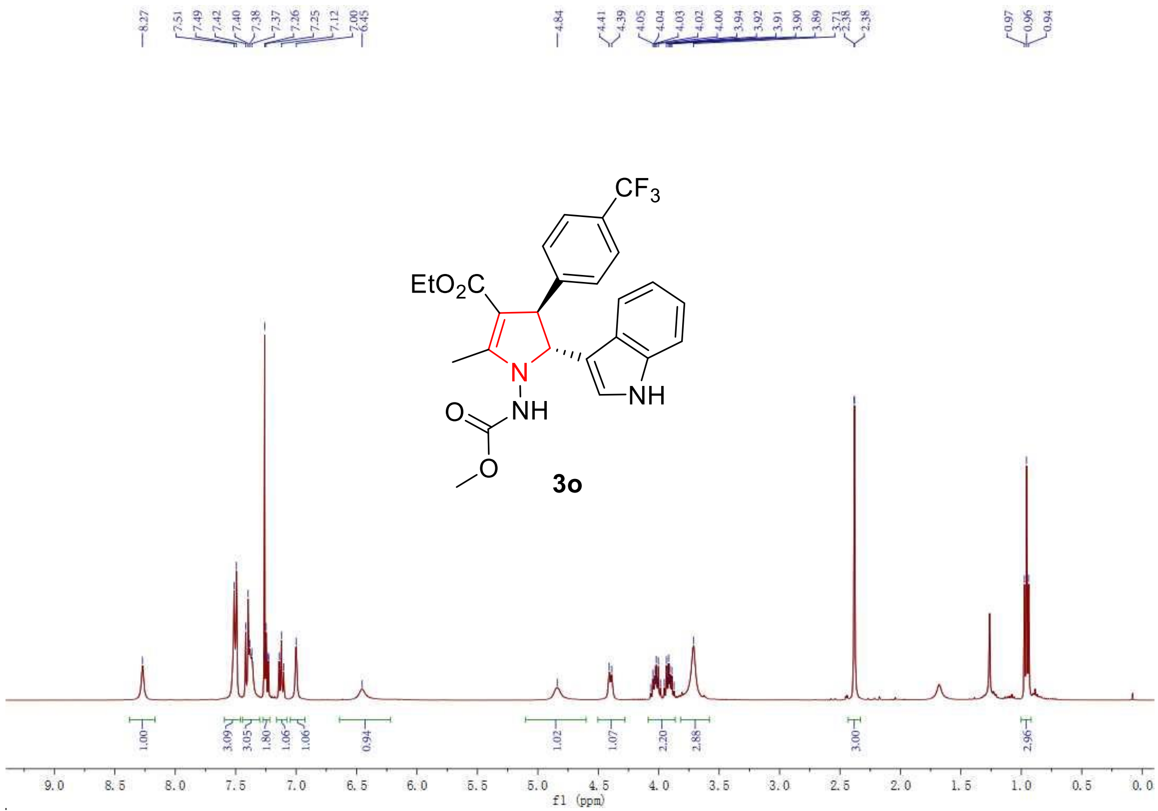
8.27
7.51 7.49 7.42 7.40 7.38 7.37 7.26 7.25 7.12 7.00 6.45
4.84
4.41 4.39
4.05 4.04 4.03 4.02 4.00 3.94 3.92 3.91 3.90 3.89 3.71 2.38 2.38
0.97 0.96 0.94
CF3
EtO2C
N
NH
O
NH
O
3o
1.00 3.09 3.05 1.80 1.06 1.06 0.94 1.02 1.07 2.20 2.88 3.00 2.96
f1 (ppm)

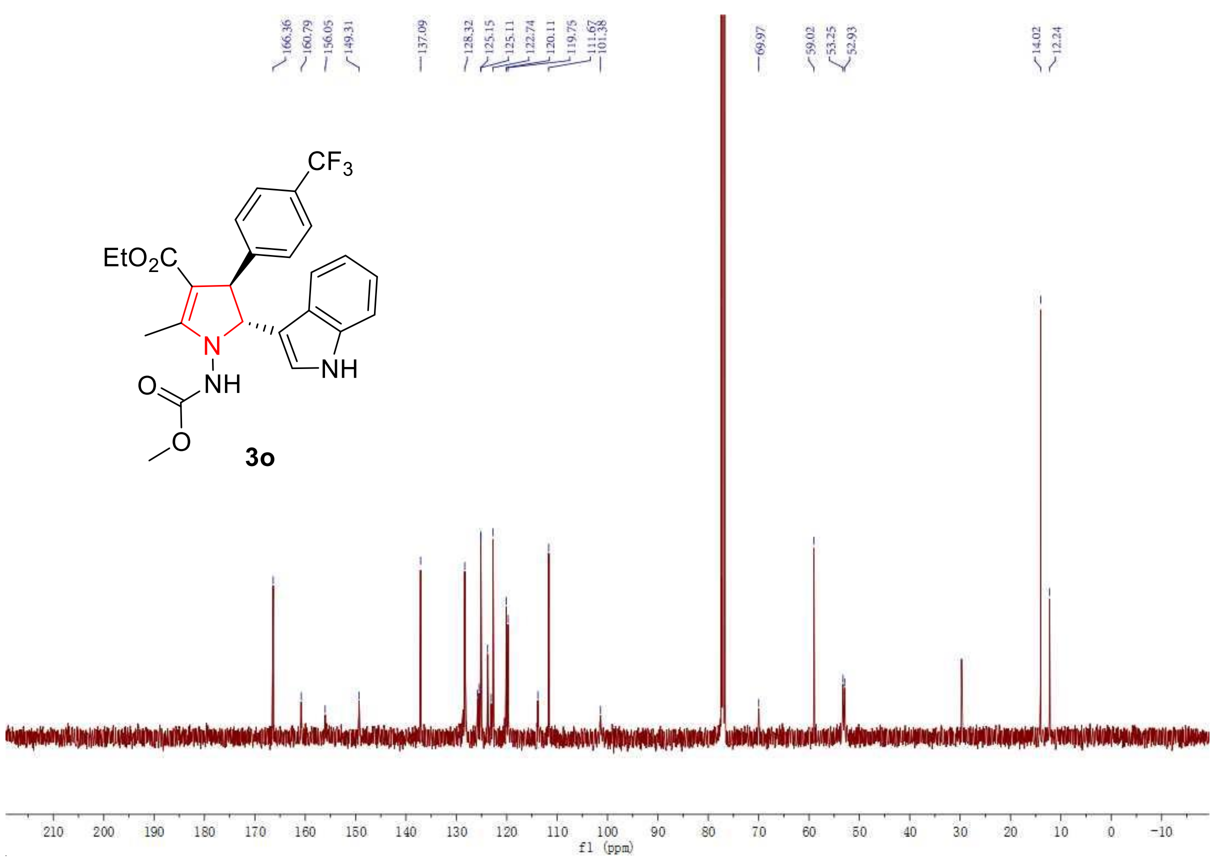
166.36 160.79 156.05 149.31
137.09
128.32 125.15 125.11 122.74 120.11 119.75 111.67 101.38
69.97
59.02 53.25 52.93
14.02 12.24
CF3
EtO2C
N
NH
O
NH
O
3o
f1 (ppm)

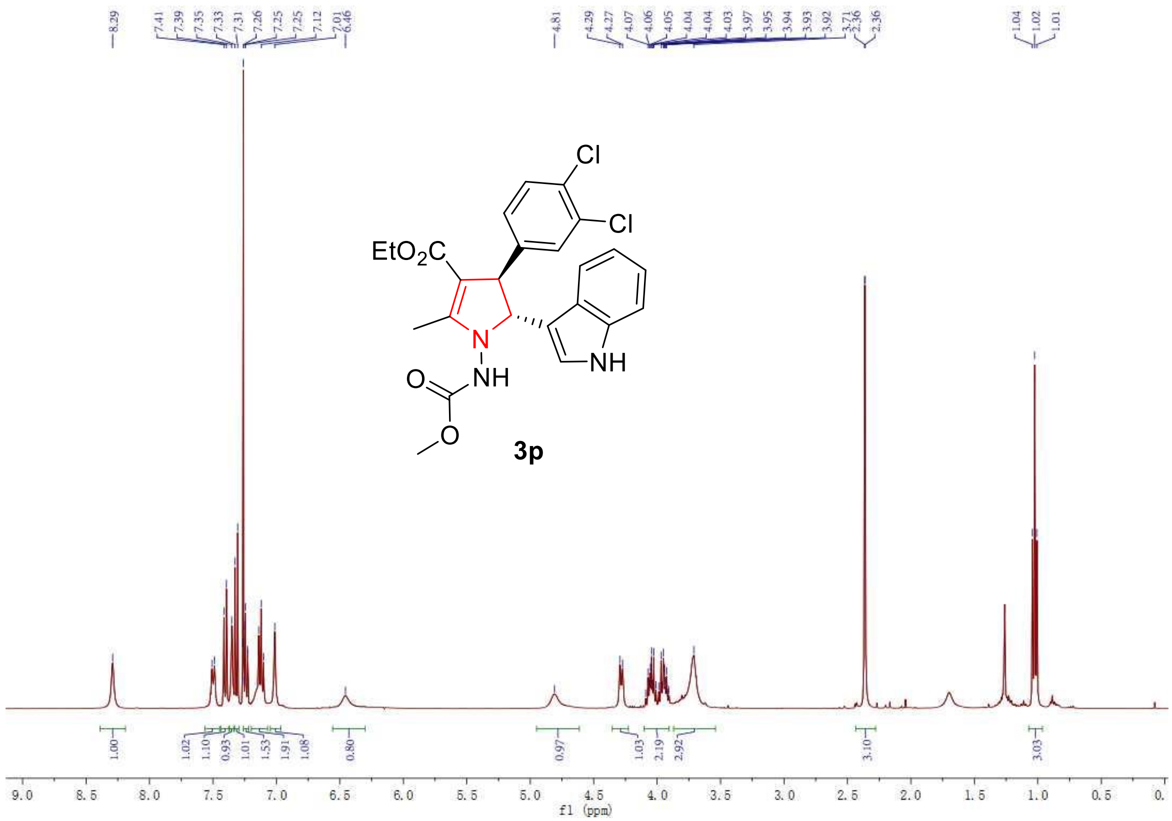
8.29
7.41
7.39
7.35
7.33
7.31
7.26
7.25
7.25
7.12
7.01
6.46
4.81
4.29
4.27
4.07
4.06
4.05
4.04
4.04
4.03
3.97
3.95
3.94
3.93
3.92
3.71
2.36
2.36
1.04
1.02
1.01
EtO2C
Cl
Cl
N
NH
NH
O
O
3p
1.00
1.02
1.10
0.93
1.01
1.53
1.91
1.08
0.80
0.97
1.03
2.19
2.92
3.10
3.03
f1 (ppm)

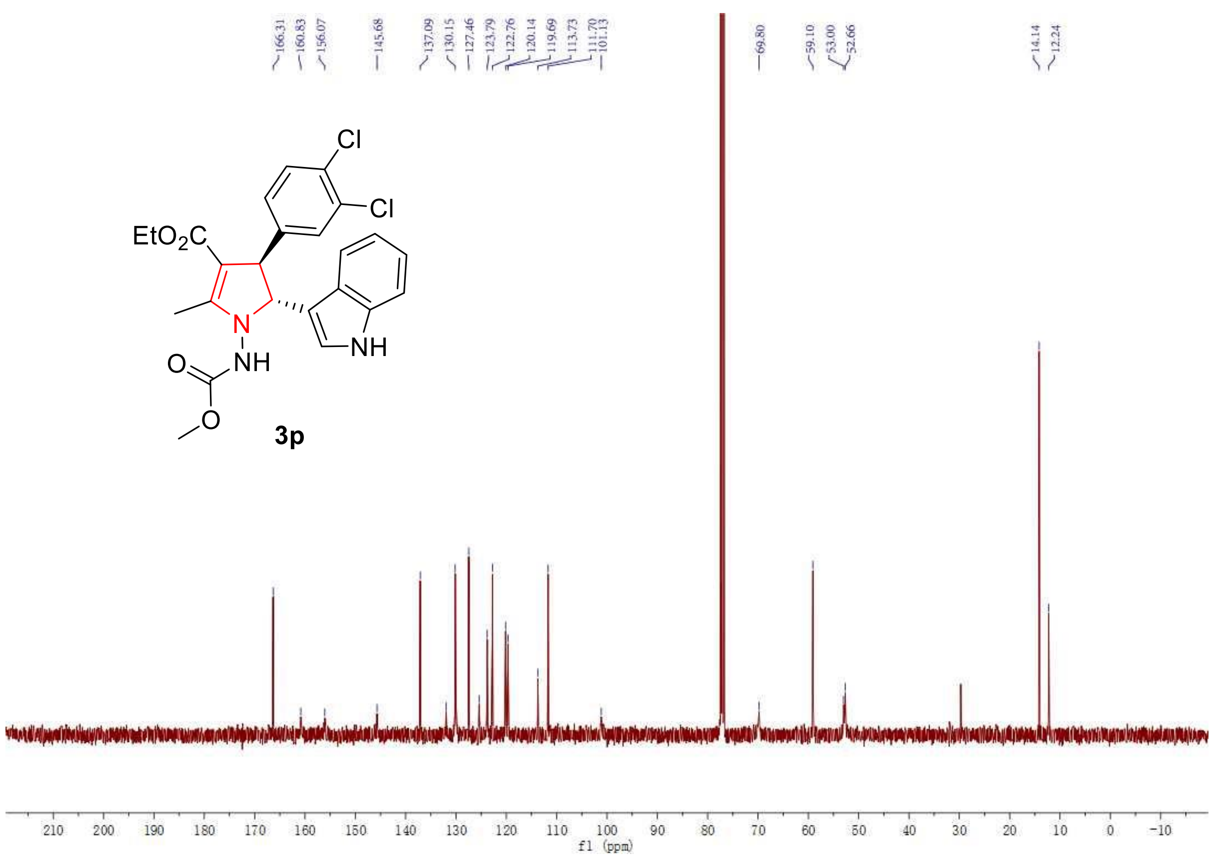
166.31
160.83
156.07
145.68
137.09
130.15
127.46
123.79
122.76
120.14
119.69
113.73
111.70
101.13
69.80
59.10
53.00
52.66
14.14
12.24
EtO2C
Cl
Cl
N
NH
NH
O
O
3p
f1 (ppm)

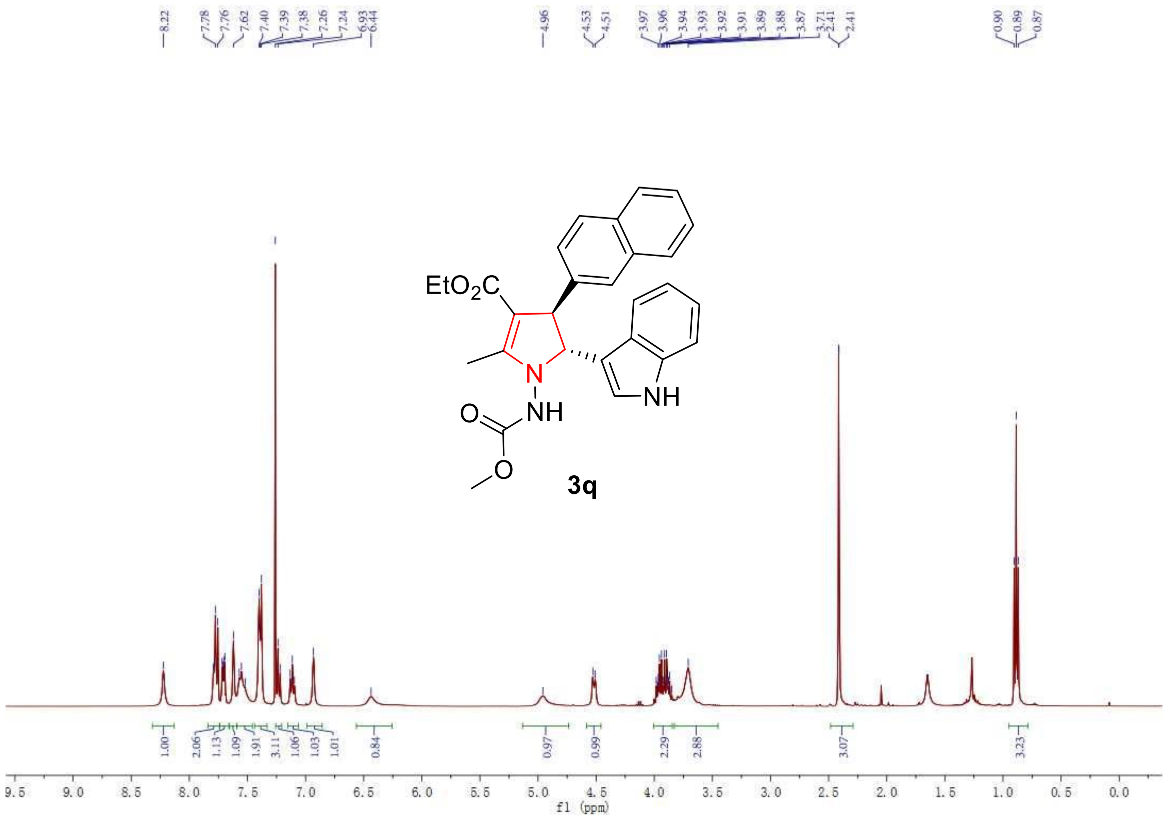

8.22
7.78
7.76
7.62
7.40
7.39
7.38
7.26
7.24
6.93
6.44
4.96
4.53
4.51
3.97
3.96
3.94
3.93
3.92
3.91
3.89
3.88
3.87
3.71
2.41
2.41
0.90
0.89
0.87
EtO2C
N
NH
O
O
NH
3q
1.00
2.06
1.13
1.09
1.91
3.11
1.06
1.03
1.01
0.84
0.97
0.99
2.29
2.88
3.07
3.23
9.5
9.0
8.5
8.0
7.5
7.0
6.5
6.0
5.5
5.0
4.5
4.0
3.5
3.0
2.5
2.0
1.5
1.0
0.5
0.0
f1 (ppm)

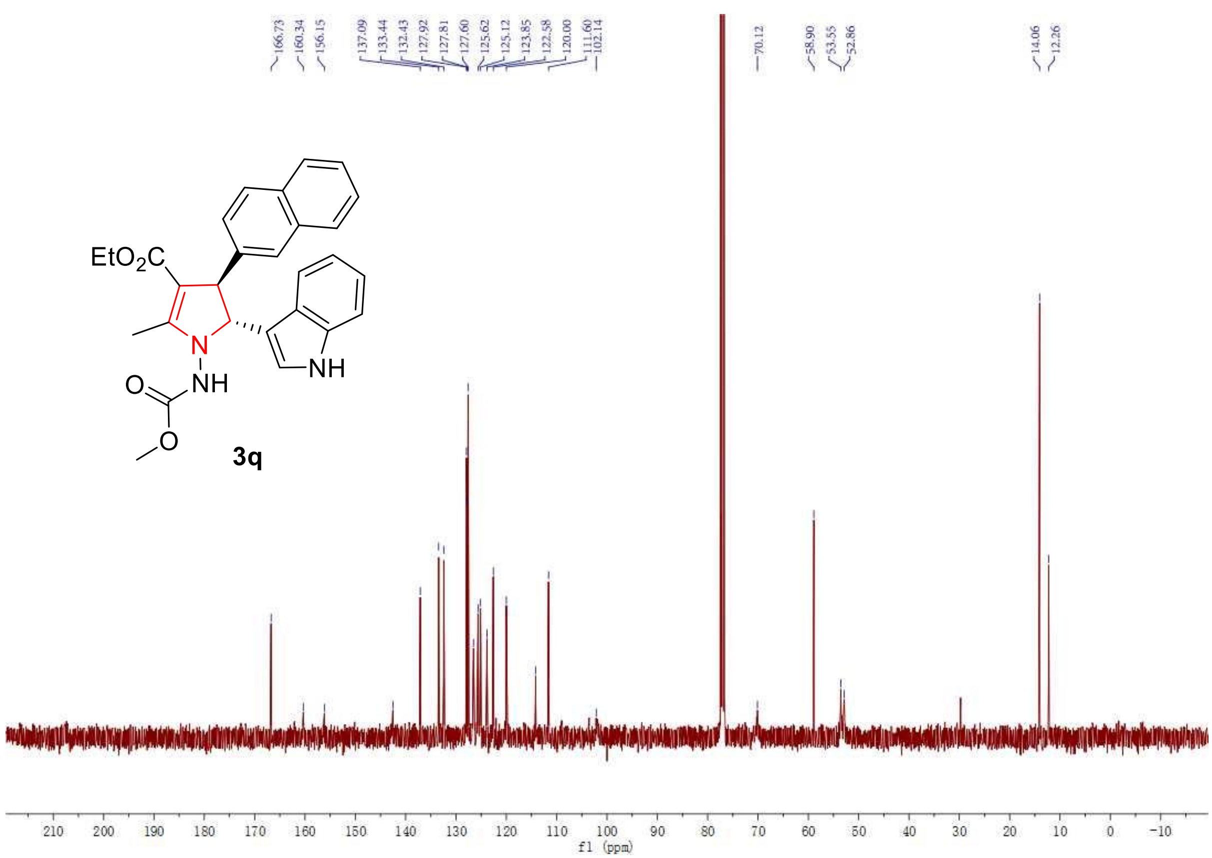

166.73
160.34
156.15
137.09
133.44
132.43
127.92
127.81
127.60
125.62
125.12
123.85
122.58
120.00
111.60
102.14
70.12
58.90
53.55
52.86
14.06
12.26
EtO2C
N
NH
O
O
NH
3q
210
200
190
180
170
160
150
140
130
120
110
100
90
80
70
60
50
40
30
20
10
0
-10
f1 (ppm)

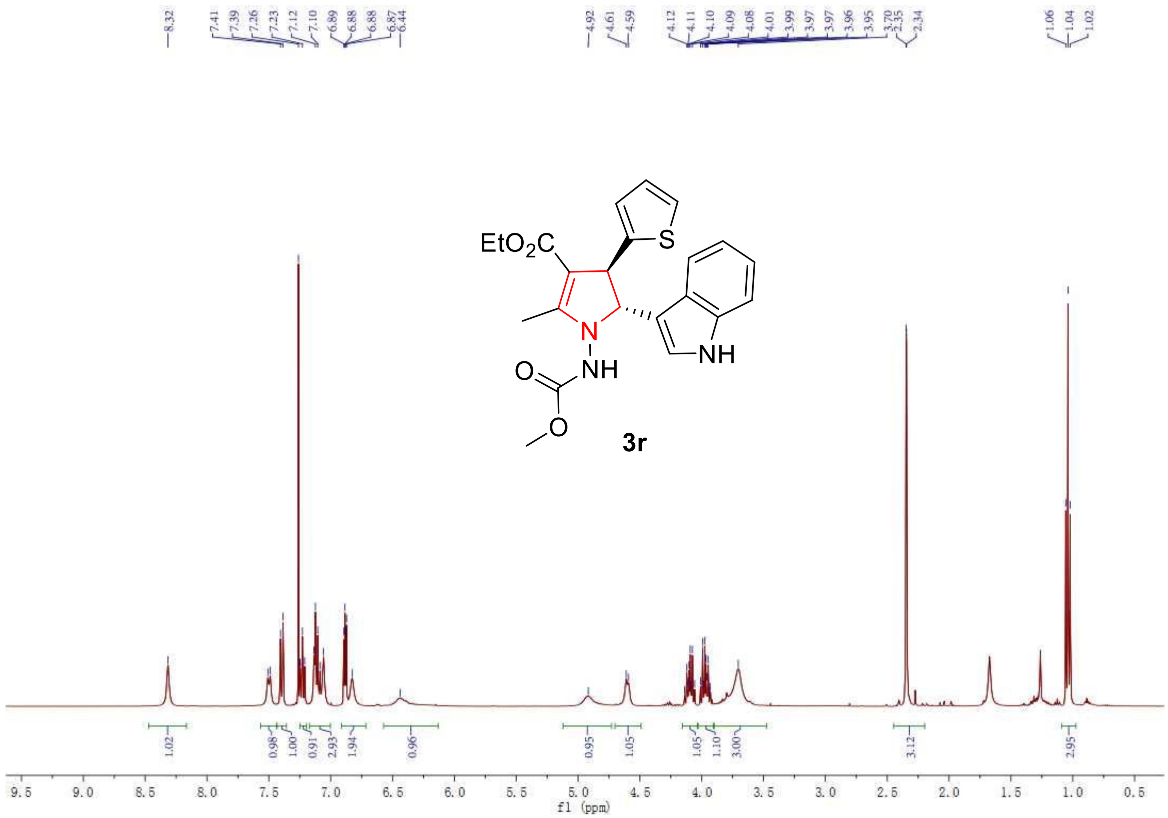
8.32 7.41 7.39 7.26 7.23 7.12 7.10 6.89 6.88 6.88 6.87 6.44
4.92 4.61 4.59 4.12 4.11 4.10 4.09 4.08 4.01 3.99 3.97 3.97 3.96 3.95 3.70 2.35 2.34
1.06 1.04 1.02
EtO2C
S
N
NH
NH
O
O
3r
1.02 0.98 1.00 0.91 2.93 1.94 0.96 0.95 1.05 1.05 1.10 3.00 3.12 2.95
f1 (ppm)

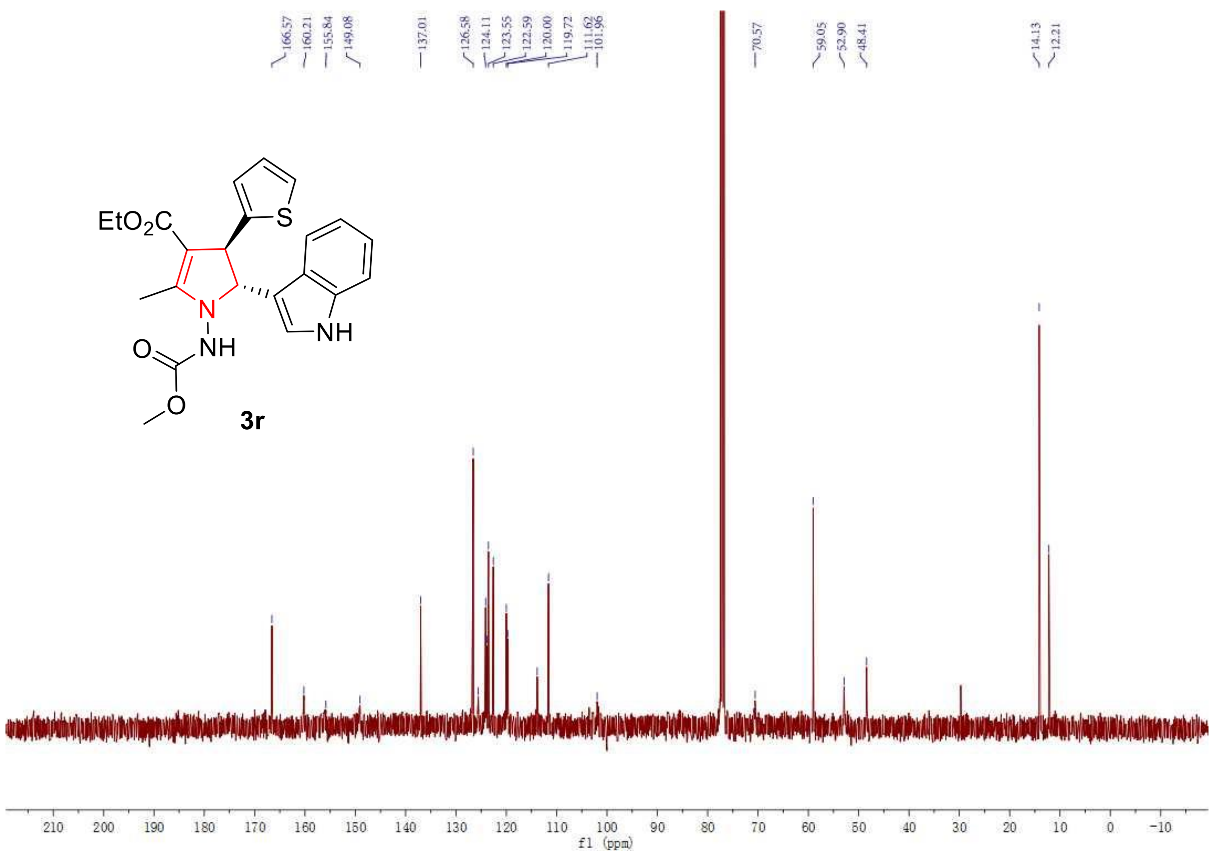
166.57 160.21 155.84 149.08 137.01 126.58 124.11 123.55 122.59 120.00 119.72 111.62 101.96
70.57 59.05 52.90 48.41 14.13 12.21
EtO2C
S
N
NH
NH
O
O
3r
f1 (ppm)

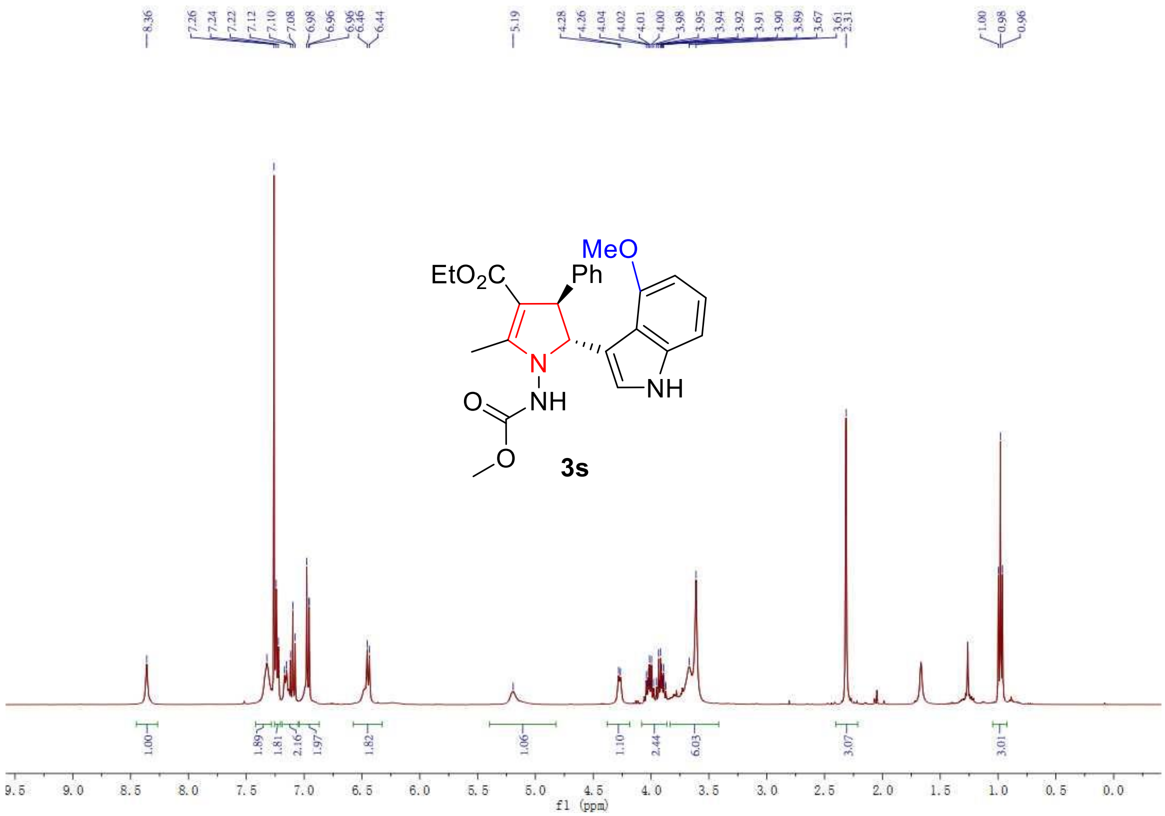
8.36, 7.26, 7.24, 7.22, 7.12, 7.10, 7.08, 6.98, 6.96, 6.96, 6.46, 6.44, 5.19, 4.28, 4.26, 4.04, 4.02, 4.01, 4.00, 3.98, 3.95, 3.94, 3.92, 3.91, 3.90, 3.89, 3.67, 3.61, 2.31, 1.00, 0.98, 0.96
MeO
EtO2C
Ph
N
NH
O
NH
O
3s
1.00
1.89
1.81
2.16
1.97
1.82
1.06
1.10
2.44
6.03
3.07
3.01
9.5 9.0 8.5 8.0 7.5 7.0 6.5 6.0 5.5 5.0 4.5 4.0 3.5 3.0 2.5 2.0 1.5 1.0 0.5 0.0
f1 (ppm)

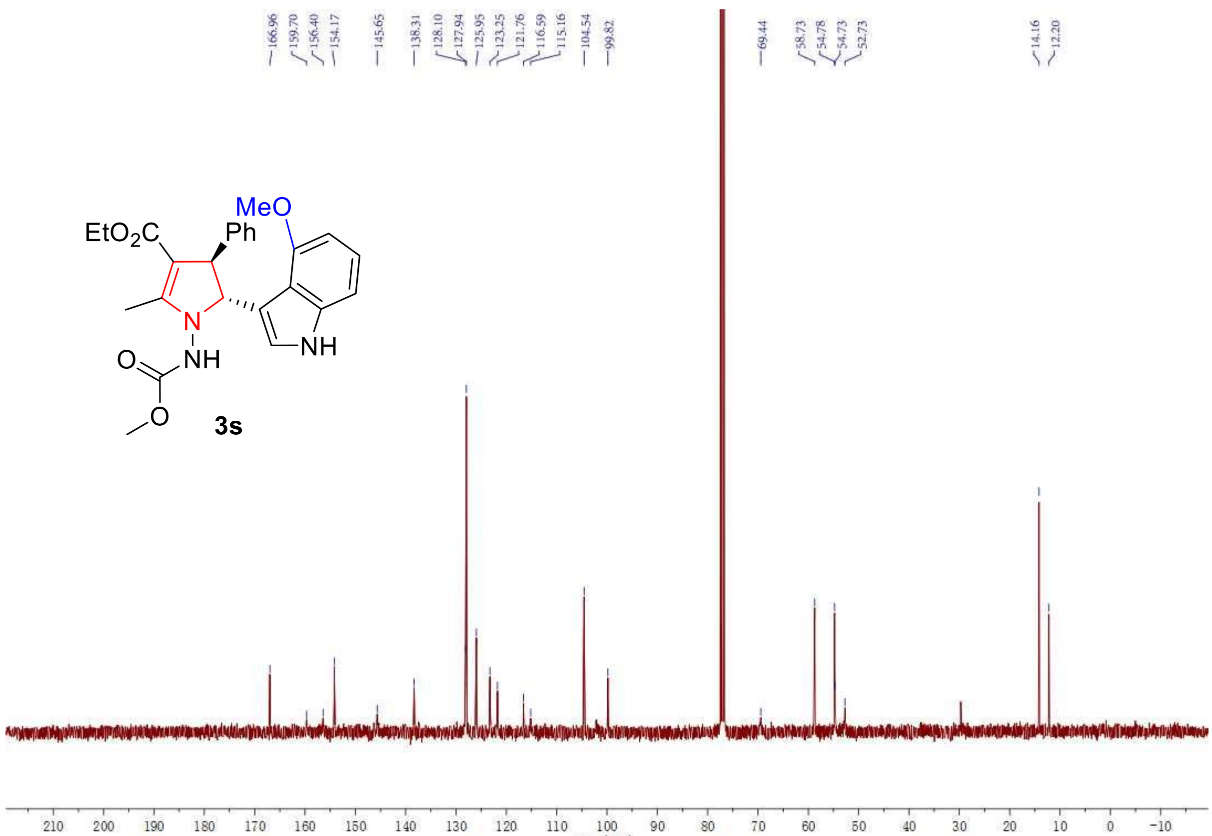
166.96, 159.70, 156.40, 154.17, 145.65, 138.31, 128.10, 127.94, 125.95, 123.25, 121.76, 116.59, 115.16, 104.54, 99.82, 69.44, 58.73, 54.78, 54.73, 52.73, 14.16, 12.20
MeO
EtO2C
Ph
N
NH
O
NH
O
3s
210 200 190 180 170 160 150 140 130 120 110 100 90 80 70 60 50 40 30 20 10 0 -10
f1 (ppm)

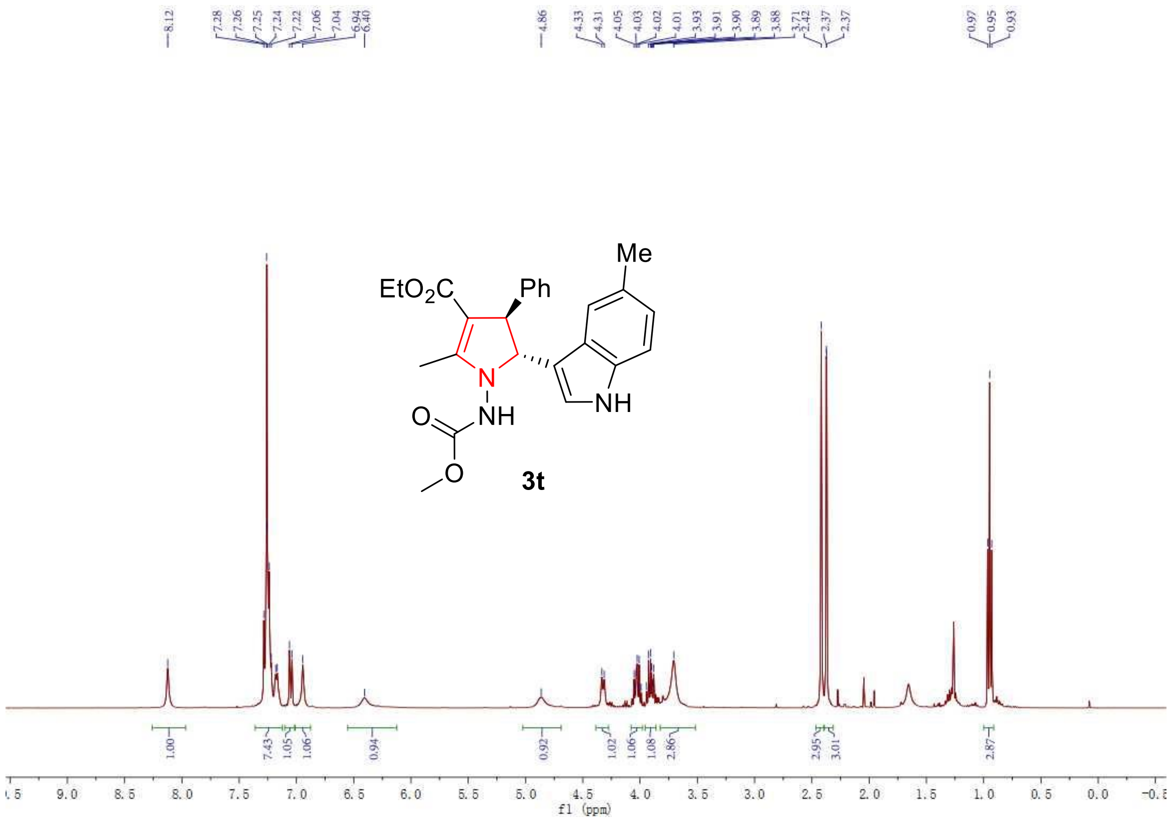
8.12
7.28
7.26
7.25
7.24
7.22
7.06
7.04
6.94
6.40
4.86
4.33
4.31
4.05
4.03
4.02
4.01
3.93
3.91
3.90
3.89
3.88
3.71
2.42
2.37
2.37
0.97
0.95
0.93
EtO2C
Ph
Me
N
NH
O
O
NH
3t
1.00
7.43
1.05
1.06
0.94
0.92
1.02
1.06
1.08
2.86
2.95
3.01
2.87
f1 (ppm)

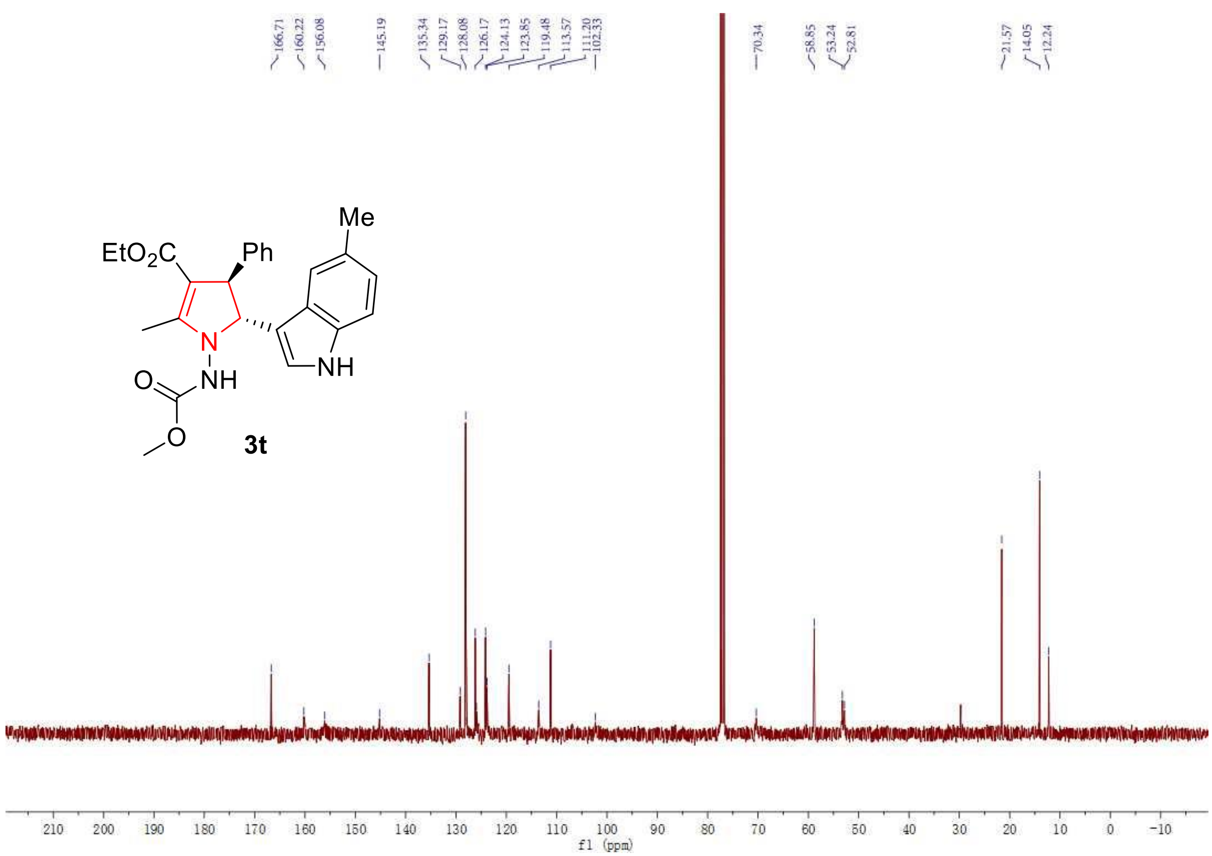
166.71
160.22
156.08
145.19
135.34
129.17
128.08
126.17
124.13
123.85
119.48
113.57
111.20
102.33
70.34
58.85
53.24
52.81
21.57
14.05
12.24
EtO2C
Ph
Me
N
NH
O
O
NH
3t
f1 (ppm)

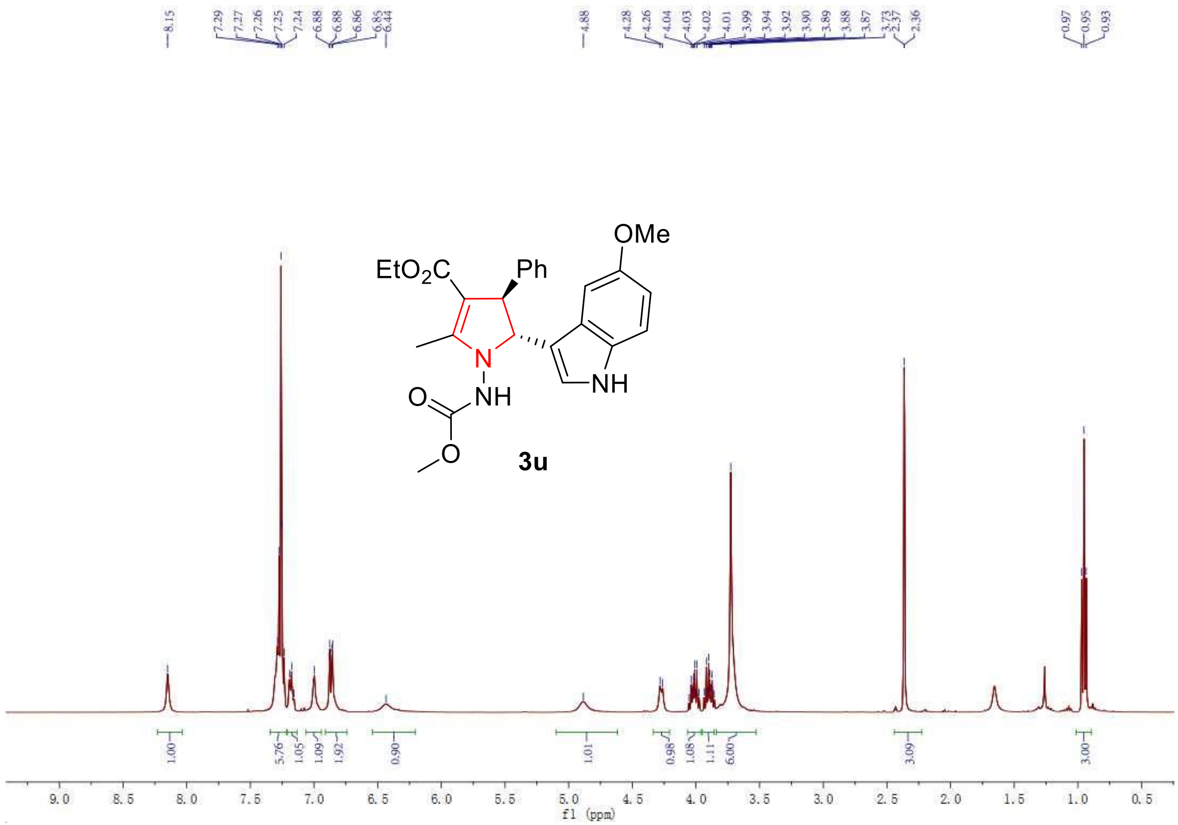
8.15
7.29
7.27
7.26
7.25
7.24
6.88
6.88
6.86
6.85
6.44
4.88
4.28
4.26
4.04
4.03
4.02
4.01
3.99
3.94
3.92
3.90
3.89
3.88
3.87
3.73
2.37
2.36
0.97
0.95
0.93
OMe
EtO_2C
Ph
N
NH
O
O
NH
3u
1.00
5.76
1.05
1.09
1.92
0.90
1.01
0.98
1.08
1.11
6.00
3.09
3.00
f1 (ppm)

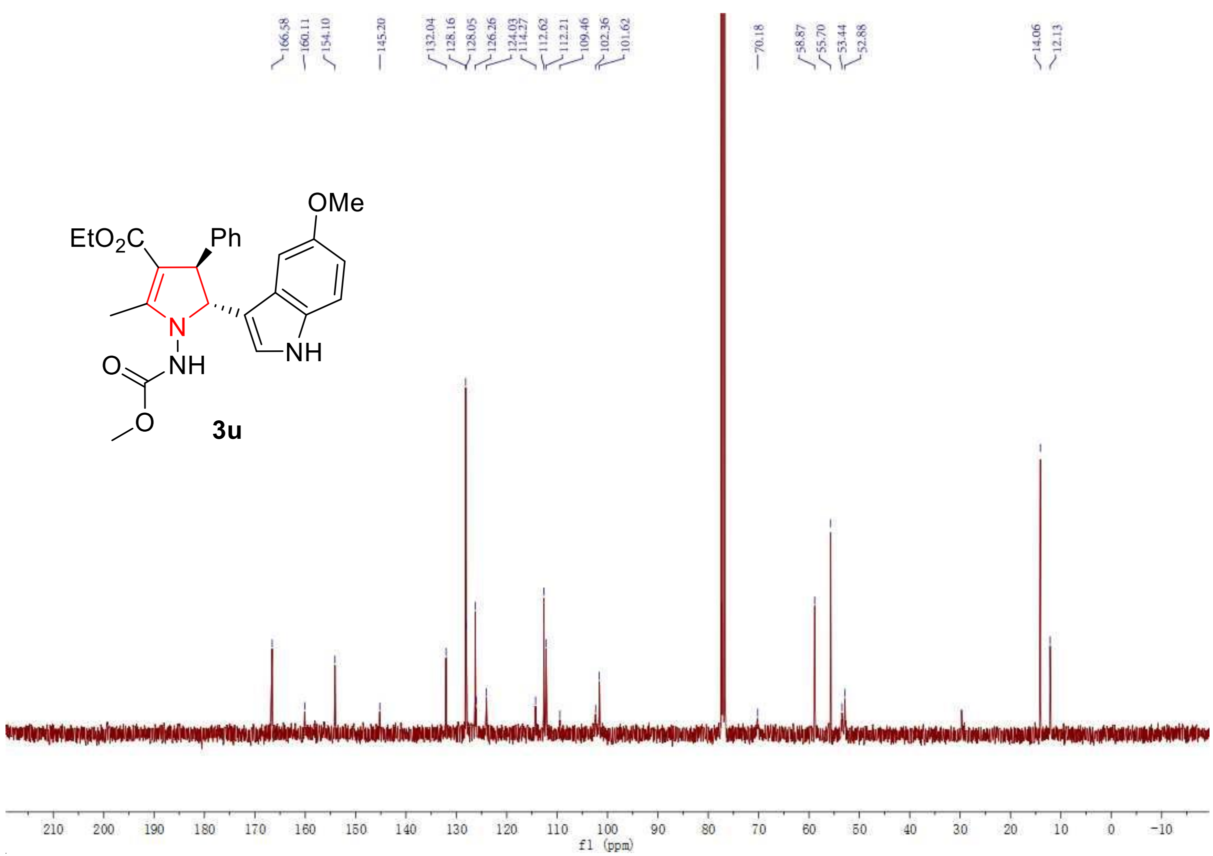
166.58
160.11
154.10
145.20
132.04
128.16
128.05
126.26
124.03
114.27
112.62
112.21
109.46
102.36
101.62
70.18
58.87
55.70
53.44
52.88
14.06
12.13
OMe
EtO_2C
Ph
N
NH
O
O
NH
3u
f1 (ppm)

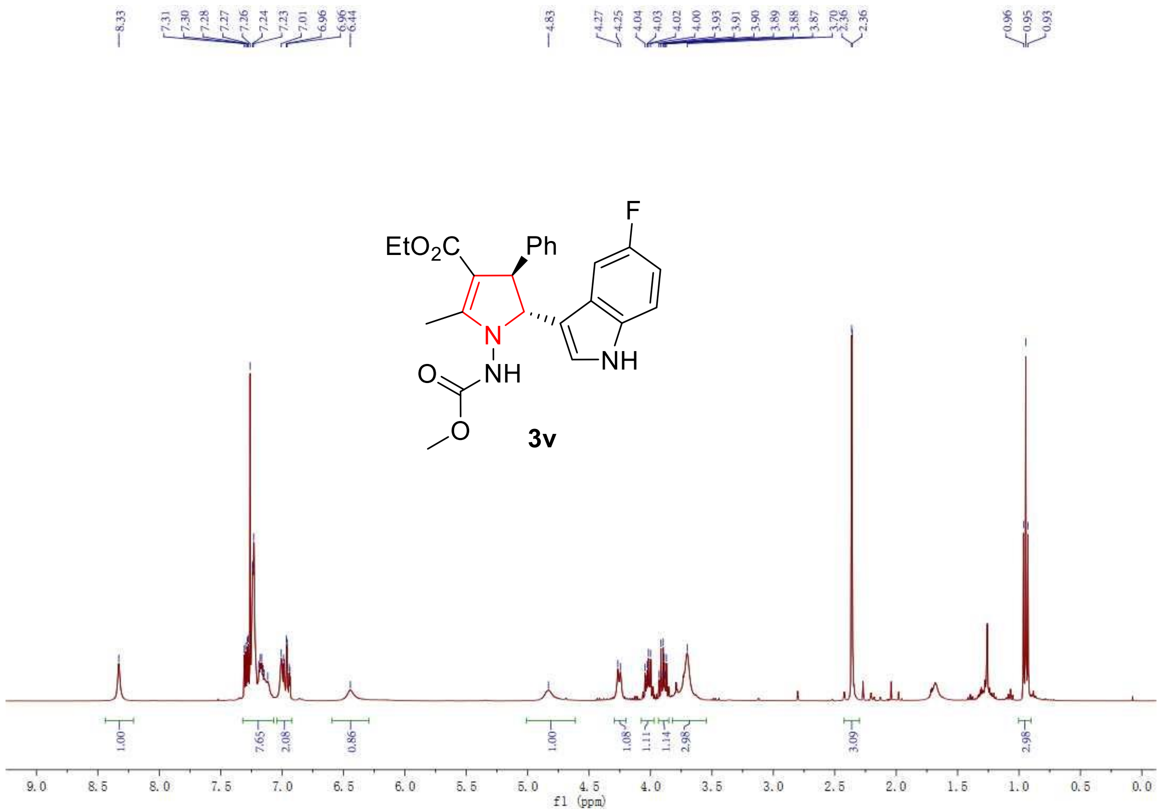
8.33
7.31
7.30
7.28
7.27
7.26
7.24
7.23
7.01
6.96
6.96
6.44
4.83
4.27
4.25
4.04
4.03
4.02
4.00
3.93
3.91
3.90
3.89
3.88
3.87
3.70
2.36
2.36
0.96
0.95
0.93
F
EtO2C
Ph
N
NH
O
NH
O
3v
1.00
7.65
2.08
0.86
1.00
1.08
1.11
1.14
2.98
3.09
2.98
9.0 8.5 8.0 7.5 7.0 6.5 6.0 5.5 5.0 4.5 4.0 3.5 3.0 2.5 2.0 1.5 1.0 0.5 0.0
f1 (ppm)

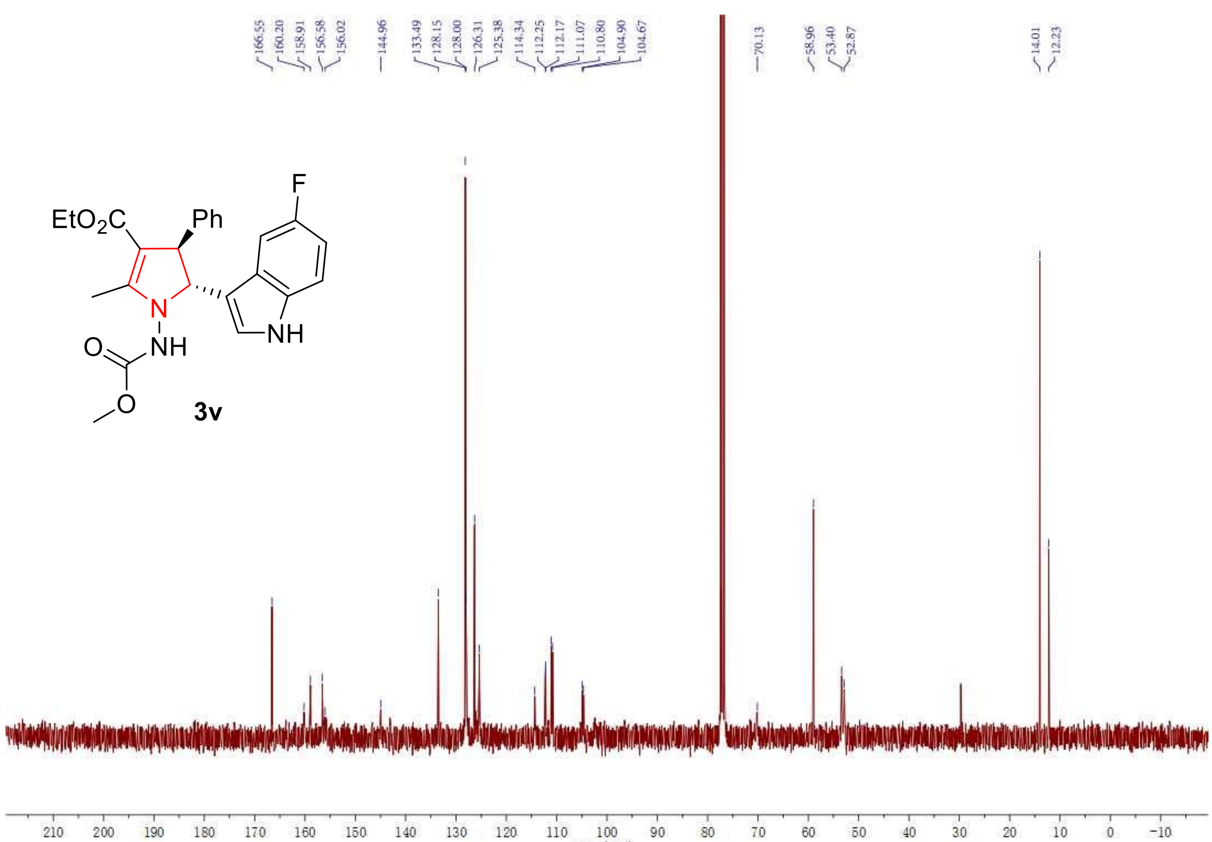
166.55
160.20
158.91
156.58
156.02
144.96
133.49
128.15
128.00
126.31
125.38
114.34
112.25
112.17
111.07
110.80
104.90
104.67
70.13
58.96
53.40
52.87
14.01
12.23
F
EtO2C
Ph
N
NH
O
NH
O
3v
210 200 190 180 170 160 150 140 130 120 110 100 90 80 70 60 50 40 30 20 10 0 -10
f1 (ppm)

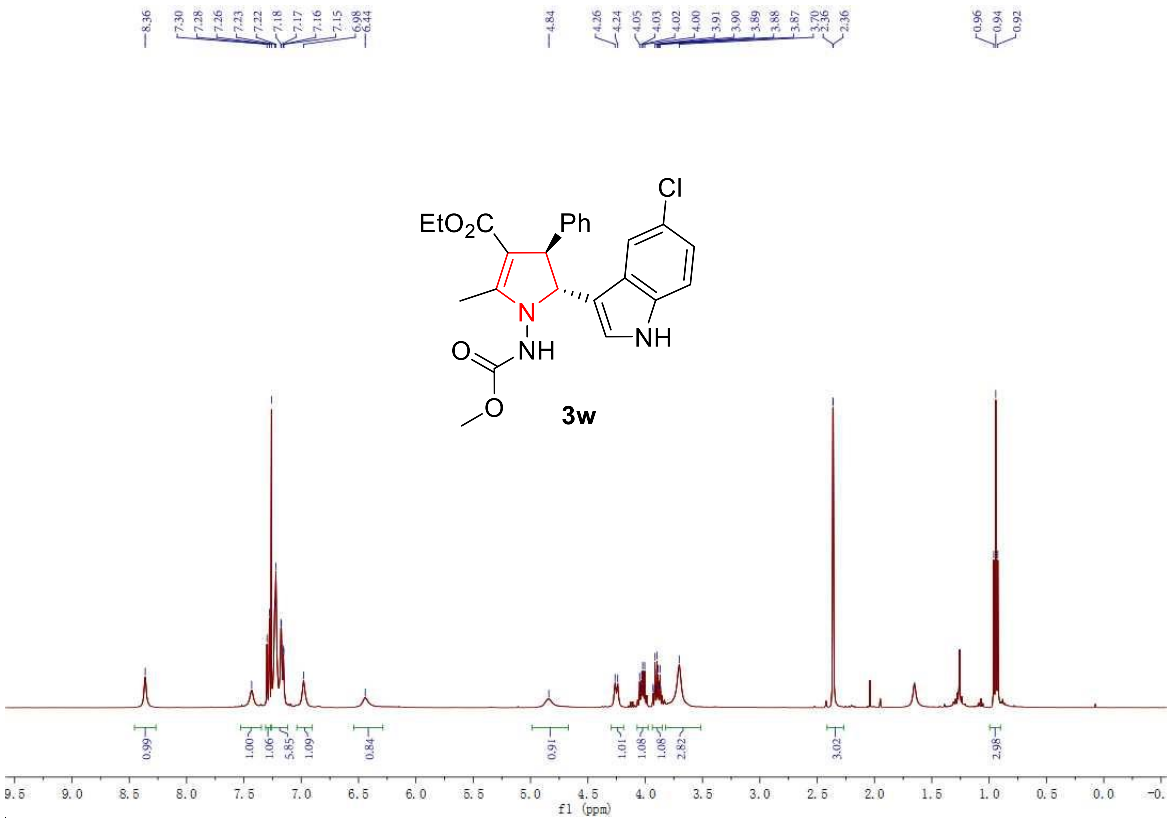
8.36
7.30
7.28
7.26
7.23
7.22
7.18
7.17
7.16
7.15
6.98
6.44
4.84
4.26
4.24
4.05
4.03
4.02
4.00
3.91
3.90
3.89
3.88
3.87
3.70
2.36
2.36
0.96
0.94
0.92
EtO2C
Ph
Cl
N
NH
NH
O
O
3w
0.99
1.00
1.06
5.85
1.09
0.84
0.91
1.01
1.08
1.08
2.82
3.02
2.98
f1 (ppm)

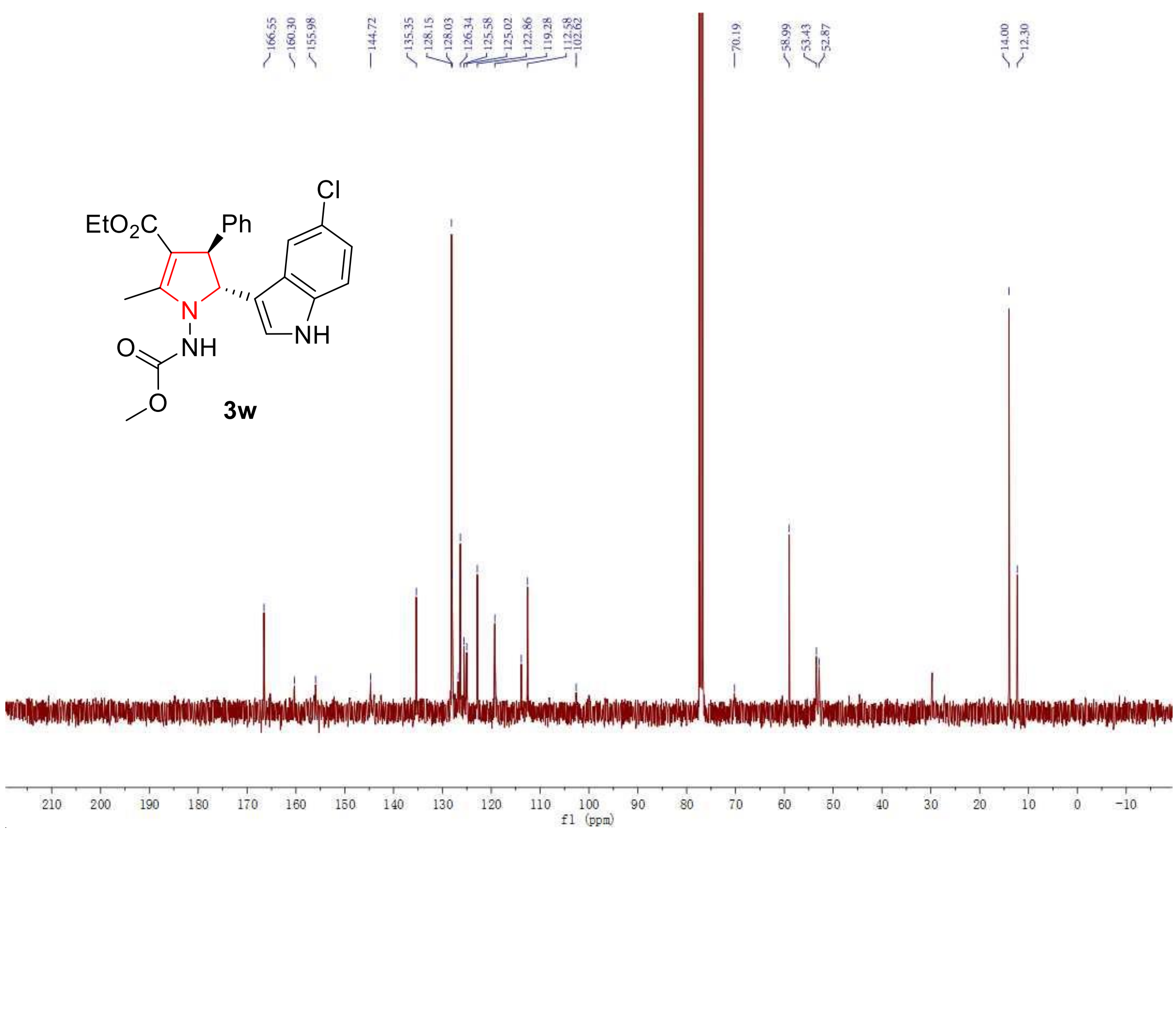
166.55
160.30
155.98
144.72
135.35
128.15
128.03
126.34
125.58
125.02
122.86
119.28
112.58
102.62
70.19
58.99
53.43
52.87
14.00
12.30
EtO2C
Ph
Cl
N
NH
NH
O
O
3w
f1 (ppm)

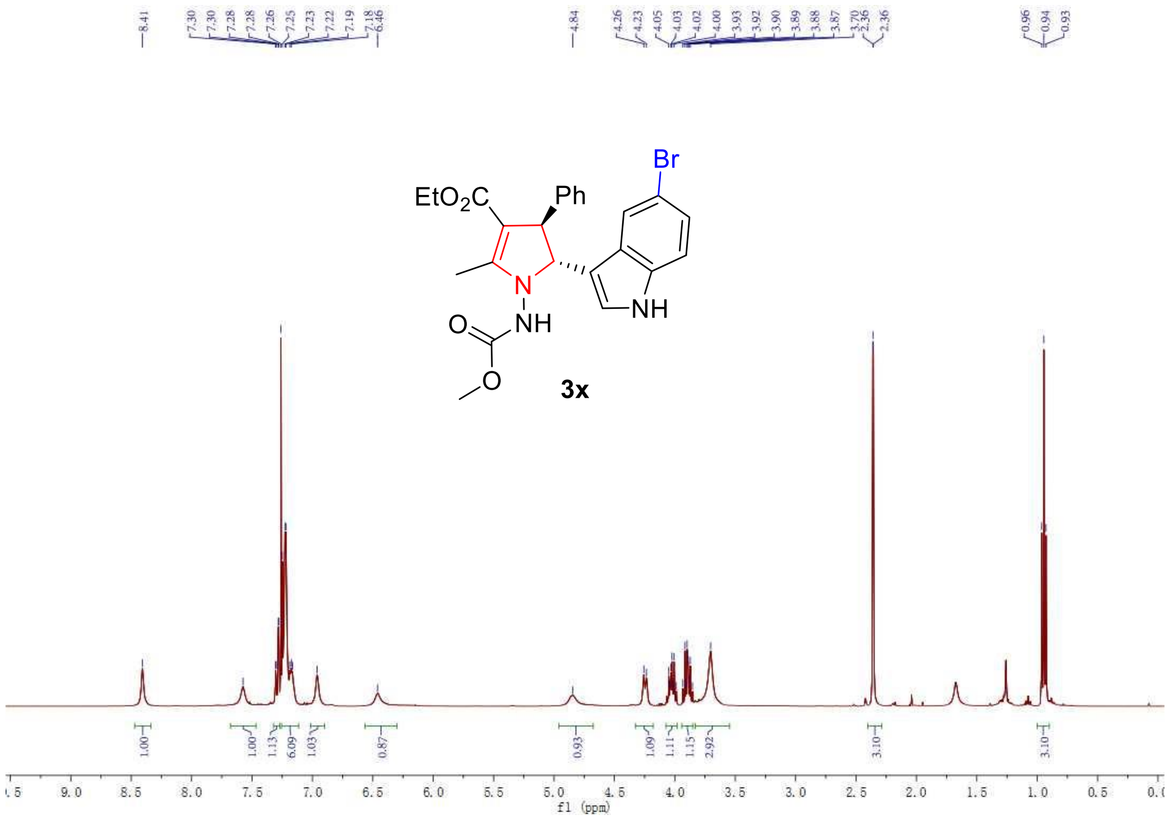
8.41 7.30 7.30 7.28 7.28 7.26 7.25 7.23 7.22 7.19 7.18 6.46
4.84 4.26 4.23 4.05 4.03 4.02 4.00 3.93 3.92 3.90 3.89 3.88 3.87 3.70 2.36 2.36
0.96 0.94 0.93
EtO2C
Ph
Br
N
NH
O
O
NH
3x
1.00 1.00 1.13 6.09 1.03 0.87 0.93 1.09 1.11 1.15 2.92 3.10 3.10
f1 (ppm)

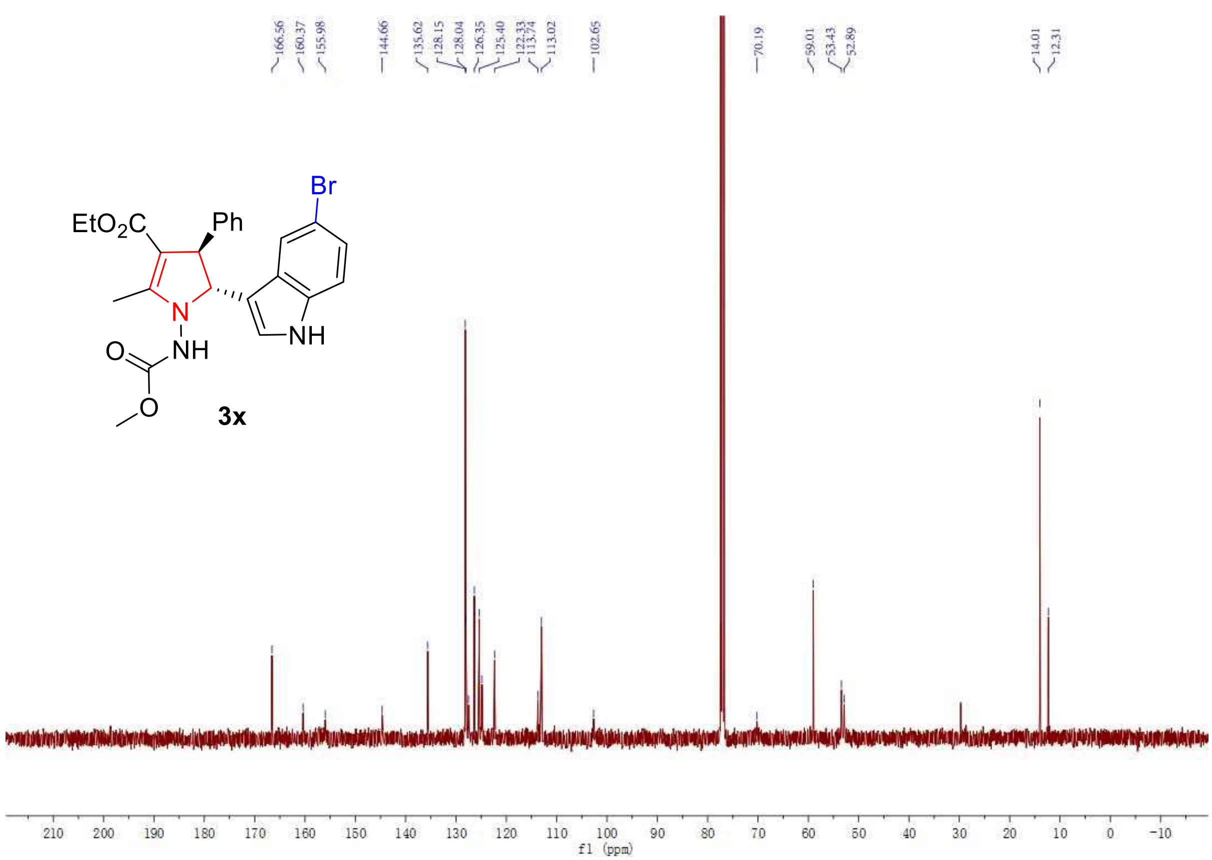
166.56 160.37 155.98 144.66 135.62 128.15 128.04 126.35 125.40 122.33 113.74 113.02 102.65 70.19 59.01 53.43 52.89 14.01 12.31
EtO2C
Ph
Br
N
NH
O
O
NH
3x
f1 (ppm)

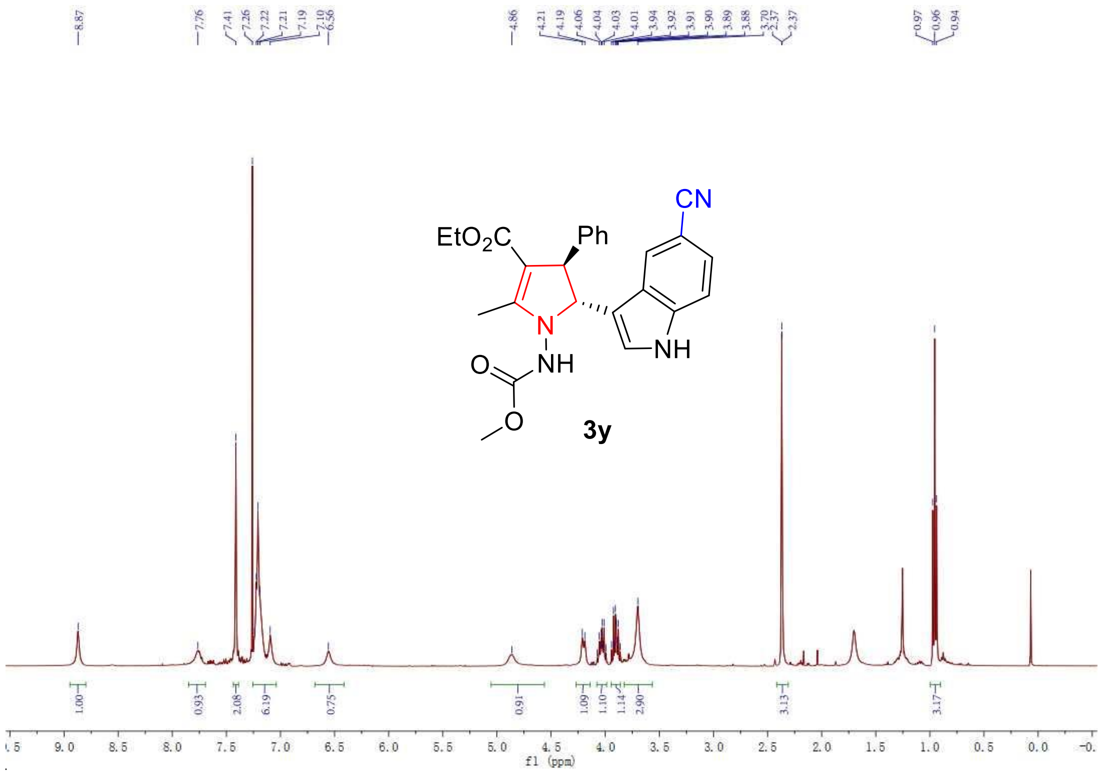
8.87
7.76
7.41
7.26
7.22
7.21
7.19
7.10
6.56
4.86
4.21
4.19
4.06
4.04
4.03
4.01
3.94
3.92
3.91
3.90
3.89
3.88
3.70
2.37
2.37
0.97
0.96
0.94
EtO2C
Ph
CN
N
NH
O
O
NH
3y
1.00
0.93
2.08
6.19
0.75
0.91
1.09
1.10
1.14
2.90
3.13
3.17
f1 (ppm)

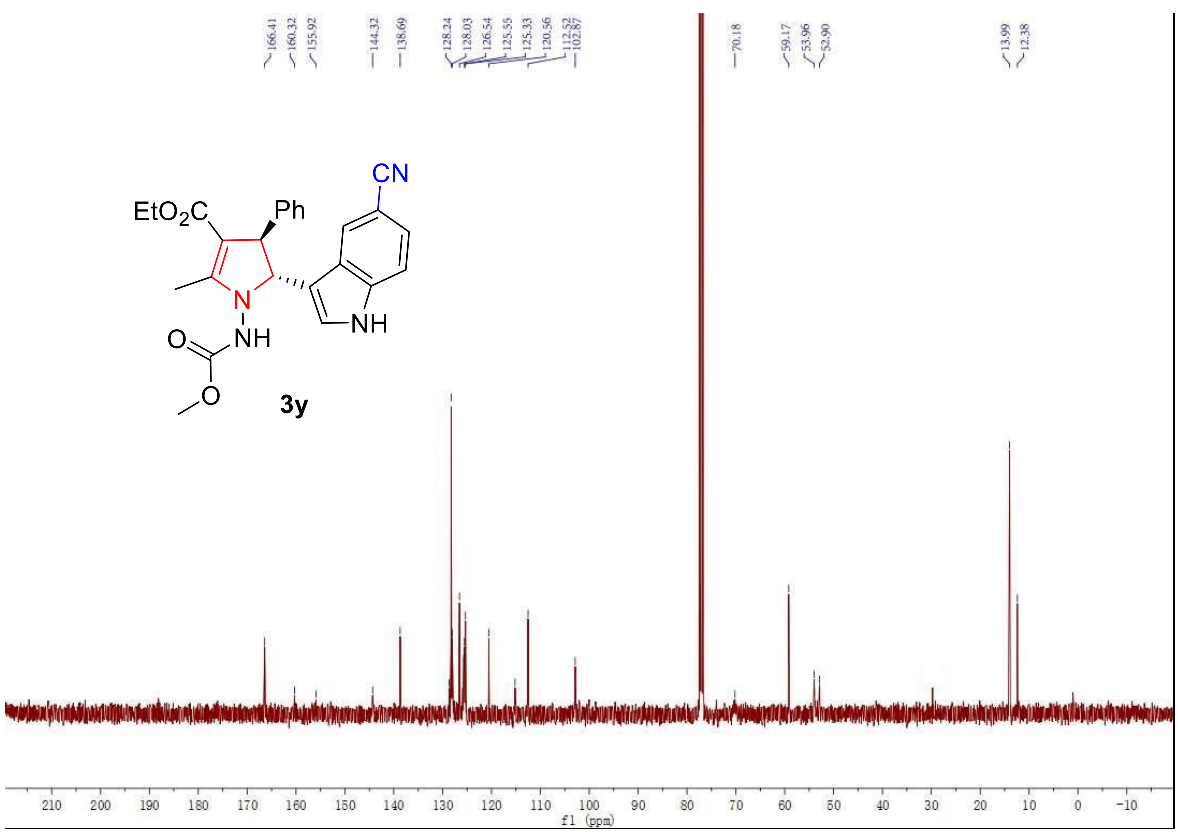
166.41
160.32
155.92
144.32
138.69
128.24
128.03
126.54
125.55
125.33
120.56
112.52
102.87
70.18
59.17
53.96
52.90
13.99
12.38
EtO2C
Ph
CN
N
NH
O
O
NH
3y
f1 (ppm)

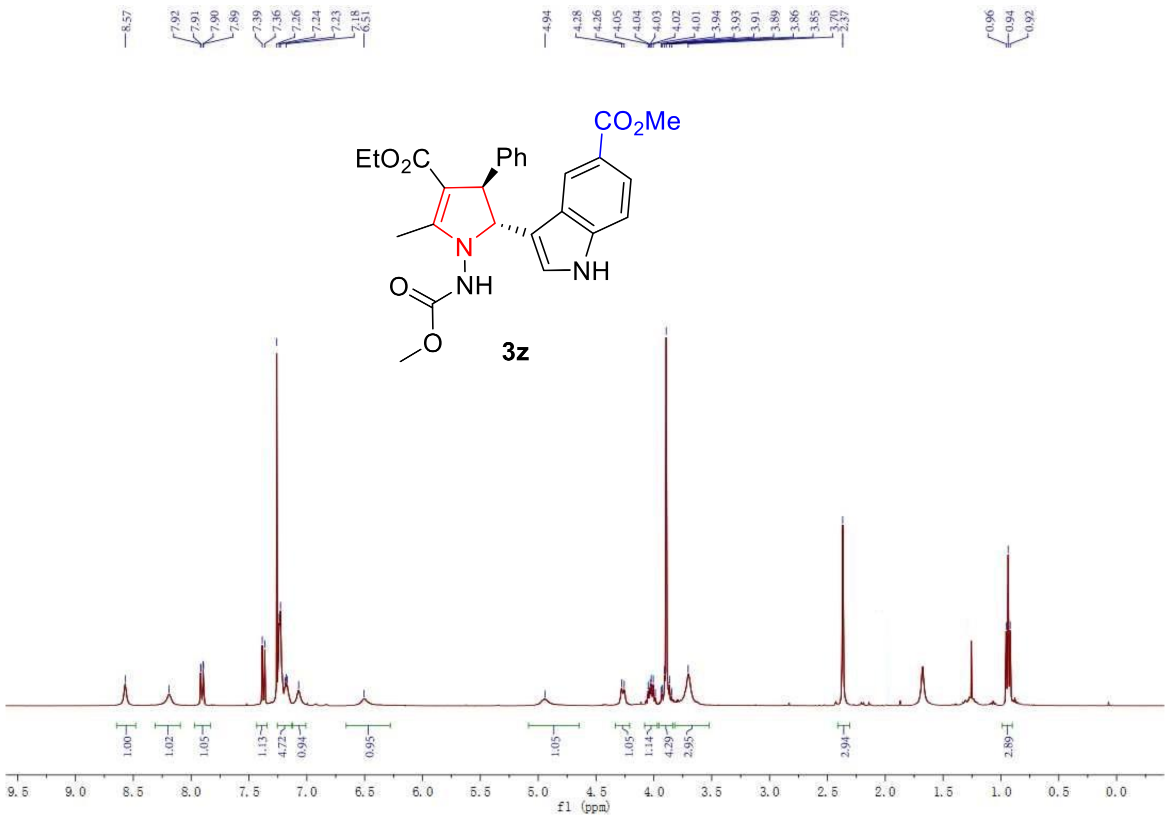
8.57
7.92 7.91 7.90 7.89 7.39 7.36 7.26 7.24 7.23 7.18 6.51
4.94
4.28 4.26 4.05 4.04 4.03 4.02 4.01 3.94 3.93 3.91 3.89 3.86 3.85 3.70 2.37
0.96 0.94 0.92
CO2Me
EtO2C
Ph
N
NH
O
NH
O
3z
1.00 1.02 1.05 1.13 4.72 0.94 0.95 1.05 1.05 1.14 4.29 2.95 2.94 2.89
f1 (ppm)

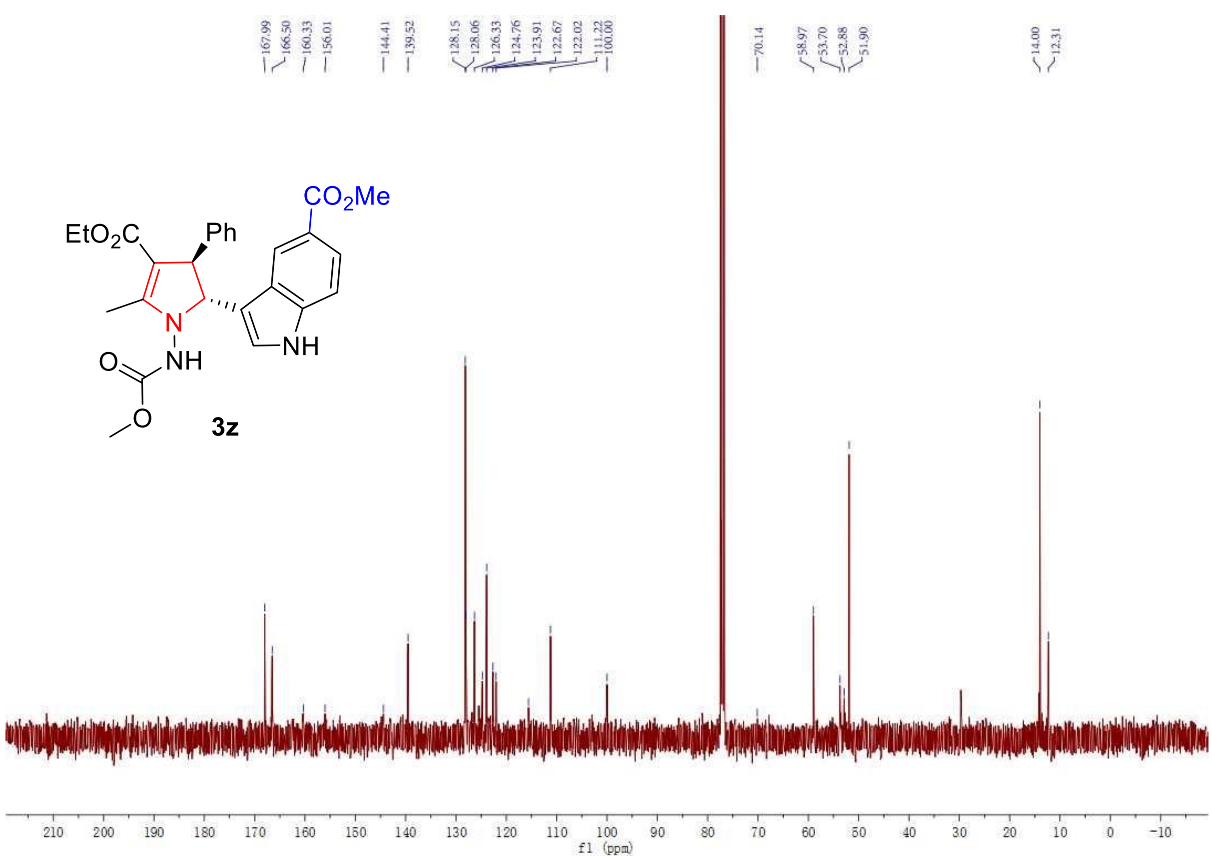
167.99 166.50 160.33 156.01 144.41 139.52 128.15 128.06 126.33 124.76 123.91 122.67 122.02 111.22 100.00
70.14 58.97 53.70 52.88 51.90 14.00 12.31
CO2Me
EtO2C
Ph
N
NH
O
NH
O
3z
f1 (ppm)

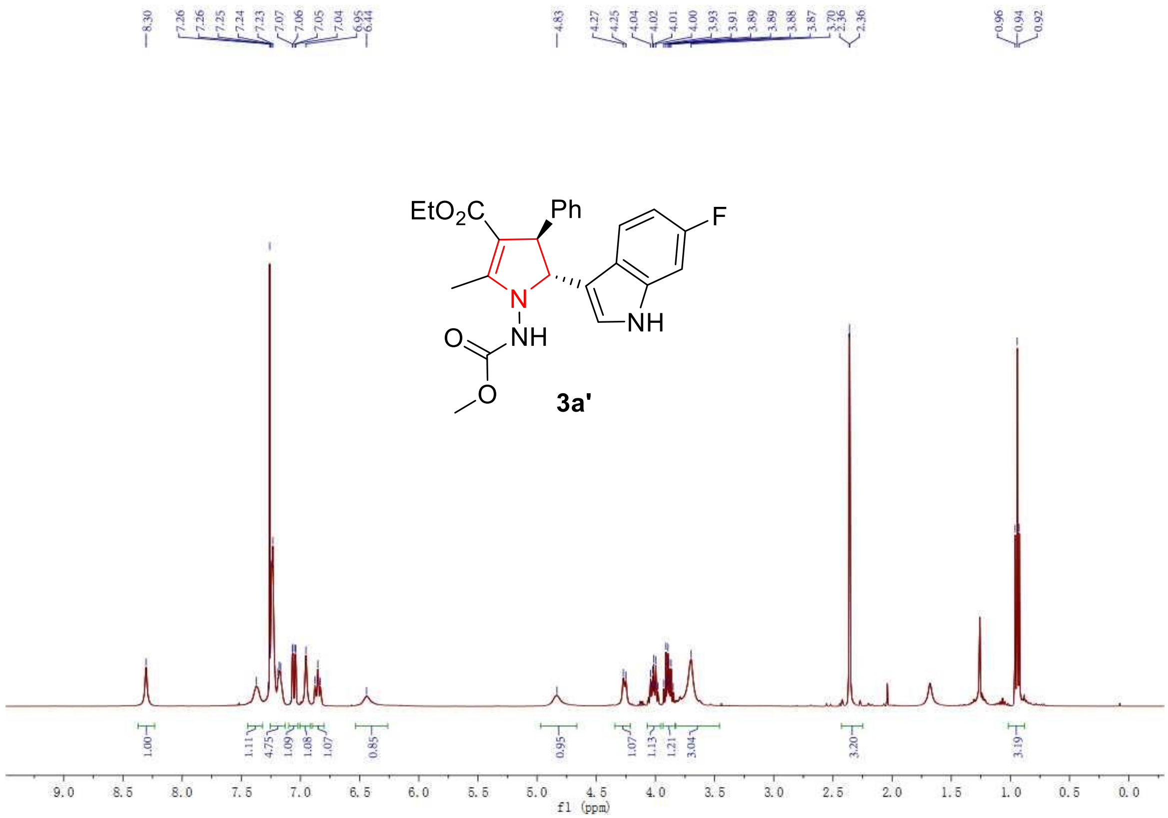
8.30
7.26
7.26
7.25
7.24
7.23
7.07
7.06
7.05
7.04
6.95
6.44
4.83
4.27
4.25
4.04
4.02
4.01
4.00
3.93
3.91
3.89
3.89
3.88
3.87
3.70
2.36
2.36
0.96
0.94
0.92
EtO2C
Ph
F
N
NH
NH
O
O
1.00
1.11
4.75
1.09
1.08
1.07
0.85
0.95
1.07
1.13
1.21
3.04
3.20
3.19
f1 (ppm)

3a'

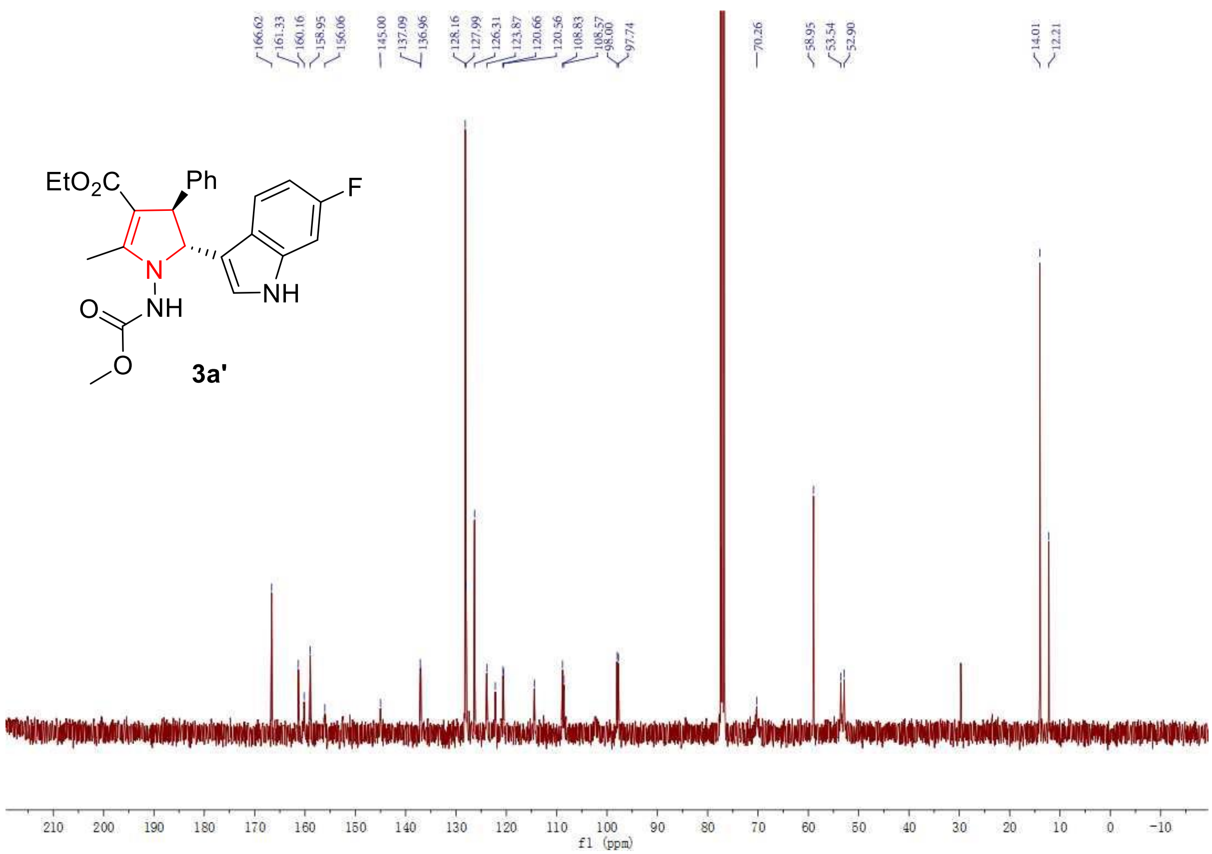
166.62
161.33
160.16
158.95
156.06
145.00
137.09
136.96
128.16
127.99
126.31
123.87
120.66
120.56
108.83
108.57
98.00
97.74
70.26
58.95
53.54
52.90
14.01
12.21
EtO2C
Ph
F
N
NH
NH
O
O
f1 (ppm)

3a'

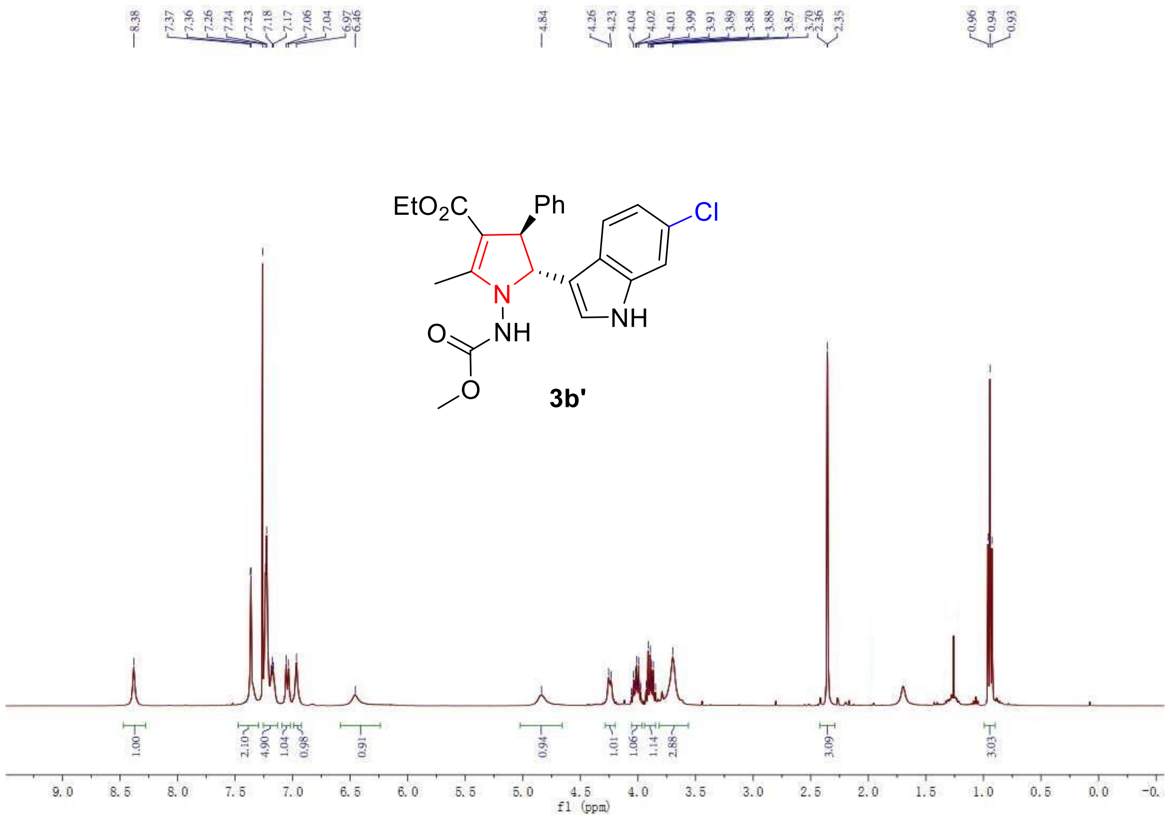
8.38
7.37 7.36 7.26 7.24 7.23 7.18 7.17 7.06 7.04 6.97 6.46
4.84
4.26 4.23 4.04 4.02 4.01 3.99 3.91 3.89 3.88 3.88 3.87 3.70 2.36 2.35
0.96 0.94 0.93
EtO2C
Ph
Cl
N
NH
O
NH
O
3b'
1.00
2.10
4.90
1.04
0.98
0.91
0.94
1.01
1.06
1.14
2.88
3.09
3.03
f1 (ppm)

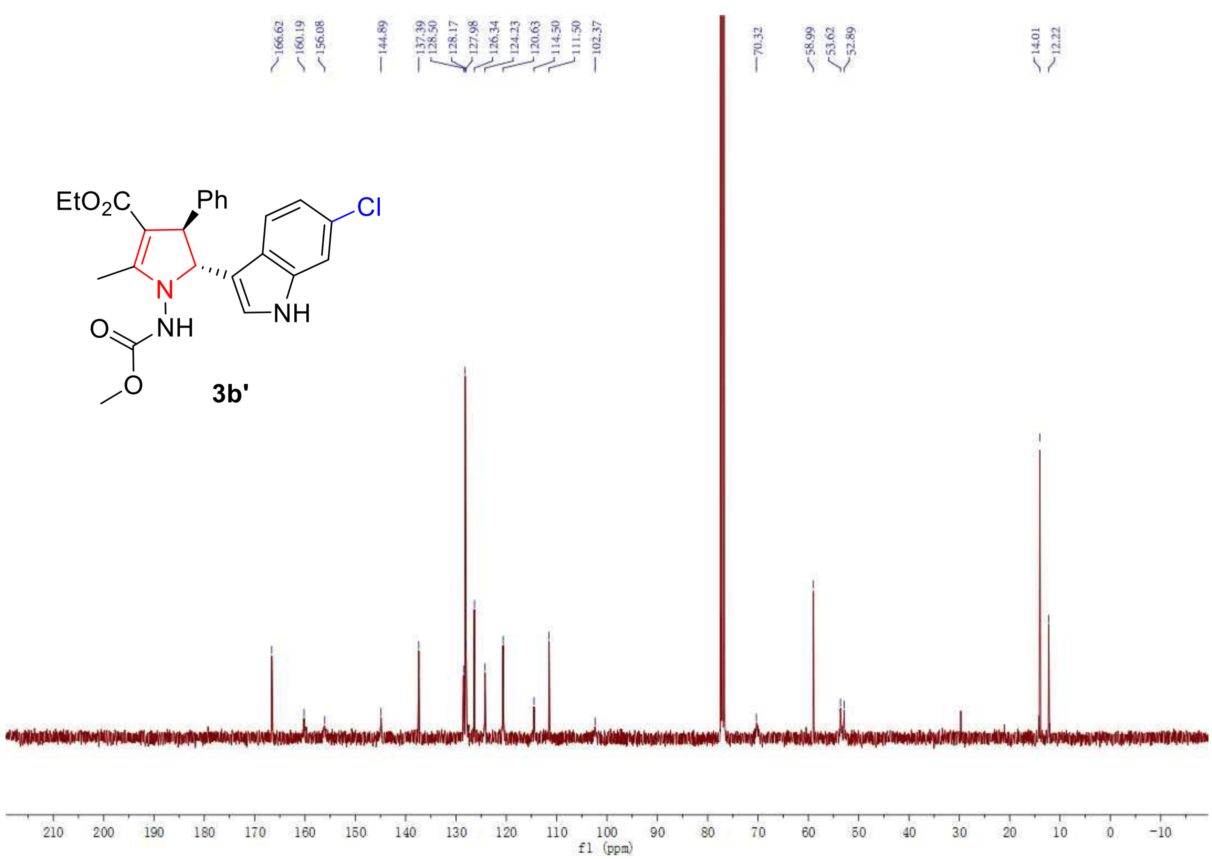
166.62 160.19 156.08
144.89
137.39 128.50 128.17 127.98 126.34 124.23 120.63 114.50 111.50
102.37
70.32
58.99 53.62 52.89
14.01 12.22
EtO2C
Ph
Cl
N
NH
O
NH
O
3b'
f1 (ppm)

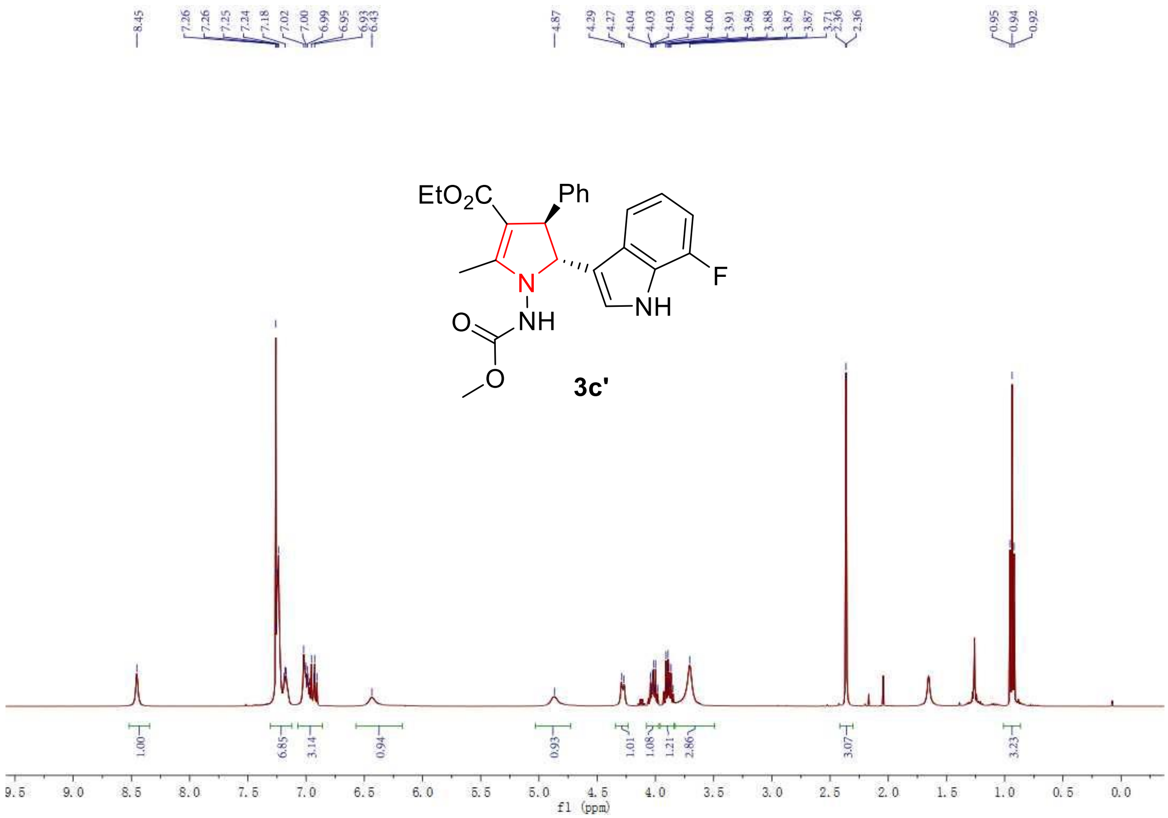
8.45
7.26 7.26 7.25 7.24 7.18 7.02 7.00 6.99 6.95 6.93 6.43
4.87
4.29 4.27 4.04 4.03 4.03 4.02 4.00 3.91 3.89 3.88 3.87 3.87 3.71 2.36 2.36
0.95 0.94 0.92
EtO2C
Ph
F
N
NH
NH
O
O
3c'
1.00 6.85 3.14 0.94 0.93 1.01 1.08 1.21 2.86 3.07 3.23
9.5 9.0 8.5 8.0 7.5 7.0 6.5 6.0 5.5 5.0 4.5 4.0 3.5 3.0 2.5 2.0 1.5 1.0 0.5 0.0
f1 (ppm)

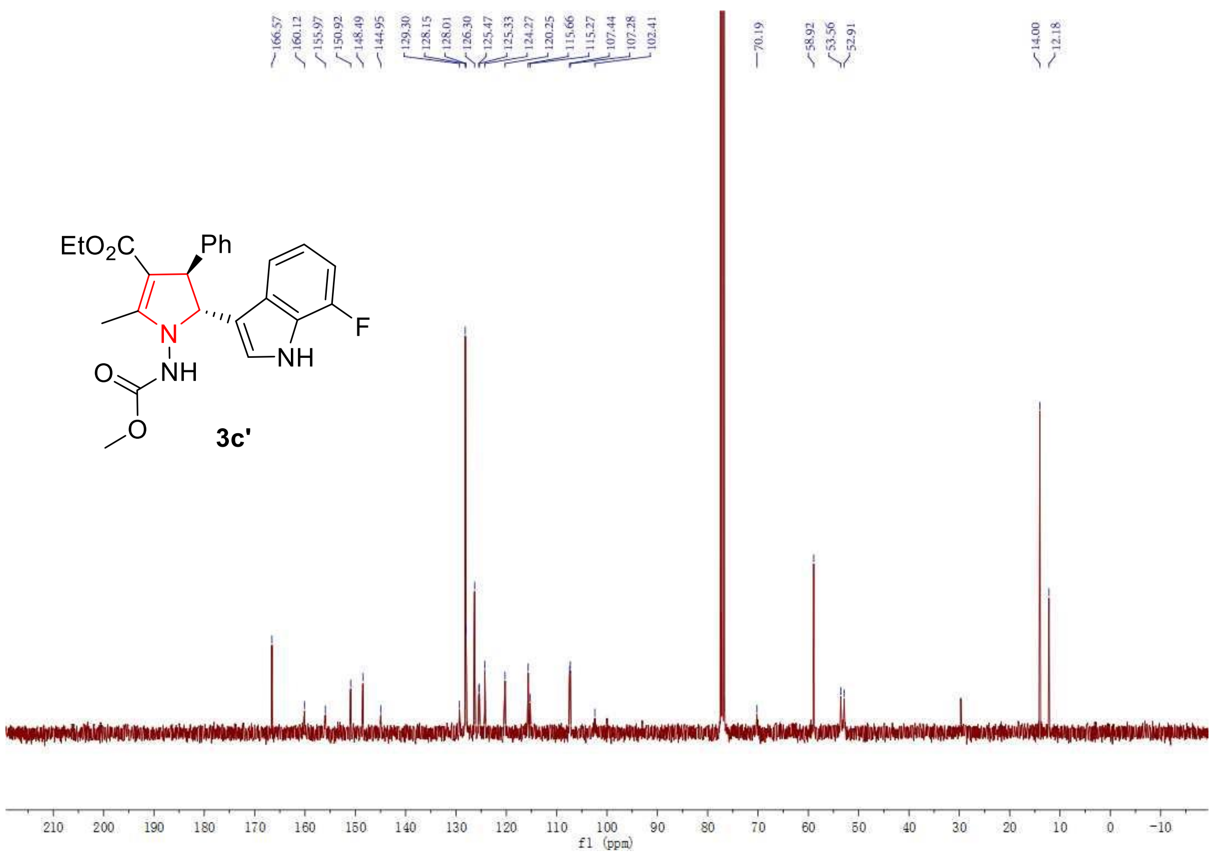
166.57 160.12 155.97 150.92 148.49 144.95
129.30 128.15 128.01 126.30 125.47 125.33 124.27 120.25 115.66 115.27 107.44 107.28 102.41
70.19
58.92 53.56 52.91
14.00 12.18
EtO2C
Ph
F
N
NH
NH
O
O
3c'
210 200 190 180 170 160 150 140 130 120 110 100 90 80 70 60 50 40 30 20 10 0 -10
f1 (ppm)

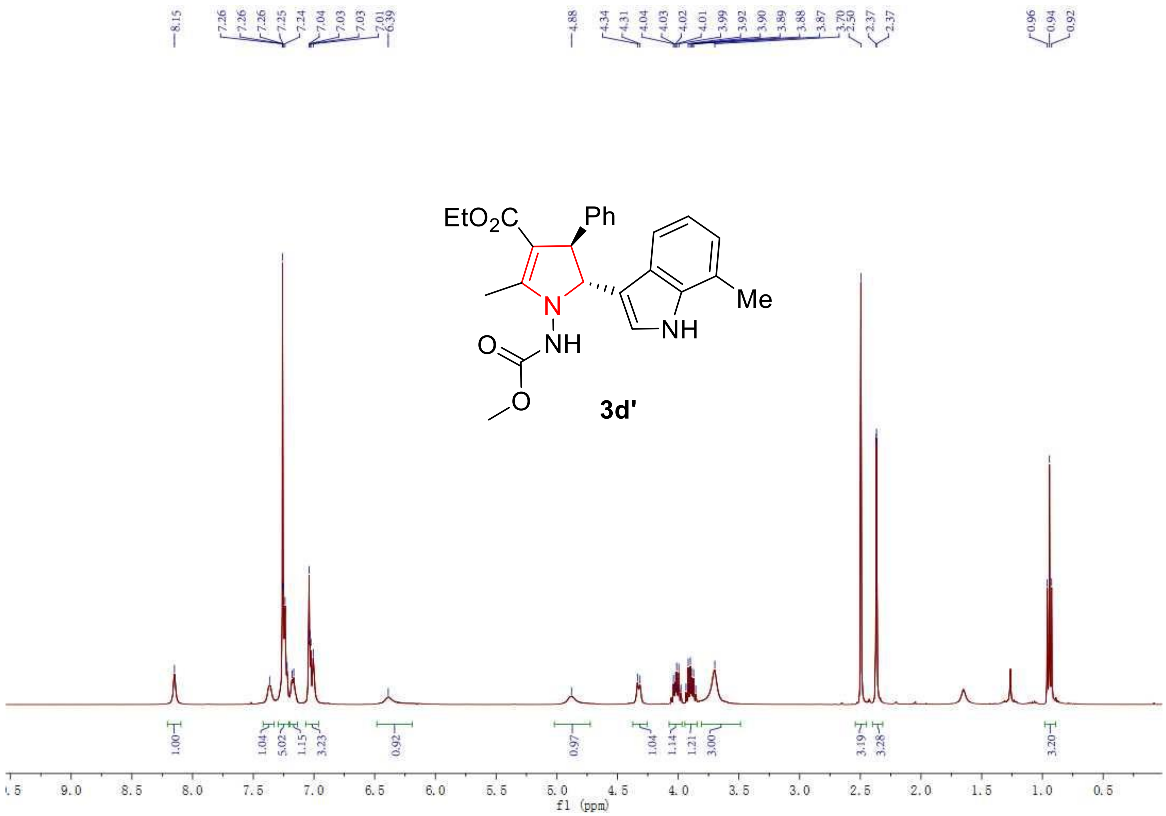
8.15
7.26
7.26
7.26
7.25
7.24
7.04
7.03
7.03
7.01
6.39
4.88
4.34
4.31
4.04
4.03
4.02
4.01
3.99
3.92
3.90
3.89
3.88
3.87
3.70
2.50
2.37
2.37
0.96
0.94
0.92
EtO2C
Ph
Me
N
NH
O
O
NH
3d'
1.00
1.04
5.02
1.15
3.23
0.92
0.97
1.04
1.14
1.21
3.00
3.19
3.28
3.20
f1 (ppm)

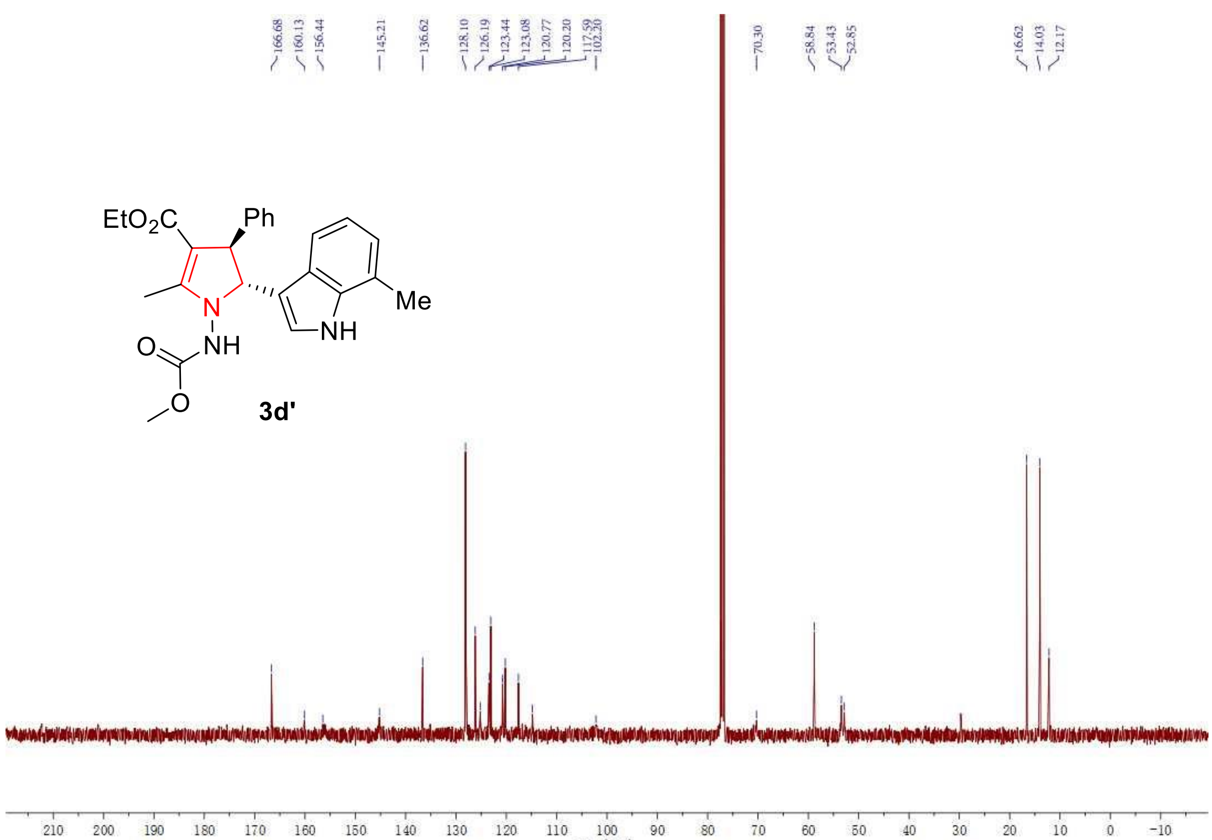
166.68
160.13
156.44
145.21
136.62
128.10
126.19
123.44
123.08
120.77
120.20
117.59
102.20
70.30
58.84
53.43
52.85
16.62
14.03
12.17
EtO2C
Ph
Me
N
NH
O
O
NH
3d'
f1 (ppm)

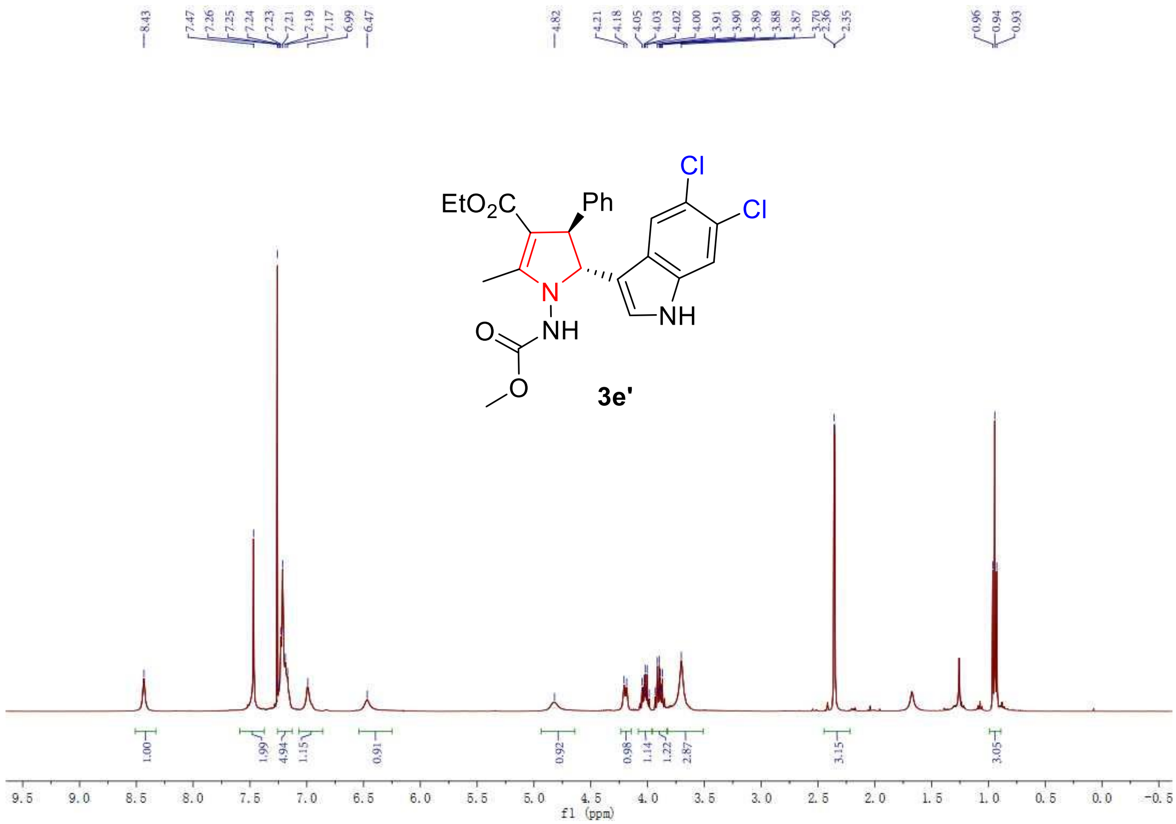

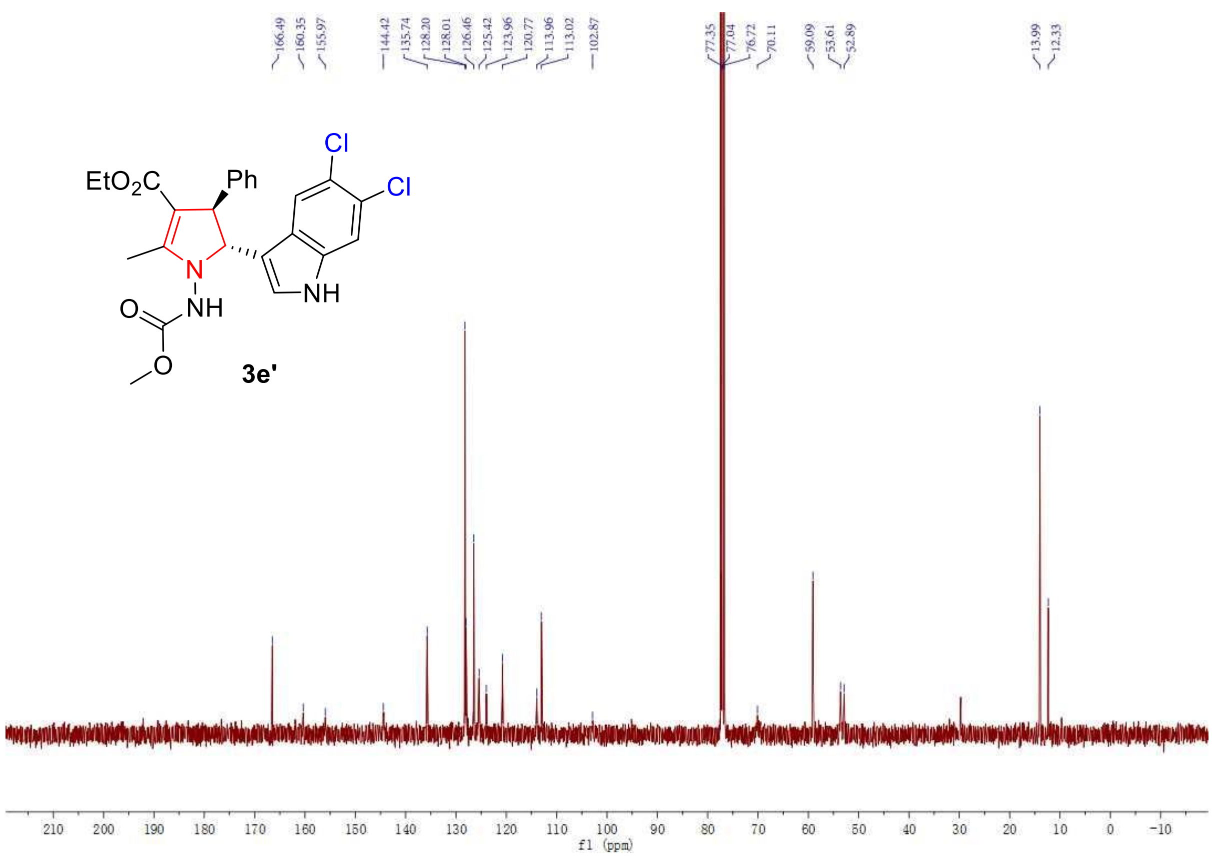

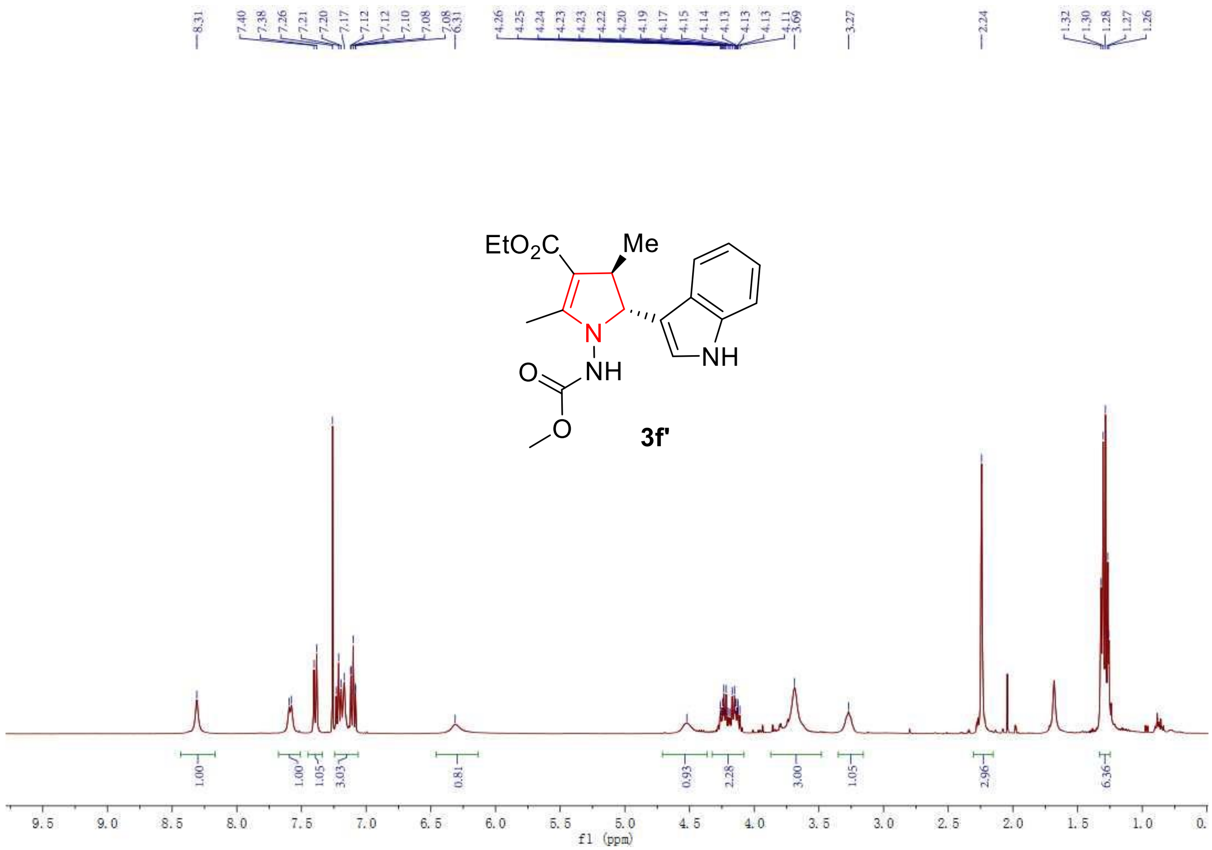
8.31
7.40 7.38 7.26 7.21 7.20 7.17 7.12 7.12 7.10 7.08 7.08 6.31
4.26 4.25 4.24 4.23 4.23 4.22 4.20 4.19 4.17 4.15 4.14 4.13 4.13 4.13 4.11 3.69
3.27
2.24
1.32 1.30 1.28 1.27 1.26
EtO2C
Me
N
NH
O
O
NH
3f'
1.00
1.00
1.05
3.03
0.81
0.93
2.28
3.00
1.05
2.96
6.36
9.5 9.0 8.5 8.0 7.5 7.0 6.5 6.0 5.5 5.0 4.5 4.0 3.5 3.0 2.5 2.0 1.5 1.0 0.
f1 (ppm)

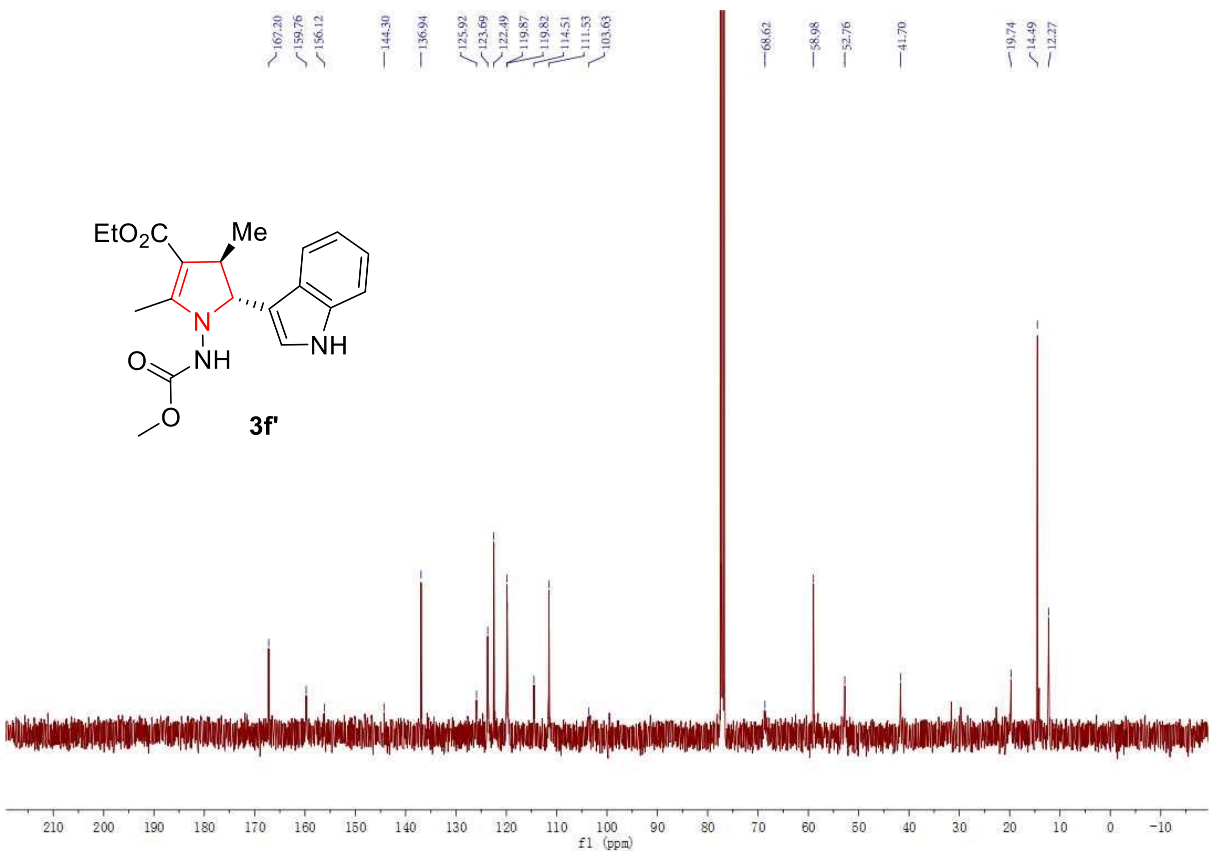
167.20 159.76 156.12
144.30 136.94
125.92 123.69 122.49 119.87 119.82 114.51 111.53 103.63
68.62
58.98
52.76
41.70
19.74 14.49 12.27
EtO2C
Me
N
NH
O
O
NH
3f'
210 200 190 180 170 160 150 140 130 120 110 100 90 80 70 60 50 40 30 20 10 0 -10
f1 (ppm)

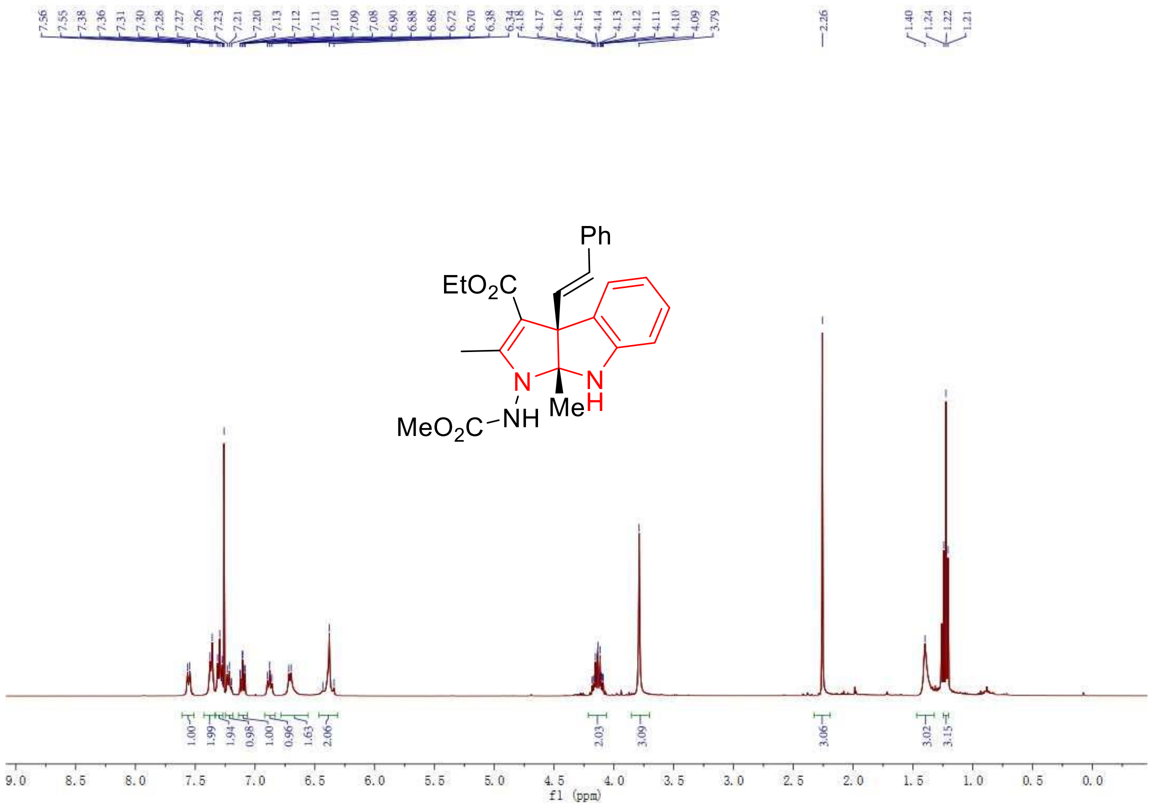

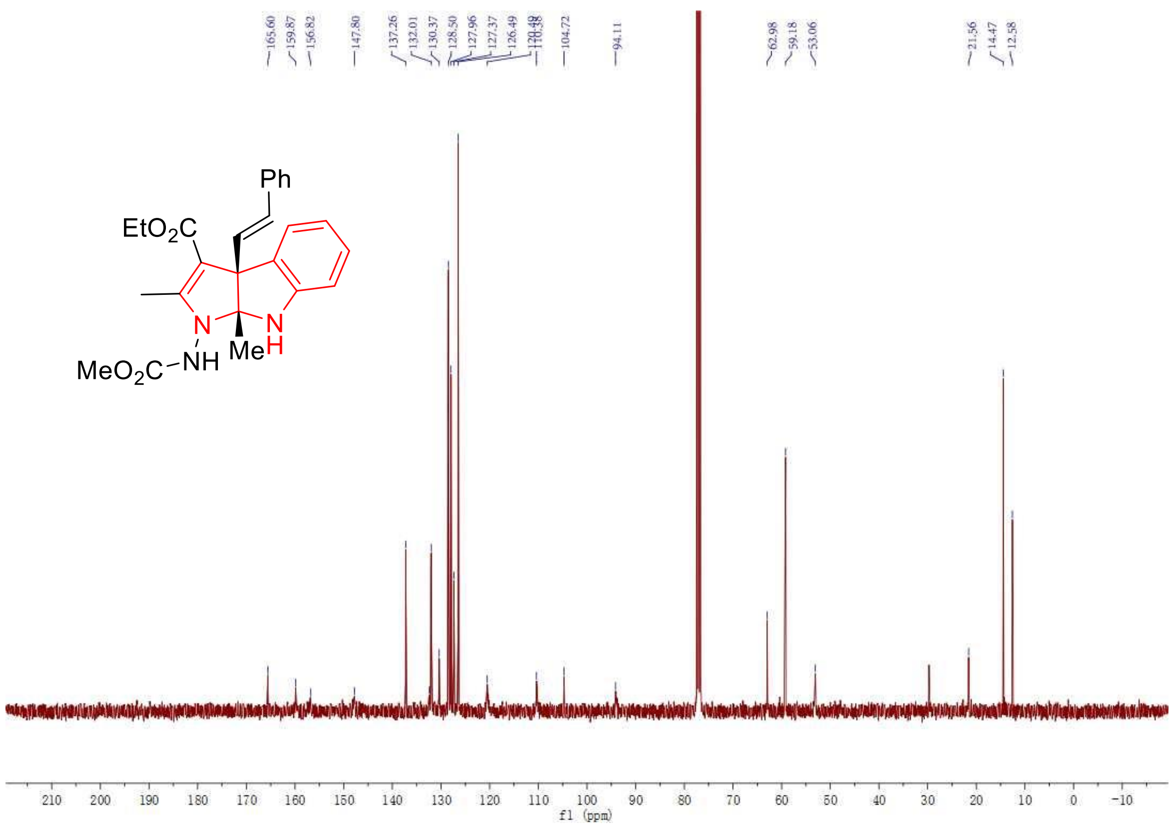

Data S2. Product Characterizations: Related to Table 2, Figures 4,5 and Scheme 1

Ethyl (4*R*,5*R*)-5-(1*H*-indol-3-yl)-1-((methoxycarbonyl)amino)-2-methyl-4-phenyl-4,5-dihydro-1*H*-pyrrole-3-carboxylate **3a**

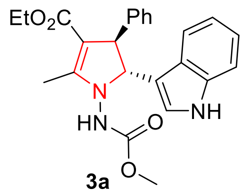

3a

A colorless oil; isolated yield = 96%, dr >20:1; $[\alpha]_D^{25}$ = –87 (c 2.0, $CHCl_3$); ^{1}H NMR (400 MHz, $CDCl_3$) δ 8.34 (s, 1H), 7.51 (d, *J* = 6.7 Hz, 1H), 7.38 (d, *J* = 8.2 Hz, 1H), 7.31 – 7.13 (m, 6H), 7.11 – 7.08 (m, 1H), 6.96 (s, 1H), 6.48 (s, 1H), 4.88 (s, 1H), 4.33 (d, *J* = 7.9 Hz, 1H), 4.07 – 3.99 (m, 1H), 3.95 – 3.85 (m, 1H), 3.70 (s, 3H), 2.37 (s, 3H), 0.95 (t, *J* = 7.1 Hz, 3H); ^{13}C NMR (100 MHz, $CDCl_3$) δ 166.8, 160.2, 156.2, 145.3, 137.1, 128.1, 128.0, 126.2, 125.6, 123.8, 122.5, 119.9, 114.2, 111.6, 102.1, 70.2, 58.9, 53.4, 52.8, 14.0, 12.2.; HRMS (ESI) m/z calcd for $C_{24}H_{26}N_3O_4$ $[M + H]^+$ = 420.1918, found = 420.1910; the ee value was 94%, t_R (major) = 7.0 min, t_R (minor) = 6.4 min (Chiralpak ID, λ = 254 nm, 20% *i*-PrOH/Hexane, flow rate = 1.0 mL/min).

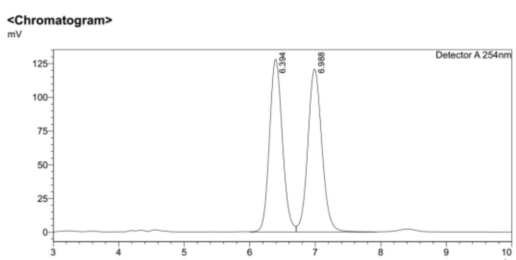

<Peak Table>

Detector A 254nm

Peak#	Ret. Time	Area	Height	Area%	Height%
1	6.394	1755002	127852	49.350	51.434
2	6.988	1801199	120722	50.650	48.566
Total		3556201	248574	100.000	100.000

Racemic **3a**

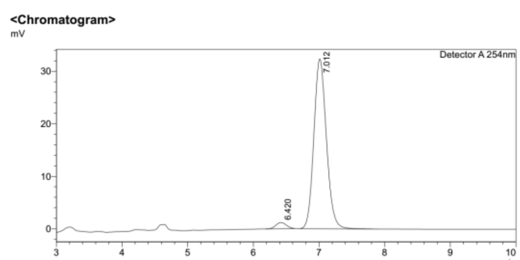

<Peak Table>

Detector A 254nm

Peak#	Ret. Time	Area	Height	Area%	Height%
1	6.420	13349	1198	3.013	3.573
2	7.012	429643	32333	96.987	96.427
Total		442992	33531	100.000	100.000

Enantioenriched **3a**

Ethyl (4*R*,5*R*)-2-ethyl-5-(1*H*-indol-3-yl)-1-((methoxycarbonyl)amino)-4-phenyl-4,5-dihydro-1*H*-pyrrole-3-carboxylate **3b**

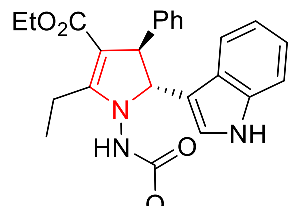

3b

A yellowish oil; isolated yield = 90%, dr >20:1; $[\alpha]_D^{25}$ = –133 (c 1.7, $CHCl_3$); ^{1}H NMR (400 MHz, $CDCl_3$) δ 8.24 (s, 1H), 7.53 (d, *J* = 7.7 Hz, 1H), 7.39 (d, *J* = 8.2 Hz, 1H), 7.33 – 7.15 (m, 7H), 7.11 (t, *J* = 7.5 Hz, 1H), 6.99 (s, 1H), 6.36 (s, 1H), 4.89 (s, 1H), 4.31 (d, *J* = 7.4 Hz, 1H), 4.08 – 3.88 (m, 2H), 3.71 (s, 3H), 3.11 – 3.06 (m, 1H), 2.66 – 2.50 (m, 1H), 1.25 (t, *J* = 7.4 Hz, 3H), 0.96 (t, *J* = 7.1 Hz, 3H); ^{13}C NMR (100 MHz, $CDCl_3$) δ 166.3, 165.1, 156.3, 145.5, 137.1, 129.1, 128.2, 128.2, 127.9, 126.2, 125.5, 123.7, 122.6, 120.0, 114.5, 111.6, 101.0, 69.9, 58.8, 53.3, 52.9, 19.2, 14.0, 12.6; HRMS (ESI) m/z calcd for $C_{25}H_{28}N_3O_4$ $[M + H]^+$ = 434.2074, found =434.2067; the ee value was 90%, t_R (major) = 5.0 min, t_R (minor) = 6.2 min (Chiralpak IA, λ = 254 nm, 20% *i*-PrOH/Hexane, flow rate = 1.0 mL/min).

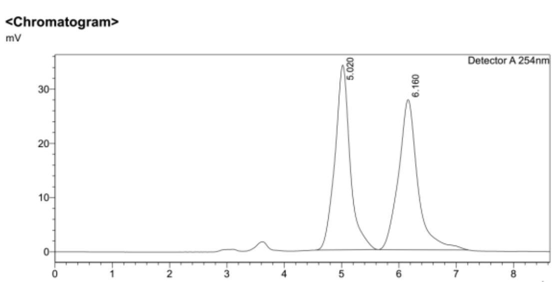

<Peak Table>

Detector A 254nm

Peak#	Ret. Time	Area	Height	Area%	Height%
1	5.020	626270	34038	49.248	55.171
2	6.160	645405	27658	50.752	44.829
Total		1271674	61697	100.000	100.000

Racemic **3b**

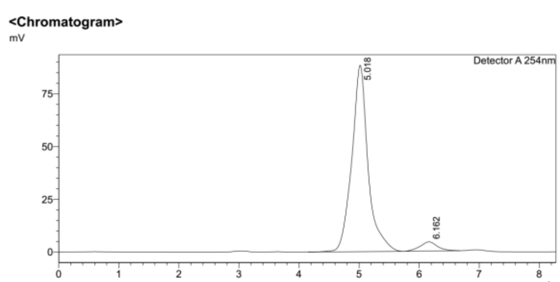

<Peak Table>

Detector A 254nm

Peak#	Ret. Time	Area	Height	Area%	Height%
1	5.018	1662347	88318	95.073	95.327
2	6.162	86151	4330	4.927	4.673
Total		1748499	92647	100.000	100.000

Enantioenriched **3b**

Ethyl (4*R*,5*R*)-5-(1*H*-indol-3-yl)-1-((methoxycarbonyl)amino)-4-phenyl-2-propyl-4,5-dihydro-1*H*-pyrrole-3-carboxylate **3c**

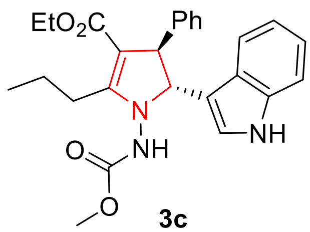

3c

A yellowish oil; isolated yield = 94%, dr >20:1; $[\alpha]_D^{25}$ = –110 (c 2.0, $CHCl_3$); ^{1}H NMR (400 MHz, $CDCl_3$) δ 8.24 (s, 1H), 7.53 (d, *J* = 7.5 Hz, 1H), 7.39 (d, *J* = 8.2 Hz, 1H), 7.34 – 7.15 (m, 6H), 7.13 – 7.09 (m, 1H), 6.98 (s, 1H), 6.34 (s, 1H), 4.89 (s, 1H), 4.33 (d, *J* = 7.5 Hz, 1H), 4.08 – 3.88 (m, 2H), 3.71 (s, 3H), 3.08 (d, *J* = 12.0 Hz, 1H), 2.63 – 2.41 (m, 1H), 1.71 – 1.66 (m, 2H), 1.06 (t, *J* = 7.4 Hz, 3H), 0.97 (t, *J* = 7.1 Hz, 3H); ^{13}C NMR (100 MHz, $CDCl_3$) δ 166.4, 163.6, 156.2, 145.5, 137.1, 128.1, 127.9, 126.2, 125.5, 123.8, 122.6, 119.9, 114.5, 111.6, 101.8, 69.8, 58.8, 53.3, 52.9, 27.6, 21.7, 14.2, 14.0; HRMS (ESI) m/z calcd for $C_{26}H_{30}N_3O_4$ $[M + H]^+$ = 448.2231, found = 448.2235; the ee value was 83%, t_R (major) = 7.1 min, t_R (minor) = 5.5 min (Chiralpak ID, λ = 254 nm, 20% *i*-PrOH/Hexane, flow rate = 1.0 mL/min).

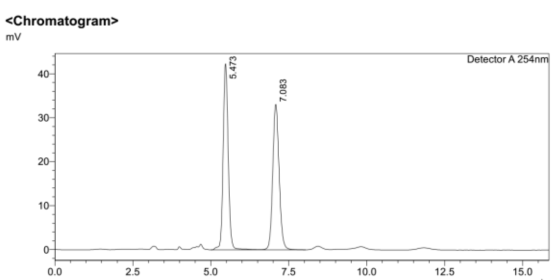

<Peak Table>
Detector A 254nm

Peak#	Ret. Time	Area	Height	Area%	Height%
1	5.473	480803	42295	50.479	56.111
2	7.083	471677	33083	49.521	43.889
Total		952481	75377	100.000	100.000

Racemic **3c**

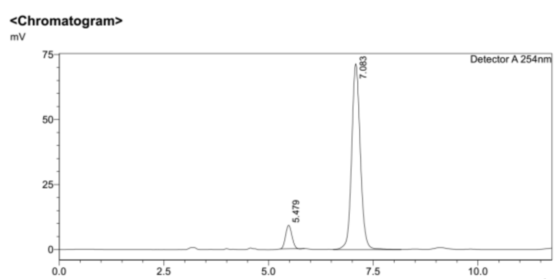

<Peak Table>
Detector A 254nm

Peak#	Ret. Time	Area	Height	Area%	Height%
1	5.479	94886	9049	8.442	11.246
2	7.083	1029042	71414	91.558	88.754
Total		1123929	80462	100.000	100.000

Enantioenriched **3c**

Methyl (4*R*,5*R*)-5-(1*H*-indol-3-yl)-1-((methoxycarbonyl)amino)-2-methyl-4-phenyl-4,5-dihydro-1*H*-pyrrole-3-carboxylate **3d**

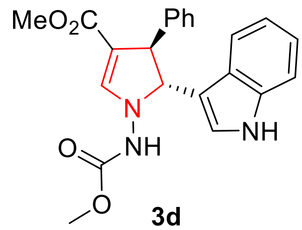

3d

A yellowish oil; isolated yield = 85%, dr >20:1; $[\alpha]_D^{25}$ = -92 (c 0.8, $CHCl_3$); ^1H NMR (400 MHz, $CDCl_3$) δ 8.17 (s, 1H), 7.51 (d, *J* = 9.0 Hz, 1H), 7.40 (d, *J* = 8.2 Hz, 1H), 7.32 – 7.15 (m, 6H), 7.13 – 7.09 (m, 1H), 7.00 (s, 1H), 6.36 (s, 1H), 4.84 (s, 1H), 4.33 (d, *J* = 7.8 Hz, 1H), 3.71 (s, 2H), 3.51 (s, 3H), 2.37 (d, *J* = 1.2 Hz, 3H); ^{13}C NMR (100 MHz, $CDCl_3$) δ 167.1, 160.3, 156.1, 145.1, 137.0, 129.0, 128.2, 127.8, 126.3, 125.6, 123.7, 122.6, 120.0, 119.9, 114.3, 111.5, 101.7, 70.2, 53.2, 52.9, 50.4, 12.2; HRMS (ESI) m/z calcd for $C_{23}H_{24}N_3O_4$ $[M + H]^+$ = 406.1761, found = 406.1751; the ee value was 94%, t_R (major) = 9.0 min, t_R (minor) = 5.5 min (Chiralpak IA, λ = 254 nm, 20% *i*-PrOH/Hexane, flow rate = 1.0 mL/min).

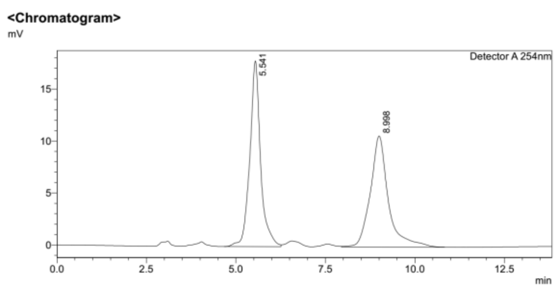

<Peak Table>
Detector A 254nm

Peak#	Ret. Time	Area	Height	Area%	Height%
1	5.541	374683	17864	50.113	62.572
2	8.998	372993	10686	49.887	37.428
Total		747676	28550	100.000	100.000

Racemic **3d**

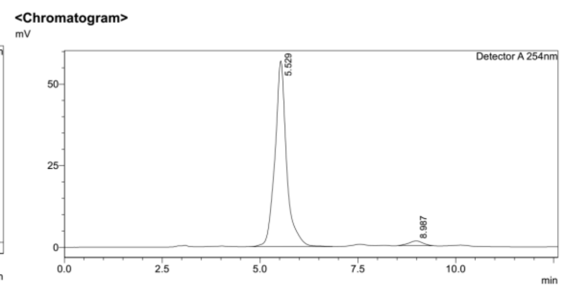

<Peak Table>
Detector A 254nm

Peak#	Ret. Time	Area	Height	Area%	Height%
1	5.529	1178249	56917	97.018	97.516
2	8.987	36210	1450	2.982	2.484
Total		1214459	58366	100.000	100.000

Enantioenriched **3d**

Tert-butyl (4*R*,5*R*)-5-(1*H*-indol-3-yl)-1-((methoxycarbonyl)amino)-4-phenyl-4,5-dihydro-1*H*-pyrrole-3-carboxylate **3e**

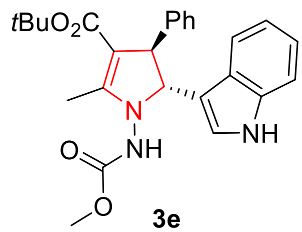

3e

A colorless oil; isolated yield = 86%, dr >20:1; $[\alpha]_D^{25}$ = -102 (c 1.0, $CHCl_3$); ^{1}H NMR (400 MHz, $CDCl_3$) δ 8.22 (s, 1H), 7.54 (s, 1H), 7.39 (d, *J* = 8.2 Hz, 1H), 7.26 – 7.15 (m, 6H), 7.12 – 7.09 (m, 1H), 6.97 (s, 1H), 6.40 (s, 1H), 4.83 (s, 1H), 4.25 (d, *J* = 8.4 Hz, 1H), 3.68 (s, 3H), 2.35 (d, *J* = 1.4 Hz, 3H), 1.15 (s, 9H); ^{13}C NMR (100 MHz, $CDCl_3$) δ 166.2, 159.8, 156.1, 145.4, 137.0, 128.2, 128.0, 126.1, 125.8, 123.7, 122.5, 120.0, 119.8, 114.4, 111.5, 103.9, 78.8, 70.4, 53.9, 52.8, 28.1, 12.1; HRMS (ESI) m/z calcd for $C_{26}H_{30}N_3O_4$ $[M + H]^+$ = 448.2231, found = 448.2219; the ee value was 92%, t_R (major) = 8.2 min, t_R (minor) = 9.2 min (Chiralpak ID, λ = 254 nm, 10% *i*-PrOH/Hexane, flow rate = 1.0 mL/min).

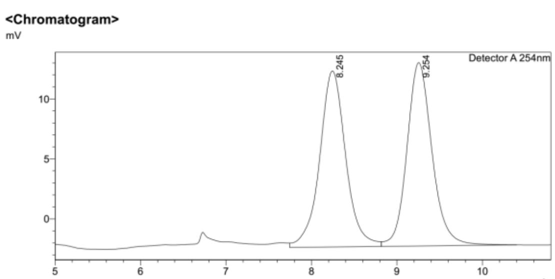

<Peak Table>

Detector A 254nm

Peak#	Ret. Time	Area	Height	Area%	Height%
1	8.245	311334	14663	49.912	48.993
2	9.254	312430	15265	50.088	51.007
Total		623764	29928	100.000	100.000

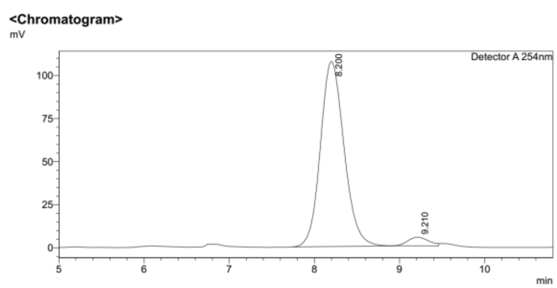

<Peak Table>

Detector A 254nm

Peak#	Ret. Time	Area	Height	Area%	Height%
1	8.200	2074389	107388	95.964	95.512
2	9.210	87249	5047	4.036	4.488
Total		2161638	112434	100.000	100.000

Racemic **3e** Enantioenriched **3e**

Benzyl (4*R*,5*R*)-5-(1*H*-indol-3-yl)-1-((methoxycarbonyl)amino)-2-methyl-4-phenyl-4,5-dihydro-1*H*-pyrrole-3-carboxylate **3f**

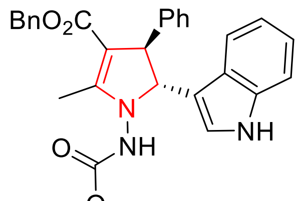

3f

A yellowish oil; isolated yield = 95%; dr >20:1; $[\alpha]_D^{25}$ = -101 (c 2.3, $CHCl_3$); ^{1}H NMR (400 MHz, $CDCl_3$) δ 8.22 (s, 1H), 7.51 (d, *J* = 7.6 Hz, 1H), 7.38 (d, *J* = 8.2 Hz, 1H), 7.30 – 7.06 (m, 10H), 6.96 (s, 1H), 6.88 – 6.81 (m, 2H), 6.43 (s, 1H), 5.12 – 4.85 (m, 3H), 4.37 (d, *J* = 7.9 Hz, 1H), 3.70 (s, 3H), 2.39 (d, *J* = 1.3 Hz, 3H); ^{13}C NMR (100 MHz, $CDCl_3$) δ 166.5, 161.2, 156.1, 145.2, 137.0, 136.8, 128.3, 128.1, 127.3, 126.3, 125.6, 123.8, 122.6, 120.0, 119.8, 114.1, 111.6, 101.4, 70.4, 64.8, 53.3, 52.9, 12.3; HRMS (ESI) m/z calcd for $C_{29}H_{28}N_3O_4$ $[M + H]^+$ = 482.2074, found = 482.2065; the ee value was 91%, t_R (major) = 17.0 min, t_R (minor) = 14.7 min (Chiralpak IC, λ = 254 nm, 10% *i*-PrOH/Hexane, flow rate = 1.0 mL/min).

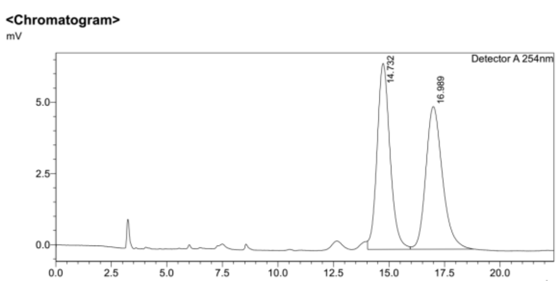

<Peak Table>

Detector A 254nm

Peak#	Ret. Time	Area	Height	Area%	Height%
1	14.732	264686	6528	50.281	56.578
2	16.989	261724	5010	49.719	43.422
Total		526409	11538	100.000	100.000

Racemic **3f**

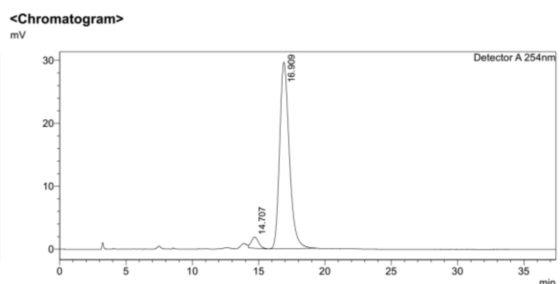

<Peak Table>

Detector A 254nm

Peak#	Ret. Time	Area	Height	Area%	Height%
1	14.707	68406	1773	4.360	5.651
2	16.909	1500522	29611	95.640	94.349
Total		1568928	31384	100.000	100.000

Enantioenriched **3f**

Isopropyl (4*R*,5*R*)-5-(1*H*-indol-3-yl)-1-((methoxycarbonyl)amino)-2-methyl-4-phenyl-4,5-dihydro-1*H*-pyrrole-3-carboxylate **3g**

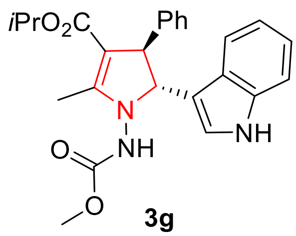

3g

A yellowish oil; isolated yield = 92%; dr >20:1; $[\alpha]_D^{25}$ = –106 (c 1.5, $CHCl_3$); ^1H NMR (400 MHz, $CDCl_3$) δ 8.27 (s, 1H), 7.52 (s, 1H), 7.39 (d, *J* = 8.2 Hz, 1H), 7.32 – 7.05 (m, 7H), 6.99 (s, 1H), 6.43 (s, 1H), 4.90 – 4.82 (m, 2H), 4.30 (d, *J* = 8.3 Hz, 1H), 3.70 (s, 3H), 2.37 (d, *J* = 1.4 Hz, 3H), 1.07 (d, *J* = 6.2 Hz, 3H), 0.75 (d, *J* = 6.2 Hz, 3H); ^{13}C NMR (100 MHz, $CDCl_3$) δ 166.2, 160.0, 156.1, 145.4, 137.0, 128.0, 126.1, 125.7, 123.7, 122.5, 119.9, 119.9, 114.3, 111.5, 102.7, 70.3, 65.9, 53.5, 52.8, 22.0, 21.4, 12.1; HRMS (ESI) m/z calcd for $C_{25}H_{28}N_3O_4$ $[M + H]^+$ = 434.2074, found = 434.2063; the ee value was 91%, t_R (major) = 6.3 min, t_R (minor) = 5.7 min (Chiralpak ID, λ = 254 nm, 20% *i*-PrOH/Hexane, flow rate = 1.0 mL/min).

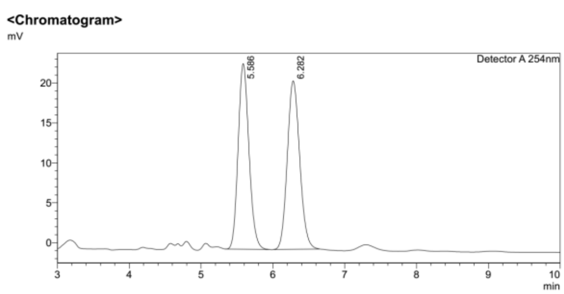

<Peak Table>
Detector A 254nm

Peak#	Ret. Time	Area	Height	Area%	Height%
1	5.586	243453	23228	49.053	52.394
2	6.282	252854	21105	50.947	47.606
Total		496307	44334	100.000	100.000

Racemic **3g**

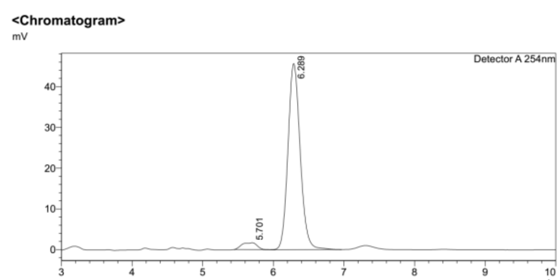

<Peak Table>
Detector A 254nm

Peak#	Ret. Time	Area	Height	Area%	Height%
1	5.701	25501	1700	4.437	3.592
2	6.289	549260	45625	95.563	96.408
Total		574761	47326	100.000	100.000

Enantioenriched **3g**

Ethyl (4*R*,5*R*)-5-(1*H*-indol-3-yl)-1-((methoxycarbonyl)amino)-2-methyl-4-(*o*-tolyl)-4,5-dihydro-1*H*-pyrrole-3-carboxylate **3h**

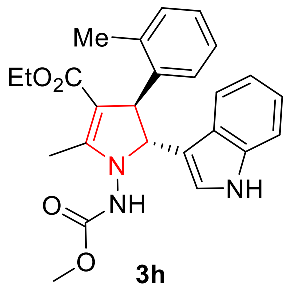

3h

A yellowish oil; isolated yield = 99%; dr >20:1; $[\alpha]_D^{25}$ = –94 (c 2.4, $CHCl_3$); ^{1}H NMR (400 MHz, $CDCl_3$) δ 8.26 (s, 1H), 7.52 (d, *J* = 3.6 Hz, 2H), 7.38 (d, *J* = 8.2 Hz, 1H), 7.24 – 7.16 (m, 2H), 7.13 – 7.02 (m, 2H), 6.98 (s, 2H), 6.41 (s, 1H), 4.87 (s, 1H), 4.70 (d, *J* = 7.8 Hz, 1H), 4.03 – 3.85 (m, 2H), 3.69 (s, 3H), 2.37 (d, *J* = 0.9 Hz, 3H), 1.94 (s, 3H), 0.91 (t, *J* = 7.1 Hz, 3H); ^{13}C NMR (100 MHz, $CDCl_3$) δ 166.6, 160.0, 156.1, 143.8, 137.0, 135.8, 129.4, 127.7, 126.4, 125.9, 125.6, 123.6, 122.5, 119.9, 119.8, 114.5, 111.5, 102.5, 70.3, 58.9, 52.8, 48.3, 19.6, 13.9, 12.1; HRMS (ESI) m/z calcd for $C_{25}H_{28}N_3O_4$ $[M + H]^+$ = 434.2074, found = 434.2070; the ee value was 90%, t_R (major) = 6.1 min, t_R (minor) = 5.0 min (Chiralpak IA, λ = 254 nm, 20% *i*-PrOH/Hexane, flow rate = 1.0 mL/min).

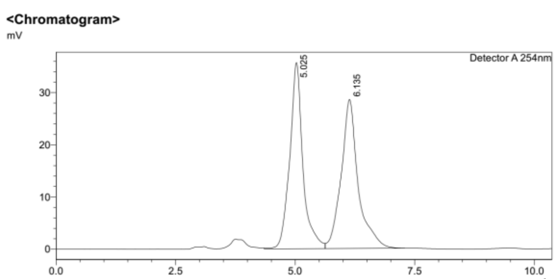

<Peak Table>
Detector A 254nm

Peak#	Ret. Time	Area	Height	Area%	Height%
1	5.025	678889	35641	49.041	55.525
2	6.135	705427	28548	50.959	44.475
Total		1384316	64189	100.000	100.000

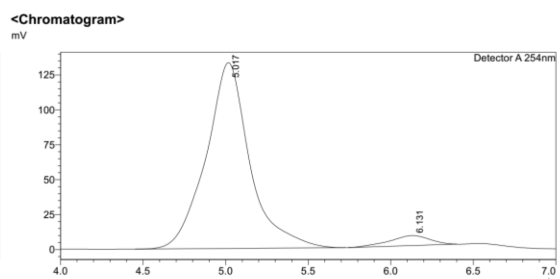

<Peak Table>
Detector A 254nm

Peak#	Ret. Time	Area	Height	Area%	Height%
1	5.017	2454563	133052	95.261	94.920
2	6.131	122118	7121	4.739	5.080
Total		2576681	140173	100.000	100.000

Racemic **3h**

Enantioenriched **3h**

Ethyl (4*R*,5*R*)-5-(1*H*-indol-3-yl)-1-((methoxycarbonyl)amino)-2-methyl-4-(*m*-tolyl)-4,5-dihydro-1*H*-pyrrole-3-carboxylate **3i**

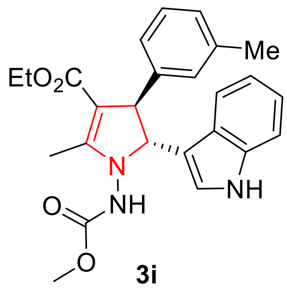

3i

A colorless oil; isolated yield = 75%; dr >20:1; $[\alpha]_D^{25}$ = –93 (c 0.6, $CHCl_3$); ^{1}H NMR (400 MHz, $CDCl_3$) δ 8.27 (s, 1H), 7.58 – 7.48 (m, 1H), 7.38 (d, *J* = 8.2 Hz, 1H), 7.23 (dd, *J* = 11.3, 3.9 Hz, 1H), 7.16 – 7.02 (m, 4H), 6.98 (s, 2H), 6.40 (s, 1H), 4.87 (s, 1H), 4.30 (d, *J* = 8.0 Hz, 1H), 4.09 – 4.01 (m, 1H), 3.96 – 3.88 (m, 1H), 3.70 (s, 2H), 2.36 (d, *J* = 1.1 Hz, 3H), 2.28 (s, 3H), 0.97 (t, *J* = 7.1 Hz, 3H); ^{13}C NMR (100 MHz, $CDCl_3$) δ 166.8, 159.9, 156.2, 145.1, 137.5, 137.0, 128.8, 128.0, 127.0, 125.6, 125.0, 123.8, 122.5, 119.9, 114.3, 111.6, 102.2, 70.2, 58.9, 53.2, 21.4, 14.1, 12.2; HRMS (ESI) m/z calcd for $C_{25}H_{28}N_3O_4$ $[M + H]^+$ = 434.2074, found = 434.2068; the ee value was 92%, t_R (major) = 7.5 min, t_R (minor) = 6.4 min (Chiralpak IC, λ = 254 nm, 20% *i*-PrOH/Hexane, flow rate = 1.0 mL/min).

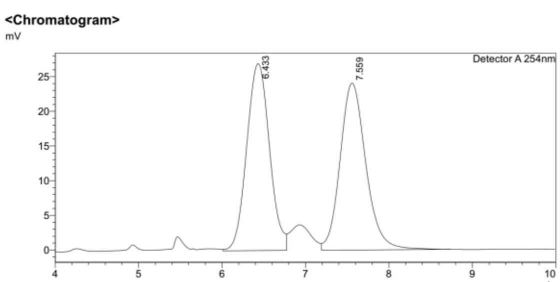

<Peak Table>
Detector A 254nm

Peak#	Ret. Time	Area	Height	Area%	Height%
1	6.433	513119	26975	49.763	52.830
2	7.559	518015	24084	50.237	47.170
Total		1031134	51059	100.000	100.000

Racemic **3i**

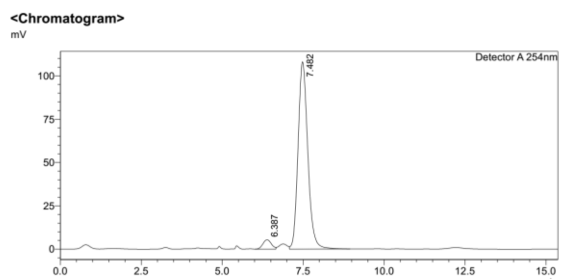

<Peak Table>
Detector A 254nm

Peak#	Ret. Time	Area	Height	Area%	Height%
1	6.387	98068	5367	4.158	4.733
2	7.482	2260374	108025	95.842	95.267
Total		2358442	113393	100.000	100.000

Enantioenriched **3i**

Ethyl (4*R*,5*R*)-4-(3-chlorophenyl)-5-(1*H*-indol-3-yl)-1-((methoxycarbonyl)amino)-2-methyl-4,5-dihydro-1*H*-pyrrole-3-carboxylate **3j**

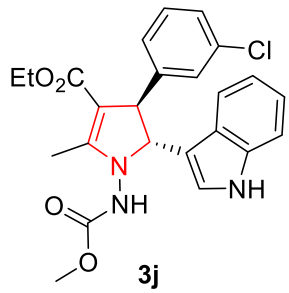

3j

A yellowish oil; isolated yield = 80%; dr >20:1; $[\alpha]_D^{25}$ = -109 (c 1.7, $CHCl_3$); ^1H NMR (400 MHz, $CDCl_3$) δ 8.24 (s, 1H), 7.51 (d, *J* = 8.2 Hz, 1H), 7.40 (d, *J* = 8.2 Hz, 1H), 7.29 – 7.08 (m, 6H), 7.01 (s, 1H), 6.41 (s, 1H), 4.85 (s, 1H), 4.30 (d, *J* = 8.1 Hz, 1H), 4.08 – 4.01 (m, 1H), 3.95 – 3.87 (m, 1H), 3.71 (s, 3H), 2.37 (d, *J* = 1.2 Hz, 3H), 0.98 (t, *J* = 7.1 Hz, 3H); ^{13}C NMR (100 MHz, $CDCl_3$) δ 166.4, 160.6, 154.4, 147.4, 137.1, 133.8, 129.4, 128.3, 126.4, 126.2, 125.4, 123.8, 122.7, 120.1, 119.8, 113.9, 111.6, 101.6, 69.9, 58.9, 53.1, 52.9, 14.1, 12.2; HRMS (ESI) m/z calcd for $C_{24}H_{25}ClN_3O_4$ $[M + H]^+$ = 454.1528, found = 454.1521; the ee value was 94%, t_R (major) = 5.0 min, t_R (minor) = 7.3 min (Chiralpak IA, λ = 254 nm, 20% *i*-PrOH/Hexane, flow rate = 1.0 mL/min).

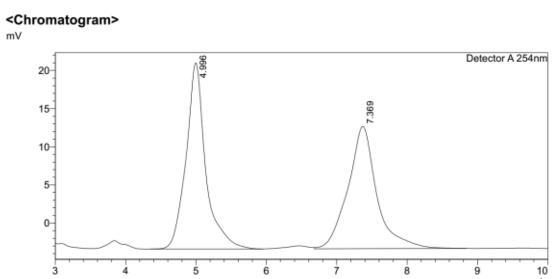

<Peak Table>

Detector A 254nm

Peak#	Ret. Time	Area	Height	Area%	Height%
1	4.996	472137	24377	50.890	60.345
2	7.369	455620	16020	49.110	39.655
Total		927757	40397	100.000	100.000

Racemic **3j**

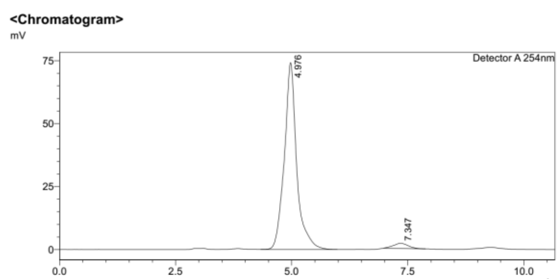

<Peak Table>

Detector A 254nm

Peak#	Ret. Time	Area	Height	Area%	Height%
1	4.976	1377390	74187	96.802	97.326
2	7.347	45497	2038	3.198	2.674
Total		1422887	76226	100.000	100.000

Enantioenriched **3j**

Ethyl (4*R*,5*R*)-5-(1*H*-indol-3-yl)-1-((methoxycarbonyl)amino)-2-methyl-4-(*p*-tolyl)-4,5-dihydro-1*H*-pyrrole-3-carboxylate **3k**

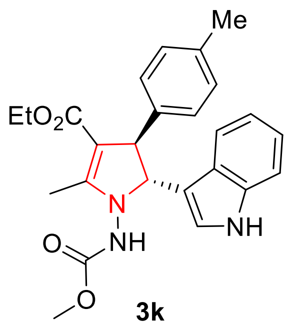

3k

A yellowish oil; isolated yield = 99%; dr >20:1; $[\alpha]_D^{25}$ = –130 (c 2.2, $CHCl_3$); ^1H NMR (400 MHz, $CDCl_3$) δ 8.24 (s, 1H), 7.52 (d, *J* = 7.2 Hz, 1H), 7.38 (d, *J* = 8.2 Hz, 1H), 7.23 (dd, *J* = 11.3, 3.9 Hz, 1H), 7.18 – 7.03 (m, 5H), 6.98 (s, 1H), 6.41 (s, 1H), 4.84 (s, 1H), 4.30 (d, *J* = 7.6 Hz, 1H), 4.06 – 3.88 (m, 2H), 3.70 (s, 3H), 2.36 (d, *J* = 0.9 Hz, 3H), 2.30 (s, 3H), 0.99 (t, *J* = 7.1 Hz, 3H); ^{13}C NMR (100 MHz, $CDCl_3$) δ 166.8, 159.8, 156.1, 142.3, 137.0, 135.6, 128.8, 127.8, 125.6, 123.7, 122.5, 119.9, 114.4, 111.5, 102.2, 70.3, 58.9, 52.9, 52.9, 21.1, 14.1, 12.2; HRMS (ESI) m/z calcd for $C_{25}H_{28}N_3O_4$ $[M + H]^+$ = 434.2074, found = 434.2062; the ee value was 90%, t_R (major) = 6.8 min, t_R (minor) = 5.5 min (Chiralpak IA, λ = 254 nm, 20% *i*-PrOH/Hexane, flow rate = 1.0 mL/min).

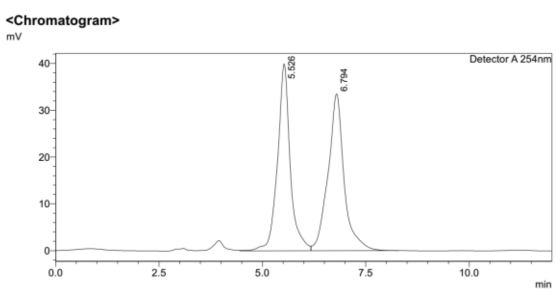

<Peak Table>

Detector A 254nm

Peak#	Ret. Time	Area	Height	Area%	Height%
1	5.526	854911	39927	48.590	54.389
2	6.794	904535	33483	51.410	45.611
Total		1759446	73410	100.000	100.000

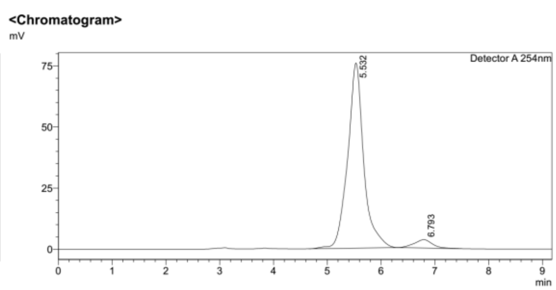

<Peak Table>

Detector A 254nm

Peak#	Ret. Time	Area	Height	Area%	Height%
1	5.532	1571574	75760	95.063	95.641
2	6.793	81610	3453	4.937	4.359
Total		1653184	79212	100.000	100.000

Racemic **3k**   Enantioenriched **3k**

Ethyl (4*R*,5*R*)-4-(4-fluorophenyl)-5-(1*H*-indol-3-yl)-1-((methoxycarbonyl)amino)-2-methyl-4,5-dihydro-1*H*-pyrrole-3-carboxylate **3l**

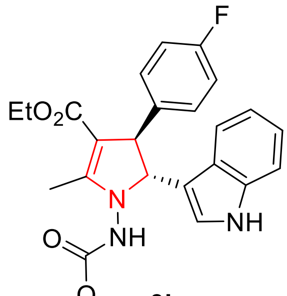

3l

A yellowish oil; isolated yield = 92%; dr >20:1; $[\alpha]_D^{25}$ = –124 (c 1.8, $CHCl_3$); ^{1}H NMR (400 MHz, $CDCl_3$) δ 8.28 (s, 1H), 7.49 (d, *J* = 7.3 Hz, 1H), 7.39 (d, *J* = 8.2 Hz, 1H), 7.26 – 7.16 (m, 3H), 7.10 (t, *J* = 7.5 Hz, 1H), 7.00 (s, 1H), 6.93 (t, *J* = 8.7 Hz, 2H), 6.45 (s, 1H), 4.83 (s, 1H), 4.30 (d, *J* = 8.1 Hz, 1H), 4.07 – 3.99 (m, 1H), 3.95 – 3.86 (m, 1H), 3.71 (s, 3H), 2.36 (d, *J* = 1.1 Hz, 3H), 0.98 (t, *J* = 7.1 Hz, 3H); ^{13}C NMR (100 MHz, $CDCl_3$) δ 166.6, 161.5 (d, *J* = 242 Hz), 160.3, 156.1, 141.1, 137.1, 129.4, 125.6, 123.6, 122.6, 119.9 (d, *J* = 19 Hz), 114.8 (d, *J* = 21 Hz), 114.1, 111.6, 102.0, 70.2, 58.9, 52.9, 52.8, 14.1, 12.2; ^{19}F NMR (376 MHz, $CDCl_3$) δ -117.4; HRMS (ESI) m/z calcd for $C_{24}H_{25}FN_3O_4$ $[M + H]^+$ = 438.1824, found = 438.1815; the ee = value was 94%, t_R (major) = 5.2 min, t_R (minor) = 7.9 min (Chiralpak IA, λ = 254 nm, 20% *i*-PrOH/Hexane, flow rate = 1.0 mL/min).

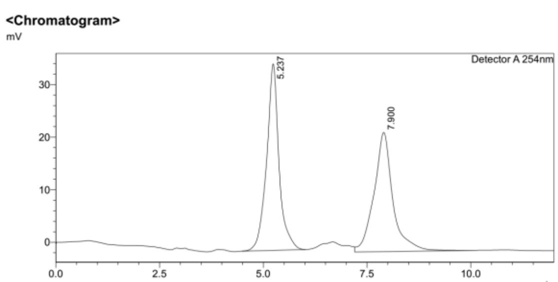

<Peak Table>
Detector A 254nm

Peak#	Ret. Time	Area	Height	Area%	Height%
1	5.237	738553	35458	50.734	60.982
2	7.900	717182	22687	49.266	39.018
Total		1455734	58145	100.000	100.000

Racemic **3l**

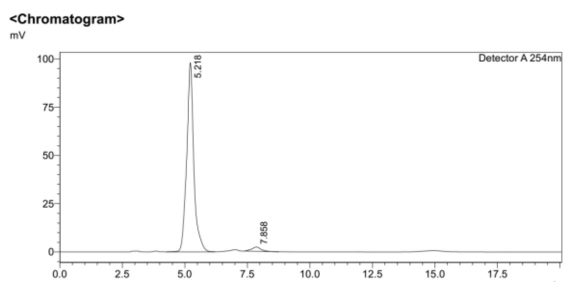

<Peak Table>
Detector A 254nm

Peak#	Ret. Time	Area	Height	Area%	Height%
1	5.218	1937815	97892	97.029	97.775
2	7.858	59334	2227	2.971	2.225
Total		1997149	100120	100.000	100.000

Enantioenriched **3l**

Ethyl (4*R*,5*R*)-4-(4-chlorophenyl)-5-(1*H*-indol-3-yl)-1-((methoxycarbonyl)amino)-2-methyl-4,5-dihydro-1*H*-pyrrole-3-carboxylate **3m**

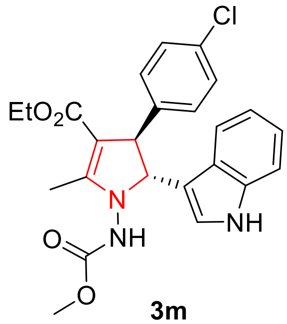

3m

A yellowish oil; isolated yield = 99%; dr >20:1; $[\alpha]_D^{25}$ = –120 (c 2.3, $CHCl_3$); ^{1}H NMR (400 MHz, $CDCl_3$) δ 8.27 (s, 1H), 7.50 (d, *J* = 7.4 Hz, 1H), 7.39 (d, *J* = 8.2 Hz, 1H), 7.26 – 7.14 (m, 5H), 7.11 (t, *J* = 7.5 Hz, 1H), 7.00 (s, 1H), 6.45 (s, 1H), 4.81 (s, 1H), 4.30 (d, *J* = 8.0 Hz, 1H), 4.08 – 3.88 (m, 2H), 3.71 (s, 3H), 2.36 (d, *J* = 0.9 Hz, 3H), 0.99 (t, *J* = 7.1 Hz, 3H); ^{13}C NMR (100 MHz, $CDCl_3$) δ 166.5, 160.5, 156.0, 143.8, 137.1, 131.9, 129.4, 128.3, 125.5, 123.7, 122.7, 120.0, 119.8, 114.0, 111.6, 101.8, 70.1, 59.0, 52.9, 14.1, 12.2; HRMS (ESI) m/z calcd for $C_{24}H_{25}ClN_3O_4$ $[M + H]^+$ = 454.1528, found = 454.1518; the ee value was 94%, t_R (major) = 5.5 min, t_R (minor) = 7.4 min (Chiralpak IA, λ = 254 nm, 20% *i*-PrOH/Hexane, flow rate = 1.0 mL/min).

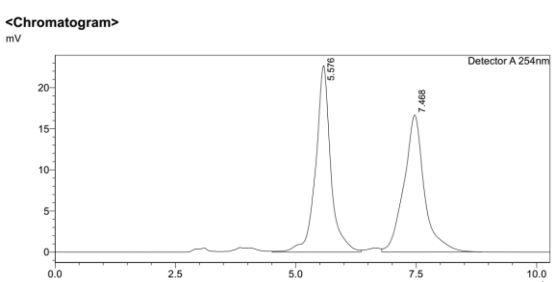

<Peak Table>
Detector A 254nm

Peak#	Ret. Time	Area	Height	Area%	Height%
1	5.576	491905	22668	50.163	57.647
2	7.468	488718	16654	49.837	42.353
Total		980624	39323	100.000	100.000

Racemic **3m**

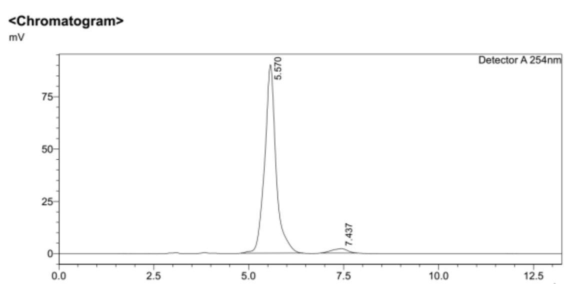

<Peak Table>
Detector A 254nm

Peak#	Ret. Time	Area	Height	Area%	Height%
1	5.570	1867381	89961	96.916	97.744
2	7.437	59423	2076	3.084	2.256
Total		1926804	92037	100.000	100.000

Enantioenriched **3m**

Ethyl (4*R*,5*R*)-5-(1*H*-indol-3-yl)-1-((methoxycarbonyl)amino)-2-methyl-4-(4-nitrophenyl)-4,5-dihydro-1*H*-pyrrole-3-carboxylate **3n**

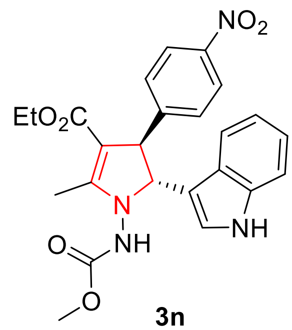

3n

A yellowish oil; isolated yield = 91%; dr >20:1; $[a]_D^{25}$ = –119 (c 2.0, $CHCl_3$); ^{1}H NMR (400 MHz, $CDCl_3$) δ 8.26 (s, 1H), 8.12 (d, *J* = 8.7 Hz, 2H), 7.58 – 7.37 (m, 4H), 7.28 – 7.08 (m, 2H), 7.01 (d, *J* = 1.7 Hz, 1H), 6.47 (s, 1H), 4.84 (s, 1H), 4.46 (d, *J* = 8.5 Hz, 1H), 4.05 – 3.90 (m, 2H), 3.73 (s, 3H), 2.39 (d, *J* = 1.3 Hz, 3H), 0.98 (t, *J* = 7.1 Hz, 3H); ^{13}C NMR (100 MHz, $CDCl_3$) δ 166.1, 161.2, 156.0, 152.9, 146.6, 137.1, 129.0, 128.9, 128.2, 125.3, 123.8, 123.6, 122.9, 120.2, 119.6, 113.5, 111.7, 101.1, 69.6, 59.1, 53.4, 53.0, 14.1, 12.3; HRMS (ESI) m/z calcd for $C_{24}H_{25}N_4O_6$ $[M + H]^+$ = 465.1769, found = 465.1753; the ee value was 95%, t_R (major) = 6.3 min, t_R (minor) = 9.9 min (Chiralpak IA, λ = 254 nm, 20% *i*-PrOH/Hexane, flow rate = 1.0 mL/min).

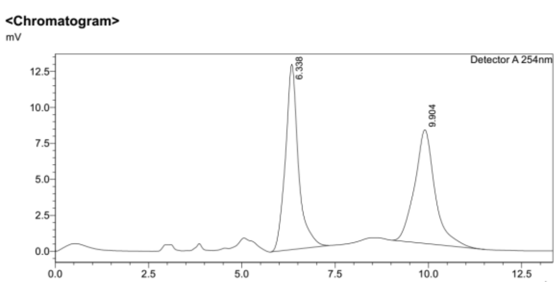

<Peak Table>
Detector A 254nm

Peak#	Ret. Time	Area	Height	Area%	Height%
1	6.338	311094	12865	50.934	61.953
2	9.904	299689	7901	49.066	38.047
Total		610783	20766	100.000	100.000

Racemic **3n**

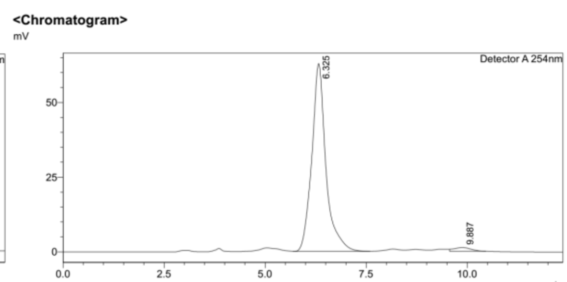

<Peak Table>
Detector A 254nm

Peak#	Ret. Time	Area	Height	Area%	Height%
1	6.325	1527017	62840	97.591	97.984
2	9.887	37698	1293	2.409	2.016
Total		1564716	64133	100.000	100.000

Enantioenriched **3n**

Ethyl (4*R*,5*R*)-5-(1*H*-indol-3-yl)-1-((methoxycarbonyl)amino)-2-methyl-4-(4-(trifluoromethyl)phenyl)-4,5-dihydro-1*H*-pyrrole-3-carboxylate **3o**

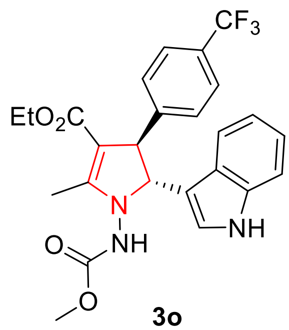

3o

A yellowish oil; isolated yield = 95%; dr >20:1; $[\alpha]_D^{25}$ = –116 (c 2.2, $CHCl_3$); ^{1}H NMR (400 MHz, $CDCl_3$) δ 8.27 (s, 1H), 7.50 (d, *J* = 8.0 Hz, 3H), 7.39 (dd, *J* = 12.8, 7.5 Hz, 3H), 7.28 – 7.22 (m, 1H), 7.14 – 7.10 (m, 1H), 7.00 (s, 1H), 6.45 (s, 1H), 4.84 (s, 1H), 4.40 (d, *J* = 8.3 Hz, 1H), 4.08 – 3.88 (m, 2H), 3.71 (s, 3H), 2.38 (d, *J* = 0.7 Hz, 3H), 0.96 (t, *J* = 7.1 Hz, 3H); ^{13}C NMR (100 MHz, $CDCl_3$) δ 166.4, 160.8, 156.0, 149.3, 137.1, 128.7, 128.3, 125.8 (t, *J* = 270 Hz,), 125.5, 125.1 (d, *J* = 4 Hz,), 123.8, 123.1, 122.7, 120.1, 119.7, 113.8, 111.7, 101.4, 69.9, 59.0, 53.2, 52.9, 14.0, 12.2; ^{19}F NMR (376 MHz, $CDCl_3$) δ -62.2; HRMS (ESI) m/z calcd for $C_{25}H_{25}F_3N_3O_4$ $[M + H]^+$ = 488.1792, found = 488.1773; the ee value was 93%, t_R (major) = 4.6 min, t_R (minor) = 6.9 min (Chiralpak IA, λ = 254 nm, 20% *i*-PrOH/Hexane, flow rate = 1.0 mL/min).

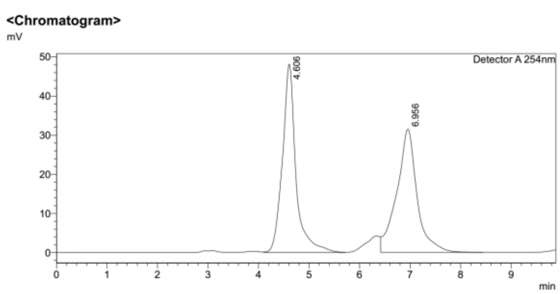

<Peak Table>

Detector A 254nm

Peak#	Ret. Time	Area	Height	Area%	Height%
1	4.606	892154	48142	50.430	60.467
2	6.956	876951	31475	49.570	39.533
Total		1769104	79617	100.000	100.000

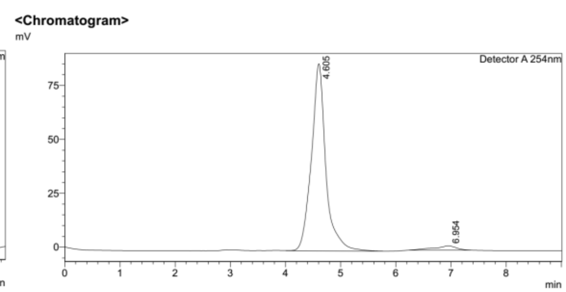

<Peak Table>

Detector A 254nm

Peak#	Ret. Time	Area	Height	Area%	Height%
1	4.605	1574911	86724	96.561	97.773
2	6.954	56087	1975	3.439	2.227
Total		1630999	88699	100.000	100.000

Racemic **3o** Enantioenriched **3o**

Ethyl (4*R*,5*R*)-4-(3,4-dichlorophenyl)-5-(1*H*-indol-3-yl)-1-((methoxycarbonyl)amino)-2-methyl-4,5-dihydro-1*H*-pyrrole-3-carboxylate **3p**

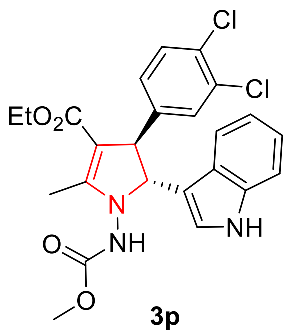

3p

A yellowish oil; isolated yield = 99%; dr >20:1; $[\alpha]_D^{25}$ = -154 (c 2.4, $CHCl_3$); ^{1}H NMR (400 MHz, $CDCl_3$) δ 8.29 (s, 1H), 7.50 (d, *J* = 7.8 Hz, 1H), 7.40 (d, *J* = 8.2 Hz, 1H), 7.35 (s, 1H), 7.32 (d, *J* = 8.2 Hz, 1H), 7.26 – 7.21 (m, 1H), 7.14 – 7.10 (m, 2H), 7.01 (s, 1H), 6.46 (s, 1H), 4.81 (s, 1H), 4.28 (d, *J* = 8.1 Hz, 1H), 4.10 – 3.90 (m, 2H), 3.71 (s, 3H), 2.36 (d, *J* = 1.0 Hz, 3H), 1.02 (t, *J* = 7.1 Hz, 3H); ^{13}C NMR (100 MHz, $CDCl_3$) δ 166.3, 160.8, 156.1, 145.7, 137.1, 131.9, 130.1, 127.5, 125.4, 123.8, 122.8, 120.1, 119.7, 113.7, 111.7, 101.1, 69.8, 59.1, 53.0, 52.7, 14.1, 12.2; HRMS (ESI) m/z calcd for $C_{24}H_{24}Cl_2N_3O_4$ $[M + H]^+$ = 488.1138, found = 488.1120; the ee value was 95%, t_R (major) = 5.0 min, t_R (minor) = 7.1 min (Chiralpak IA, λ = 254 nm, 20% *i*-PrOH/Hexane, flow rate = 1.0 mL/min).

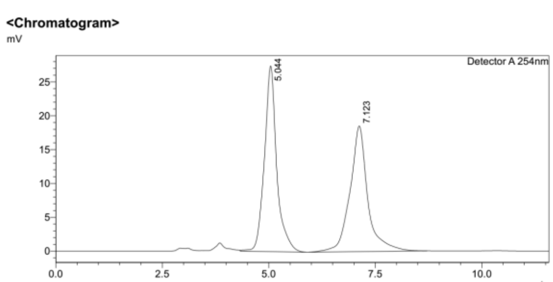

<Peak Table>
Detector A 254nm

Peak#	Ret. Time	Area	Height	Area%	Height%
1	5.044	551626	27422	50.691	59.634
2	7.123	536584	18562	49.309	40.366
Total		1088210	45983	100.000	100.000

Racemic **3p**

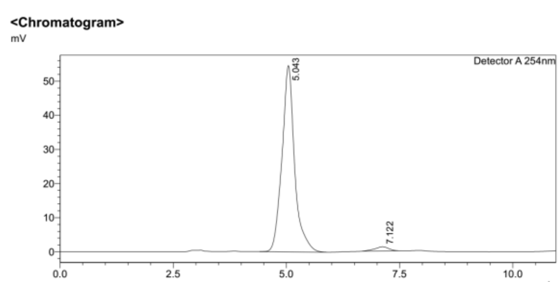

<Peak Table>
Detector A 254nm

Peak#	Ret. Time	Area	Height	Area%	Height%
1	5.043	1059206	54583	97.503	97.749
2	7.122	27123	1257	2.497	2.251
Total		1086329	55840	100.000	100.000

Enantioenriched **3p**

Ethyl (4*R*,5*R*)-5-(1*H*-indol-3-yl)-1-((methoxycarbonyl)amino)-2-methyl-4-(naphthalen-2-yl)-4,5-dihydro-1*H*-pyrrole-3-carboxylate **3q**

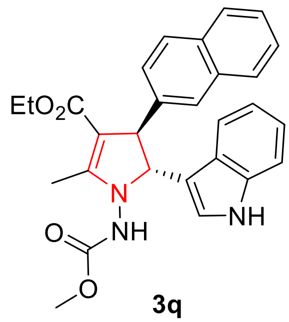

3q

A yellowish solid; isolated yield = 98%; dr >20:1; $[\alpha]_D^{25}$ = -150 (c 2.5, $CHCl_3$); ^{1}H NMR (400 MHz, $CDCl_3$) δ 8.22 (s, 1H), 7.78 (dd, *J* = 9.8, 5.9 Hz, 2H), 7.71 (dd, *J* = 6.1, 3.4 Hz, 1H), 7.62 (s, 1H), 7.59 – 7.46 (m, 2H), 7.43 – 7.34 (m, 3H), 7.28 – 7.21 (m, 1H), 7.11 (t, *J* = 7.4 Hz, 1H), 6.93 (s, 1H), 6.44 (s, 1H), 4.96 (s, 1H), 4.52 (d, *J* = 8.2 Hz, 1H), 4.00 – 3.84 (m, 2H), 3.71 (s, 3H), 2.41 (d, *J* = 1.2 Hz, 3H), 0.89 (t, *J* = 7.1 Hz, 3H); ^{13}C NMR (100 MHz, $CDCl_3$) δ 166.7, 160.3, 156.1, 142.5, 137.1, 133.4, 132.4, 127.9, 127.8, 127.6, 126.5, 125.6, 125.1, 123.8, 122.6, 120.0, 114.2, 111.6, 102.1, 70.1, 58.9, 53.5, 52.9, 14.1, 12.3; HRMS (ESI) m/z calcd for $C_{28}H_{28}N_3O_4$ $[M + H]^+$ = 470.2074, found = 470.2074; the ee value was 95%, t_R (major) = 7.0min, t_R (minor) = 8.6 min (Chiralpak IA, λ = 254 nm, 20% *i*-PrOH/Hexane, flow rate = 1.0 mL/min).

<Chromatogram>

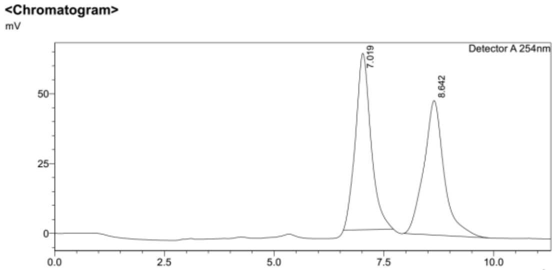

<Peak Table>

Detector A 254nm

Peak#	Ret. Time	Area	Height	Area%	Height%
1	7.019	1556480	63183	50.220	56.752
2	8.642	1542825	48149	49.780	43.248
Total		3099305	111332	100.000	100.000

Racemic **3q**

<Chromatogram>

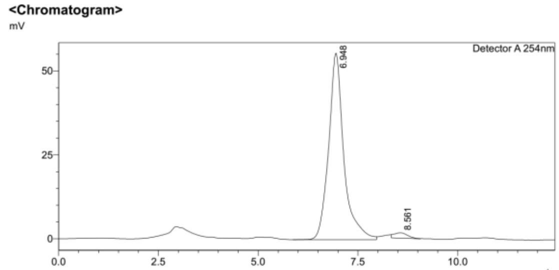

<Peak Table>

Detector A 254nm

Peak#	Ret. Time	Area	Height	Area%	Height%
1	6.948	1473428	55594	97.457	97.221
2	8.561	38449	1589	2.543	2.779
Total		1511877	57183	100.000	100.000

Enantioenriched **3q**

Ethyl (4*R*,5*R*)-5-(1*H*-indol-3-yl)-1-((methoxycarbonyl)amino)-2-methyl-4-(thiophen-2-yl)-4,5-dihydro-1*H*-pyrrole-3-carboxylate **3r**

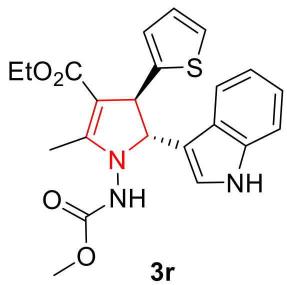

3r

A yellowish oil; isolated yield = 91%; dr >20:1; $[a]_D^{25}$ = -106 (c 1.8, $CHCl_3$); ^{1}H NMR (400 MHz, $CDCl_3$) δ 8.32 (s, 1H), 7.50 (d, *J* = 7.5 Hz, 1H), 7.40 (d, *J* = 8.2 Hz, 1H), 7.23 (dd, *J* = 11.2, 3.9 Hz, 1H), 7.16 – 7.02 (m, 3H), 6.91 – 6.75 (m, 2H), 6.44 (s, 1H), 4.92 (s, 1H), 4.60 (d, *J* = 7.2 Hz, 1H), 4.16 – 4.07 (m, 1H), 4.02 – 3.94 (m, 1H), 3.70 (s, 3H), 2.35 (d, *J* = 1.1 Hz, 3H), 1.04 (t, *J* = 7.1 Hz, 3H); ^{13}C NMR (100 MHz, $CDCl_3$) δ 166.6, 160.2, 155.8, 149.1, 137.0, 126.6, 125.6, 124.1, 123.9, 123.5, 122.6, 120.0, 119.7, 113.9, 111.6, 101.9, 70.6, 59.0, 52.9, 48.4, 14.1, 12.2; HRMS (ESI) m/z calcd for $C_{22}H_{24}N_3O_4S$ $[M + H]^+$ = 426.1482, found = 426.1489; the ee value was 95%, t_R (major) = 9.0 min, t_R (minor) = 7.2 min (Chiralpak IC, λ = 254 nm, 20% *i*-PrOH/Hexane, flow rate = 1.0 mL/min).

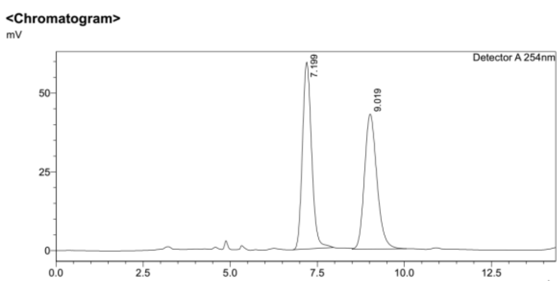

<Peak Table>

Detector A 254nm

Peak#	Ret. Time	Area	Height	Area%	Height%
1	7.199	1082801	59264	50.361	58.046
2	9.019	1067266	42835	49.639	41.954
Total		2150067	102099	100.000	100.000

Racemic **3r**

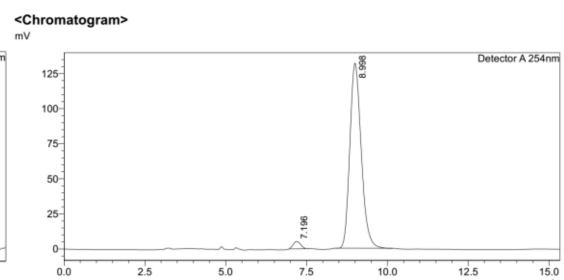

<Peak Table>

Detector A 254nm

Peak#	Ret. Time	Area	Height	Area%	Height%
1	7.196	83611	5244	2.517	3.823
2	8.998	3237691	131935	97.483	96.177
Total		3321302	137179	100.000	100.000

Enantioenriched **3r**

Ethyl (4*R*,5*R*)-5-(4-methoxy-1*H*-indol-3-yl)-1-((methoxycarbonyl)amino)-2-methyl-4-phenyl-4,5-dihydro-1*H*-pyrrole-3-carboxylate **3s**

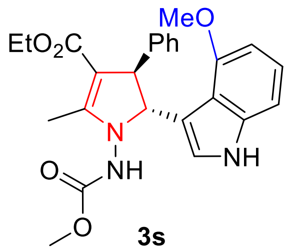

3s

A colorless oil; isolated yield= 98%; dr >20:1; $[\alpha]_D^{25}$ = –126 (c 2.4, $CHCl_3$); ^{1}H NMR (400 MHz, $CDCl_3$) δ 8.36 (s, 1H), 7.32 (s, 2H), 7.27 – 7.21 (m, 2H), 7.19 – 7.06 (m, 2H), 7.02 – 6.90 (m, 2H), 6.45 (d, J = 7.7 Hz, 2H), 5.19 (s, 1H), 4.27 (d, J = 6.4 Hz, 1H), 4.05 – 3.87 (m, 2H), 3.82 – 3.42 (m, 6H), 2.31 (s, 3H), 0.98 (t, J = 7.1 Hz, 3H); ^{13}C NMR (100 MHz, $CDCl_3$) δ 166.9, 159.7, 156.4, 154.2, 145.6, 138.3, 128.1, 127.9, 125.9, 123.2, 121.8, 116.6, 115.2, 104.5, 99.8, 69.4, 58.7, 54.8, 52.7, 52.7, 14.2, 12.2; HRMS (ESI) m/z calcd for $C_{25}H_{28}N_3O_5$ $[M + H]^+$ = 450.2023, found = 450.2020; the ee value was 92%, t_R (major) = 7.8 min, t_R (minor) = 7.1 min (Chiralpak IC, λ = 254 nm, 20% *i*-PrOH/Hexane, flow rate = 1.0 mL/min).

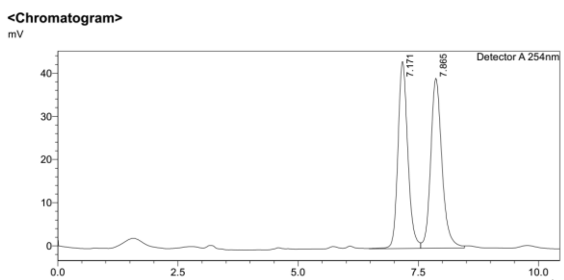

<Peak Table>

Detector A 254nm

Peak#	Ret. Time	Area	Height	Area%	Height%
1	7.171	618994	43257	49.025	52.362
2	7.865	643616	39355	50.975	47.638
Total		1262610	82613	100.000	100.000

Racemic **3s**

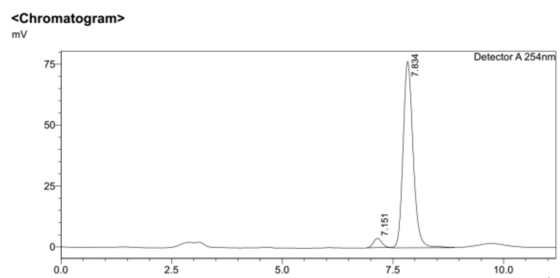

<Peak Table>

Detector A 254nm

Peak#	Ret. Time	Area	Height	Area%	Height%
1	7.151	50582	3815	4.020	4.752
2	7.834	1207526	76467	95.980	95.248
Total		1258107	80282	100.000	100.000

Enantioenriched **3s**

Ethyl (4*R*,5*R*)-1-((methoxycarbonyl)amino)-2-methyl-5-(5-methyl-1*H*-indol-3-yl)-4-phenyl-4,5-dihydro-1*H*-pyrrole-3-carboxylate **3t**

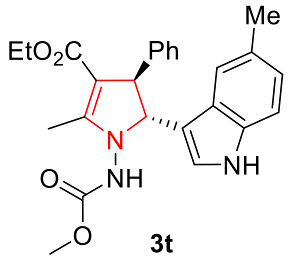

3t

A colorless oil; isolated yield= 88%; dr >20:1; $[\alpha]_D^{25}$ = –105 (c 1.8, $CHCl_3$); ^{1}H NMR (400 MHz, $CDCl_3$) δ 8.12 (s, 1H), 7.34 – 7.12 (m, 7H), 7.05 (d, *J* = 8.4 Hz, 1H), 6.94 (s, 1H), 6.40 (s, 1H), 4.86 (s, 1H), 4.32 (d, *J* = 8.4 Hz, 1H), 4.07 – 4.00 (m, 1H), 3.94 – 3.87 (m, 1H), 3.71 (s, 3H), 2.42 (s, 3H), 2.37 (d, *J* = 1.2 Hz, 3H), 0.95 (t, *J* = 7.1 Hz, 3H); ^{13}C NMR (100 MHz, $CDCl_3$) δ 166.7, 160.2, 156.1, 145.2, 135.3, 129.2, 128.1, 126.2, 125.9, 124.1, 123.8, 119.5, 113.6, 111.2, 102.3, 70.3, 58.8, 53.2, 52.8, 21.57, 14.0, 12.2; HRMS (ESI) m/z calcd for $C_{25}H_{28}N_3O_4$ $[M + H]^+$ = 434.2074, found = 434.2068; the ee value was 90%, t_R (major) = 6.5 min, t_R (minor) = 5.8 min (Chiralpak ID, λ = 254 nm, 20% *i*-PrOH/Hexane, flow rate = 1.0 mL/min).

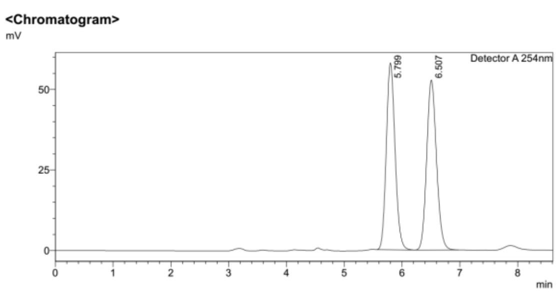

<Peak Table>
Detector A 254nm

Peak#	Ret. Time	Area	Height	Area%	Height%
1	5.799	610876	57910	49.528	52.363
2	6.507	622514	52685	50.472	47.637
Total		1233390	110595	100.000	100.000

Racemic **3t**

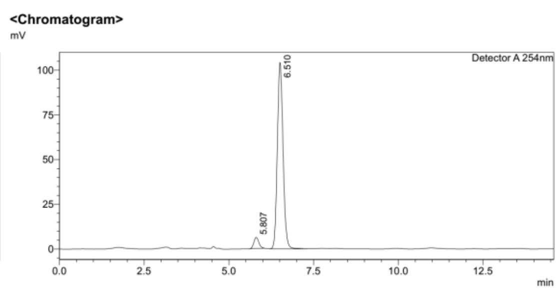

<Peak Table>
Detector A 254nm

Peak#	Ret. Time	Area	Height	Area%	Height%
1	5.807	64307	6264	5.004	5.678
2	6.510	1220682	104065	94.996	94.322
Total		1284989	110329	100.000	100.000

Enantioenriched **3t**

Ethyl (4*R*,5*R*)-5-(5-methoxy-1*H*-indol-3-yl)-1-((methoxycarbonyl)amino)-2-methyl-4-phenyl-4,5-dihydro-1*H*-pyrrole-3-carboxylate **3u**

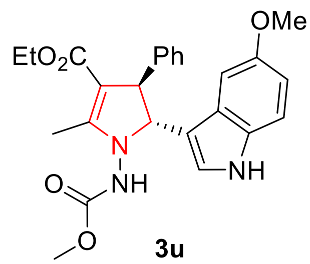

3u

A yellow oil; isolated yield = 85%; dr >20:1; $[\alpha]_D^{25}$ = -116 (c 1.8, $CHCl_3$); ^{1}H NMR (400 MHz, $CDCl_3$) δ 8.15 (s, 1H), 7.36 – 7.22 (m, 5H), 7.19 – 7.16 (m, 1H), 7.00 (s, 1H), 6.88 – 6.85 (m, 2H), 6.44 (s, 1H), 4.88 (s, 1H), 4.27 (d, *J* = 7.4 Hz, 1H), 4.07 – 3.98 (m, 1H), 3.95 – 3.87 (m, 1H), 3.73 (s, 6H), 2.36 (d, *J* = 1.1 Hz, 3H), 0.95 (t, *J* = 7.1 Hz, 3H); ^{13}C NMR (100 MHz, $CDCl_3$) δ 166.6, 160.1, 154.1, 145.2, 132.0, 128.2, 128.0, 126.3, 126.1, 124.0, 114.3, 112.6, 112.2, 109.5, 102.4, 101.6, 70.2, 58.9, 55.7, 53.4, 52.9, 14.1, 12.1; HRMS (ESI) m/z calcd for $C_{25}H_{28}N_3O_5$ $[M + H]^+$ = 450.2023, found = 450.2015; the ee value was 90%, t_R (major) = 14.0 min, t_R (minor) = 6.2 min (Chiralpak IA, λ = 254 nm, 10% *i*-PrOH/Hexane, flow rate = 1.0 mL/min).

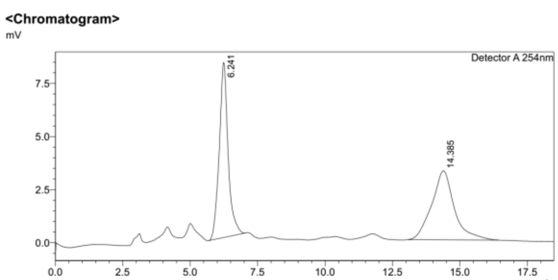

<Peak Table>
Detector A 254nm

Peak#	Ret. Time	Area	Height	Area%	Height%
1	6.241	188720	8242	49.862	71.702
2	14.385	189762	3253	50.138	28.298
Total		378483	11495	100.000	100.000

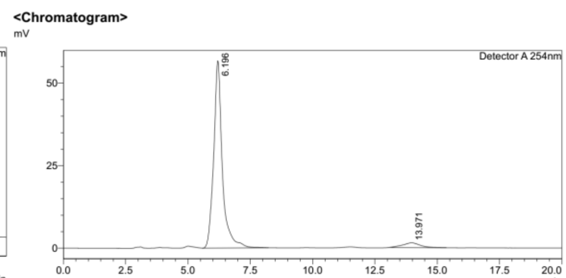

<Peak Table>
Detector A 254nm

Peak#	Ret. Time	Area	Height	Area%	Height%
1	6.196	1376159	56704	94.975	97.517
2	13.971	72817	1444	5.025	2.483
Total		1448976	58148	100.000	100.000

Racemic **3u** Enantioenriched **3u**

Ethyl (4*R*,5*R*)-5-(5-fluoro-1*H*-indol-3-yl)-1-((methoxycarbonyl)amino)-2-methyl-4-phenyl-4,5-dihydro-1*H*-pyrrole-3-carboxylate **3v**

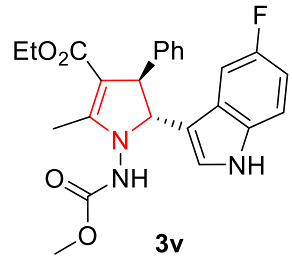

3v

A yellow oil; isolated yield = 83%; dr >20:1; $[\alpha]_D^{25}$ = -98 (c 1.7, $CHCl_3$); ^1H NMR (400 MHz, $CDCl_3$) δ 8.33 (s, 1H), 7.32 – 7.10 (m, 7H), 7.03 – 6.93 (m, 2H), 6.44 (s, 1H), 4.83 (s, 1H), 4.26 (d, *J* = 8.2 Hz, 1H), 4.08 – 3.98 (m, 1H), 3.95 – 3.86 (m, 1H), 3.70 (s, 3H), 2.36 (d, *J* = 1.3 Hz, 3H), 0.95 (t, *J* = 7.1 Hz, 3H); ^{13}C NMR (100 MHz, $CDCl_3$) δ 166.5, 160.2, 157.7 (d, *J* = 233 Hz), 156.0, 145.0, 133.5, 128.1, 128.0, 126.3, 125.4, 114.34, 112.2 (d, *J* = 8 Hz), 110.9 (d, *J* = 27 Hz), 104.7 (d, *J* = 23 Hz), 70.1, 59.0, 53.4, 52.9, 14.0, 12.2; ^{19}F NMR (376 MHz, $CDCl_3$) δ -123.6; HRMS (ESI) m/z calcd for $C_{24}H_{25}FN_3O_4$ $[M + H]^+$ = 438.1824, found = 438.1813; the ee value was 93%, t_R (major) = 6.1 min, t_R (minor) = 5.4 min (Chiralpak ID, λ = 254 nm, 20% *i*-PrOH/Hexane, flow rate = 1.0 mL/min).

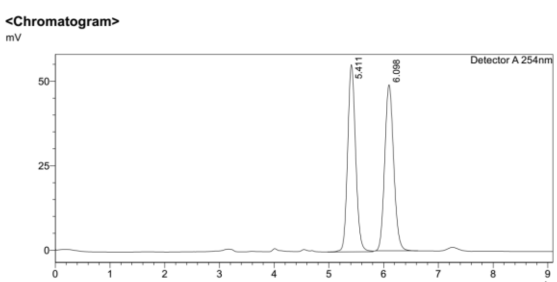

<Peak Table>
Detector A 254nm

Peak#	Ret. Time	Area	Height	Area%	Height%
1	5.411	563443	55348	50.215	52.979
2	6.098	558619	49123	49.785	47.021
Total		1122063	104472	100.000	100.000

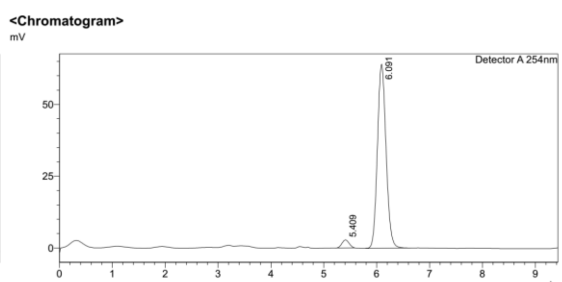

<Peak Table>
Detector A 254nm

Peak#	Ret. Time	Area	Height	Area%	Height%
1	5.409	26205	2781	3.477	4.161
2	6.091	727422	64055	96.523	95.839
Total		753627	66836	100.000	100.000

Racemic **3v** Enantioenriched **3v**

Ethyl (4*R*,5*R*)-5-(5-chloro-1*H*-indol-3-yl)-1-((methoxycarbonyl)amino)-2-methyl-4-phenyl-4,5-dihydro-1*H*-pyrrole-3-carboxylate **3w**

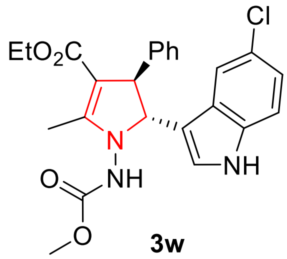

3w

A yellow oil; isolated yield = 76%; dr >20:1; $[\alpha]_D^{25}$ = -107 (c 1.6, $CHCl_3$); ^1H NMR (400 MHz, $CDCl_3$) δ 8.36 (s, 1H), 7.43 (s, 1H), 7.29 (d, *J* = 8.6 Hz, 1H), 7.26 – 7.12 (m, 6H), 6.98 (s, 1H), 6.44 (s, 1H), 4.84 (s, 1H), 4.25 (d, *J* = 9.2 Hz, 1H), 4.06 – 3.99 (m, 1H), 3.94 – 3.86 (m, 1H), 3.70 (s, 3H), 2.36 (d, *J* = 1.4 Hz, 3H), 0.94 (t, *J* = 7.1 Hz, 3H); ^{13}C NMR (100 MHz, $CDCl_3$) δ 166.5, 160.3, 156.0, 144.7, 135.3, 128.1, 128.0, 126.8, 126.3, 125.6, 125.0, 122.9, 119.3, 113.9, 112.6, 102.6, 70.2, 59.0, 53.4, 52.9, 14.0, 12.3; HRMS (ESI) m/z calcd for $C_{24}H_{25}ClN_3O_4$ $[M + H]^+$ = 454.1528, found = 454.1535; the ee value was 94%, t_R (major) = 5.7 min, t_R (minor) = 5.0 min (Chiralpak ID, λ = 254 nm, 20% *i*-PrOH/Hexane, flow rate = 1.0 mL/min).

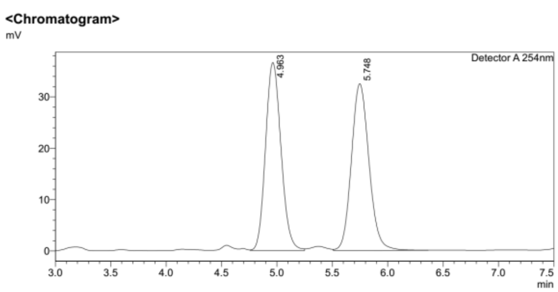

<Peak Table>

Detector A 254nm

Peak#	Ret. Time	Area	Height	Area%	Height%
1	4.963	356029	36594	49.839	52.981
2	5.748	358329	32476	50.161	47.019
Total		714357	69070	100.000	100.000

Racemic **3w**

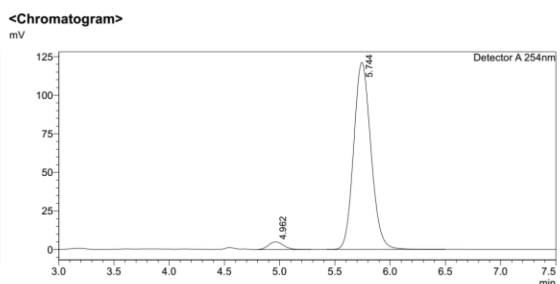

<Peak Table>

Detector A 254nm

Peak#	Ret. Time	Area	Height	Area%	Height%
1	4.962	47014	4953	3.439	3.925
2	5.744	1319906	121244	96.561	96.075
Total		1366919	126197	100.000	100.000

Enantioenriched **3w**

Ethyl (4*R*,5*R*)-5-(5-chloro-1*H*-indol-3-yl)-1-((methoxycarbonyl)amino)-2-methyl-4-phenyl-4,5-dihydro-1*H*-pyrrole-3-carboxylate **3x**

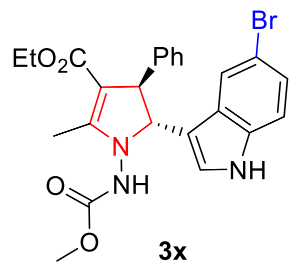

A yellowish solid; isolated yield = 70%; dr >20:1; $[\alpha]_D^{25}$ = -109 (c 1.5, $CHCl_3$); ^{1}H NMR (400 MHz, $CDCl_3$) δ 8.41 (s, 1H), 7.57 (s, 1H), 7.33 – 7.14 (m, 7H), 6.96 (s, 1H), 6.46 (s, 1H), 4.84 (s, 1H), 4.25 (d, *J* = 8.9 Hz, 1H), 4.08 – 4.00 (m, 1H), 3.95 – 3.87 (m, 1H), 3.70 (s, 3H), 2.36 (d, *J* = 1.3 Hz, 3H), 0.94 (t, *J* = 7.1 Hz, 3H); ^{13}C NMR (100 MHz, $CDCl_3$) δ 166.6, 160.4, 156.0, 144.7, 135.6, 128.1, 128.0, 127.5, 126.3, 125.4, 124.8, 122.3, 113.7, 113.0, 102.6, 70.2 59.0, 53.4, 52.9, 14.0, 12.3; HRMS (ESI) m/z calcd for $C_{24}H_{25}BrN_3O_4$ $[M + H]^+$ = 498.1023, found = 498.1011; the ee value was 94%, t_R (major) = 7.6 min, t_R (minor) = 4.9 min (Chiralpak IC, λ = 254 nm, 10% *i*-PrOH/Hexane, flow rate = 1.0 mL/min).

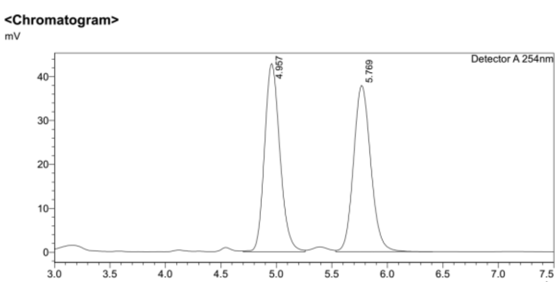

<Peak Table>
Detector A 254nm

Peak#	Ret. Time	Area	Height	Area%	Height%
1	4.957	413665	42879	50.209	53.090
2	5.769	410214	37887	49.791	46.910
Total		823879	80766	100.000	100.000

Racemic **3x**

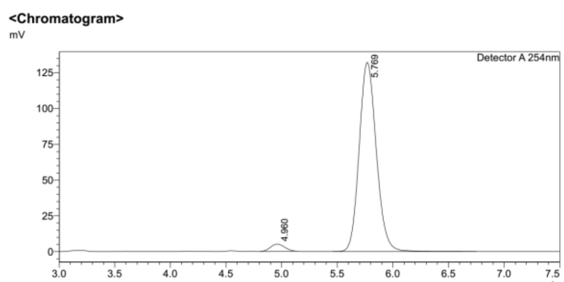

<Peak Table>
Detector A 254nm

Peak#	Ret. Time	Area	Height	Area%	Height%
1	4.960	44788	5063	3.061	3.688
2	5.769	1418609	132214	96.939	96.312
Total		1463397	137278	100.000	100.000

Enantioenriched **3x**

Ethyl (4*R*,5*R*)-5-(5-cyano-1*H*-indol-3-yl)-1-((methoxycarbonyl)amino)-2-methyl-4-phenyl-4,5-dihydro-1*H*-pyrrole-3-carboxylate **3y**

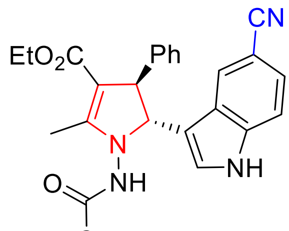

3y

A yellowish solid; isolated yield = 73%; dr >20:1; $[\alpha]_D^{25}$ = –82 (c 1.5, $CHCl_3$); ^1H NMR (400 MHz, $CDCl_3$) δ 8.87 (s, 1H), 7.76 (s, 1H), 7.41 (s, 2H), 7.25 – 7.04 (m, 6H), 6.56 (s, 1H), 4.86 (s, 1H), 4.20 (d, *J* = 9.2 Hz, 1H), 4.08 – 4.00 (m, 1H), 3.94 – 3.86 (m, 1H), 3.70 (s, 3H), 2.37 (d, *J* = 1.3 Hz, 3H), 0.96 (t, *J* = 7.1 Hz, 3H); ^{13}C NMR (100 MHz, $CDCl_3$) δ 166.4, 160.3, 155.9, 144.3, 138.7, 128.7, 128.2, 128.0, 126.5, 125.7, 125.6, 125.3, 120.6, 115.2, 112.5, 102.9, 70.2, 59.2, 53.9, 52.9, 14.0, 12.4; HRMS (ESI) m/z calcd for $C_{25}H_{25}N_4O_4$ $[M + H]^+$ = 445.1870, found = 445.1870; the ee value was 91%, t_R (major) = 8.1 min, t_R (minor) = 6.1 min (Chiralpak ID, λ = 254 nm, 20% *i*-PrOH/Hexane, flow rate = 1.0 mL/min).

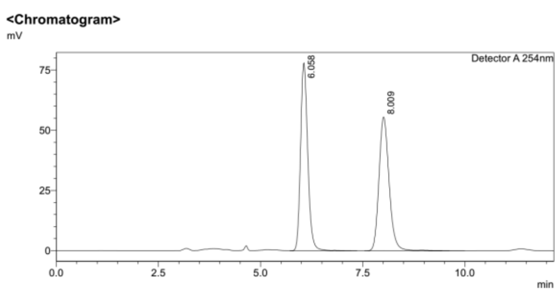

<Peak Table>

Detector A 254nm

Peak#	Ret. Time	Area	Height	Area%	Height%
1	6.058	957207	77956	49.843	58.366
2	8.009	963249	55609	50.157	41.634
Total		1920455	133565	100.000	100.000

Racemic **3y**

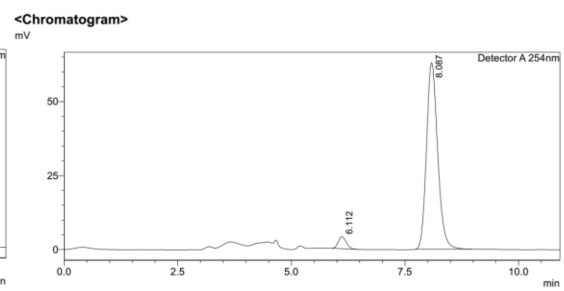

<Peak Table>

Detector A 254nm

Peak#	Ret. Time	Area	Height	Area%	Height%
1	6.112	49810	4059	4.419	6.055
2	8.087	1077452	62985	95.581	93.945
Total		1127263	67044	100.000	100.000

Enantioenriched **3y**

Ethyl (3a*S*,8a*R*)-3a-(3-methoxy-3-oxopropyl)-1-((methoxycarbonyl)amino)-2-methyl-1,3a,8,8a-tetrahydropyrrolo[2,3-*b*]indole-3-carboxylate **3z**

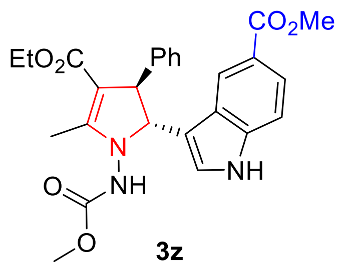

3z

A colorless oil; isolated yield = 70%; dr >20:1; $[\alpha]_D^{25}$ = -10 (c 1.2, $CHCl_3$); ^1H NMR (400 MHz, $CDCl_3$) δ 8.57 (s, 1H), 8.19 (s, 1H), 7.91 (dd, *J* = 8.6, 1.2 Hz, 1H), 7.37 (d, *J* = 8.6 Hz, 1H), 7.25 – 7.13 (m, 5H), 7.07 (s, 1H), 6.51 (s, 1H), 4.94 (s, 1H), 4.27 (d, *J* = 8.4 Hz, 1H), 4.05 – 3.99 (m, 1H), 3.95 – 3.84 (m, 4H), 3.70 (s, 3H), 2.37 (s, 3H), 0.94 (t, *J* = 7.1 Hz, 3H); ^{13}C NMR (100 MHz, $CDCl_3$) δ 168.0, 166.5, 160.3, 156.0, 144.4, 139.5, 128.1, 128.1, 126.3, 124.8, 123.9, 122.7, 122.0, 115.6, 111.2, 100.0, 70.1, 58.9, 53.70, 52.9, 51.9, 14.0, 12.3; HRMS (ESI) m/z calcd for $C_{26}H_{28}N_3O_6$ $[M + H]^+$ = 478.1973, found = 478.1960; the ee value was 91%, t_R (major) = 5.6 min, t_R (minor) = 7.7 min (Chiralpak IA, λ = 254 nm, 20% *i*-PrOH/Hexane, flow rate = 1.0 mL/min).

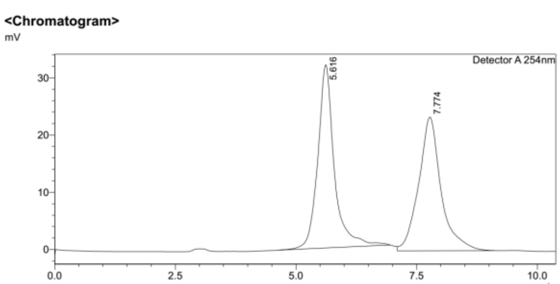

<Peak Table>

Detector A 254nm

Peak#	Ret. Time	Area	Height	Area%	Height%
1	5.616	761757	31993	50.242	57.794
2	7.774	754408	23363	49.758	42.206
Total		1516165	55356	100.000	100.000

Racemic **3z**

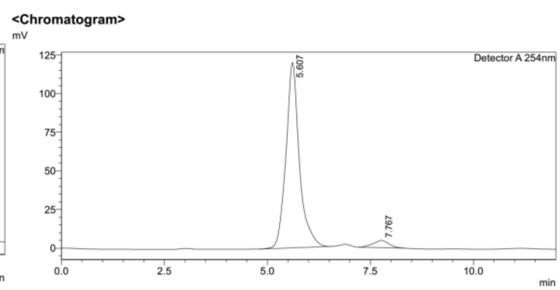

<Peak Table>

Detector A 254nm

Peak#	Ret. Time	Area	Height	Area%	Height%
1	5.607	2706716	119814	95.591	96.260
2	7.767	124844	4656	4.409	3.740
Total		2831560	124470	100.000	100.000

Enantioenriched **3z**

Ethyl (4*R*,5*R*)-5-(6-fluoro-1*H*-indol-3-yl)-1-((methoxycarbonyl)amino)-2-methyl-4-phenyl-4,5-dihydro-1*H*-pyrrole-3-carboxylate **3a'**

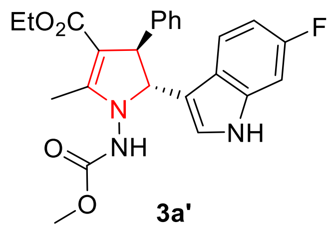

3a'

A colorless oil; isolated yield = 87%; dr >20:1; $[\alpha]_D^{25}$ = -99 (c 1.8, $CHCl_3$); ^1H NMR (400 MHz, $CDCl_3$) δ 8.30 (s, 1H), 7.37 (s, 1H), 7.26 – 7.13 (m, 5H), 7.05 (dd, *J* = 9.5, 2.2 Hz, 1H), 6.95 (s, 1H), 6.85 (t, *J* = 9.1 Hz, 1H), 6.44 (s, 1H), 4.83 (s, 1H), 4.26 (d, *J* = 8.2 Hz, 1H), 4.06 – 3.99 (m, 1H), 3.94 – 3.86 (m, 1H), 3.70 (s, 3H), 2.36 (d, *J* = 1.3 Hz, 3H), 0.94 (t, *J* = 7.1 Hz, 3H); ^{13}C NMR (100 MHz, $CDCl_3$) δ 166.62, 160.1, 160.1 (d, *J* = 238 H), 156.1, 145.0, 137.0 (d, *J* = 13 Hz), 128.2, 127.9, 126.3, 123.9, 122.2, 120.6 (d, *J* = 10 Hz), 114.4, 108.7 (d, *J* = 26 Hz), 97.8 (d, *J* = 26 Hz), 70.3, 58.9, 53.5, 52.9, 14.0, 12.2; ^{19}F NMR (376 MHz, $CDCl_3$) δ -120.3; HRMS (ESI) m/z calcd for $C_{24}H_{25}FN_3O_4$ $[M + H]^+$ = 438.1824, found = 438.1815; the ee value was 94%, t_R (major) = 5.9 min, t_R (minor) = 5.3 min (Chiralpak ID, λ = 254 nm, 20% *i*-PrOH/Hexane, flow rate = 1.0 mL/min).

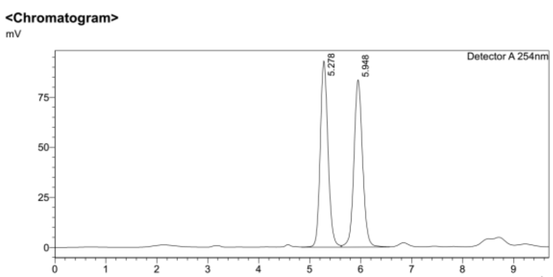

<Peak Table>

Detector A 254nm

Peak#	Ret. Time	Area	Height	Area%	Height%
1	5.278	988633	92932	50.131	52.676
2	5.948	983470	83489	49.869	47.324
Total		1972103	176421	100.000	100.000

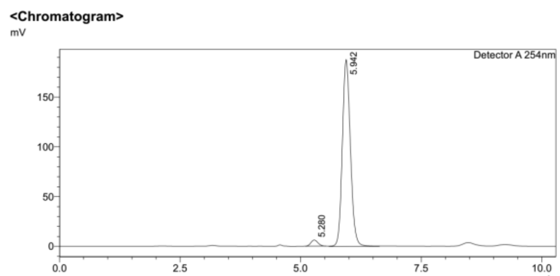

<Peak Table>

Detector A 254nm

Peak#	Ret. Time	Area	Height	Area%	Height%
1	5.280	62592	6129	2.783	3.162
2	5.942	2186309	187688	97.217	96.838
Total		2248901	193817	100.000	100.000

Racemic **3a'**

Enantioenriched **3a'**

Ethyl (4*R*,5*R*)-5-(6-chloro-1*H*-indol-3-yl)-1-((methoxycarbonyl)amino)-2-methyl-4-phenyl-4,5-dihydro-1*H*-pyrrole-3-carboxylate **3b'**

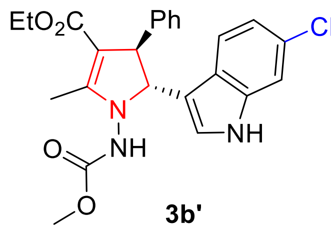

3b'

A yellowish solid; isolated yield = 97%; dr >20:1; $[\alpha]_D^{25}$ = -121 (c 2.1, $CHCl_3$); ^1H NMR (400 MHz, $CDCl_3$) δ 8.38 (s, 1H), 7.36 (d, *J* = 1.6 Hz, 2H), 7.26 – 7.12 (m, 5H), 7.05 (d, *J* = 8.3 Hz, 1H), 6.97 (s, 1H), 6.46 (s, 1H), 4.84 (s, 1H), 4.24 (d, *J* = 8.3 Hz, 1H), 4.07 – 3.99 (m, 1H), 3.94 – 3.85 (m, 1H), 2.36 (d, *J* = 1.2 Hz, 3H), 0.94 (t, *J* = 7.1 Hz, 3H); ^{13}C NMR (100 MHz, $CDCl_3$) δ 166.6, 160.2, 156.1, 144.9, 137.4, 128.5, 128.2, 127.9, 126.3, 124.2, 120.6, 114.5, 111.5, 102.4, 70.3, 58.9, 53.6, 52.9, 14.0, 12.2; HRMS (ESI) m/z calcd for $C_{24}H_{25}ClN_3O_4$ $[M + H]^+$ = 454.1528, found = 454.1516; the ee value was 91%, t_R (major) = 6.0 min, t_R (minor) = 5.5 min (Chiralpak ID, λ = 254 nm, 20% *i*-PrOH/Hexane, flow rate = 1.0 mL/min).

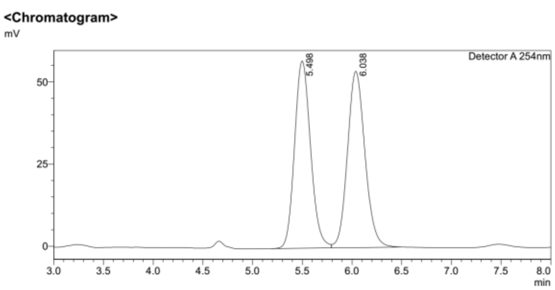

<Peak Table>

Detector A 254nm

Peak#	Ret. Time	Area	Height	Area%	Height%
1	5.498	637621	56921	49.258	51.522
2	6.038	656839	53557	50.742	48.478
Total		1294460	110478	100.000	100.000

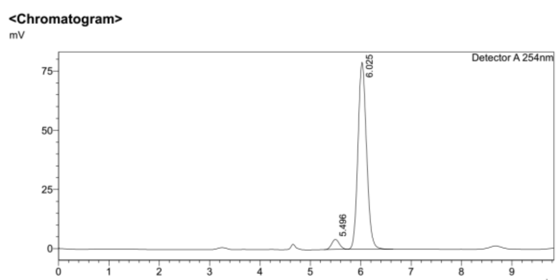

<Peak Table>

Detector A 254nm

Peak#	Ret. Time	Area	Height	Area%	Height%
1	5.496	44586	4198	4.548	5.053
2	6.025	935783	78875	95.452	94.947
Total		980369	83073	100.000	100.000

Racemic **3b'** Enantioenriched **3b'**

Ethyl (4*R*,5*R*)-5-(7-fluoro-1*H*-indol-3-yl)-1-((methoxycarbonyl)amino)-2-methyl-4-phenyl-4,5-dihydro-1*H*-pyrrole-3-carboxylate **3c'**

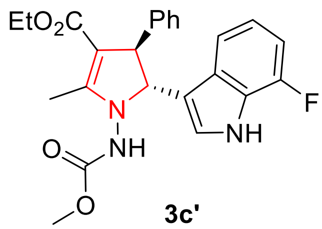

3c'

A colorless oil; isolated yield = 78%; dr >20:1; $[\alpha]_D^{25}$ = -116 (c 1.6, $CHCl_3$); ^{1}H NMR (400 MHz, $CDCl_3$) δ 8.45 (s, 1H), 7.31 – 7.13 (m, 6H), 7.04 – 6.86 (m, 3H), 6.43 (s, 1H), 4.87 (s, 1H), 4.28 (d, *J* = 8.3 Hz, 1H), 4.07 – 3.99 (m, 1H), 3.94 – 3.86 (m, 1H), 3.71 (s, 3H), 2.36 (d, *J* = 1.4 Hz, 3H), 0.94 (t, *J* = 7.1 Hz, 3H); ^{13}C NMR (101 MHz, $CDCl_3$) δ 166.6, 160.1, 155.9, 149.7 (d, *J* = 243 Hz), 144.9, 129.3, 128.1, 128.0, 126.3, 125.4 (d, *J* = 14 Hz), 124.3, 120.2, 115.7, 115.3, 107.3 (d, *J* = 16 Hz), 102.4, 70.2, 58.9, 53.6, 52.9, 14.0, 12.2; ^{19}F NMR (376 MHz, $CDCl_3$) δ -134.7; HRMS (ESI) m/z calcd for $C_{24}H_{25}FN_3O_4$ $[M + H]^+$ = 438.1824, found = 438.1813; the ee value was 92%, t_R (major) = 12.1 min, t_R (minor) = 13.9 min (Chiralpak IC, λ = 254 nm, 10% *i*-PrOH/Hexane, flow rate = 1.0 mL/min).

<Chromatogram>

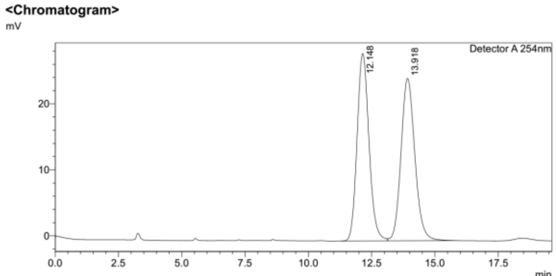

<Peak Table>

Detector A 254nm

Peak#	Ret. Time	Area	Height	Area%	Height%
1	12.148	930397	28419	49.797	53.581
2	13.918	937969	24620	50.203	46.419
Total		1868366	53039	100.000	100.000

Racemic **3c'**

<Chromatogram>

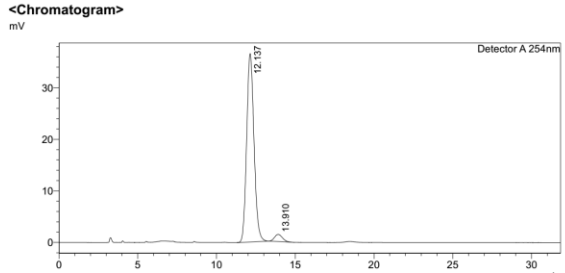

<Peak Table>

Detector A 254nm

Peak#	Ret. Time	Area	Height	Area%	Height%
1	12.137	1182640	36546	96.020	96.306
2	13.910	49019	1402	3.980	3.694
Total		1231659	37947	100.000	100.000

Enantioenriched **3c'**

Ethyl (4*R*,5*R*)-1-((methoxycarbonyl)amino)-2-methyl-5-(7-methyl-1*H*-indol-3-yl)-4-phenyl-4,5-dihydro-1*H*-pyrrole-3-carboxylate **3d'**

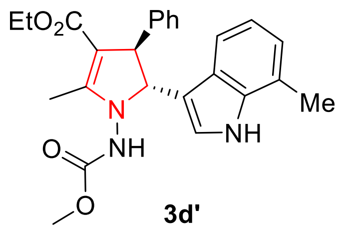

3d'

A yellowish solid; isolated yield = 97%; dr >20:1; $[\alpha]_D^{25}$ = -107 (c 2.1, $CHCl_3$); ^{1}H NMR (400 MHz, $CDCl_3$) δ 8.15 (s, 1H), 7.37 (s, 1H), 7.30 – 7.21 (m, 4H), 7.17 (d, *J* = 5.7 Hz, 1H), 7.04 – 7.01 (m, 3H), 6.39 (s, 1H), 4.88 (s, 1H), 4.32 (d, *J* = 8.0 Hz, 1H), 4.07 – 3.99 (m, 1H), 3.94 – 3.86 (m, 1H), 3.70 (s, 3H), 2.50 (s, 3H), 2.37 (d, *J* = 1.2 Hz, 3H), 0.94 (t, *J* = 7.1 Hz, 3H); ^{13}C NMR (100 MHz, $CDCl_3$) δ 166.7, 160.1, 156.4, 145.2, 136.6, 128.1, 126.2, 125.2, 123.4, 123.1, 120.8, 120.2, 117.6, 114.8, 102.2, 70.3, 58.8, 53.4, 52.8, 16.6, 14.0, 12.2; HRMS (ESI) m/z calcd for $C_{25}H_{28}N_3O_4$ $[M + H]^+$ = 434.2074, found = 434.2058; the ee value was 90%, t_R (major) = 6.6 min, t_R (minor) = 5.8 min (Chiralpak ID, λ = 254 nm, 20% *i*-PrOH/Hexane, flow rate = 1.0 mL/min).

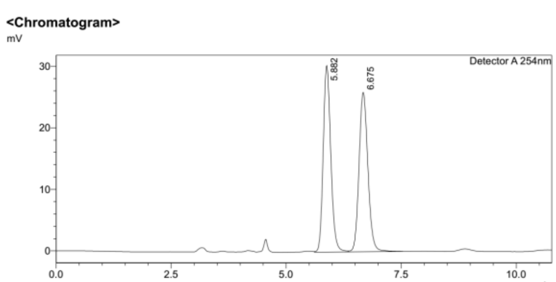

<Peak Table>
Detector A 254nm

Peak#	Ret. Time	Area	Height	Area%	Height%
1	5.882	346513	30289	49.939	53.899
2	6.675	347357	25907	50.061	46.101
Total		693870	56196	100.000	100.000

Racemic **3d'**

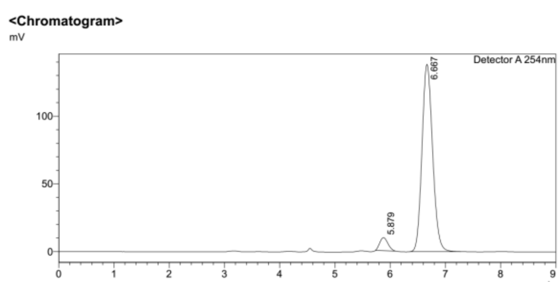

<Peak Table>
Detector A 254nm

Peak#	Ret. Time	Area	Height	Area%	Height%
1	5.879	99545	9636	5.107	6.516
2	6.667	1849703	138249	94.893	93.484
Total		1949248	147885	100.000	100.000

Enantioenriched **3d'**

Ethyl (4*R*,5*R*)-5-(5,6-dichloro-1*H*-indol-3-yl)-1-((methoxycarbonyl)amino)-2-methyl-4-phenyl-4,5-dihydro-1*H*-pyrrole-3-carboxylate **3e'**

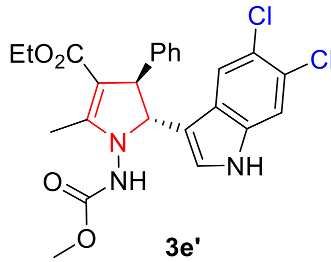

3e'

A colorless oil; isolated yield = 94%; dr >20:1; $[a]_D^{25}$ = –82 (c 2.3, $CHCl_3$); ^1H NMR (400 MHz, $CDCl_3$) δ 8.43 (s, 1H), 7.47 (s, 2H), 7.25 – 7.13 (m, 5H), 6.99 (s, 1H), 6.47 (s, 1H), 4.82 (s, 1H), 4.20 (d, *J* = 9.2 Hz, 1H), 4.08 – 3.98 (m, 1H), 3.95 – 3.84 (m, 1H), 3.70 (s, 3H), 2.36 (d, *J* = 1.2 Hz, 3H), 0.94 (t, *J* = 7.1 Hz, 3H); ^{13}C NMR (101 MHz, $CDCl_3$) δ 166.5, 160.3, 155.9, 144.4, 135.7, 128.2, 128.0, 126.5, 125.4, 123.9, 120.8, 113.9, 113.0, 102.8, 77.3, 77.0, 76.7, 70.1, 59.1, 53.6, 52.9, 14.0, 12.3; HRMS (ESI) m/z calcd for $C_{24}H_{24}Cl_2N_3O_4$ $[M + H]^+$ = 488.1138, found = 488.1114; the ee value was 92%, t_R (major) = 5.2 min, t_R (minor) = 4.5 min (Chiralpak ID, λ = 254 nm, 20% *i*-PrOH/Hexane, flow rate = 1.0 mL/min).

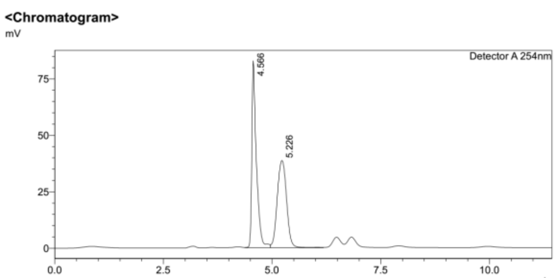

<Peak Table>

Detector A 254nm

Peak#	Ret. Time	Area	Height	Area%	Height%
1	4.566	596871	82795	50.958	68.186
2	5.226	574439	38630	49.042	31.814
Total		1171310	121424	100.000	100.000

Racemic **3e'**

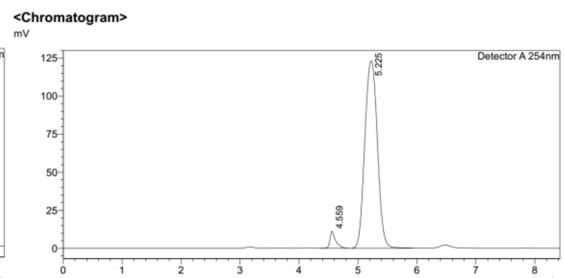

<Peak Table>

Detector A 254nm

Peak#	Ret. Time	Area	Height	Area%	Height%
1	4.559	74522	11200	3.914	8.332
2	5.225	1829527	123213	96.086	91.668
Total		1904049	134413	100.000	100.000

Enantioenriched **3e'**

Ethyl (4*R*,5*R*)-5-(1*H*-indol-3-yl)-1-((methoxycarbonyl)amino)-2,4-dimethyl-4,5-dihydro-1*H*-pyrrole-3-carboxylate **3f'**

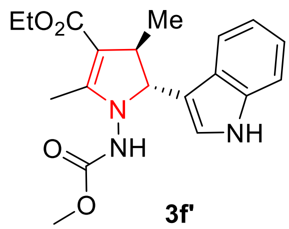

3f'

A colorless oil; isolated yield = 84%; dr >20:1; ^{1}H NMR (400 MHz, $CDCl_3$) δ 8.31 (s, 1H), 7.59 (d, *J* = 7.6 Hz, 1H), 7.39 (d, *J* = 8.1 Hz, 1H), 7.24 – 7.06 (m, 3H), 6.31 (s, 1H), 4.52 (s, 1H), 4.30 – 4.10 (m, 2H), 3.69 (s, 3H), 3.27 (s, 1H), 2.24 (s, 3H), 1.37 – 1.22 (m, 6H).; ^{13}C NMR (100 MHz, $CDCl_3$) δ 167.2, 159.7, 156.1, 144.3, 136.9, 125.9, 123.7, 122.5, 119.9, 119.8, 114.5, 111.5, 103.6, 68.6, 58.9, 52.8, 41.7, 19.7, 14.5, 12.3; HRMS (ESI) m/z calcd for $C_{19}H_{24}N_3O_4$ $[M + H]^+$ = 358.1761, found = 358.1755; the ee value was 64%, t_R (major) = 6.4 min, t_R (minor) = 5.7 min (Chiralpak ID, λ = 254 nm, 20% *i*-PrOH/Hexane, flow rate = 1.0 mL/min).

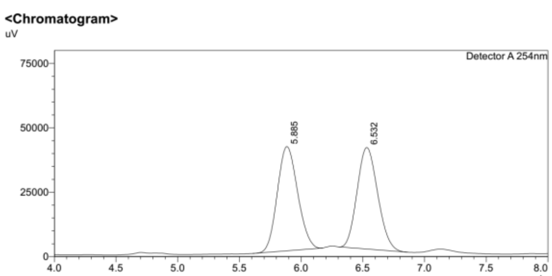

<Peak Table>

Detector A 254nm

Peak#	Ret. Time	Area	Height	Area%	Height%
1	5.885	465215	40487	50.372	50.664
2	6.532	458351	39426	49.628	49.336
Total		923565	79913	100.000	100.000

Racemic **3f'**

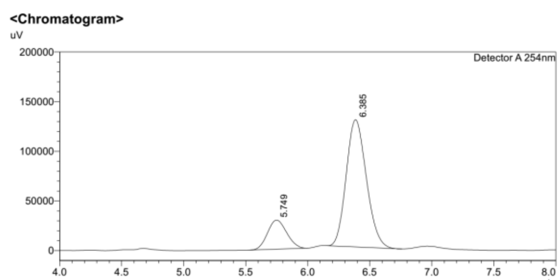

<Peak Table>

Detector A 254nm

Peak#	Ret. Time	Area	Height	Area%	Height%
1	5.749	316835	29333	17.883	18.612
2	6.385	1454871	128269	82.117	81.388
Total		1771706	157602	100.000	100.000

Enantioenriched **3f'**

Ethyl (3*S*,8*R*)-1-((methoxycarbonyl)amino)-2,8-dimethyl-3-((E)-styryl)-1,3,8,8-tetrahydropyrrolo[2,3-*b*]indole-3-carboxylate **5**

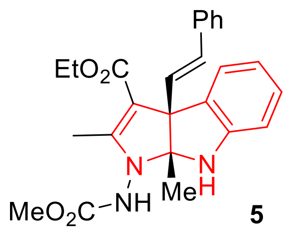

5

A colorless oil; isolated yield = 88%; $[\alpha]_D^{25}$ = –98 (c 1.6, $CHCl_3$); dr >20:1; ^{1}H NMR (400 MHz, $CDCl_3$) δ 7.55 (d, *J* = 4 Hz, 1H), 7.37 (d, *J* = 7.3 Hz, 2H), 7.31 – 7.28 (m, 2H), 7.23 – 7.20 (m, 1H), 7.13 – 7.08 (m, 1H), 6.90 – 6.86 (m, 1H), 6.72 – 6.70 (m, 2H), 6.47 – 6.30 (m, 2H), 4.21 – 4.06 (m, 2H), 3.79 (s, 3H), 2.26 (s, 3H), 1.40 (s, 3H), 1.22 (t, J = 7.1 Hz, 3H); ^{13}C NMR (100 MHz, $CDCl_3$) δ 165.6, 159.8, 156.8, 147.8, 137.3, 132.4, 132.0, 130.4, 128.5, 127.9, 127.4, 126.5, 120.5, 110.4, 104.7, 94.1, 62.9, 59.2, 53.1, 21.6, 14.5, 12.6; HRMS (ESI) m/z calcd for $C_{25}H_{28}N_3O_4$ $[M + H]^+$ = 434.2074, found = 434.2083; the ee value was 95%, t_R (major) = 6.9 min, t_R (minor) = 12.4 min (Chiralpak IC, λ = 254 nm, 20% *i*-PrOH/Hexane, flow rate = 1.0 mL/min).

<Chromatogram>

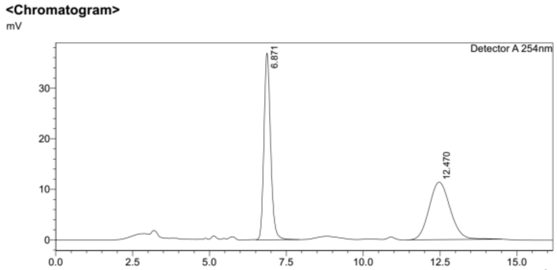

<Peak Table>

Detector A 254nm

Peak#	Ret. Time	Area	Height	Height%	Area%
1	6.871	554150	36851	76.451	50.540
2	12.470	542319	11351	23.549	49.460
Total		1096470	48202	100.000	100.000

Racemic **5**

<Chromatogram>

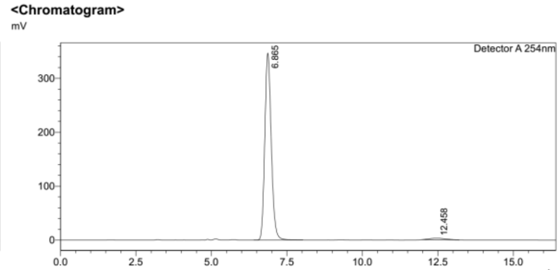

<Peak Table>

Detector A 254nm

Peak#	Ret. Time	Area	Height	Height%	Area%
1	6.865	5138197	346282	99.176	97.842
2	12.458	113325	2876	0.824	2.158
Total		5251522	349158	100.000	100.000

Enantioenriched **5**

X-Ray Crystallographic Analysis

Determination of the Absolute Configurations of the Product 3y

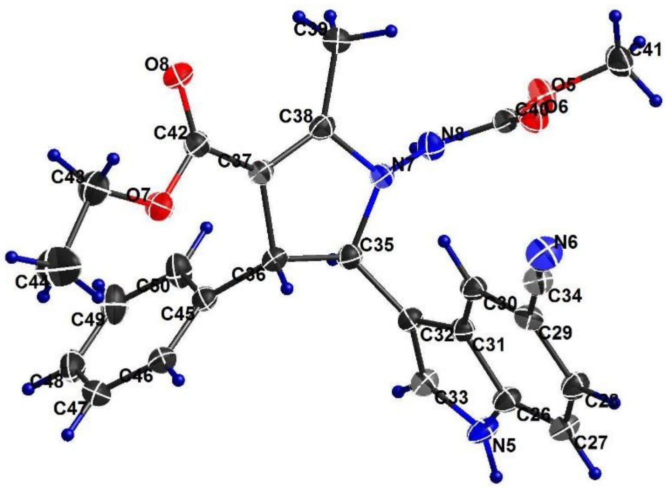

Figure S1. X ray structure of **3y** (CCDC 1957145). Related to Figure 5.

Table S1. Crystal data and structure refinement for j518. Related to Figure 5.

Identification code	j518	
Empirical formula	C25 H24 N4 O4	
Formula weight	444.48	
Temperature	100(2) K	
Wavelength	1.54178 Å	
Crystal system	Triclinic	
Space group	P1	
Unit cell dimensions	a = 9.6507(9) Å	= 76.217(4)°.
	b = 10.4976(10) Å	= 80.536(4)°.

	c = 13.0255(12) Å	= 62.679(3)°.
Volume	1136.32(19) Å^3	
Z	2	
Density (calculated)	1.299 Mg/m^3	
Absorption coefficient	0.734 mm^{-1}	
F(000)	468	
Crystal size	0.312 x 0.107 x 0.098 mm^3	
Theta range for data collection	3.501 to 72.253°.	
Index ranges	-11<=h<=11, -12<=k<=12, -16<=l<=16	
Reflections collected	80402	
Independent reflections	8646 [R(int) = 0.0508]	
Completeness to theta = 67.679°	99.3 %	
Absorption correction	Semi-empirical from equivalents	
Max. and min. transmission	0.7533 and 0.6811	
Refinement method	Full-matrix least-squares on F^2	
Data / restraints / parameters	8646 / 3 / 617	
Goodness-of-fit on F^2	1.034	
Final R indices [I>2sigma(I)]	R1 = 0.0289, wR2 = 0.0741	
R indices (all data)	R1 = 0.0298, wR2 = 0.0747	
Absolute structure parameter	0.07(4)	
Extinction coefficient	n/a	
Largest diff. peak and hole	0.259 and -0.194 e.Å^{-3}	

Preliminary Modeling Approach

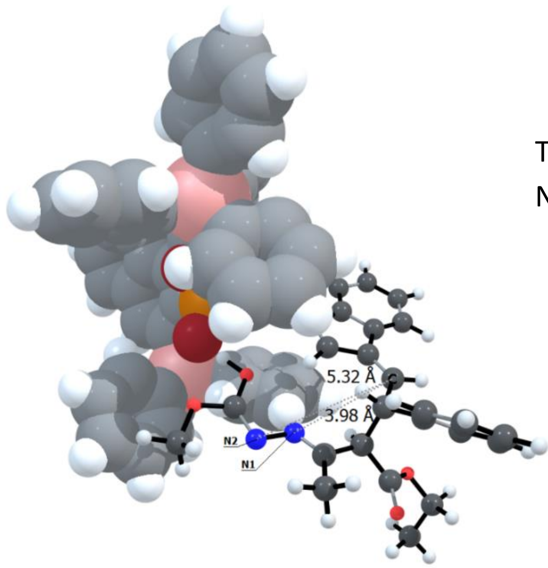

The distance N1-C is 3.98 Å and N2-C is 5.32 Å.

Figure S2. Distances between key atoms in intermediate **A**. Related to Figure 6.

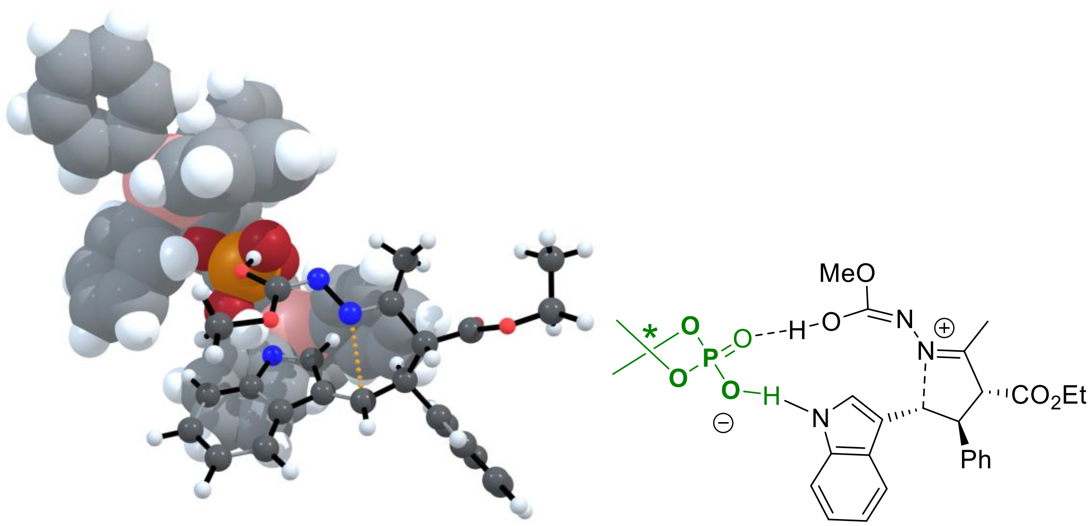

Figure S3. 5-exo attack from intermediate **A**. Related to Figure 6.

TS1 (Favored)

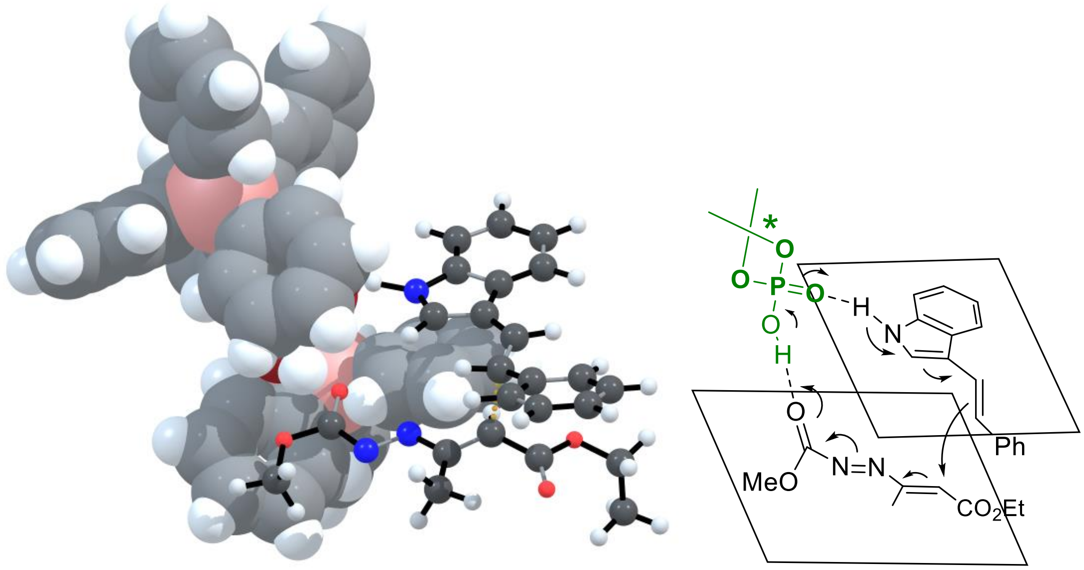

Figure S4. Plausible Transition states. Related to Figure 6.

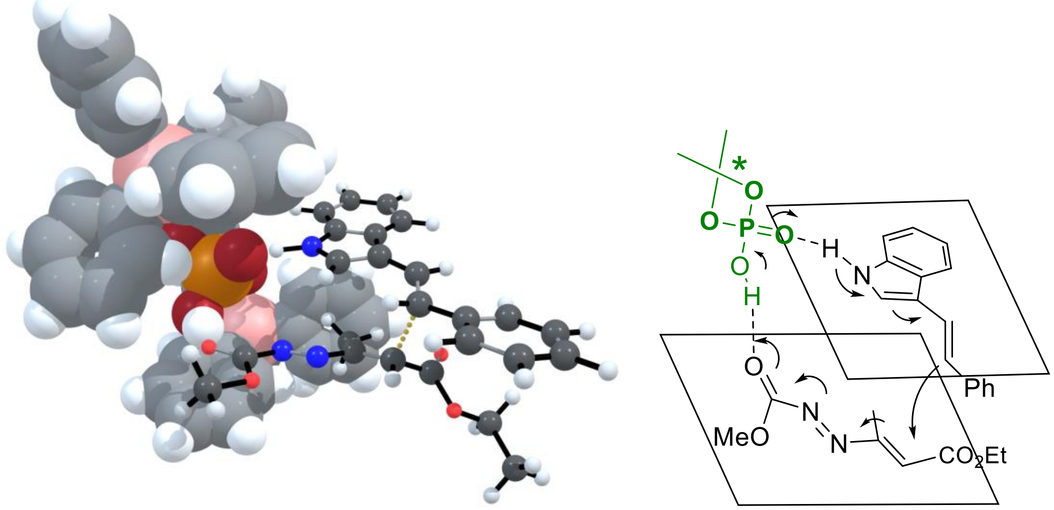

Figure S5. TS1’ (6.2 kcal/mol higher). Related to Figure 6.

Data S3. Geometries at HF/STO-3G: Related to Figure 6

A
Geometry at E(RHF/STO-3G)
C -0.6467264862 0.0147821728 -4.2140516052
C -0.6913260990 -1.2084051870 -3.2898311757
C -0.4244216584 -1.1814786826 -1.9911851084
C -0.0120152508 -0.0141576701 -1.1452175820
N 0.1537800605 -0.3115923509 0.1036127583
C -0.1368518674 -1.7375949711 0.2350790013
C -0.4752319679 -2.2932740233 -1.0036111369
C -0.0981431068 -2.4990613584 1.3878970706
C -0.4084687993 -3.8513316661 1.2805149627
C -0.7452943059 -4.4109441468 0.0552341468
C -0.7836900244 -3.6370243245 -1.1009821659
H -0.9337668683 0.8720911377 -3.6100800236
H 0.2639390850 0.7313925527 1.3256478897
C -1.6692324506 -0.0877367415 -5.3600964681
C -1.7434926172 -1.2058044073 -6.1877976497
C -2.6756976381 -1.2691987829 -7.2097826665
C -3.5524481079 -0.2158489229 -7.4224552827
C -3.4900505166 0.9001499382 -6.6043751426
C -2.5561005659 0.9610021474 -5.5813259219
H -0.9611904823 -2.1561044464 -3.7461824851
H 0.1848907760 0.9955639359 -1.5076594938
H 0.1647244638 -2.0596553031 2.3417765266
H -0.3867052512 -4.4758319722 2.1646597537
H -0.9820342417 -5.4658898102 -0.0013264319
H -1.0490209164 -4.0854756500 -2.0501445693
H -1.0663344304 -2.0355963827 -6.0366474634
H -2.7185554228 -2.1459289339 -7.8436518400
H -4.2811435077 -0.2666702622 -8.2212711641
H -4.1712831574 1.7271371289 -6.7601561506
H -2.5184008999 1.8359246436 -4.9449952146
C 0.8463937914 0.3071420008 -4.6748140006
C 1.1575895801 1.8115306720 -4.5037037225
N 1.5254867091 2.1022228021 -3.3077006427
C 1.1817949948 -0.2764570784 -6.0723344998
C 0.9278994062 2.7903318321 -5.6512485858
N 1.7856793966 3.5044303996 -3.0542238144
C 1.7282770851 3.6800766538 -1.7501704375
O 1.1858938022 0.2996943537 -7.1416185344
O 1.4971692986 -1.6311029854 -5.9392460812
C 1.8707401093 -2.2545805469 -7.1832499278
C 3.3374763140 -1.9673145553 -7.5750279791
O 1.3670388778 2.7769885852 -0.8378406067
O 2.0054230906 4.9291710738 -1.2119620633
C 2.4114304632 5.8960610488 -2.1916455633
H 1.4932231336 -0.2188902413 -3.9753081304
H 1.6870582254 2.6695689473 -6.4192590420
H 0.9738596132 3.8039250424 -5.2689392140
H -0.0410032964 2.6210965226 -6.1125405441
H 1.2027306073 -1.9387340954 -7.9907284910
H 1.7355520352 -3.3288608124 -7.0277550263
H 3.5923798384 -2.5305671599 -8.4673693765
H 4.0079748526 -2.2621317791 -6.7736068680
H 3.4795688381 -0.9111193761 -7.7802754917
H 2.6345538571 6.8146681454 -1.6452444072
H 1.6189799788 6.0931545610 -2.9185219152
H 3.3034131372 5.5733270510 -2.7345860136
C -0.4205001986 -1.5414744412 8.0178324051
C 0.9869990337 -1.4995823348 7.8087492366
C 1.5351483842 -0.5520527783 7.0119282365
C 0.7152707077 0.4228741732 6.3585388327
C -0.6744439281 0.3672667954 6.5498495338
C -1.2220340975 -0.6377666703 7.4076294745
C 1.2519595058 1.4284545019 5.4751743854
C 0.3833862646 2.2189808675 4.7780777709
C -1.0342438913 2.2463198006 5.0263668943
C -1.5151249800 1.3291749141 5.9005492213
C 3.7226319768 2.6708575166 8.8085810267
C 5.1265465616 2.8446388046 8.6478028180
C 5.6939493667 2.6452866045 7.4364870819
C 4.9016886983 2.2528548499 6.3115753713
C 3.5229148277 2.0507021417 6.4712226769
C 2.9513269261 2.2893962305 7.7638069179
C 5.4881068309 2.0760756392 5.0204719419
C 4.7647064072 1.7598017727 3.9175334679
C 3.3449994081 1.5823302162 4.0959684606
C 2.7400585283 1.6571317387 5.3232207455
O 2.5952891973 1.2236078948 2.9617167175
O 0.9042845933 3.1071936886 3.8076786155
P 1.4163901454 2.2947837006 2.4356571676
O 1.9438081803 3.3624450110 1.3842236596
O 0.1470312543 1.3167079650 2.1405054784
Si -2.1183455753 3.5725663973 4.2658132503
C -1.4742058357 5.2717748450 4.7001911572
C -2.1671162451 6.3965195677 4.2501430439
C -1.7584719601 7.6796431795 4.5741227463
C -0.6392852197 7.8699006681 5.3703068470
C 0.0569367988 6.7684529937 5.8382549025
C -0.3608269050 5.4873070034 5.5064508658
C -2.2351542589 3.3507963772 2.4174406841
C -1.7721701361 4.3110720919 1.5233909146
C -1.8869827083 4.1382087158 0.1510428007
C -2.4721647431 2.9908479504 -0.3567898931
C -2.9305093040 2.0147297748 0.5154222598
C -2.8076240791 2.1955290455 1.8830114911
C -3.8203800375 3.4625588545 5.0355341148
C -3.9655654615 3.6496597136 6.4112635086
C -5.2073363243 3.6144386890 7.0232509936
C -6.3476016375 3.3954418302 6.2647635623
C -6.2296058888 3.2189987324 4.8968505531
C -4.9795063409 3.2552628215 4.2946021807
Si 5.6617580341 1.5992739098 2.2790986030
C 7.3661198990 0.9274398230 2.6696998754
C 7.5290725440 -0.1390746839 3.5545965349
C 8.7785155733 -0.6677766284 3.8351499687
C 9.9080194301 -0.1364768650 3.2320238903
C 9.7721247285 0.9249592557 2.3533124527
C 8.5155051973 1.4455655557 2.0794090804
C 4.8330780742 0.4312229665 1.0805143301
C 4.9598896383 -0.9506001522 1.2107676841
C 4.3869069968 -1.8185171262 0.2948532253
C 3.6726014015 -1.3196157247 -0.7831985338
C 3.5299386274 0.0505924527 -0.9309647412
C 4.1026221580 0.9083976071 -0.0043935717
C 5.8216071851 3.2941480608 1.5121637515
C 5.4882261235 4.4504927956 2.2117094677
C 5.6322806796 5.7086860585 1.6455909944
C 6.1197075872 5.8372193057 0.3556914355
C 6.4593239983 4.6998762889 -0.3606296028
C 6.3102900596 3.4481295881 0.2144158547
H -0.8378153177 -2.3043017934 8.6626433345
H 1.6146475810 -2.2375130004 8.2922639111
H 2.6036365925 -0.5286545517 6.8483445737
H -2.2947350393 -0.6613433772 7.5527999329
H -2.5715370297 1.2947963815 6.1364079606
H 3.2761222373 2.8530955355 9.7779670648
H 5.7251981104 3.1452741822 9.4980845803
H 6.7578755445 2.7844594721 7.2916664044
H 1.8856077929 2.1733284602 7.8959521938
H 6.5591848595 2.2204561878 4.9482784542
H -3.0502499752 6.2761861781 3.6338174772
H -2.3150255334 8.5327418465 4.2072754227
H -0.3155356946 8.8706082861 5.6268764484
H 0.9287616698 6.9042782576 6.4656439591
H 0.2029387655 4.6481844044 5.8929253090
H -1.3085484673 5.2175187178 1.8922183826
H -1.5168160727 4.9024439395 -0.5206086608
H -2.5671220088 2.8550418335 -1.4266132435
H -3.3835513751 1.1106037645 0.1290309774
H -3.1643254195 1.4130168142 2.5422261368
H -3.0920686070 3.8313809918 7.0263374084
H -5.2871916623 3.7609939223 8.0929717547
H -7.3210144925 3.3678826291 6.7377871327
H -7.1132120516 3.0546731894 4.2931214214
H -4.9215830847 3.1222823481 3.2219065283
H 6.6667416871 -0.5686329113 4.0497905274
H 8.8715040200 -1.4951422442 4.5272338451
H 10.8866235869 -0.5456467699 3.4485650647
H 10.6467932007 1.3515574299 1.8787277407
H 8.4428751630 2.2784944436 1.3917089161
H 5.5221364703 -1.3705418940 2.0349788745
H 4.5033807542 -2.8875813119 0.4201121438
H 3.2305637663 -1.9966024699 -1.5031805468
H 2.9713215123 0.4632207890 -1.7627304845
H 3.9731385484 1.9738016765 -0.1438866133
H 5.1050094396 4.3805525411 3.2222299874
H 5.3617599038 6.5895532936 2.2139744167
H 6.2334613611 6.8172071832 -0.0901731297
H 6.8401238468 4.7878219900 -1.3702839478
H 6.5792622655 2.5766868371 -0.3703594707
H 1.6191079237 3.1021849971 0.1434337938

TS1
Geometry at E(RHF/STO-3G)
C -1.0349648106 -0.1495039922 -4.1008105053
C -0.7797841342 -1.1746772153 -3.1955204310
C -0.4001082876 -1.0302984250 -1.8486829702
C -0.2863371230 0.1658785715 -1.1049758752
N 0.1156362253 -0.0446660804 0.1530970594
C 0.2664826592 -1.4445728581 0.3035549335
C -0.0369423963 -2.0810793470 -0.9085015984
C 0.6509911327 -2.1686703921 1.4379891999
C 0.7266536272 -3.5363034793 1.3342318596
C 0.4278991787 -4.1866058092 0.1241016074
C 0.0499055828 -3.4776405178 -0.9904688815
H -1.2382706130 0.8183458205 -3.6673419445
H 0.1558250287 0.8188186637 1.0339381733
C -1.7755488394 -0.3805370835 -5.3837617492
C -1.8285188605 -1.6182764323 -6.0302093803
C -2.5316882497 -1.7750814642 -7.2118342542
C -3.1989982649 -0.7018414705 -7.7815837791
C -3.1548992495 0.5339027709 -7.1548651890
C -2.4522485920 0.6910807935 -5.9733367937
H -0.7916731346 -2.1950059759 -3.5704845216
H -0.4835226302 1.1741686038 -1.4536725481
H 0.8819851744 -1.6633238469 2.3667409028
H 1.0202069917 -4.1266587355 2.1922935598
H 0.4982183988 -5.2656066385 0.0769958085
H -0.1779296757 -3.9929249208 -1.9147808618
H -1.3152497145 -2.4713603285 -5.6098332321
H -2.5591603457 -2.7450514996 -7.6923798749
H -3.7481164445 -0.8277074616 -8.7053190636
H -3.6722534763 1.3804630582 -7.5885912425
H -2.4278323804 1.6596984154 -5.4918379346
C 0.9907411555 0.4017995605 -4.5805436022
C 1.0860773256 1.7889491850 -4.4944400914
N 1.3493936082 2.2310577780 -3.2057855593
C 1.1463301382 -0.3559712051 -5.9015943215
C 0.8025105494 2.7649310614 -5.6236623246
N 1.3784531725 3.5456370128 -3.0710676324
C 1.6303002414 3.8208833585 -1.6696833976
O 1.0090290506 0.0904004648 -7.0261967957
O 1.5031203971 -1.6770392922 -5.6368433853
C 1.7315998479 -2.4532209434 -6.8296858330
C 3.1343290843 -2.2146302792 -7.4319163350
O 1.6731445044 2.9862197165 -0.7512575469
O 1.7969453645 5.1471972434 -1.3260012457
C 1.7616758056 6.0718625592 -2.4265648187
H 1.4055338637 -0.1395030622 -3.7358374968
H 0.6610820202 2.2280861074 -6.5548513443
H 1.6303186059 3.4603094730 -5.7406306968
H -0.0893330610 3.3532276035 -5.4171089815
H 0.9631022081 -2.2430529623 -7.5799984404
H 1.6352140025 -3.4985272135 -6.5226020371
H 3.2878735127 -2.8866473414 -8.2705163225
H 3.9026579811 -2.4039757484 -6.6885405136
H 3.2317769912 -1.1930296638 -7.7851628297
H 1.9262715184 7.0613304718 -1.9948730854
H 0.7960561676 6.0588836257 -2.9378914764
H 2.5469356444 5.8644190160 -3.1575293163
C -0.7767109472 -1.7193792146 7.6485599492
C 0.6337086664 -1.7577176822 7.4560201226
C 1.2563265154 -0.7891391861 6.7439734904
C 0.5125392679 0.2885169098 6.1652410685
C -0.8804586510 0.3150667682 6.3399710099
C -1.5070246730 -0.7164278431 7.1081707913
C 1.1263508511 1.3223667121 5.3708355800
C 0.3221242259 2.2267502159 4.7388226550
C -1.0919781045 2.3354423802 4.9749160766
C -1.6444681299 1.3833401326 5.7669878647
C 3.6003215564 2.1735948866 8.8136402157
C 5.0125487250 2.2969151519 8.6835472917
C 5.5895220737 2.1631072518 7.4676184114
C 4.7984351361 1.8899641301 6.3073266535
C 3.4101803415 1.7384184153 6.4343234751
C 2.8293241071 1.9056328700 7.7337497862
C 5.3981583448 1.7818738855 5.0144444466
C 4.6818368060 1.5734449477 3.8822799820
C 3.2518502555 1.4534316165 4.0298055176
C 2.6281758966 1.4696741552 5.2492174506
O 2.5093900849 1.2207024070 2.8529629768
O 0.9279415396 3.1413715776 3.8382292360
P 1.3582598675 2.3559528991 2.4258051364
O 2.0812117791 3.5366286186 1.5767157313
O 0.0517588661 1.6346291765 1.8609973001
Si -2.0759136147 3.7967691472 4.3326241562
C -1.3263527265 5.3972967562 4.9397096157
C -1.9546293209 6.6025005605 4.6220351232
C -1.4665500258 7.8176618558 5.0729588035
C -0.3300034162 7.8562290541 5.8665042204
C 0.3034626739 6.6723540654 6.2038918148
C -0.1938481659 5.4604499781 5.7454669180
C -2.1718940292 3.7706819336 2.4701148951
C -1.6512906579 4.7960642580 1.6869584736
C -1.7530523195 4.7733364516 0.3031977723
C -2.3831452334 3.7149710907 -0.3290398744
C -2.9007023370 2.6763888881 0.4306704624
C -2.7902056912 2.7069512117 1.8111807086
C -3.7937364033 3.7234100224 5.0692776593
C -3.9516565416 3.8139354867 6.4532837425
C -5.2036281879 3.7982251153 7.0448925142
C -6.3407620784 3.6967648807 6.2573496115
C -6.2093005873 3.6169660897 4.8815891196
C -4.9491330191 3.6326034929 4.2997415269
Si 5.5791409777 1.4815520898 2.2370144160
C 7.3509460836 0.9922903591 2.5968874802
C 7.6509114000 -0.0719775415 3.4484000219
C 8.9575461135 -0.4609114841 3.6950605191
C 10.0079471332 0.2119642377 3.0902933845
C 9.7357890952 1.2732955000 2.2437123921
C 8.4231394619 1.6534140584 2.0038783008
C 4.8475951790 0.2174710715 1.0730061342
C 5.1502465148 -1.1369024084 1.1983114318
C 4.6491959375 -2.0771623201 0.3117436452
C 3.8296203646 -1.6799112447 -0.7324904031
C 3.5118302087 -0.3386774534 -0.8735747836
C 4.0140861700 0.5918007059 0.0221886821
C 5.5659848185 3.1738714877 1.4490084342
C 5.2115195140 4.3120073669 2.1682370985
C 5.2377429554 5.5731650070 1.5911867170
C 5.6262917047 5.7231695830 0.2702399793
C 5.9879435355 4.6048082321 -0.4648662315
C 5.9574402919 3.3498026193 0.1217187804
H -1.2537096630 -2.5019179125 8.2248434245
H 1.2026054210 -2.5739279011 7.8832860895
H 2.3262386740 -0.8251797312 6.5918214329
H -2.5807873307 -0.6781596076 7.2418248880
H -2.7036853377 1.4030001516 5.9920248643
H 3.1469934263 2.3023243755 9.7884603676
H 5.6104434149 2.5068415769 9.5612129255
H 6.6605513212 2.2653515273 7.3464033433
H 1.7578589814 1.8272637848 7.8445662653
H 6.4745846804 1.8879822009 4.9680829304
H -2.8494861660 6.6003323605 4.0108476033
H -1.9746579159 8.7360870530 4.8075231372
H 0.0556097537 8.8032201600 6.2222931575
H 1.1880154713 6.6891894695 6.8279488693
H 0.3224848341 4.5537186969 6.0325358905
H -1.1531149323 5.6363038653 2.1543077801
H -1.3396453696 5.5865436838 -0.2797611253
H -2.4690248325 3.6963922206 -1.4082265382
H -3.3888970871 1.8400816469 -0.0535152107
H -3.1929680295 1.8772220856 2.3800627498
H -3.0802370268 3.9026426070 7.0913476262
H -5.2937509103 3.8680761105 8.1215320583
H -7.3220919484 3.6848948776 6.7144606961
H -7.0899618574 3.5443423466 4.2559453793
H -4.8801977312 3.5768944060 3.2209141016
H 6.8533399206 -0.6115360187 3.9442140020
H 9.1567309931 -1.2903346125 4.3618030021
H 11.0306128354 -0.0881447040 3.2803398176
H 10.5471222199 1.8092175961 1.7674943170
H 8.2429295803 2.4892134028 1.3397005467
H 5.7973234729 -1.4785438983 1.9955482912
H 4.9029964512 -3.1224061974 0.4346882504
H 3.4383084047 -2.4107875348 -1.4287576845
H 2.8689851215 -0.0097463659 -1.6797718042
H 3.7464722508 1.6309983216 -0.1181791590
H 4.9053642161 4.2248144080 3.2036048228
H 4.9533403172 6.4393085609 2.1751850954

H 5.6480500070 6.7055259250 -0.1843133180
H 6.2955744362 4.7103575684 -1.4975062816
H 6.2455217644 2.4933050743 -0.4759417017
H 1.9195585125 3.3753327837 0.5722135719

TS1'
Geometry at E(RHF/STO-3G)
C 2.6066071648 6.4271005647 -3.7331247849
C 2.8710115195 7.0422226325 -2.5151486196
C 2.9759106203 6.3614886497 -1.2913077522
C 2.8825325636 4.9699857768 -1.1006588475
N 2.8447676639 4.6298410397 0.1984977893
C 2.9542699275 5.8296218111 0.9383113875
C 3.0405342885 6.9155805483 0.0546907211
C 3.0051135475 6.0096619950 2.3258768210
C 3.1393819787 7.2897012595 2.8057143152
C 3.2182790808 8.3869803419 1.9303300682
C 3.1684978160 8.2128574337 0.5681698136
H 2.8738464117 5.3821546937 -3.8030829105
H 2.6780790241 3.4944943720 0.5637765750
C 2.7334269474 7.1492198243 -5.0436670047
C 2.6193510859 8.5354706051 -5.1688123462
C 2.7404639338 9.1500490199 -6.4032697699
C 2.9737418185 8.3972984936 -7.5437628350
C 3.0837666281 7.0194679947 -7.4375046410
C 2.9635487462 6.4049590652 -6.2034379877
H 2.8807402761 8.1271373863 -2.4689212142
H 2.8708726972 4.2013101329 -1.8639650843
H 2.9447484397 5.1647631292 2.9984851736
H 3.1865612437 7.4615676432 3.8732499727
H 3.3227224666 9.3818608997 2.3430140133
H 3.2335239486 9.0655960700 -0.0957349863
H 2.4326467371 9.1455800694 -4.2961294452
H 2.6513689622 10.2267918273 -6.4752378850
H 3.0684834389 8.8806692398 -8.5071990425
H 3.2655320928 6.4202755845 -8.3208681770
H 3.0534479310 5.3287710271 -6.1313680999
C 0.5819494576 5.8950916436 -3.5906987767
C 0.2984433368 5.1231785410 -2.4635069564
N 0.5253344795 3.7560566781 -2.6556925191
C -0.0664745691 7.2714638624 -3.7770219081
C -0.3269359363 5.6532116899 -1.1822868074
N 0.2192006346 2.9904709504 -1.6336555809
C 0.5018986046 1.6054285314 -2.0032597088
O -0.1401198816 8.1701515273 -2.9592934773
O -0.5975544668 7.3627961961 -5.0620026107
C -1.2417064892 8.6286770031 -5.3029667732
C -1.7688456494 8.6217578133 -6.7504680169
O 0.5348273527 0.6853086055 -1.1774256517
O 0.6981763204 1.3641382105 -3.3499078304
C 0.9524397726 -0.0241510537 -3.6328881749
H 0.6767025772 5.3503954490 -4.5255496629
H 0.1418158173 5.2154921135 -0.3064295904
H -1.3872417816 5.4093324808 -1.1415889549
H -0.2236851349 6.7312610661 -1.1315310725
H -0.5336166782 9.4523271163 -5.1601082970
H -2.0667979925 8.7787233881 -4.5974579035
H -2.2628455886 9.5641745424 -6.9668953841
H -2.4803993433 7.8138284510 -6.8901835085
H -0.9491097046 8.4874411917 -7.4494433764
H 1.0817270383 -0.1000403018 -4.7136442315
H 0.1170167679 -0.6586906416 -3.3248826150
H 1.8603230496 -0.3776394149 -3.1366849668
C -0.0017270713 1.3641850820 8.9039942511
C 1.3775393518 1.2511605813 8.5691457828
C 1.8177821917 1.5971077278 7.3367409345
C 0.9105871501 2.0830313338 6.3397198261
C -0.4499797920 2.1650697308 6.6649328142
C -0.8852747739 1.8039488346 7.9790248368
C 1.3287360876 2.4481106400 5.0068286480
C 0.3796888998 2.7659842379 4.0703052638
C -1.0217550826 2.8950572274 4.3960353420
C -1.3792844249 2.6030753793 5.6712759411
C 4.3852967412 4.9832025882 6.8617033859
C 5.7598300448 4.7922888455 6.5382368508
C 6.1170818820 3.8590059360 5.6268530340
C 5.1286381442 3.0509049447 4.9793170797
C 3.7758057044 3.2211803009 5.3142997767
C 3.4293782567 4.2264887043 6.2745716814
C 5.4932164715 2.0765772917 3.9976771677
C 4.5814738491 1.3349437671 3.3154681804
C 3.2027525531 1.5561003124 3.6533876237
C 2.7974265141 2.4038677878 4.6456384920
O 2.1904652318 0.8475512237 2.9600277791
O 0.7726139075 3.0886070398 2.7476317297
P 1.4495024865 1.8497191721 1.8446463760
O 2.5476366897 2.3285657844 0.7904486978
O 0.2277853635 0.9582400115 1.2563066199
Si -2.3490642008 3.4675887352 3.1967623303
C -2.0219063752 5.1815529080 2.5387561073
C -3.0370104530 5.8370590028 1.8394440114
C -2.8829908453 7.1352914574 1.3838158672
C -1.7005964237 7.8183611190 1.6263735247
C -0.6832018078 7.1904570317 2.3241992470
C -0.8467823956 5.8871078326 2.7733926742
C -2.5910220902 2.2026649370 1.8482840392
C -2.7539917577 2.5550556340 0.5125220594
C -3.0016845434 1.5987873719 -0.4622244453
C -3.0932847224 0.2612571650 -0.1160049411
C -2.9301873636 -0.1134608309 1.2091663370
C -2.6819384587 0.8487952575 2.1740161120
C -3.9477419600 3.6043538503 4.1645034434
C -4.1393821980 4.6727758315 5.0420253566
C -5.3110899457 4.8182933591 5.7658398548
C -6.3320781907 3.8901308089 5.6257249915
C -6.1666318118 2.8242403997 4.7580023610
C -4.9873125535 2.6881629221 4.0388368025
Si 5.1857682608 0.0816213064 2.0578401191
C 6.6833079435 -0.7452324582 2.8159619594
C 6.7004730967 -1.0998949271 4.1647297577
C 7.7920682271 -1.7348622837 4.7351747735
C 8.9034073543 -2.0324365779 3.9619136564
C 8.9098377433 -1.6881294233 2.6203598542
C 7.8109574908 -1.0535687694 2.0598531754
C 3.9047734273 -1.2252044672 1.6820329991
C 3.7864002013 -2.3660566311 2.4721079689
C 2.8424052461 -3.3437392102 2.1961761010
C 1.9897447683 -3.1996165754 1.1140185395
C 2.0906993971 -2.0727700843 0.3132059319
C 3.0379900280 -1.1021355563 0.5977328124
C 5.6894168681 0.9457790938 0.4821249637
C 5.8951116873 2.3214332302 0.4246707042
C 6.2998715619 2.9454402333 -0.7462166497
C 6.5111284985 2.1985003633 -1.8935454433
C 6.3137333983 0.8268691584 -1.8595611926
C 5.9085963856 0.2138369640 -0.6847169986
H -0.3309946661 1.0868216662 9.8972534918
H 2.0719847578 0.8793834350 9.3120046500
H 2.8645300662 1.4957235732 7.0894681613
H -1.9394693282 1.8857663125 8.2119152864
H -2.4139637851 2.6841372304 5.9783680526
H 4.1140162631 5.7453026564 7.5814625730
H 6.5078522661 5.4062212275 7.0236003427
H 7.1566793034 3.7089195578 5.3642228016
H 2.3870485460 4.3808744370 6.5162506743
H 6.5522826965 1.9527996609 3.8041657917
H -3.9771066180 5.3321240474 1.6517188266
H -3.6875986423 7.6173829855 0.8432222267
H -1.5749083834 8.8343710773 1.2740930337
H 0.2440006558 7.7134000171 2.5199215754
H -0.0332955598 5.4252158887 3.3175666676
H -2.6859136765 3.5929884208 0.2125322562
H -3.1249695167 1.9025343207 -1.4940387318
H -3.2892659974 -0.4869244222 -0.8736058680
H -2.9960162986 -1.1567794593 1.4905663062
H -2.5543286710 0.5297446832 3.2019014093
H -3.3595676983 5.4149507155 5.1663489094
H -5.4298674588 5.6577640809 6.4391424356
H -7.2507132163 4.0000425492 6.1879264002
H -6.9579756688 2.0952011879 4.6375531083
H -4.8896031588 1.8469255830 3.3643318256
H 5.8489309456 -0.8734735312 4.7950407727
H 7.7760627993 -1.9970953817 5.7854970137
H 9.7590596408 -2.5274954070 4.4033261521
H 9.7732120326 -1.9129687643 2.0069188825
H 7.8462961049 -0.7930409655 1.0093794075
H 4.4431441713 -2.5088550915 3.3211110110
H 2.7740033663 -4.2204221277 2.8278470356
H 1.2513118961 -3.9605071911 0.8952927894
H 1.4275992923 -1.9452081274 -0.5330464683
H 3.0961720660 -0.2310715086 -0.0437593796
H 5.7348565512 2.9313171504 1.3050333942
H 6.4487622610 4.0177795282 -0.7612077747
H 6.8269615423 2.6819303068 -2.8093686604
H 6.4759313456 0.2330973859 -2.7501968343
H 5.7591042559 -0.8592457070 -0.6868165242
H 0.3263616601 0.8772165648 0.2442772348

TS2
Geometry at E(RHF/STO-3G)
C 0.4102202172 0.8574107716 -4.4259384817
C 0.1870086950 -0.4066703070 -3.5663988331
C -0.2595122602 -0.4631173198 -2.2742077109
C 0.1070196010 0.4280244664 -1.1846502544
N -0.1051058780 -0.0799412791 0.0062790799
C -0.7337356269 -1.3557199683 -0.2169190853
C -0.8191514832 -1.6304372235 -1.5858845099
C -1.2138620707 -2.2479651988 0.7388590966
C -1.7899592316 -3.4219888504 0.2969190920
C -1.8843355309 -3.7033045824 -1.0702644760
C -1.4058567129 -2.8199130955 -2.0169350984
H 0.5322271461 1.7141187894 -3.7663492746
H 0.5570867351 0.1747093410 1.3413816529
C -0.8330268446 1.1010483503 -5.3010126927
C -1.2181455824 0.1953467789 -6.2869526150
C -2.3404010319 0.4314894402 -7.0624939262
C -3.0968436051 1.5774072827 -6.8644537959
C -2.7230168870 2.4840011573 -5.8861370114
C -1.5989065272 2.2456477184 -5.1095099903
H 0.0249170490 -1.3040261602 -4.1660751992
H 0.6075316488 1.3864326375 -1.3016921433
H -1.1405467812 -2.0228855961 1.7953683570
H -2.1780921438 -4.1342189017 1.0130628247
H -2.3431150824 -4.6313128486 -1.3872147169
H -1.4875991913 -3.0505145567 -3.0712172318
H -0.6391452605 -0.7032439330 -6.4544763388
H -2.6264394085 -0.2818146109 -7.8250875499
H -3.9740363355 1.7614454466 -7.4714859905
H -3.3070179802 3.3813243658 -5.7251026660
H -1.3113987184 2.9598696850 -4.3484658151
C 1.7304666853 0.7055795281 -5.2432152544
C 2.7839847699 0.2644706511 -4.2026517473
N 2.2803550721 -0.5576033249 -3.3595354742
C 2.1002697286 2.0322484893 -5.9535510855
C 4.1814031717 0.8668951164 -4.1667535992
N 2.9651729235 -0.7471525483 -2.1106192902
C 2.6343340185 -1.9038365932 -1.5504991461
O 1.7439315588 3.1451109888 -5.6191589295
O 2.9068514666 1.7772246633 -7.0592150510
C 3.2751996627 2.9673789389 -7.7843675234
C 4.4575463107 3.7217140162 -7.1361145288
O 2.8836556056 -2.1579354834 -0.2776130508
O 2.0508952603 -2.9159137227 -2.2967126215
C 1.8928318740 -4.1425254981 -1.5617585508
H 1.6219188437 -0.0573512048 -6.0152014822
H 4.6813091004 0.7179377280 -5.1208537022
H 4.7555316366 0.3942777304 -3.3770550599
H 4.1309434122 1.9356755507 -3.9708583635
H 2.4164549477 3.6388696405 -7.8831098422
H 3.5597963192 2.6260520300 -8.7838096800
H 4.7459589027 4.5547157889 -7.7696716542
H 5.3113933303 3.0612734767 -7.0202304221
H 4.1781891280 4.1093428017 -6.1616831137
H 1.4186357931 -4.8493276164 -2.2450764883
H 1.2568625668 -4.0146097933 -0.6829671887
H 2.8565553686 -4.5475319023 -1.2414278831
C 3.0054185742 3.9265987493 8.3186386908
C 3.9789781898 2.8989778792 8.1652434921
C 4.2206715302 2.3553004266 6.9493255777
C 3.5027462587 2.7956440126 5.7903277644
C 2.5273689028 3.7888696056 5.9504425872
C 2.3023384233 4.3543471999 7.2450485614
C 3.7070515596 2.2342435286 4.4770599550
C 2.8729842342 2.5992769350 3.4540050252
C 1.9068709019 3.6660066240 3.5800029701
C 1.7781670177 4.2208119284 4.8120063113
C 7.9167178928 3.2165590443 5.0086115986
C 8.9093518969 2.2003447532 4.9055110053
C 8.5495949549 0.9350659631 4.5908370103
C 7.1775592364 0.5989083511 4.3619180022
C 6.1945942781 1.5917777109 4.4879009368
C 6.6101651293 2.9246233601 4.8101084440
C 6.7874007864 -0.7310139042 4.0107981062
C 5.5077339319 -1.0743939199 3.7158393286
C 4.5239399468 -0.0249017243 3.8011098881
C 4.8189682097 1.2340492578 4.2475262079
O 3.1778411570 -0.3192602432 3.4928305145
O 3.0329259860 1.9944509351 2.1925288175
P 2.6492046495 0.3690263040 2.0617425225
O 3.4482841331 -0.1343551873 0.7815447738
O 1.0390735948 0.2480935661 2.2486874032
Si 0.8318174354 4.3575350814 2.1997177006
C 1.7092004397 4.7678506942 0.5985699052
C 1.1334538502 5.7282719172 -0.2362123929
C 1.7131078768 6.0882716946 -1.4412724867
C 2.8986783830 5.4935319542 -1.8445730252
C 3.4891165059 4.5407461697 -1.0323048255
C 2.8984950289 4.1847727990 0.1721257777
C -0.6203876153 3.2232469136 1.9011003008
C -1.3182874945 3.2399979328 0.6957851050
C -2.4549387706 2.4692822193 0.5063972578
C -2.9213372579 1.6579571226 1.5285105315
C -2.2423187353 1.6249891372 2.7360008046
C -1.1082547971 2.4021826722 2.9156346925
C 0.1518618767 5.9831806608 2.8357409819
C 0.9775068084 7.1046769903 2.9276810293
C 0.5027800421 8.3196837372 3.3924735322
C -0.8233984900 8.4435912905 3.7799878000
C -1.6612595318 7.3447680665 3.6974156642
C -1.1739357624 6.1316735365 3.2307420401
Si 5.1321222786 -2.8634999338 3.2913978556
C 6.2290151477 -3.9329049755 4.3709999718
C 5.8004183914 -4.4470375102 5.5923196575
C 6.6301525749 -5.2262802680 6.3846964884
C 7.9205051373 -5.5116914160 5.9696714441
C 8.3690582801 -5.0142682016 4.7565655890
C 7.5304503514 -4.2374674332 3.9727320432
C 3.3465290174 -3.2914493889 3.6229828529
C 2.7423991431 -2.9417413701 4.8322163896
C 1.4325940829 -3.2902004407 5.1149271855
C 0.6889970355 -4.0038657292 4.1864874338
C 1.2659790764 -4.3558308106 2.9787556760
C 2.5797790936 -4.0008203102 2.7045902289
C 5.6180718364 -3.2005313145 1.5216439043
C 5.9846074471 -2.1856742343 0.6431476179
C 6.3766621896 -2.4619583107 -0.6592951487
C 6.4110464170 -3.7702781158 -1.1110301966
C 6.0539361726 -4.7983851086 -0.2514541778
C 5.6660491007 -4.5118040466 1.0468009804
H 2.8321305938 4.3508377940 9.2993363219
H 4.5221823974 2.5528981450 9.0355667154
H 4.9532476158 1.5678970610 6.8444550668
H 1.5517447253 5.1282615463 7.3449672292
H 1.0742995503 5.0264126673 4.9759999654
H 8.2206928564 4.2287005834 5.2440697996
H 9.9479335200 2.4551406832 5.0736672885
H 9.2927217564 0.1529430571 4.4997596858
H 5.8635129410 3.7029416275 4.8797706101
H 7.5736820718 -1.4750298644 3.9796040163
H 0.2126474587 6.2176777004 0.0568692867
H 1.2403274476 6.8354762053 -2.0658117513
H 3.3566870408 5.7721026992 -2.7851977066
H 4.4145121388 4.0674554409 -1.3352829148
H 3.3735051102 3.4271937319 0.7808062151
H -0.9766427384 3.8665647759 -0.1189363732
H -2.9779880028 2.5020256554 -0.4409800584
H -3.8081320790 1.0538547111 1.3840825023
H -2.5972655669 0.9945635293 3.5413861558
H -0.5990418200 2.3616856598 3.8710986379
H 2.0169544973 7.0354785028 2.6289298064
H 1.1669119980 9.1726319970 3.4523361609
H -1.1993917492 9.3916901574 4.1429471094
H -2.6983805686 7.4298345056 3.9964050535
H -1.8518970455 5.2887476665 3.1755775900
H 4.7957882295 -4.2486417117 5.9425838410
H 6.2662884476 -5.6125528610 7.3284252375
H 8.5709305077 -6.1200638455 6.5851731028
H 9.3739758273 -5.2333622819 4.4184415884
H 7.9054206884 -3.8704596367 3.0249958324
H 3.2957177429 -2.3751588124 5.5714740573
H 0.9896370749 -3.0037450784 6.0602626619
H -0.3352799045 -4.2790749624 4.4038280474
H 0.6932115393 -4.9075442090 2.2443181686
H 3.0021851359 -4.2813937314 1.7480796163
H 5.9630125598 -1.1523461425 0.9671263114
H 6.6532569705 -1.6509844100 -1.3209830717
H 6.7165236483 -3.9897761641 -2.1262446766
H 6.0823037644 -5.8254261824 -0.5926680746
H 5.4040437632 -5.3344443939 1.7017125327
H 3.1416595383 -1.2240748934 0.2198797662

Transparent Methods

A. General Information

Unless otherwise specified, all reactions were conducted under an inert atmosphere and anhydrous conditions. All the solvents were purified according to the standard procedures. All chemicals which are commercially available were employed without further purification. Thin-layer chromatography (TLC) was performed on silica gel plates (60F-254) using UV-light (254 and 365 nm). Flash chromatography was conducted on silica gel (200–300 mesh). ^{1}H and ^{13}C NMR spectra were recorded at ambient temperature in $CDCl_3$ on a Bruker AMX500 (500 MHz) or AMX400 (400 MHz) spectrometer. Chemical shifts were reported in parts per million (ppm). The data are reported as follows: for ^{1}H NMR, chemical shift in ppm from tetramethylsilane with the solvent as internal standard ($CDCl_3$ δ 7.26 ppm), multiplicity (s = singlet, d = doublet, t = triplet, q = quartet, m = multiplet or overlap of non-equivalent resonances), integration; for ^{13}C NMR, chemical shift in ppm from tetramethylsilane with the solvent as internal indicator ($CDCl_3$ δ 77.1 ppm), multiplicity with respect to protons. All high-resolution mass spectra were performed by the MS service at the chemistry department, National University of Singapore, and were obtained on a Finnigan/MAT 95XL-T spectrometer to be given in m/z. Optical rotations were measured using an Anton Paar MCP-100 digital polarimeter using a 1 cm glass cell. Enantiomeric excesses were determined by HPLC analysis on a chiral stationary phase using CHIRALPAK® columns (IA and ID) eluting with hexane/isopropanol mixtures as indicated.

B. Representative Procedures

General Procedure for synthesis of 3:

To a stirring anhydrous $CHCl_3$ solution (1 ml) of azoalkenes **1** (0.12 mmol) and olefins **2** (0.1 mmol) was added CPA **4f** (1 mol%) at rt. The reaction mixture was stirred until completion of reaction (0.5 h, as monitored by TLC). The solvent was then removed under reduced pressure and the residue was purified by flash column chromatography on silica gel (PE:EtOAc = 4:1) to afford cycloadducts **3**.

Synthesis of 3a at a gram-scale:

To a stirring anhydrous $CHCl_3$ solution (15 ml) of azoalkenes **1a** (4.8 mmol) and indoles **2a** (4 mmol) was added CPA **4f** (1 mol%) at rt. The reaction mixture was stirred until completion of reaction (1.5 h, as monitored by TLC). Water was added and the mixture was extracted with AcOEt (2 × 20 mL). The combined organic layer was washed with brine, separated, dried over Na_2SO_4 and filtered. The solvent was then removed under reduced pressure and the residue was purified by flash column chromatography on silica gel (PE:EtOAc = 4:1) to afford product **3a** (1.5 g) in 90% yield with 92% ee.

C. Calculations

Because the system contains large and flexible binaphthol backbone and SiPh3 groups, selected geometries of the plausible transition states and intermediate were pre-modeled at the HF/STO-3G level of theory to provide visual guidance. The computed energies are thus for providing qualitative insights but subjected to errors. (Frisch et al. 2016) Post-processing visualization was carried out with the ChemCraft program. (Zhurko, http://www.chemcraftprog.com.)

Supplemental References

Attanasi, O., Filippone, P., Mei, A. and Santeusanio, S. (1984). Effect of Metal Ions in Organic Synthesis; Part XXIII. Easy and High-Yield Direct Synthesis of 3-Aminocarbonyl-1-ureidopyrroles by the Copper(II) Chloride-Catalyzed Reaction of Aminocarbonylazoalkenes with 3-Oxoalkanamides. Synthesis *1984*, 671-672.

Attanasi, O., Filippone, P., Mei, A. and Santeusanio, S. (1984). Effect of Metal Ions in Organic Synthesis; Part XXIV. Facile One-Flask Synthesis of 1-Alkoxycarbonylamino-3-aminocarbonylpyrroles by Reaction of Alkoxycarbonylazoalkenes with 3-Oxoalkanamides under Copper(II) Chloride Catalysis. Synthesis *1984*, 873-874.

Cheng, H.-G., Lu, L.-Q., Wang, T., Yang, Q.-Q., Liu, X.-P., Li, Y., Deng, Q.-H., Chen, J.-R. and Xiao, W.-J. (2013). Highly Enantioselective Friedel – Crafts Alkylation/N – Hemiacetalization Cascade Reaction with Indoles. Angew. Chem. Int. Ed. *52,* 3250-3254.

Frisch, M. J., Trucks, G. W., Schlegel, H. B., Scuseria, G. E., Robb, M. A., Cheeseman, J. R., Scalmani, G., Barone, V., Petersson, G. A., Nakatsuji, H., Li, X., Caricato, M., Marenich, A. V., Bloino, J., Janesko, B. G., Gomperts, R., Mennucci, B., Hratchian, H. P., Ortiz, J. V., Izmaylov, A. F., Sonnenberg, J. L., Williams, Ding, F., Lipparini, F., Egidi, F., Goings, J., Peng, B., Petrone, A., Henderson, T., Ranasinghe, D., Zakrzewski, V. G., Gao, J., Rega, N., Zheng, G., Liang, W., Hada, M., Ehara, M., Toyota, K., Fukuda, R., Hasegawa, J., Ishida, M., Nakajima, T., Honda, Y., Kitao, O., Nakai, H., Vreven, T., Throssell, K., Montgomery Jr., J. A., Peralta, J. E., Ogliaro, F., Bearpark, M. J., Heyd, J. J., Brothers, E. N., Kudin, K. N., Staroverov, V. N., Keith, T. A., Kobayashi, R., Normand, J., Raghavachari, K., Rendell, A. P., Burant, J. C., Iyengar, S. S., Tomasi, J., Cossi, M., Millam, J. M., Klene, M., Adamo, C., Cammi, R., Ochterski, J. W., Martin, R. L., Morokuma, K., Farkas, O., Foresman, J. B. and Fox, D. J. *Gaussian 16 Rev. B.01*, Wallingford, CT, **2016**.

Preti, L., Attanasi, O. A., Caselli, E., Favi, G., Ori, C., Davoli, P., Felluga, F. and Prati, F. (2010) One-Pot Synthesis of Imidazole-4-Carboxylates by Microwave-Assisted 1,5-Electrocyclization of Azavinyl Azomethine Ylides. Eur. J. Org. Chem. *2010*, 4312-4320.

Zhurko, G. A., http://www.chemcraftprog.com.